AD-A034 159 CALSPAN CORP BUFFALO N Y F/G 19/1

CASELESS AMMUNITION HEAT TRANSFER. VOLUME III.(U)

APR 76 D E ADAMS, F A VASSALLO DAAG25-70-C-0454

UNCLASSIFIED CALSPAN-GM-2948-Z-3-VOL-3 NL

1 OF 3

AD A034159

AD A034159

(1)

Calspan

Technical Report

DDC
RECEIVED
DEC 3 1976
C

COPY AVAILABLE TO DDC DOES NOT
PERMIT FULLY LEGIBLE PRODUCTION

DISTRIBUTION STATEMENT A
Approved for public release;
Distribution Unlimited

Calspan Corporation
Buffalo, New York 14221

(1)

Calspan

(9) Rept. for Apr 70 - Apr 76,

DDC
RECEIVED
DEC 8 1976
C

(6) CASELESS AMMUNITION HEAT TRANSFER.
VOLUME III.

(10) D.E. Adams and F.A. Vassallo

Calspan Report No. GM-2948-Z-3

(14) CALSPAN-GM-2948-Z-3-Vol-3

Prepared For:

DEPARTMENT OF THE ARMY
FRANKFORD ARSENAL
PHILADELPHIA, PENNSYLVANIA 19137

(15) DAAG-25-70-C-0454 supp. I

(11) APRIL 1976
CONTRACT NO. DAAA25-70-C0454 ✓

(12) 241 p.

PREPARED BY: D E Adams
D.E. Adams
Thermal Research Center

APPROVED BY: Gerald A. Sterbutzel
Gerald A. Sterbutzel
Thermal Research Center

Franklin A. Vassallo
F.A. Vassallo
Thermal Research Center

DISTRIBUTION STATEMENT A
Approved for public release;
Distribution Unlimited

[redacted]

Calspan Corporation
Buffalo, New York 14221

407727

B

FOREWORD

This report was prepared by Calspan Corporation, Buffalo, New York, 14221, to cover the work accomplished from April 1970 to April 1976 under Contract No. DAAG25-70-C-0454. The program was administered by Ms. Theresa Elmendorf and Mr. Peter Ayyoub of Frankford Arsenal. At Calspan, the work was under the supervision of Mr. Franklin A. Vassallo.

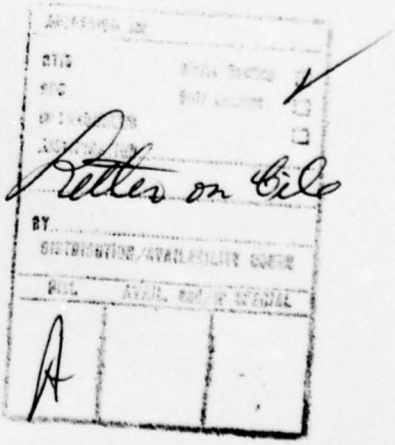

ABSTRACT

Heat transfer studies were performed for small and medium caliber caseless ammunition (1) to evaluate the thermal performance of existing fixtures and ammunition, (2) devise and evaluate mathematical techniques by which the thermal behavior of future weapons may be predicted and problem areas identified prior to weapon design and (3) obtain information which can lead to improvement in future weapons and ammunition.

The study continues previous work on 5.56mm and 27mm caseless ammunition. Some measurements of the heating of an M16 rifle firing cased 5.56mm ammunition are initially reported as a basis of comparison of caseless ammunition. The primary emphasis of the 5.56mm testing is directed towards High Ignition Temperature Propellant (HITP) rounds. Firing tests and laboratory cook-off tests were conducted with HITP and analysis was conducted to evaluate the potential of caseless ammunition during burst firing schedules.

The 27mm evaluations consist of the results of single-shot and rapid-fire testing, laboratory cook-off tests, and predictions of gun heating to be expected during rapid-fire bursts.

A mathematical model was developed which provides an adequate tool by which the thermal effects of rapid fire may be predicted based upon single-shot testing.

TABLE OF CONTENTS

Section	Title	Page
	FOREWORD	i
	ABSTRACT	ii
	LIST OF ILLUSTRATIONS	v
	LIST OF TABLES	x
I	INTRODUCTION	1
II	SUMMARY AND CONCLUSIONS	5
III	5.56MM AMMUNITION	10
	A. Cased Ammunition	10
	B. Thermal Characteristics of Molded Propellants	20
	1. Controlled Temperature Plate Tests	20
	2. Rapidly Cooling Surface Tests	24
	3. Firing Tests	26
	4. Cook-Off Tests	37
	5. Heat Transfer Evaluations	40
	6. Temperature Predictions	44
IV	27MM AMMUNITION	50
	A. Single-Shot Tests	50
	B. Rapid-Fire Tests	59
	C. Cook-Off Tests	72
	D. Thermal Evaluations	81
	1. Heat Transfer Parameters	81
	2. Comparisons Between Measured and Calculated Temperatures	81
	3. Weapon Thermal Conductivity Effects	90
	4. Cook-Off Limits	100
	5. Covered Caseless Ammunition	106

TABLE OF CONTENTS (CONT'D.)

Section	Title	Page
V	REFERENCES	113
VI	APPENDICES	
	A. Mathematical Models and Computer Routines Used In Evaluation of Caseless Ammunition Heat Transfer	114
	B. Thermal Instrumentation	220

LIST OF ILLUSTRATIONS

Figure No.	Title	Page
1	COOK-OFF TIMES FOR 5.56MM CASED AMMUNITION IN PREHEATED M16 RIFLE	11
2	EXTERNAL CHAMBER AND BARREL TEMPERATURES IN M16 RIFLE DURING RAPID FIRE SCHEDULE	13
3	EXTERNAL CHAMBER AND BARREL TEMPERATURES IN M16 RIFLE DURING RAPID FIRE SCHEDULE	14
4	TEMPERATURE HISTORY OF INSTRUMENTED 5.56MM BRASS CASE	15
5	ESTIMATED EXTERNAL BARREL TEMPERATURES IN A SINGLE BURST OF AN M16 RIFLE	19
6	COOK-OFF TEMPERATURES ON CONSTANT TEMPERATURES STEEL PLATE, 5.56MM PROPELLANTS	22
7	COOK-OFF TEMPERATURES ON CONSTANT TEMPERATURE STEEL PLATE, 5.56MM PROPELLANTS	23
8	ROCK ISLAND BARREL MODIFIED TO M16 CONFIGURATION SHOWING IN-WALL AND EXTERNAL THERMOCOUPLE POSITIONS	27
9	AVERAGE TEMPERATURE RISE VS. BURST LENGTH (R1-M16 CASELESS FIXTURE)	29
10	IN-WALL TEMPERATURES AT THE REAR CHAMBER DURING A 20 ROUND BURST (R1-M16 FIXTURE)	30
11	FIRING PIN FOR DETERMINING HEAT INPUT	33
12	FIRING PIN HEATING, 5.56MM CASELESS AMMUNITION	34
13	CALCULATED FIRING PIN TEMPERATURE DURING BURST OF 5.56MM CASELESS AMMUNITION	36
14	INITIAL FIRING PIN TEMPERATURE REQUIRED TO COOK-OFF PROPELLANT AS A FUNCTION OF DISTANCE BETWEEN FIRING PIN AND PROPELLANT	38
15	DISTANCE BETWEEN FIRING PIN AND PROPELLANT REQUIRED TO PREVENT COOK-OFF IN A BURST OF 5.56MM CASELESS AMMUNITION	39
16	MEASURED AND COMPUTED TEMPERATURES AFT OF THE STOP SHOULDER DURING 5 ROUND BURST AT 300 RDS/MIN, ROCK ISLAND 5.56MM CASELESS FIXTURE	47

LIST OF ILLUSTRATIONS (CONT'D.)

Figure No.	Title	Page
17	COMPARISON OF RESIDUAL IN-WALL TEMPERATURE AT STOP SHOULDER AS A FUNCTION OF FIRING RATE AND NUMBER OF ROUNDS FIRED (R1-M16 CASELESS FIXTURE)	48
18	INSTRUMENTATION LOCATIONS IN CALSPAN SINGLE-SHOT CHAMBER SIMULATING PHILCO-FORD 27MM CASELESS FIXTURE, CAW-T2	51
19	MACHINED AND MYLAR-COVERED 27MM ROUND CONFIGURATION (HERCULES AND OLIN AMMUNITION)	55
20	CAW-T2 AUTOMATIC FIXTURE IN-WALL TEMPERATURE LOCATIONS	60
21	IN-WALL TEMPERATURES DURING A 10 ROUND BURST OF AEROJET AMMUNITION IN THE PHILCO-FORD CAW-T2 AUTOMATIC 27MM FIXTURE	61
22	IN-WALL TEMPERATURES DURING A 25 ROUND BURST OF HERCULES AMMUNITION IN THE PHILCO-FORD CAW-T2 AUTOMATIC 27MM FIXTURE	62
23	IN-WALL TEMPERATURES DURING A 15 ROUND BURST OF OLIN AMMUNITION IN THE PHILCO-FORD CAW-T2 AUTOMATIC 27MM FIXTURE	63
24	IN-WALL TEMPERATURES DURING A 7 ROUND BURST OF COVERED AEROJET AMMUNITION IN THE PHILCO-FORD CAW-T2 AUTOMATIC 27MM FIXTURE	66
25	IN-WALL TEMPERATURES DURING A 10 ROUND BURST OF COVERED HERCULES AMMUNITION IN THE PHILCO-FORD CAW-T2 AUTOMATIC 27MM FIXTURE	75
26	IN-WALL TEMPERATURES DURING A 9 ROUND BURST OF COVERED OLIN AMMUNITION IN THE PHILCO-FORD CAW-T2 AUTOMATIC 27MM FIXTURE	76
27	COOK-OFF TEMPERATURES ON CONSTANT TEMPERATURE STEEL PLATE, AEROJET 27MM CASELESS PROPELLANT	77
28	COOK-OFF TEMPERATURES ON CONSTANT TEMPERATURE STEEL PLATE, HERCULES 27MM CASELESS PROPELLANT	78

LIST OF ILLUSTRATIONS (CONT'D.)

Figure No.	Title	Page
29	COOK-OFF TEMPERATURES ON CONSTANT TEMPERATURE STEEL PLATE, OLIN 27MM CASELESS PROPELLANT	79
30	PROPELLANT GAS TEMPERATURE, CHAMBER PRESSURE, AND PROJECTILE VELOCITY AS A FUNCTION OF TIME FOR AEROJET 27MM CASELESS AMMUNITION	82
31	PROPELLANT GAS TEMPERATURE, CHAMBER PRESSURE, AND PROJECTILE VELOCITY AS A FUNCTION OF TIME FOR HERCULES 27MM CASELESS AMMUNITION	83
32	PROPELLANT GAS TEMPERATURE, CHAMBER PRESSURE, AND PROJECTILE VELOCITY AS A FUNCTION OF TIME FOR OLIN 27MM CASELESS AMMUNITION	84
33	COMPUTED HEAT TRANSFER COEFFICIENTS IN THE PHILCO-FORD CAW-T2 AUTOMATIC 27MM FIXTURE, AEROJET AMMUNITION	85
34	COMPUTED HEAT TRANSFER COEFFICIENTS IN THE PHILCO-FORD CAW-T2 AUTOMATIC 27MM FIXTURE, HERCULES AMMUNITION	86
35	COMPUTED HEAT TRANSFER COEFFICIENTS IN THE PHILCO-FORD CAW-T2 AUTOMATIC 27MM FIXTURE, OLIN AMMUNITION	87
36	COMPARISON OF MEASURED AND CALCULATED RESIDUAL TEMPERATURES AT STOP-SHOULDER OF CAW-T2 27MM AUTOMATIC FIXTURE, HERCULES AMMUNITION	88
37	COMPARISON OF MEASURED AND CALCULATED RESIDUAL TEMPERATURES AT NECK OF CAW-T2 27MM AUTOMATIC FIXTURE, HERCULES AMMUNITION	89
38	CALCULATED EFFECT OF THERMAL CONDUCTIVITY ON INTERNAL SURFACE TEMPERATURE AT THE STOP-SHOULDER OF A 27MM CASELESS CHAMBER DURING A 40 ROUND BURST	91
39	CALCULATED EFFECT OF THERMAL CONDUCTIVITY ON AVERAGE STOP SHOULDER TEMPERATURE FOR A 27MM CASELESS CHAMBER DURING A 40 ROUND BURST	92
40	CALCULATED EFFECT OF THERMAL CONDUCTIVITY ON HEAT INPUT TO STOP SHOULDER FOR A 27MM CASELESS CHAMBER DURING A 40 ROUND BURST	93

LIST OF ILLUSTRATIONS (CONT'D.)

Figure No.	Title	Page
41	EFFECT OF COATING THERMAL CONDUCTIVITY ON RESIDUAL AND AVERAGE TEMPERATURES AT THE STOP SHOULDER DURING A 25 ROUND BURST (27MM, 600 RDS/MIN)	95
42	EFFECT OF COATING THERMAL CONDUCTIVITY ON HEAT INPUT TO STOP SHOULDER DURING A 25 ROUND BURST (27MM, 600 RDS/MIN)	96
43	EFFECT OF COATING THERMAL CONDUCTIVITY ON RESIDUAL TEMPERATURE AT STOP SHOULDER AFTER 25 ROUNDS (27MM, 600 RDS/MIN)	97
44	EFFECT OF COATING THICKNESS ON RESIDUAL SURFACE TEMPERATURE AT THE STOP SHOULDER (27MM, 600 RDS/MIN)	98
45	EFFECT OF COATING THICKNESS ON HEAT TRANSFER TO THE STOP SHOULDER (27MM, 600 RDS/MIN)	99
46	CALCULATED RESIDUAL STOP-SHOULDER TEMPERATURES IN 27MM CAW-T2 FIXTURE, 270 RDS/MIN	102
47	CALCULATED AVERAGE BOLT CAVITY TEMPERATURES IN 27MM CAW-T2 FIXTURE, 270 RDS/MIN	104
48	CALCULATED STOP-SHOULDER TEMPERATURES FOR 27MM AEROJET CASELESS AMMUNITION IN CAW-T2 FIXTURE, 270 RDS/MIN	108
49	CALCULATED STOP-SHOULDER TEMPERATURES FOR 27MM HERCULES CASELESS AMMUNITION IN CAW-T2 FIXTURE, 270 RDS/MIN	109
50	CALCULATED STOP-SHOULDER TEMPERATURES FOR 27MM OLIN CASELESS AMMUNITION IN CAW-T2 FIXTURE, 270 RDS/MIN	110
A-1	CROSS SECTIONAL VIEW AT A TYPICAL CHAMBER AXIAL SECTION	164
A-2	TYPICAL AXIAL CHAMBER SECTIONS	166
A-3	TIME FACTORS FOR COMPUTER SIMULATION OF RAPID FIRE	169
A-4	GENERAL SUBDIVISION OF AXIAL SECTIONS INTO RADIAL ELEMENTS	172

LIST OF ILLUSTRATIONS (CONT'D.)

Figure No.	Title	Page
B-1	TYPICAL IN-WALL THERMOCOUPLE INSTALLATION	222
B-2	HEAT INPUT CALCULATED FROM IN-WALL TEMPERATURES	224
B-3	ACCURACY OF IN-WALL THERMOCOUPLE TECHNIQUE	226
B-4	CORRECTION FACTOR FOR HEAT INPUT CALCULATED FROM IN-WALL THERMOCOUPLES	228

LIST OF TABLES

Table No.	Title	Page
I	COOK-OFF TEST OF M193 BALL PROPELLANT AMMUNITION IN M16 RIFLE (THERMAL GRADIENTS PRODUCED BY TORCH)	17
II	INCIDENCE OF FLAMES IN CONSTANT TEMPERATURE PLATE COOK-OFF TESTS	21
III	COOK-OFF THRESHOLDS ESTABLISHED BY THE CONTROLLED TEMPERATURE PLATE TESTS	21
IV	RESIDUAL TEMPERATURE COOK-OFF TESTS	25
V	RESIDUAL TEMPERATURE COOK-OFF RESULTS	26
VI	5.56MM HITP COOK-OFF TEST RESULTS	41
VII	5.56MM HITP FIRING TEST RESULTS	43
VIII	COMPARATIVE 5.56MM HITP AND IMR COOK-OFF DATA	45
IX	TEST RESULTS - 27MM CASELESS AMMUNITION	53
X	TEST RESULTS - 27MM COVERED AMMUNITION (AS COVERED FOR RAPID-FIRE TESTS)	56
XI	RAPID-FIRE TEST DATA AT STOP-SHOULDER AFTER 10 ROUNDS	67
XII	COMPARISON OF MEASURED RESIDUAL TEMPERATURES FOR CALSPAN-COVERED AND UNCOVERED 27MM CASELESS AMMUNITION	68
XIII	FIRST ROUND HEAT INPUT DATA FOR CALSPAN-COVERED AMMUNITION IN CAW-T2 27MM AUTOMATIC FIXTURE	70
XIV	MINIMUM COOK-OFF TEMPERATURE OF PROPELLANTS IN CONTACT WITH STEEL SURFACE COOKING AT 250°F/SEC	73
XVI	RAPID-FIRE TEST DATA AT STOP-SHOULDER AFTER 10 ROUNDS	103
XVII	STOP-SHOULDER COOK-OFF DATA FOR COVERED AND UNCOVERED 27MM CASELESS AMMUNITION	112

I. INTRODUCTION

The propellant in caseless ammunition is formed into a solid material having structural integrity in comparison to standard ammunition where loose propellant grains are contained in a metal case. As presently developed, most caseless ammunition consists of the same propellants used in cased ammunition except that they are bonded with nitrocellulose into a hollow cylinder. A variation of this type of ammunition is nitrocellulose formed into a single grain of propellant. Also under development are ammunitions containing High Ignition Temperature Propellants (HITP) which have varied chemical compositions designed to require higher ignition temperatures than nitrocellulose.

Substitution of caseless ammunition for standard cased ammunition in rapid-fire weapons can alter weapon design techniques in that problem areas associated with over-heating of gun parts and ammunition can be significantly different for the two types of ammunition. In the chamber area of the weapon, the caseless propellant burns in close contact with the wall. Hence, heat transferred to the wall may be retarded only by the gas boundary layer. By contrast, cased ammunition provides a barrier to heat penetration which, at high rates of fire, can totally prevent heat transfer to the chamber walls prior to extraction of the case. Additionally, the cold brass case offers a cooling action, in that heat is conducted from the hot chamber walls to the case during its residence in the chamber. Hence, the residual chamber temperatures are expected to be significantly less when cased ammunition is used. (Residual temperature is defined as the inside surface temperature at the time the succeeding round is chambered.)

Chamber wall temperatures can have a direct bearing on the acceptability of a weapon because thermally initiated ignition (cook-off) may occur. Most rapid-fire weapons, both caseless and cased, are designed to be open-bolt weapons; that is, to stop at the end of a burst with no chambered round. Even if a weapon is of the open-bolt type, a round may be left chambered if there is a malfunction; and cook-off in this instance must be avoided if at all possible

because of the extreme hazard that is involved. Because chamber wall temperatures can be higher and direct contact of propellant with the wall is possible using caseless ammunition, cook-off probability may be greater for this ammunition. In fact, very short time cook-off (within milliseconds) is made possible in situations where the caseless propellant is forced into direct contact with the chamber prior to reduction of chamber wall temperatures. This type of cook-off has, heretofore, been prevented by the brass case.

Short-time cook-off is cook-off due to contact with the rapidly falling temperature at the time of chambering (residual temperature). Long-time cook-off is the cook-off due to the average temperature across the chamber cross-section. This average temperature is the temperature to which the residual temperature equilibrates given enough time. Cook-off is a function of both temperature and time. For given circumstances, a cook-off may occur after a short time due to contact with the high residual temperature or after a long time due to contact with the lower average temperature. The residual temperature decreases rapidly due to heat conduction into the chamber metal. The average temperature decreases slowly because heat conduction and convection into the surrounding environment are the only sources of heat loss.

Even though caseless ammunition may have heat transfer problems, it does offer impressive advantages in weight, logistics, and strategic materials. In many instances, these advantages can far outweigh problems of weapon heating. To obtain the fullest advantage from caseless ammunition, techniques by which the altered heat transfer problems can be overcome are needed. As a first step in this direction, the magnitude of the heat problem must be defined and the areas of greatest concern determined. The first report of the current study by Calspan (formerly Cornell Aeronautical Laboratory) deals with heat transfer for both cased and caseless ammunition in guns utilizing 7.62mm ammunition.[1] In addition, a general experimental-analytical technique was evolved by which weapon design criteria could be established. The desire to predict temperatures during bursts from single-shot data arises from the fact that single-shot data are available much earlier in the development cycle than multiple-shot

data; in the form of basic Mann barrel data it can be available during the initial design stages. Predictions based on single-shot data can be used in modifying proposed designs to satisfy mission requirements before the weapon development has reached the point where changes are costly and time consuming.

The general experimental-analytical approach developed in Reference 1 began with the realization that although heat transfer rates can be viewed as quantities for which theoretical interpretation is possible, they have yet to be accurately predicted without the use of extensive empirical evaluations. Generally, the theory serves as a means of interpreting between existing designs for which experimental observations have been made. For this reason, it has been regarded most efficient to evaluate by experiments the heat transfer within a number of weapons using both caseless and cased ammunition and to correlate the measured data in terms of pressure, velocity, and position. This was the approach that was used in Reference 1 for studying the heat transfer to 7.62mm fixtures and it is the approach that has been followed in a second report which is primarily concerned with the heat transfer to 5.56mm and 27mm caseless ammunition fixtures.[2]

Heat transfer to chamber and stop-shoulder areas of weapons are most vital to understanding the effects of replacement of standard ammunition with caseless ammunition as these are the areas of outstanding difference between cased and caseless ammunition. For this reason, prime emphasis in Reference 2 was placed on measurement of heat transfer in these areas and its effects on weapon performance in both single and multiple burst operation. Small heat flux sensors were installed in selected guns, and the time history of chamber heat flux was evaluated in single-shot firings using caseless ammunition. Through computer calculations, chamber wall temperatures were obtained for simulated rapid-fire conditions, and temperature values were compared with critical cook-off temperatures experimentally determined for the propellant. By this means, areas of greatest cook-off hazard could be delineated. The effectiveness of ammunition coatings for reducing net heat transfer and for preventing propellant ignition was also investigated in this work, both experimentally and analytically. Additional studies by Calspan of coated

caseless ammunition have been reported in References 3, 4, and 5. The mathematical models and computer routines developed in the present program for evaluating heat transfer are presented in Reference 6, which is reproduced as an Appendix to this report. The ignition of 5.56mm caseless ammunition was photographed through a clear sapphire chamber. These tests are reported in Reference 7. Reference 7 also includes single-shot and 20 round burst heat transfer measurements of 5.56mm cased ammunition for comparative purposes.

II. SUMMARY AND CONCLUSIONS

The objectives of these heat transfer studies of small and medium caliber caseless ammunition have been (1) to evaluate the thermal performance of existing fixtures and ammunition, (2) to devise and evaluate mathematical techniques by which the thermal behavior of future weapons employing small and medium caliber caseless ammunition may be predicted and problem areas identified prior to final weapon design, and (3) to obtain information which can lead to improvement in future weapons and ammunition. This study continues previous work on 5.56mm and 27mm caseless ammunition. The primary emphasis of the 5.56mm caseless ammunition testing is directed towards HITP rounds. Firing tests and laboratory cook-off tests were conducted with HITP and analysis was conducted to evaluate the potential of caseless ammunition during burst firing schedules. The 27mm evaluations presented in this report consist of the results of single-shot and rapid-fire testing, laboratory cook-off tests, and predictions of gun heating to be expected during rapid-fire bursts. A mathematical model was developed which provides an adequate tool by which the thermal effects of rapid fire may be predicted based upon single-shot testing.

The following conclusions were developed relative to 5.56mm ammunition:

1. Cased Ammunition

    1. Cook-off of conventional 5.56mm ball ammunition in the M16 rifle is possible after 140 rounds fired rapidly (i.e. all magazines fired in single bursts and approximately 5 seconds between magazines).

    2. For conventional 5.56mm ball propellant ammunition, cook-off at chamber temperatures below 370^{o}F is unlikely. Cook-off within 1.5 sec of chambering is not expected for any chamber temperature.

3. Generally, cook-off in the M16 rifle is due to heating of propellant in contact with the projectile, not the case.

2. Caseless Propellants

1. Molded caseless ammunition which is unprotected by a covering exhibits similar characteristics to cased ammunition but limiting cook-off conditions are different.
2. Limiting long-time cook-off temperature for caseless propellants as given in Table III is better than that for 5.56mm ball propellant cased ammunition.
3. By comparison with IMR propellant which flames at cook-off, flaming of the newly developed high ignition temperature propellants (HITP) is unlikely at temperatures expected during use in a rapid fire weapon.
4. The HITP generally provide some measurable increase in limiting long-time cook-off temperature level over that of IMR.
5. Short-time cook-off temperature thresholds of HITP are significantly greater than IMR (Table V).
6. Rapid fire of molded caseless ammunition has been performed at nominally 600 rounds/min and at burst lengths up to 40 rounds.
7. Short-time cook-off in less than one second has been experienced in the firing of molded IMR caseless ammunition but is attributable to inappropriate selection of firing mechanism for use with caseless ammunition.

8. HITP generally show less chamber heating than IMR propellants but reductions are believed due in part to incomplete combustion and in part to insulating effects of residue in the chamber.
9. The HITP generally show increased chamber residue over that of IMR; HITP 8602.1 appears closest to IMR in cleanliness of burning.
10. It appears that the increased ignition temperature of HITP in general may allow a severalfold increase in burst length over that of IMR.

Based upon the results of the heat transfer studies and the above conclusions, the following recommendations relative to 5.56mm caseless ammunition are made.

1. Efforts should be directed to the design and fabrication of a rapid fire system thermally compatible with caseless ammunition. It is suggested that a multiple chamber, fixed breech design be investigated. A multiple chamber would allow time between round insertions for the residual temperature to reduce and a fixed breech would reduce heating at the base of the round.
2. Means by which contact of the propellant to the stop-shoulder may be prevented must be sought and developed. Plastic shoulder discs may be very effective.
3. Limited effort should be continued on the development of HITP propellant with especial attention given to modifications of the 8600 series propellants.

The following conclusions were developed for the tested 27mm caseless ammunition.

1. Ballistic performance comparable to standard brass cased ammunition can be obtained with molded charge caseless ammunition with little chamber residue.
2. Cook-off of molded propellants is not likely at chamber temperatures below 400°F, or about equivalent to the cook-off threshold for brass cased ammunition. Above 600°F, cook-off of uncovered caseless ammunition can be expected prior to equilibration of chamber wall temperature gradients.
3. Use of covered caseless ammunition can defeat substantially the limitations on allowable burst length caused by chamber wall thermal gradients. This is due in part to the insulating effect of the covering and in part to the heating reductions afforded by the covering during the interior ballistic cycle. Computer assessment of thermal information indicates that burst length limited by cook-off can be made equivalent to that of standard brass cased ammunition when covered caseless ammunition is used.
4. The tested molded ball propellant ammunition was found to exhibit generally less chamber heating than the other ammunition types tested (molded double base extruded propellant and cast monolithic, single grain propellant). Additionally, the ball propellant ammunition produced more uniform interior ballistic performance
5. For the ammunitions tested, the most rounds that can be fired in a burst in the automatic test fixture without a cook-off possibility will occur with the molded ball propellant. Next will be the molded double base extruded propellant ammunition and third the monolithic, single grain propellant ammunition.

6. In the design of future rapid-fire weapons, thermal factors must be given prime consideration especially in critical chamber and bolt/breech areas. Use of low thermal conductivity materials and unnecessary protrusions must be avoided.

III. 5.56MM AMMUNITION

A. Cased Ammunition

Early efforts in the study program were devoted to the investigation of cook-off characteristics of cased 5.56mm ammunition when used in the M16 rifle. The ultimate objective of these investigations was to establish the cook-off performance which ideally must be bettered or at least matched by caseless ammunition.

Cook-off times recorded for 5.56mm cased ammunition placed into a preheated M16 rifle chamber are shown in Figure 1. Midchamber temperatures up to 800°F were utilized in tests of three types, (1) natural chamber cooling, (2) constant chamber temperature, and (3) rapid fire cook-off of a 20 round magazine during natural cooling of the chamber. Results obtained for the three types of tests (Figure 1) indicate typically the same values. This is as expected inasmuch as the natural cooling of the chamber produced insignificant temperature drop in the cook-off times recorded, especially at high chamber temperatures. Inspection of the data indicates two limiting conditions:

1. Cook-off is not expected at chamber temperatures below 370°F.
2. Cook-off times shorter than 1.5 sec would not be expected in this ammunition-rifle combination.

For comparison, the solid curve of Figure 1 represents the locus of minimum cook-off times observed for cased 7.62mm ammunition obtained in earlier work using an M60 machine gun.[2] Differences in observed cook-off times are minor and are likely due to differences in barrel-chamber geometries rather than ammunition-propellant effects.

Chamber and barrel temperature rises for the M16 rifle during rapid fire of multiple magazines were recorded in order to determine rapid fire conditions leading to cook-off. In particular, it was desired to estimate the

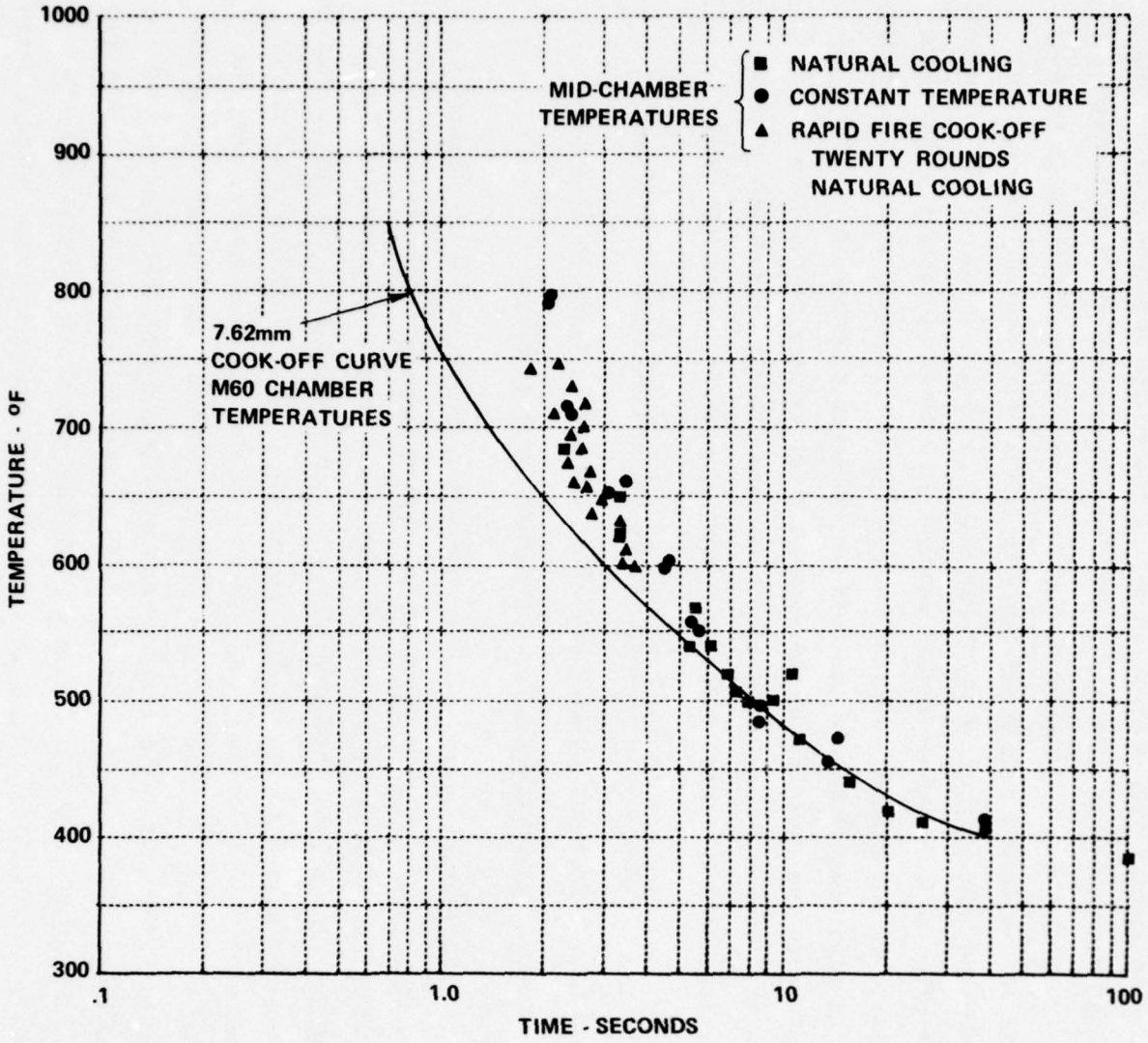

Figure 1 COOK-OFF TIMES FOR 5.56mm CASED AMMUNITION IN PREHEATED M16 RIFLE

single burst cook-off limit for the cased 5.56mm ammunition fired in the M16 chamber configuration. Figure 2 illustrates temperatures and cook-off times recorded in rapid fire of about 11 magazines (219 rounds) in the M16 rifle. A failure to eject followed by a jam during the fourth magazine allowed some cooling of the weapon to take place and thus compromised the data somewhat, but it is clear that this number of rounds is more than sufficient to produce cook-off in the weapon. Cook-off times as short as 18 seconds are observed. A second test, the results of which are shown in Figure 3, was found to produce no cook-off. Here 7 magazines (140 rounds) were fired as rapidly as possible (approximately 46 seconds) with the cook-off round chambered within 12 seconds after the final magazine. No cook-off was observed although the barrel temperature in the vicinity of the stop-shoulder is seen to be above 400^{o}F (Figure 3). Cook-off conditions must have been closely approached in this test as indicated by tests at Aberdeen Proving Grounds[8] which reported:

1. Cook-off in 41.2 sec after 140 rounds fired in 46.7 sec.
2. Cook-off in 42.7 sec after 140 rounds fired in 51.2 sec.
3. No cook-off after 120 rounds fired in 32 sec.

In order to obtain a more fundamental understanding of chamber cook-off and to reduce the expenditure of ammunition, several tests were conducted in which an inert round of ammunition containing temperature sensing thermocouples was placed into preheated chambers. In these tests, the barrel section near the chamber was heated by an external gas torch. High heat flux can be obtained with this technique, and thermal gradients in the chamber area which are representative of those in rapid fire can be obtained. After heating the chamber with the torch, the instrumented round was immediately cycled into the chamber by the bolt. Figure 4 shows case temperature histories for a specific thermal gradient and where the barrel near the projectile (position No. 3) was initially above 475^{o}F. The gradient closely represents that which existed at the insertion of the second cook-off round in the test shown in Figure 2 where cook-off occurred in about 18 sec. The maximum temperature internal to the case appears to occur at the base of the projectile. This maximum occurs

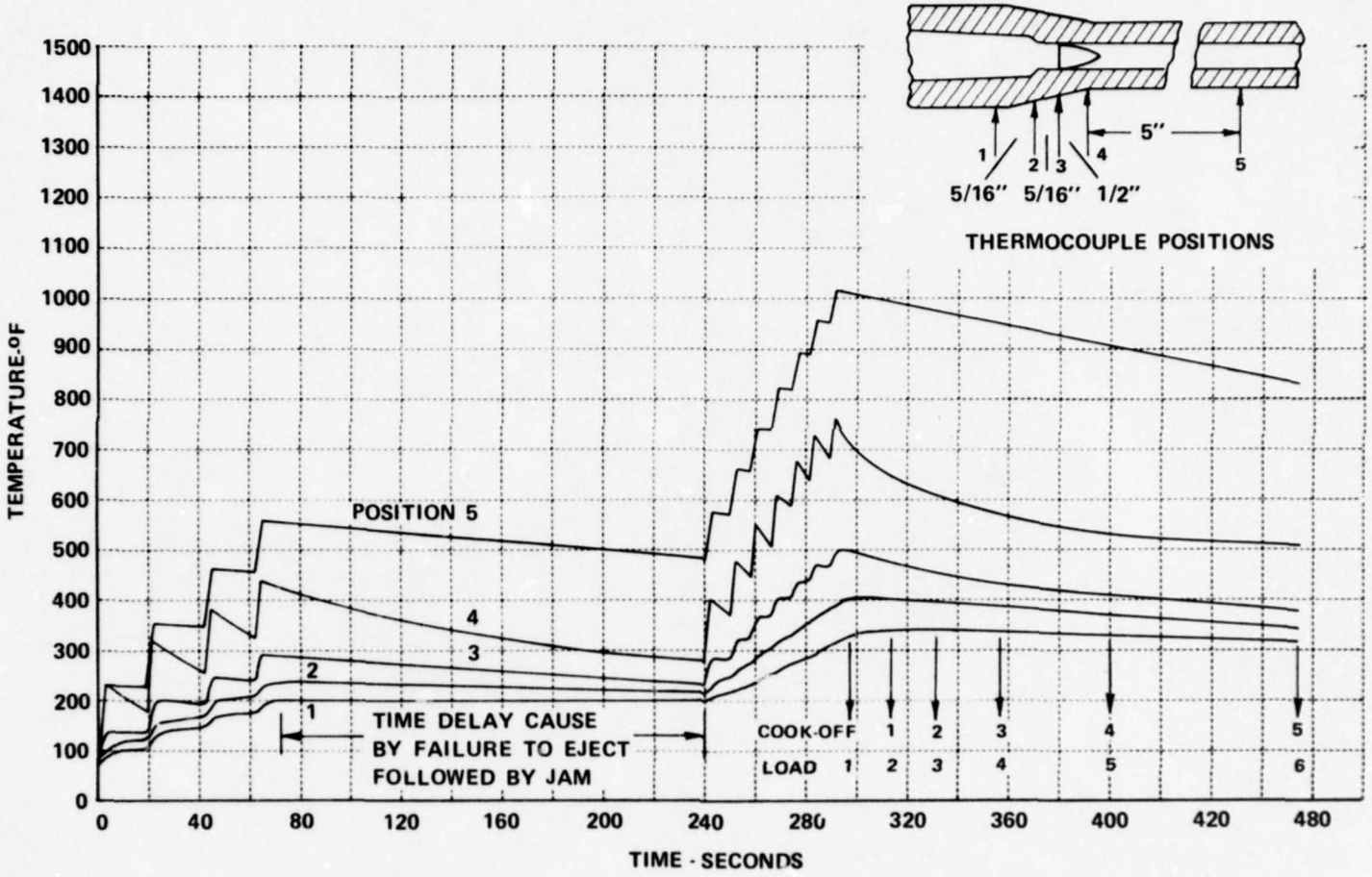

Figure 2 EXTERNAL CHAMBER AND BARREL TEMPERATURES IN M16 RIFLE DURING RAPID FIRE SCHEDULE

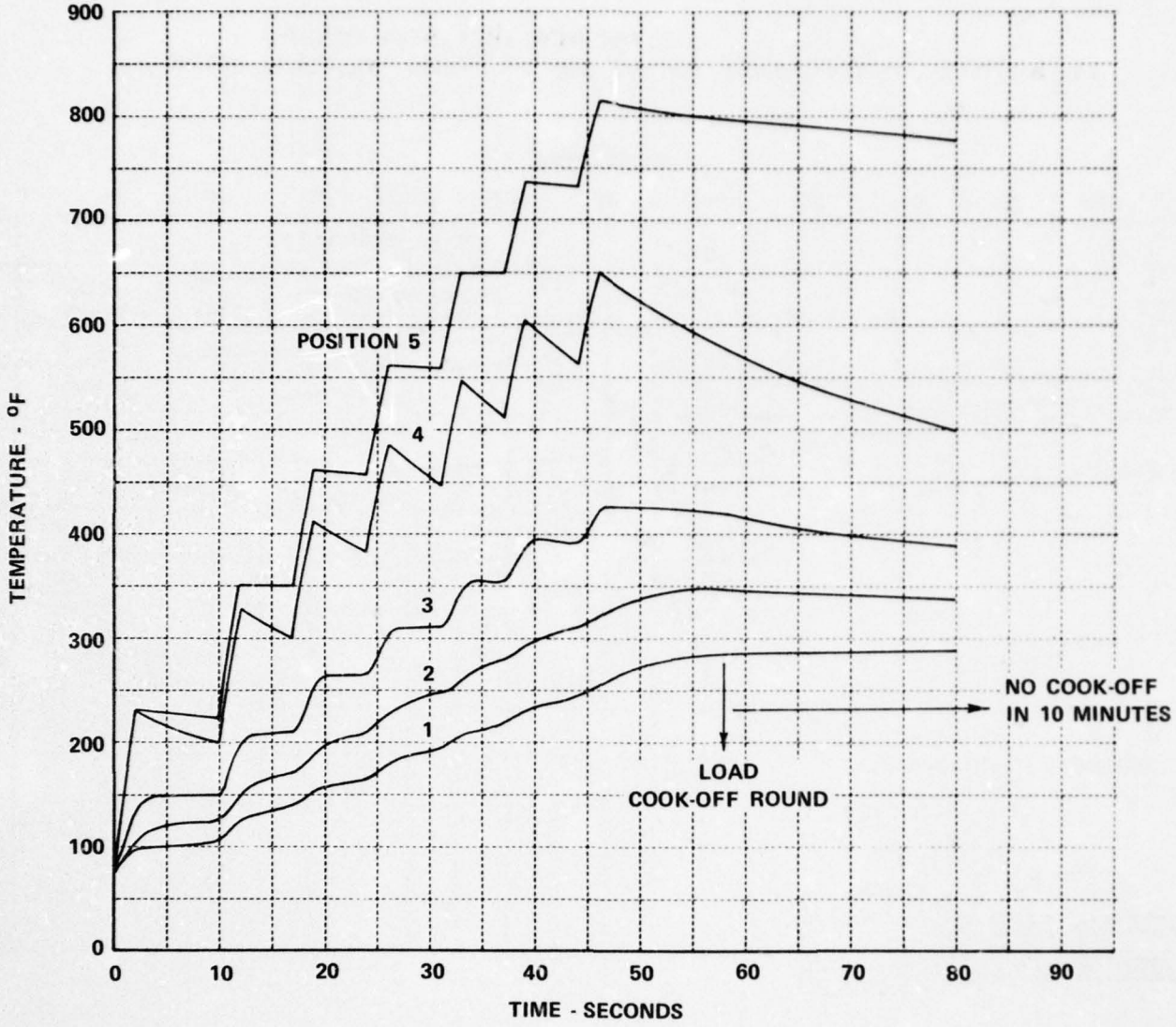

Figure 3 EXTERNAL CHAMBER AND BARREL TEMPERATURES IN M16 RIFLE DURING RAPID FIRE SCHEDULE

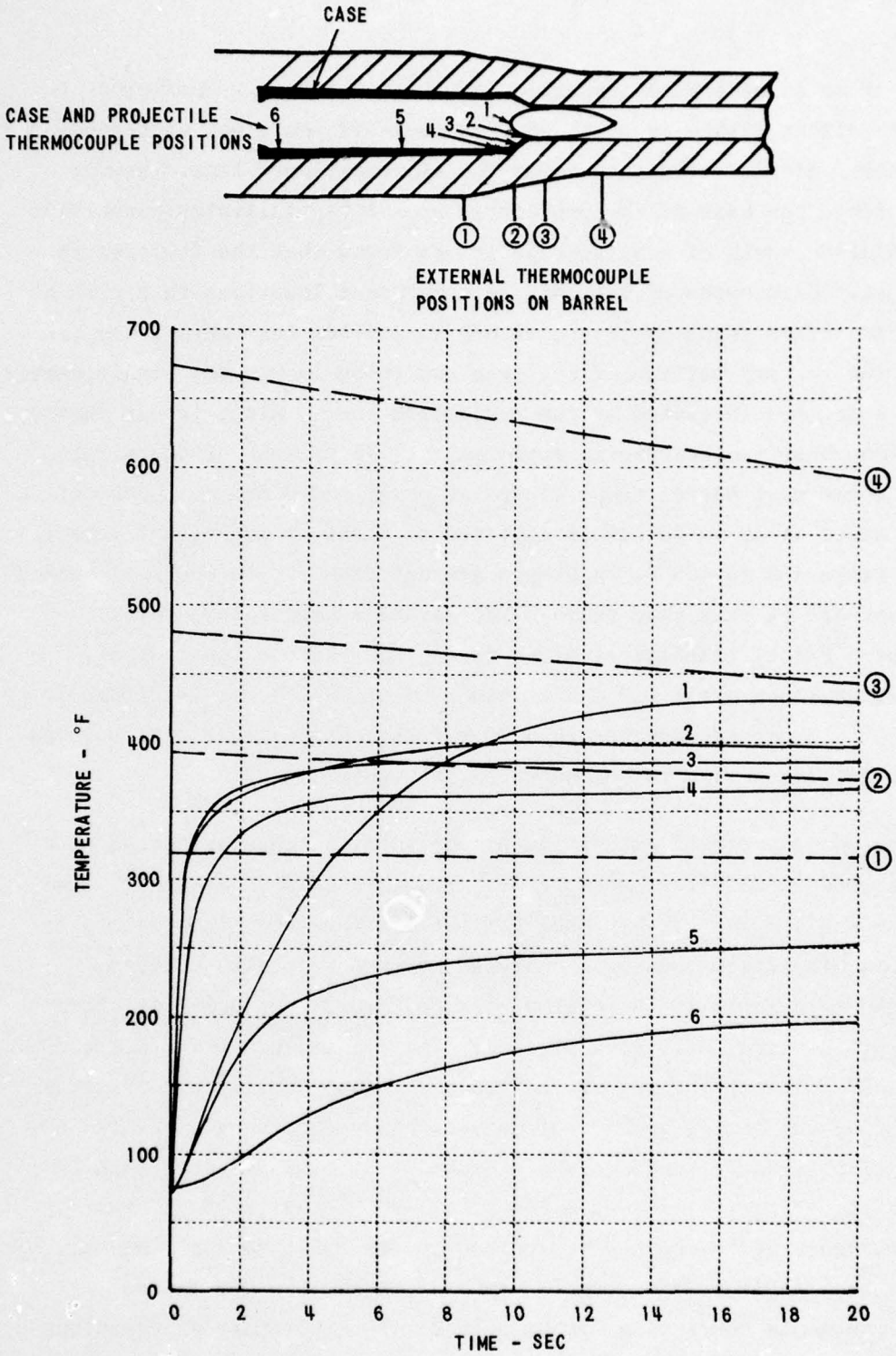

Figure 4 TEMPERATURE HISTORY OF INSTRUMENTED 5.56 mm BRASS CASE

in the order of 20 seconds after insertion of the round and is sufficient to ignite the propellant within seconds, whereas cook-off would not be produced by any of the other recorded temperatures in the aforementioned time. Hence, for this gradient, the base of the projectile apparently initiates propellant cook-off. In other tests of similar type it was found that the temperature of the projectile base exceeded that of the other case locations in a time of about 9 seconds. This suggests that cook-off in periods less than 9 sec are initiated by the forward portion of the case and those in periods significantly greater than 9 sec are initiated by the projectile base. Also, it was observed that the maximum base temperature is approximately 75 percent of the simple average of the external barrel temperatures at positions 3 and 4. Cook-off in times of the order of 10 to 20 sec is expected to occur at propellant temperatures in the range 450 to 425^{o}F. A simple average from 570 to 600^{o}F is needed to produce cook-off in this time frame. This average temperature falls rapidly (about 3^{o}F/sec) immediately after firing and because the cook-off temperature range is so small (10 sec at 450^{o}F, ∞ at 375^{o}F), it is difficult to produce cook-off in periods greater than 20 sec without having first produced it in shorter periods. This is demonstrated in Figure 2.

Data on cook-off of ammunition placed into the chamber heated by a torch was gathered in an effort to determine the threshold of cook-off. The test procedure was similar to that used for the instrumented round, but a standard 5.56mm M193 cased round was charged into the preheated chamber. Results are shown in Table I. A total of ten tests were conducted of which five did not produce cook-off, four produced cook-off in less than 20 sec, and one produced cook-off in greater than 20 sec. Considering cook-off time to be governed by the simple average of barrel temperature above, the Table shows that the temperature range in which cook-off at times greater than 20 sec occurs is rather narrow, say from 594 to 613^{o}F. Below 594^{o}F, cook-off did not occur; above 613^{o}F, cook-off occurred in less than 20 sec. Hence, one estimates the single burst cook-off temperature for the M16 firing cased ammunition to be 600^{o}F as a simple average of temperature at positions 3 and 4 of the M16 barrel.*

* It must be emphasized that this simple average temperature (600^{o}F) is not the propellant temperature.

Table I

COOK-OFF TEST OF M193 BALL PROPELLANT AMMUNITION IN M16 RIFLE
(THERMAL GRADIENTS PRODUCED BY TORCH)

TEMPERATURE AT BARREL POSITIONS				AVERAGE OF 3 AND 4	COOK-OFF TIME - SEC
1	2	3	4		
276°F	355°F	454°F	701°F	577°F	NO COOK
270	350	452	710	581	NO COOK
	274	395	773	584	NO COOK
266	345	447	727	587	NO COOK
252	334	444	744	594	NO COOK
	280	395	820	607	47
290	375	486	769	627	19.5
296	374	482	744	613	18.0
	321	442	854	648	16.5
310	395	507	783	645	14.5

The number of rounds which can be safely fired in a single burst of the M16 rifle was established by determining the barrel temperature as a function of rounds fired using rapid-fire data of the type shown in Figures 2 and 3. The resulting temperatures are shown in Figure 5 where barrel temperatures at positions 2, 3, and 4 as well as the simple average of 3 and 4 are shown as a function of rounds fired. One may observe that the average temperature reaches the 600°F threshold at about 140 rounds fired in a continuous burst. Hence, cook-off conditions have been reached for this ammunition-weapon combination in any continuous burst exceeding 140 rounds, if the weapon is above 70°F initially. The effect of ambient temperature (-65 to +165°F) is estimated to affect the allowable burst length by ± 20 rounds.

With respect to shorter burst lengths followed by short term interim cooling, say 5-10 sec, the number of rounds fired prior to cook-off conditions will not be changed greatly because the balance of heat energy in the chamber area will be relatively the same. Although thermal gradients will not be as great, the rate of average temperature decay will be somewhat less, and hence, more time will be available to heat the case and its propellant contents. This is illustrated above by the Aberdeen tests. One may, therefore, consider 140 rounds fired as rapidly as possible the probable cook-off limit for this ammunition-weapon combination. This ideally should be matched by a caseless rifle system.

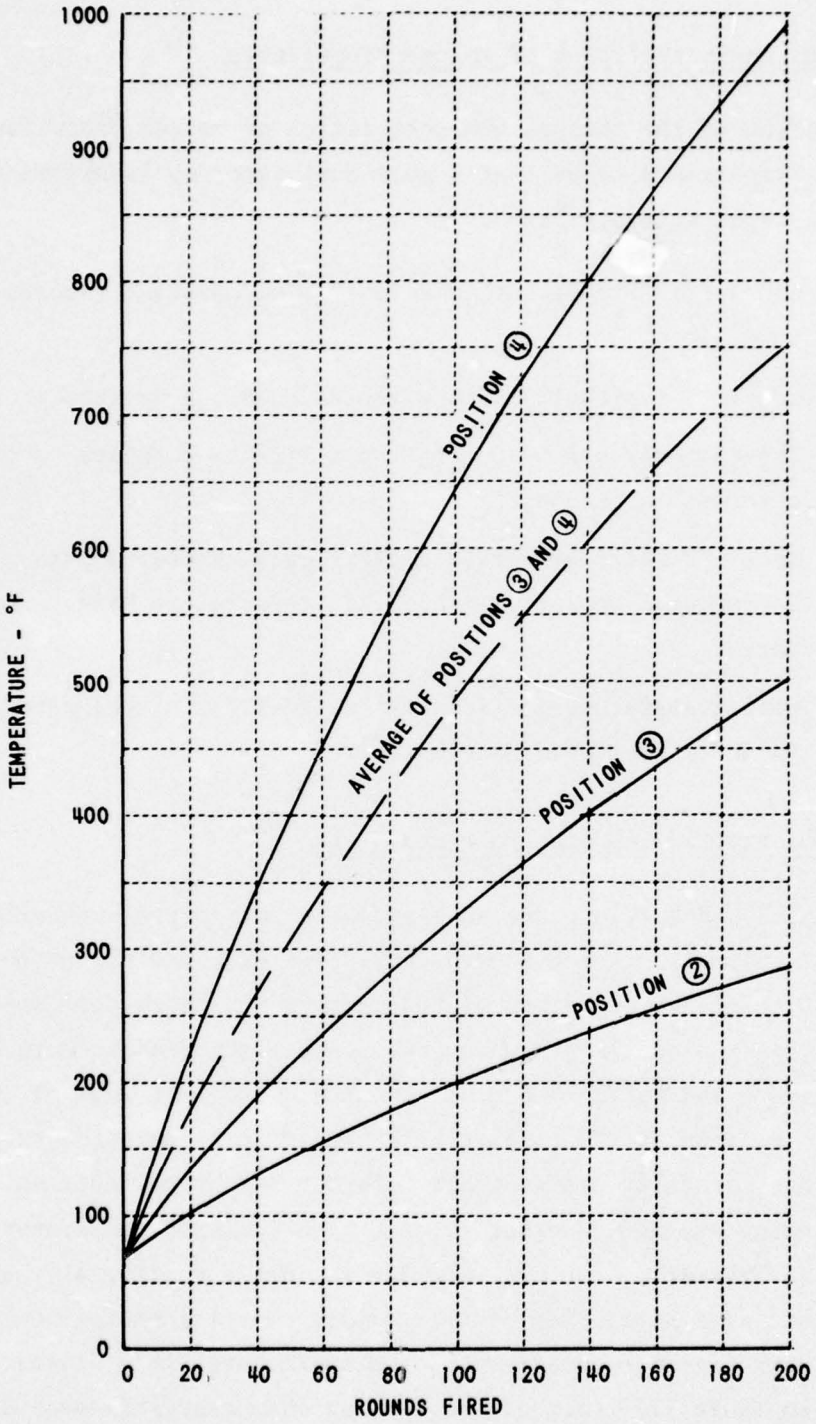

Figure 5 ESTIMATED EXTERNAL BARREL TEMPERATURES IN A SINGLE BURST OF AN M16 RIFLE

B. Thermal Characteristics of Molded Propellants

Evaluation of the thermal characteristics of molded propellants was conducted. The propellants to be tested were designated by Frankford Arsenal. Tests of several types were performed.

1. Contact of propellant to a controlled constant temperature plate.
2. Contact of propellant to a rapidly cooling surface.
3. Thermal evaluations during rapid fire of complete caseless cartridges.
4. Cook-off tests of complete cartridges chambered into a preheated essentially constant temperature Mann barrel.
5. Heat transfer evaluations of complete cartridges fired in an instrumented Mann barrel.

1. Controlled Temperature Plate Tests

Figures 6 and 7 illustrate cook-off data for several propellant types obtained using a controlled temperature plate. The data are presented in terms of cook-off time for any given plate temperature. Each test point was obtained by placing a propellant sample on a steel plate preheated to a measured temperature and noting the time at which propellant cook-off begins. Here cook-off is defined as the time at which rapid smoke emission began. It must be noted that generally, by contrast with the IMR propellants which flame at cook-off, flaming was not observed for the high ignition temperature propellants (HITP). Typically, the HITP would first begin melting at the contact surface, then at a later time, begin rapidly emitting smoke. Only in a few tests at very high temperatures did the smoke burst into flames. This is illustrated in Table II. Lack of the flaming characteristic made determination of specific cook-off time somewhat a matter of observer judgment, but the values obtained are believed adequate for purposes of comparison. Limiting cook-off temperatures appear to be as given in Table III.

TABLE II

INCIDENT OF FLAMES IN CONSTANT TEMPERATURE
PLATE COOK-OFF TESTS

Propellant	Approx. Plate Temperature, ^{O}F	No. of Tests	No. of tests Resulting in Flames
8602.1	840	8	3
8602.2	850	3	3
	820	1	1
	790	1	1
8603.1	840	4	4
GP-014	930	5	3
	870	1	1
	850	8	3
546-1	850	6	2

TABLE III

COOK-OFF THRESHOLDS ESTABLISHED
BY THE CONTROLLED TEMPERATURE PLATE TESTS

IMR 4227 - 4809	$375^{O}F$	
6090		
6145		
6151	$450^{O}F$	Picatinny Arsenal
6152		
6153		
546-1	$450^{+O}F$	Rocketdyne
GP-014	$500^{OO}F$	Thiokol
CASOL	$500^{O}F$	Rocketdyne
8602.1	$550^{O}F$	Hercules Powder Company
8602.2		
8603.1		

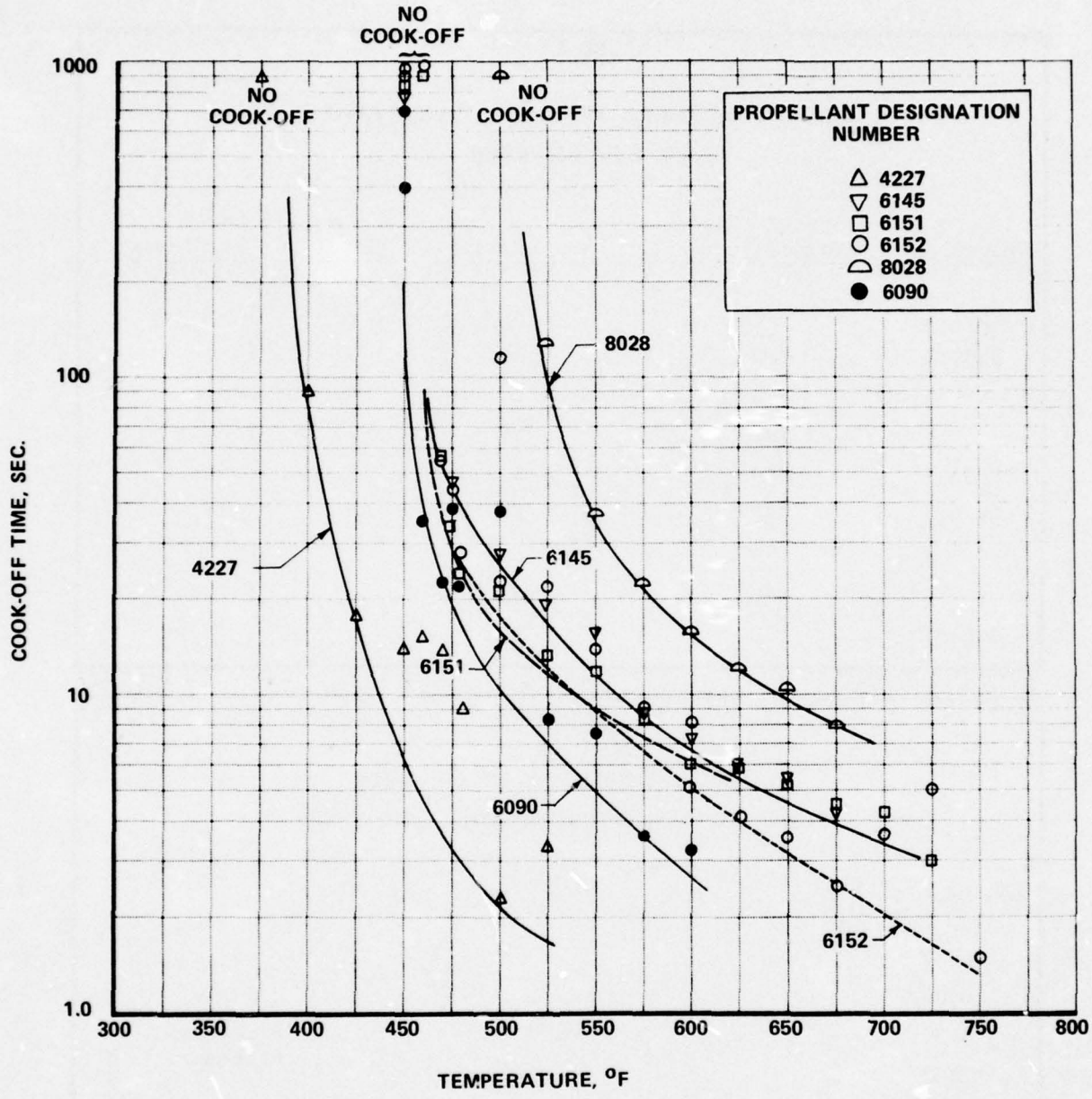

Figure 6 COOK-OFF TEMPERATURES ON CONSTANT TEMPERATURE STEEL PLATE, 5.56 MM PROPELLANTS

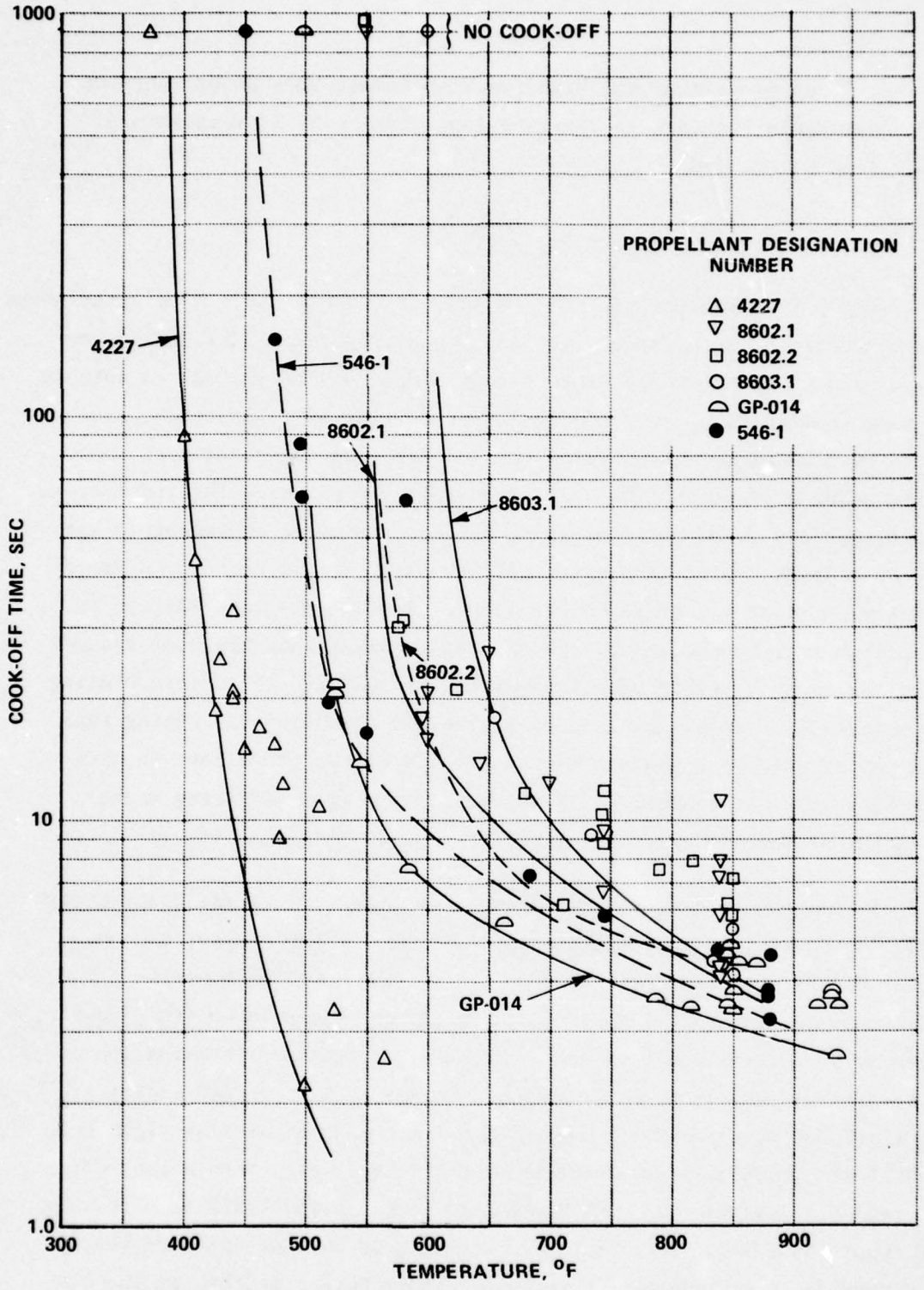

Figure 7 COOK-OFF TEMPERATURES ON CONSTANT TEMPERATURE STEEL PLATE, 5.56 MM PROPELLANTS

It is apparent that the high ignition temperature propellants provide some measurable increase in limiting long-time cook-off temperature level over that of the IMR.

2. Rapidly Cooling Surface Tests

Cook-off characteristics of IMR and various HITP were also established in tests conducted using a rapidly cooling contact surface. The device consists of a balance arm on which a propellant sample may be placed. A movable test surface containing a thermocouple, after heating by a gas torch, may be pivoted over the sample thus releasing a catch allowing contact of the propellant under a preestablished load (generally 50 grams). The temperature of the test surface is recorded on an oscilloscope via the thermocouple and the time of contact of the sample is indicated also on the scope by a microswitch which supplies a voltage to the scope. Because the test surface is heated at high rate by the torch, the thermal gradient thus produced induces rapid cooling of the surface upon removal of the source. This rapid cooling is representative of that which occurs within the chamber walls during rapid fire and can be used as a measure of the ability of the propellant to withstand contact with hot chamber walls in the early stages of firing where thermal gradients are severe.

In testing, one of several effects of high temperature contact may be noted, dependent upon the propellant, the contact temperature, or the cooling rate. First, there may be no effect on the propellant; second, the propellant may be discolored; third, some minor smoke may be emitted; fourth, there may be an initial surge of smoke followed by immediate termination of reaction; fifth, reaction might continue for a measurable period indicative of a cook-off but then terminate or quench; finally, the reaction might continue until all propellant is consumed which is here designated a cook-off. Table IV and V illustrate data obtained for several propellants at a cooling rate of about 150^{o}F/sec. As found in the long time controlled plate tests, the HITP provide some increase in cook-off temperature over that of the IMR.

TABLE IV
RESIDUAL TEMPERATURE COOK-OFF TESTS
(Surface Cooling Rate = 150° F/sec)

Propellant	Contact Temperature, °F	Result
IMR 4809	390	no effect
	450	slight smoke
	460	cook-off
	470	large smoke
	480	large smoke
	480	large smoke
	500	cook-off
	510	cook-off
	540	cook-off
	540	cook-off
	550	cook-off
	630	cook-off
HITP 6153	500	slight smoke
	580	large smoke
	630	large smoke
	670	cook-off
	740	cook-off
	740	cook-off
	800	cook-off
	860	cook-off
	880	cook-off
	1050	cook-off
HITP Casol	540	slight smoke
	580	large smoke
	630	quench
	670	quench
	690	quench
	760	cook-off
	800	cook-off
	840	cook-off
	900	cook-off
	930	cook-off
	930	cook-off
	1030	cook-off
HITP 8602.1	560	no effect
	580	no effect
	630	slight smoke
	630	slight smoke
	690	large smoke
	760	large smoke
	800	quench
	840	cook-off
	880	cook-off
	900	cook-off
HITP GP-014	770	slight smoke
	820	quench
	860	quench
	860	no effect
	870	quench
	880	quench
	930	cook-off
	930	cook-off
	950	cook-off
	950	cook-off
	990	cook-off

Table V

RESIDUAL TEMPERATURE COOK-OFF RESULTS

SURFACE COOLING RATE 150 ^{o}F/SEC

	Cook-Off Limit
IMR 4809	480 - 500^{o}F
6153	630 - 670^{o}F
CASOL	690 - 760^{o}F
8602.1	800 - 840^{o}F
GP-014	880 - 930^{o}F

It must be noted that the values in Tables IV and V apply most strictly to the cooling rate given, and will change somewhat for other cooling rates. The variation is, however, not great and therefore one expects that the order of grouping will not change with other cooling rates.

3. Firing Tests

Thermal evaluations of 5.56mm caseless ammunition during rapid fire were conducted using a test fixture supplied by Rock Island Arsenal and subsequently modified by Calspan to represent as closely as possible the M16 barrel configuration in the vicinity of the breech. The fixture was instrumented with several barrel thermocouples at the locations shown in Figure 8. Rapid fire operation of the fixture is produced by direct action of the chamber propellant gases on the firing pin and bolt face. As these gases act on the firing pin, the pin is forced rearward initiating bolt unlock through bolt rotation. Once the bolt is unlocked, breech pressure acting on the bolt face accelerates the bolt rearward compressing a driving spring which then stores sufficient energy to perform the functions of round stripping, chambering, bolt locking, and firing pin strike in the next cycle. The rate of fire is governed by the bolt mass, drive spring force constant, and buffer spring action and position. The approximate average firing rate for the fixture as assembled for the rapid fire tests was 600 rds/min, but a

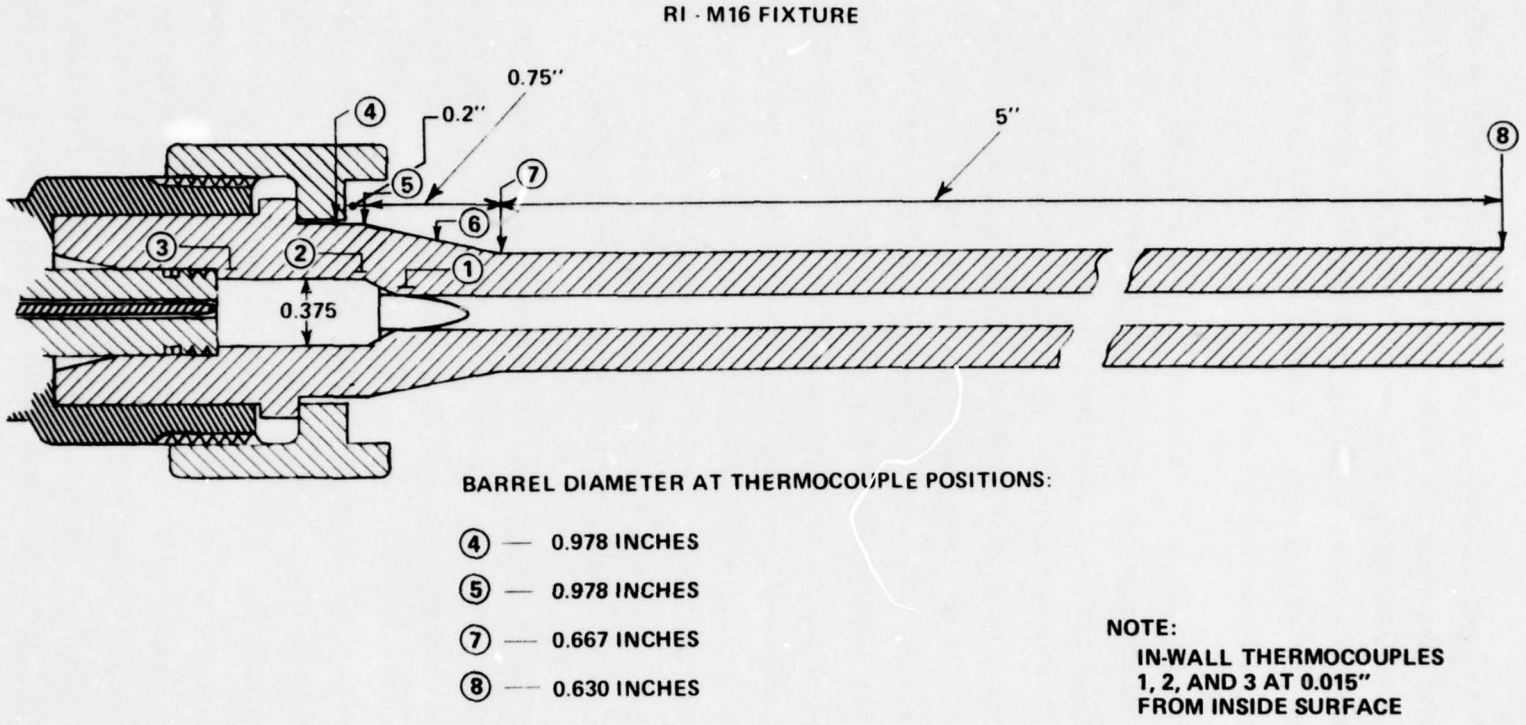

Figure 8 ROCK ISLAND BARREL MODIFIED TO M16 CONFIGURATION SHOWING IN-WALL AND EXTERNAL THERMOCOUPLE POSITIONS

special air actuated trigger release mechanism allowed reduction of effective rate of fire if desired for specific tests. Testing with this fixture was to be for the purpose of establishing chamber and barrel temperatures in rapid fire as well as to expose factors relating to ammunition performance in rapid fire conditions. For the firing tests, a magazine capable of containing up to 60 rounds was designed and fabricated.

Several short bursts of ammunition molded from IMR 4809 and supplied by Frankford Arsenal were made including a forty-round burst at 600 rounds/min. External barrel temperatures were recorded, and the average chamber temperatures were taken as the peak external temperature after each burst. Figure 9 shows the average temperature rise at each thermocouple location as a function of burst length. It has previously been established (Table III) that average temperatures near 375^{o}F are needed to produce cook-off of this propellant. Clearly, the average temperatures are insufficient to initiate a cook-off of this propellant in forty rounds. Extrapolation of the average temperature data, specifically for position No. 5 where intimate propellant contact is possible, indicates this chamber configuration to be capable of firing at least 80 rounds without cook-off initiated by excessive average temperature. An unprimed round, the last round of the forty round complement was, however, found to discharge within 0.8 sec after loading.

Thermal gradients measured in subsequent testing were found to be insufficient to account for this observed cook-off and it is postulated that the cook-off was due to excessive bolt face temperature. This is supported by recorded chamber temperatures as shown in Figure 10, which illustrates both weapon action and measured chamber wall temperature at the rear chamber position. Ignition delays on the second, seventh, thirteenth, and seventeenth rounds of a 20 round burst are clearly illustrated in Figure 10. Characteristically, each delay is preceded by an immediate primer ignition which is indicated by a slight increase of chamber wall temperature. This is followed by a variable delay period in which some propellant burning occurs, with increasing temperature and pressure. Finally, the main charge is ignited. Ignition delays of up to 0.35 sec are evident. The total time to fire 20 rounds is about 3.33

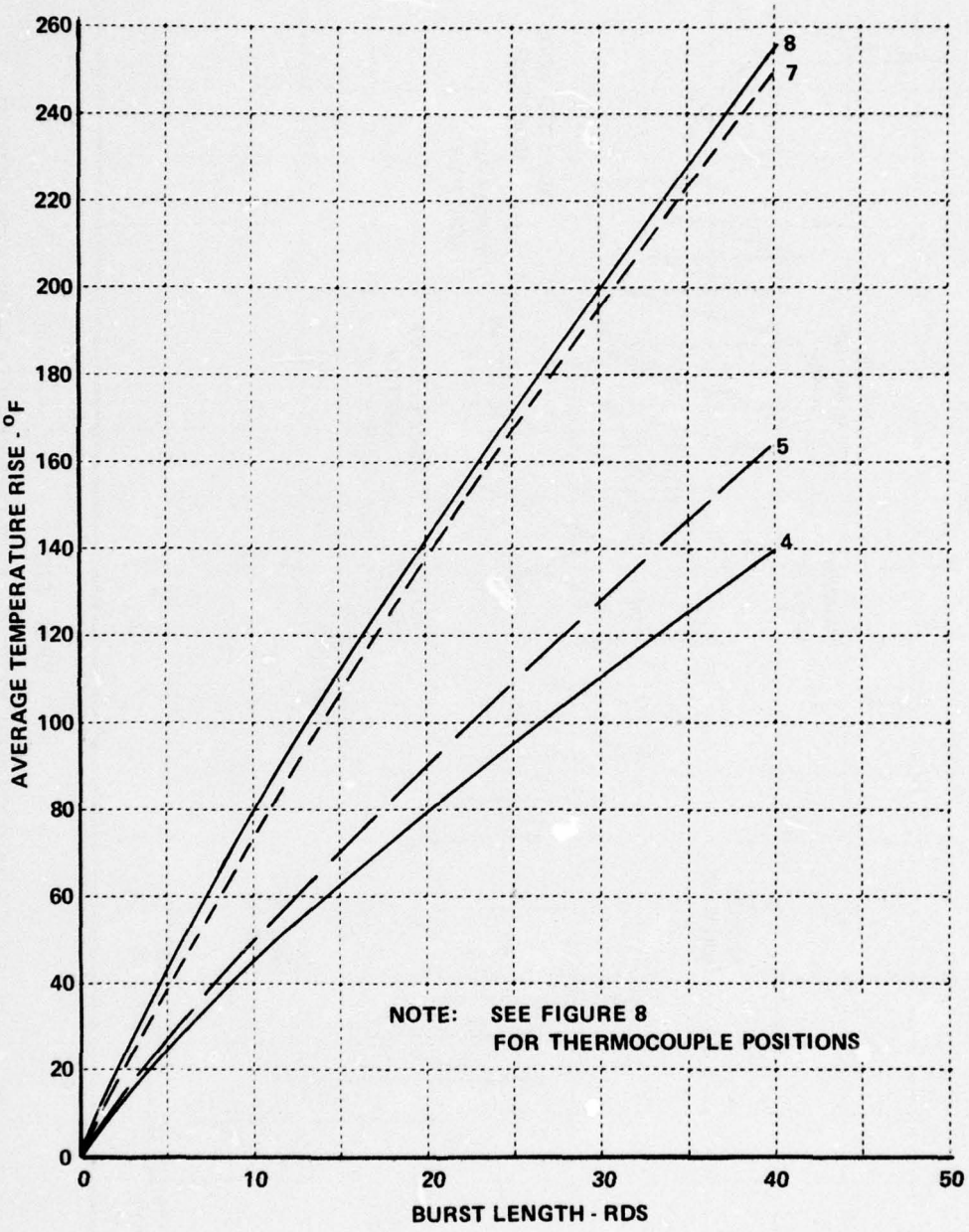

Figure 9 AVERAGE TEMPERATURE RISE VS BURST LENGTH (RI-M16 CASELESS FIXTURE)

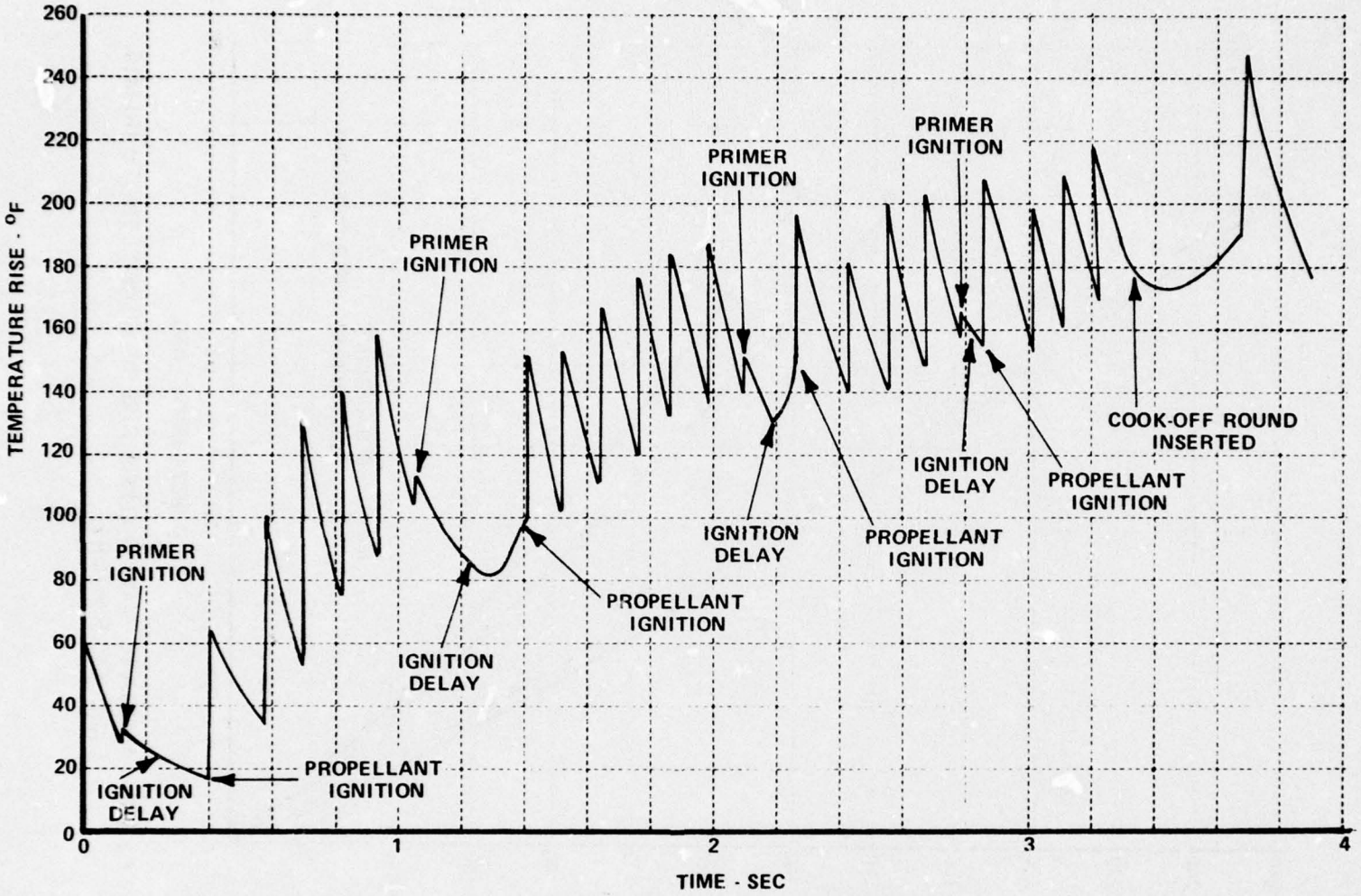

Figure 10 IN-WALL TEMPERATURES AT THE REAR CHAMBER DURING A 20 ROUND BURST (RI-M16 FIXTURE)

sec, indicating an average rate of 360 rounds/min. Excluding the rounds showing firing delays, the rate is about 520 rounds/min.

In the twenty round burst, the maximum residual rear chamber wall temperature rise is only 180°F. This is much below the cook-off threshold of the propellant. Nevertheless, the unprimed cook-off round inserted immediately upon termination of the twenty round burst was found to discharge within 0.4 sec after insertion. In fact, the rear chamber temperature indicates burning of the propellant within 0.1 sec after insertion. Because there was no primer in the cook-off round, no initial jump in wall temperature is observed, but a definite increase in chamber temperature is shown prior to discharge of this round.

The location of initial propellant ignition is interpreted to be in the vicinity of the rear chamber, because only the rear chamber temperature was found to increase prior to discharge. Temperatures recorded at the stop-shoulder and neck showed no measurable increase in this period. Their maximum residual temperature rises were 150 and 212°F respectively.

The propellant cook-off is believed to be initiated by excessive temperatures near the base of the round. The chamber wall temperature in this vicinity is not sufficient to initiate cook-off. Thus, one concludes that either the bolt or bolt parts (seal rings or firing pin) are initiating cook-off. Although the firing pin is expected to be hot enough, it does not contact combustible material in the unprimed round, but radiation from the pin might be a source of ignition. The piston rings used as a seal and the sides of the bolt contact the propellant while the bolt is moving rearward, as does the bolt face as the bolt moves forward.

A thermocouple probe was constructed and placed in a manner which would allow contact with the seal rings or the sides of the bolt when the bolt was held in its rearward position by the trigger. The thermocouple probe was spring loaded and retained by a pin such that at any desired time the probe could be released to contact a seal or the bolt. In several single-shot

firings, seal temperatures in excess of 75°F were observed, as well as average bolt temperatures in excess of 15°F at the seal location. Based on these measurements, it is conceivable that the seal temperature could have exceeded 1000°F in the twenty round burst. In addition, average bolt temperatures greater than 370°F would be expected. The maximum seal and/or bolt temperatures are difficult to assess based on these measurements but there is little doubt that either could produce rapid ignition of the propellant in a twenty round burst.

Recalling that cyclic action in this fixture is produced by chamber pressure acting on the face of the bolt, one can readily understand the excessive bolt temperatures experienced. In this action, considerable propellant gas leakage around the bolt may be obtained as the bolt moves rearward and opens. This low pressure, but very hot, gas can transfer much of its energy to the bolt and seal rings. It is evident that the weapon action to be used for rapid fire of caseless ammunition must be carefully selected to avoid generation of local hot spots which can diminish the burst length capability of the total caseless system. That extended burst capability from a thermal standpoint can be obtained using an appropriate mechanism is clearly demonstrated by the temperature data obtained in the rapid fire tests where both average chamber temperatures and chamber thermal gradients are shown insufficient to produce cook-off in multiple 20 round bursts up to 80 rounds (see Section III B-6).

Firing pin heating and firing pin temperatures required for cook-off were also determined. A single-shot 5.56mm caseless fixture was utilized for the firing pin heating tests. A special firing pin with the tip made as shown in Figure 11 was used for measuring the heat input. The temperature rise of the copper tip as indicated by the internal thermocouple is proportional to the heat input.

Propellant gas leakage around the firing pin was varied by enlarging the clearance hole through which the pin passes. The leakage was varied from no leak by virtue of an o-ring seal (verified by paper witnesses) to the leak through a 0.003 in. clearance (0.006 in. on the diameter). The results of these tests are shown in Figure 12. A total of 16 tests were conducted. The

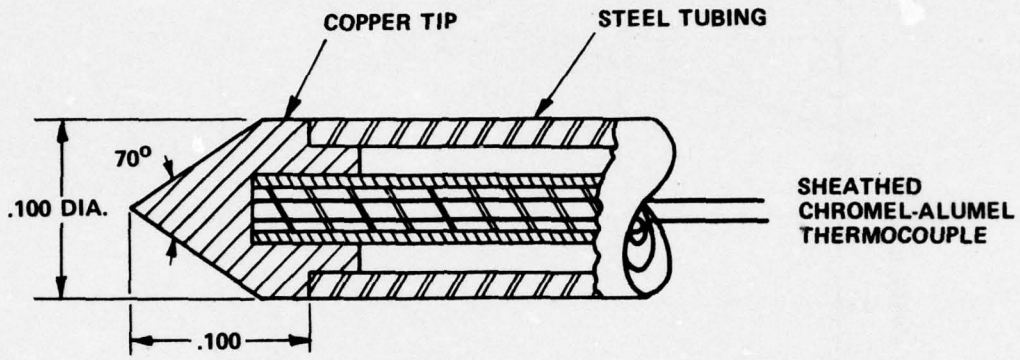

Figure 11 FIRING PIN FOR DETERMINING HEAT INPUT

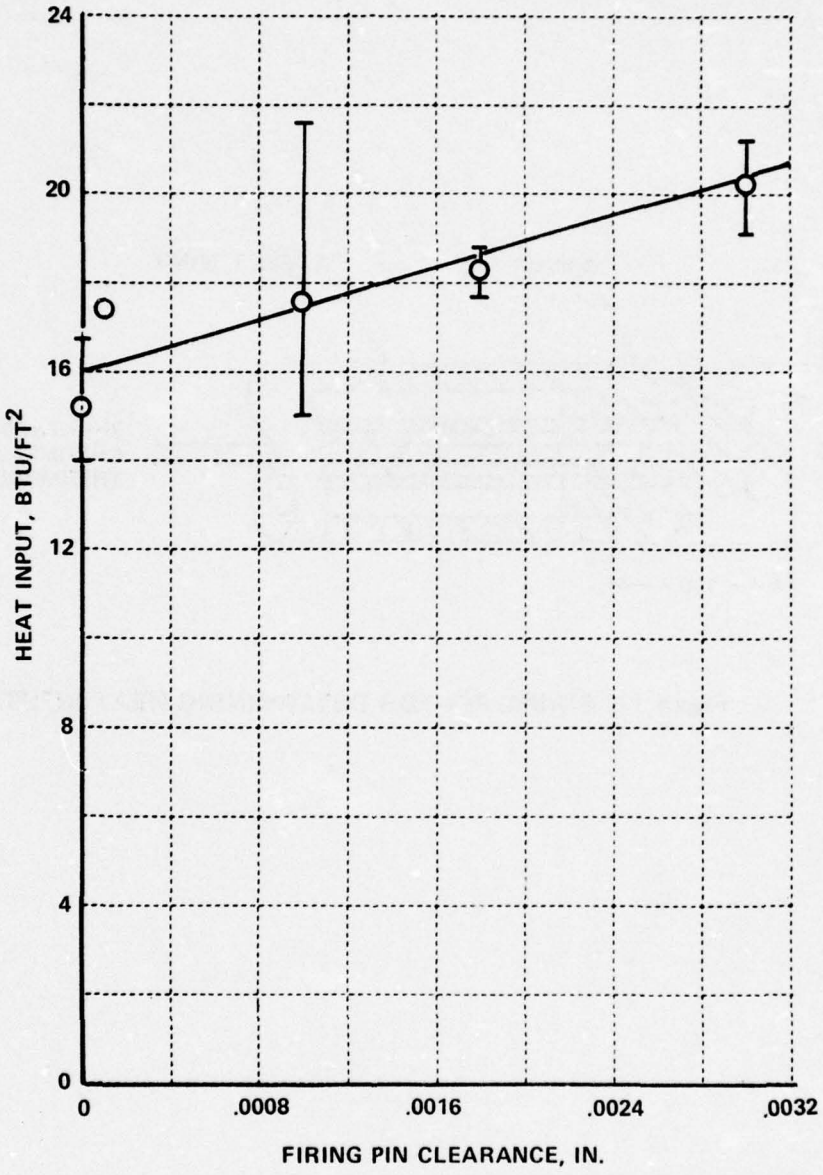

Figure 12 FIRING PIN HEATING, 5.56 MM CASELESS AMMUNITION

points on the figure represent the averages at each clearance. Although there is considerable scatter in the results, indications are that there is some increase in heat input for increased firing pin clearance (increased leakage). The single-shot temperatures were very high. The minimum average temperature rise was 173°F and the maximum was 233°F in single shots. Because these temperatures are relatively insensitive to pin material, steel firing pin temperatures would be of the same order.

The temperature of the firing pin during a burst can be calculated for determination of its cook-off potential. The heat input is about 18 Btu/ft^2 (Figure 12). The equilibrium temperature (the temperature that would be reached after a very long burst with no heat loses, i.e. at zero heat input) can be assumed to be the same as in the chamber, 2630°F (Reference 2). The heat input at ambient initial temperature and the equilibrium temperature determine the straight line variation of heat input per round as a function of firing pin temperature at the beginning of each shot. Temperature rise of the firing pin per shot is directly proportional to the heat input per shot. Therefore, knowing the heat input per shot as a function of pin temperature, the pin temperature was calculated by an iterative procedure. The result is shown in Figure 13. The firing pin temperature reaches very high values before 20 rounds are fired.

Cook-off through contact of a hot firing pin to the propellant is not a hazardous situation, inasmuch as contact of the pin in any event should be at a force sufficient to ignite the round through the primer. A problem could arise, however, if cook-off of the propellant could occur without contact of the pin. A simple test device was constructed to assess this possibility. It consisted of a 0.106 in. diameter rod, simulating a firing pin and containing a thermocouple, heated with a gas flame to various test temperatures and then inserted into a 0.120 in. diameter hole to a set distance from a disc of molded propellant at the other end of the hole. It was observed whether or not the propellant ignited as evidenced by smoke and flames, whether or not the ignition continued until the propellant was completely consumed, and the time of the initial ignition. The test was repeated for variations of propellant type, firing pin temperature, and distance between firing pin and propellant

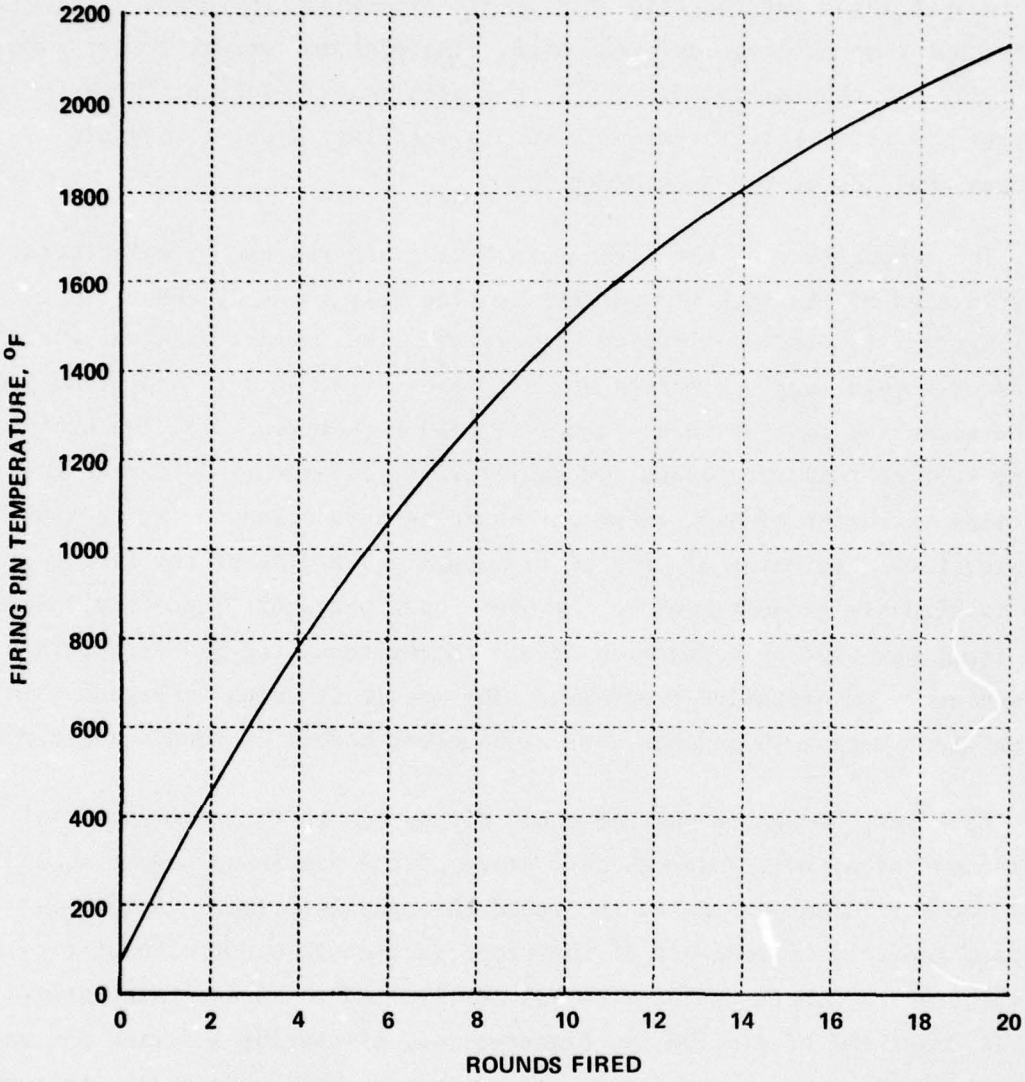

Figure 13 CALCULATED FIRING PIN TEMPERATURE DURING BURST OF 5.56 MM CASELESS AMMUNITION

until the conditions necessary to cause cook-off were delineated. The results are shown in Figure 14. Both IMR 4809 propellant and WC 870 ball propellant exhibited nearly the same relationship for cook-off, as shown in the figure. However, if the WC 870 propellant ignited, it continued burning until it was all consumed, whereas the IMR 4809 stopped burning. In all cases, if ignition occurred, it was within 2 sec after firing pin insertion. At temperatures above the minimums required for cook-off, the cook-off time decreased; but these measurements were not sufficiently definitive to determine the relations between temperature and time.

To prevent cook-off from the hot firing pin, the pin must be recessed away from the caseless propellant. Combining Figure 14 with Figure 13, the required distance between the firing pin and the propellant as a function of number of rounds fired can be determined as shown in Figure 15. For 20 rounds fired in a single burst, at least 0.053 in. between the firing pin and caseless propellant is required to prevent cook-off by radiation from the pin.

It must be emphasized that an appropriate firing fixture has yet to be established to fully exploit the benefits of caseless ammunition. Certainly, means must be sought by which local hot spots may be avoided, while at the same time providing the needed cyclic actions of loading and firing. One cannot stress too greatly the importance of minimizing contact of propellant to excessively heated parts.

4. Cook-Off Tests

Cook-off tests of complete rounds made using high ignition temperature propellant (HITP) were conducted. For these tests, a device was constructed which would insert a round (lacking a primer) into a preheated chamber. The device would then lock the breech (using a screw thread lock). Chamber temperatures were recorded using in-wall thermocouples. Although for safety purposes, chamber heating was discontinued immediately prior to insertion of the round, the relatively large mass of the chamber restricted the chamber

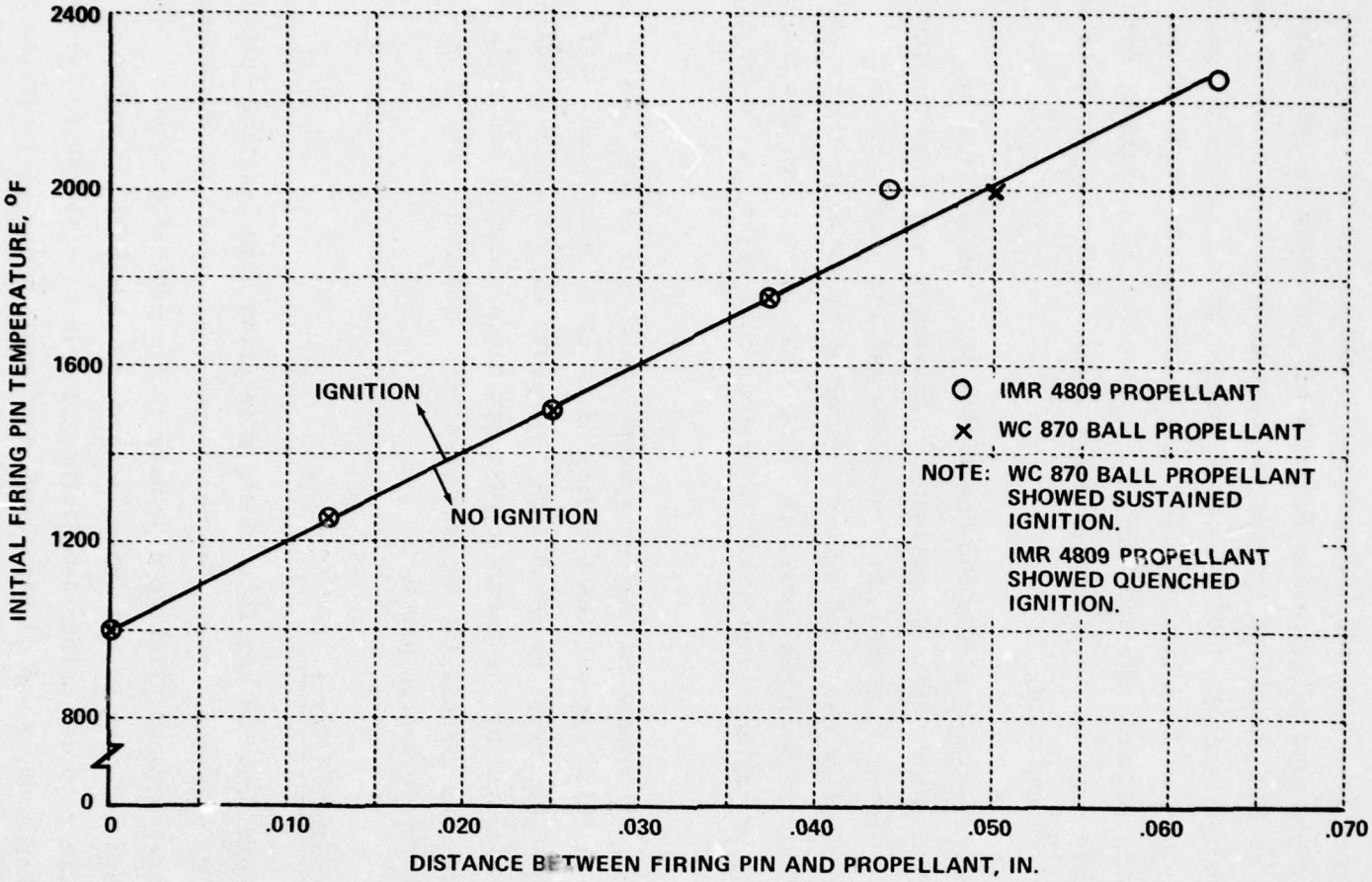

Figure 14 INITIAL FIRING PIN TEMPERATURE REQUIRED TO COOKOFF PROPELLANT AS A FUNCTION OF DISTANCE BETWEEN FIRING PIN AND PROPELLANT

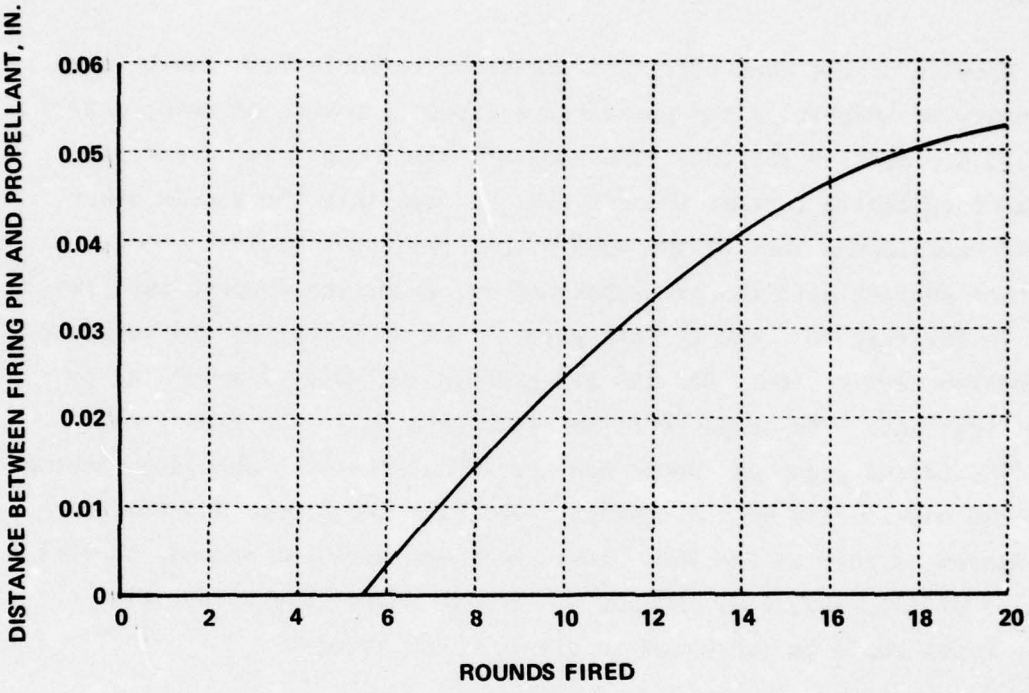

Figure 15 DISTANCE BETWEEN FIRING PIN AND PROPELLANT REQUIRED TO PREVENT COOKOFF IN A BURST OF 5.56 MM CASELESS AMMUNITION

cooling to less than 20°F/min, providing essentially a constant temperature chamber during the tests. Time-to-cook-off was sufficiently long that a stop watch could be used. Where smoke was found to be liberated at the muzzle prior to cook-off (indicated by sound), the approximate time of this occurrence was also noted.

Results of the cook-off tests are shown in Table VI. Due to the limited supply of ammunition for these tests (about 5 rounds of each) only a rather brief exploration for long time cook-off limit could be performed. Testing was complicated further when it was observed that the rounds other than GP-014 contained a core of IMR 4227 propellant which could be cooked off by either contact with the stop-shoulder or conduction through the propellant. To investigate these effects several modifications of the supplied ammunition also were tested. Results are grouped in Table VI according to these modifications. The complete rounds were as supplied by Frankford Arsenal. The second group of rounds had the IMR at the stop-shoulder machined to reduce the possibility of IMR contact. The last two groups had the projectile altered as well as the IMR. Tests were conducted at nominal chamber temperatures of 450, 500, 550, and 600°F. Due to short supply, not all ammunition types could be subjected to all test conditions.

While the cook-off test results are masked somewhat by the possible effects of the IMR substrate, it appears, as indicated in the controlled temperature plate tests, that some increase in long time cook-off temperature limit is afforded by use of HITP. The increase is up to 125°F depending upon propellant type. The results appear to confirm generally the results of plate tests. Because the plate tests were not obscured by the presence of lower cook-off temperature IMR propellant, it would appear best to use that data in comparisons of cook-off sensitivity.

5. Heat Transfer Evaluations

Chamber heating during firing of complete rounds was also obtained using an instrumented Mann barrel. Heat input was determined using in-wall

Table VI
5.56MM HITP COOK-OFF TEST RESULTS

ROUND CONFIGURATION	CASELESS ROUND TYPE	TEST NO.	CHAMBER TEMP. AT INSERTION, °F	COOK-OFF TIME, sec.	FIRST SMOKE, sec.	PROJECTILE VELOCITY, ft/sec.	RESIDUE***
COMPLETE ROUND	IMR (PL15)	1	585	1.6	–	2510	NONE
	IMR 4809	2	590	< 1	–	2880	NONE
	HITP 6153	4	590	4.9	< 3	1660	LARGE PIECES IN BARREL
	HITP CASOL	5	590	2.8	< 2	1680	SOME STUCK TO CHAMBER
	HITP 8602.1	3	590	9.7	–	1820	NONE
	HITP GP-014	6	590	6.0	NONE	2130	LARGE PIECE IN BARREL, GUMMY RESIDUE IN CHAMBER
	HITP GP-014	12	550	28.2	NONE	1080	ASH NEARLY SIZE OF ORIGINAL PROPELLANT
	IMR 4809	11	500	8.0	NONE	3050	NONE
	HITP 6153	9	500	7.0	6	1900	NONE
	HITP CASOL	8	500	1.2	NONE	2040	VERY SLIGHT AMT.
	HITP 8602.1	10	500	21.4	20	2230	VERY SLIGHT AMT.
	HITP GP-014	7	490	∞	NONE	–	RD. DISCOLORED
	IMR 4809	21	450	21.2	NONE	3120	VERY SMALL AMT. OF POWDER
IMR AT STOP-SHOULDER MACHINED*	HITP 6153	13	600	2.2	2	820	LARGE AMT. OF GUMMY RESIDUE
	HITP CASOL	15	600	2.9	2	1740	SMALL AMT. OF GUMMY RESIDUE
	HITP 8602.1	14	600	5.5	NONE	1680	SMALL AMT. OF GUMMY RESIDUE
	HITP 6153	18	450	26.0	NONE	2700	SMALL AMT. OF POWDER
	HITP CASOL	20	450	24.0	NONE	2140	SMALL AMT. OF WHITE POWDER
	HITP 8602.1	19	450	36.0	NONE	2870	PIECE IN BARREL, SMALL AMT. OF POWDER IN CHAMBER
IMR AT STOP-SHOULDER MACHINED AND PROJECTILE REPLACED W/WOOD	HITP 8602.1	16	500	SMOKE ONLY	12	–	LARGE AMT. OF BOTH ASH AND GUMMY RESIDUE
IMR AT STOP-SHOULDER MACHINED AND PROJECTILE MACHINED TO PREVENT CONTACT W/BARREL**	HITP 6153	17	500	10.4	8	1960	SMALL AMT. OF GUMMY RESIDUE
	HITP 6153	22	450	15.0	12	520	LARGE AMT. OF GUMMY RESIDUE IN CHAMBER AND BARREL

* AS RECEIVED, THE HITP ROUNDS (EXCEPT HITP GP-014) WERE APPROXIMATELY OF THE FOLLOWING CONFIGURATION:

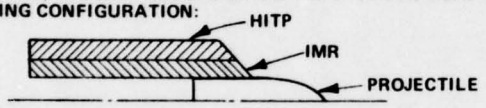

AFTER MACHINING, THE CONFIGURATION WAS AS FOLLOWS:

** THE PROJECTILE WAS CUT OFF 0.03 IN. FROM THE END OF THE PROPELLANT AND THE REMAINING PROTRUDING PROJECTILE WAS REDUCED IN DIAMETER BY 0.02 IN.

*** UNLESS OTHERWISE NOTED, ALL RESIDUE WAS LOCATED IN THE CHAMBER.

thermocouples located within 0.015 in. from the inside wall surface at the rear chamber, mid-chamber, front chamber and neck areas of the barrel. Appendix B explains the techniques required for calculation of heat input from in-wall thermocouple measurements. In addition, chamber pressure and projectile velocity were measured and the amount of residue remaining within the fixture was observed for each shot. Chamber pressure was determined through the use of a piezoelectric pressure transducer and projectile velocity through conductive grid paper velocity screens. Data are presented in Table VII. The groupings are by type of ammunition. The residue results are essentially qualitative but serve also to indicate magnitude of residue. The presence of ignition delay was inferred from the pressure-time data. If the pressure rose initially, then decreased followed by rapid rise to its peak value, an ignition delay was said to have occurred. The amount of pressure decrease was also noted.

Typically, the heat input from the HITP rounds is lower than that of the IMR rounds. The heat inputs from the Casol rounds were particularly low. The generally lower projectile velocities and increased residue of the HITP rounds are both indicative of incomplete burning and may partially account for the reduced heat input. Residue can act as a barrier to heat flow to the chamber walls thus lowering the net heat input. That observed for the Casol being well stuck to the chamber walls would be especially effective. For proper weapon functioning, however, it is desirable that no residue be produced. Elimination of residue for the propellants tested might well be expected to produce an increase in chamber heating. For this reason, the heat transfer data obtained must be viewed in this light, with conclusions regarding heat transfer taken to represent only the present state of development.

Estimates of the number of rounds of each propellant type which may be fired without cook-off were made based upon measured heat input and cook-off data. It must be realized that the large amounts of residue noted for certain of the HITP makes this assessment necessarily tentative and the ranking thus produced not necessarily representative of propellant acceptability. In general, the utilization of the actual measured heating data

Table VII

5.56 MM HITP FIRING TEST RESULTS

CASELESS ROUND TYPE	TEST NO.	HEAT INPUT, Btu/ft^2				PEAK PRESSURE, psi	PROJECTILE VELOCITY, ft/sec	RESIDUE*	IGNITION DELAY?	PRESSURE DROP AFTER IGNITION, psi***
		REAR CHAMBER	MID-CHAMBER	FRONT CHAMBER	NECK					
IMR (PL15)	1	–	13	14	16	72,500	3180	NONE	NO	–
	2	12	13	14	16	75,500	3240	NONE	YES	1500
	3	12	12	13	16	–	3180	NONE	–	–
	4	11	11	13	16	63,500	3110	NONE	–	–
	5	9	12	11	20	68,000	3150	NONE	–	–
	6	9	13	12	20	59,000	3080	NONE	NO	–
	7	11	12	12	20	60,000	3070	NONE	YES	1500
	13	10	11	12	20	78,000	3450	NONE	YES	4500
IMR 4809	8	8	11	12	20	68,500	3220	NONE	YES**	4500
	14	9	12	12	21	74,000	3330	NONE	YES**	1000
	19	7	10	14	20	36,000	2790	NONE	YES**	1500
HITP 6153	9	8	8	8	19	38,000	2450	SMALL AMT.	NO	–
	18	7	7	7	16	48,000	2670	MODERATELY LARGE AMT.	YES	4500
	20	5	8	10	16	47,000	2640	LARGE AMT.	YES	4500
HITP CASOL	10	5	4	2	15	59,000	2600	STUCK TO WALL AND POWDER	YES	2000
	17	4	3	4	15	54,000	2530	LARGE AMT. STUCK TO WALL	YES	3000
	21	5	3	6	14	51,000	2580	LARGE AMT. NEARLY COATING ALL OF CHAMBER	YES	3000
HITP 8602.1	11	8	12	12	23	48,000	2850	SMALL PIECES IN BARREL, SMALL AMT. OF POWDER IN CHAMBER	YES	500
	16	10	11	15	23	68,000	3180	SMALL PIECES	YES	6000
	22	8	10	12	23	59,000	3040	VERY SMALL AMT.	YES	3000
HITP GP-014	12	7	6	7	16	–	2720	LARGE PIECES	–	–
	15	7	8	7	19	62,000	2520	LARGE PIECES	YES	9000
	23	8	9	12	18	74,000	2720	LARGE PIECES	–	–

*UNLESS OTHERWISE NOTED, ALL RESIDUE WAS LOCATED IN THE CHAMBER.

**VERY SHARP SPIKE IN PRESSURE CURVE AT BEGINNING OF IGNITION.

***REPORTED VALUES ARE FOR ROUNDS WITH IGNITION DELAYS. PRESSURE ROSE INITIALLY, THEN DECREASED, THEN ROSE TO ITS PEAK VALUE. THE AMOUNT OF DECREASE IS THE VALUE REPORTED IN THIS COLUMN.

without account for insulating effects of residue leads to a maximizing of the allowable burst length for each propellant. The extent of increase is not the same for each, however; and elimination of residue might well change the order of ranking thus indicated.

Cook-off limit also depends upon the particular weapon being considered chiefly because of differences in mass in the chamber area available for absorbing heat. Computations of allowable burst length were made using the Rock Island-M16 5.56mm caseless fixture firing at 600 round/min inasmuch as prior data regarding this fixture are available, and it represents a typical 5.56mm rifle for which comparative estimates can be meaningful. Resulting estimates are shown in Table VIII. Two types of cook-off are considered and are designated: 1) short-time and 2) long-time cook-off. Short-time cook-off is initiated prior to relieving of the thermal gradients within the chamber wall and is a function of the residual chamber surface temperature at the time of initial propellant contact. Long-time cook-off is primarily a function of the average chamber temperature. Since residual and average temperature rises are approximately proportional to heat input and these are given for each propellant by the test data, comparative temperatures during a burst of the Rock Island-M16 caseless rifle can be calculated for each propellant type. The number of rounds which can be fired are then determined by reference to previous cook-off temperature evaluations. In the long-time cook-off evaluations, consideration was given to cook-off: 1) with and 2) without projectile heating effects. Computations as shown in Table VIII indicate substantial increase in allowable burst length using HITP compared with IMR. This is especially evident in the short-time cook-off limits where as many as three times as many rounds can be fired prior to cook-off conditions. Long time cook-off estimates suggest more than a twofold increase using HITP. Again, one is cautioned against strict use of the allowable burst length values as a ranking of the particular propellants because of the existence of residue.

6. Temperature Predictions

Heat transfer rates as they influence weapon temperatures have direct bearing upon both weapon design and effectiveness of the weapon system.

TABLE VIII

COMPARATIVE 5.56 MM HITP AND IMR COOK-OFF DATA*

Propellant	Stop-Shoulder Heat Input, Btu/Ft^2	SHORT-TIME COOK-OFF		LONG-TIME COOK-OFF			
				With Projectile Heating		Without Projectile Heating	
		Cook-off Temperature, ^oF	Allowable Burst Length Rds	Cook-off Temperature ^oF	Allowable Burst Length Rds	Cook-off Temperature ^oF	Allowable Burst Length Rds
IMR	16	480	75	375	80	375	80
HITP 6153	12	630	160	~425	125	450	130
HITP Casol	10	690	230	~425	150	500	185
HITP 8602.1	18	800	140	~425	80	550	110
HITP-GP-014	13	880	230	500	140	500	140

*Computed for Rock Island - M16 Caseless Fixture at 600 rd/min firing rate, 70^{o}F initial temperature

Weapon temperature effects are especially important where caseless ammunition is to be utilized. It has been shown that both cased and caseless ammunition are subject to cook-off given sufficient burst length. For caseless ammunition, chamber wall temperatures can produce thermally initiated ignition in extremely short periods (within milliseconds) if little regard is given to heat transfer factors in weapon and/or ammunition design. Optimization of weapon-ammunition design will be aided substantially by the availability of a suitable model which predicts weapon temperatures during rapid fire.

In Calspan's work, some effort was devoted to the development and test of a mathematical model which can predict chamber and barrel temperatures in rapid fire. For this development, it has been regarded most accurate and efficient to evaluate prime heat transfer parameters by a combined experimental-analytical approach and to determine temperatures through computer simulation of rapid-fire conditions. The total mathematical model consists of two parts. The first provides mathematical anlaysis of experimentally obtained data to formulate generalized heat transfer parameters for use in temperature computations. The second applies these parameters in simulated rapid fire conditions with resulting chamber and barrel temperatures. To allow general applicability, the two parts are not directly linked in a single computer routine. Hence, either part may be utilized without need of the other. Detailed description of the computer routines derived through this effort is given in Appendix A.

As an example of accuracy, Figure 16 shows a comparison of computed temperatures with measured values in the vicinity of the stop-shoulder during a 5 round burst of the Rock Island caseless fixture. It is evident that the computer provides excellent prediction capability for use in weapon design. One possible utilization of the computer in design evaluation is illustrated in Figure 17 where the effect of firing rate on residual chamber temperature is explored for the RI-M16 caseless configuration. Results indicate that temperatures are much below the cook-off threshold of IMR 4809 ammunition in a 20-round burst even at a firing rate of 900 rounds/min.

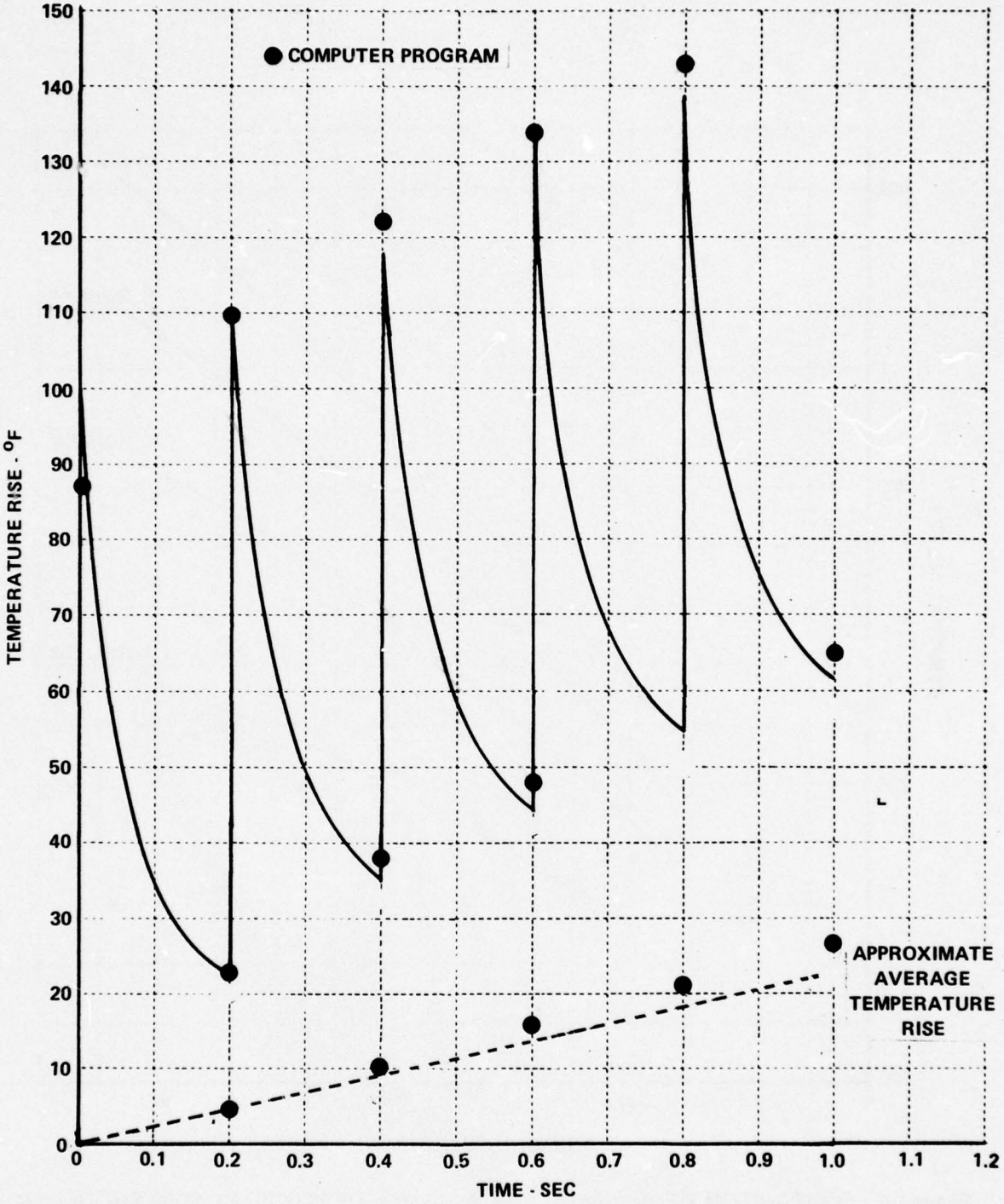

Figure 16 MEASURED AND COMPUTED TEMPERATURES AFT OF THE STOP SHOULDER DURING 5 ROUND BURST AT 300 RDS/MIN, ROCK ISLAND 5.56 MM CASELESS FIXTURE

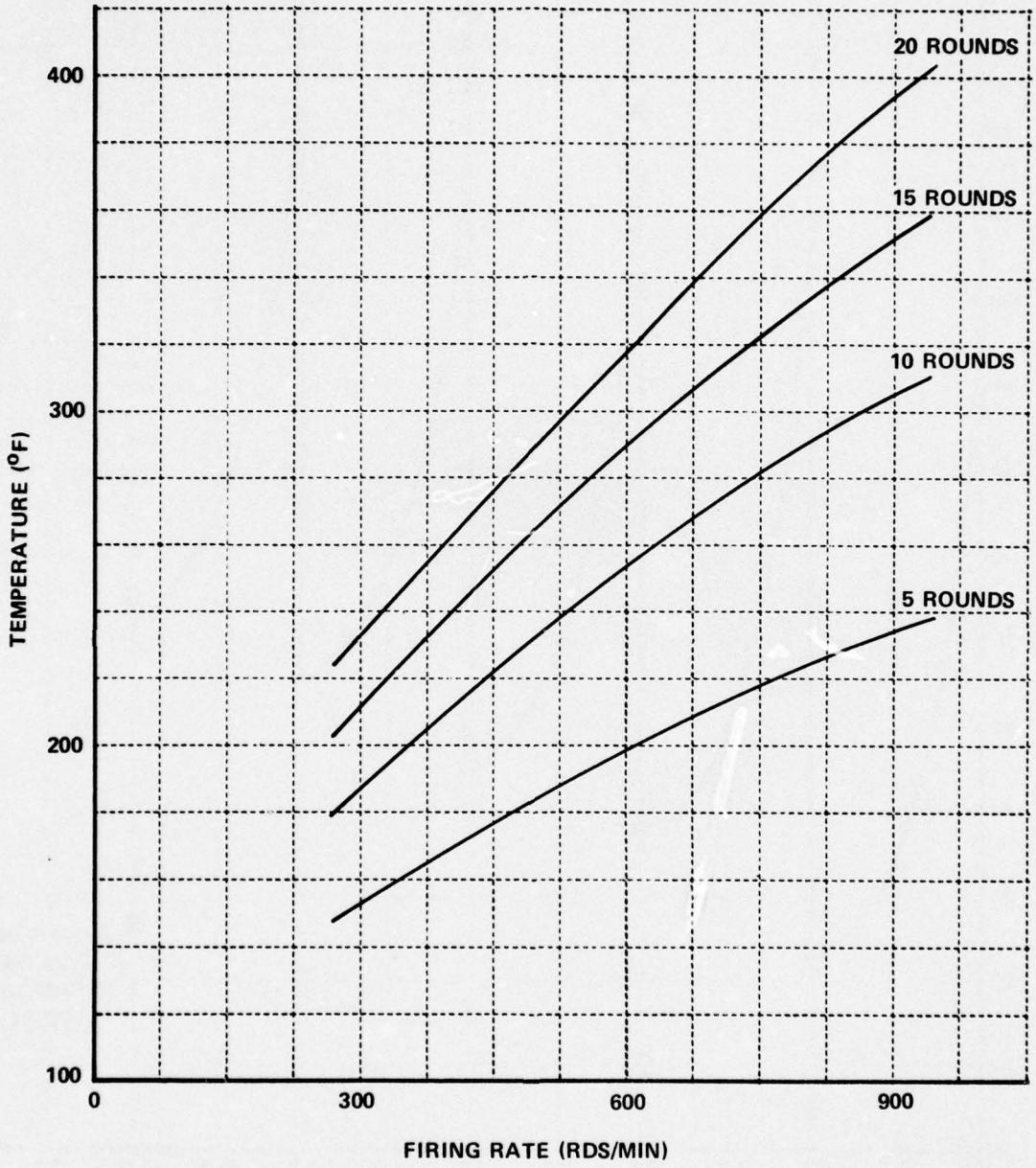

Figure 17 COMPARISON OF RESIDUAL IN-WALL TEMPERATURE AT STOP SHOULDER AS A FUNCTION OF FIRING RATE AND NUMBER OF ROUNDS FIRED (R1-M16 CASELESS FIXTURE)

Further, at 600 rounds/min firing rate, computed temperatures indicate that about 80 rounds may be fired without cook-off due to residual chamber temperature near the stop-shoulder. This limit is about equal to cook-off produced by projectile heating in the barrel as discussed earlier. It appears therefore, that extension of burst length beyond the 80 round limit for IMR 4809 may require increase in barrel mass near the projectile position. A weight increase equivalent to the weight of about fifteen brass cases is estimated to be required in order to ultimately match the cook-off performance of the M16 rifle. Hence, it is reasonable to expect a lighter weapon-magazine combination when using caseless 5.56mm ammunition than is currently in field use in the M16 rifle, provided that heat transfer factors are addressed. Through appropriate use of the computer codes developed in this work thermal evaluations of specific details of given weapon designs may be quickly performed and, where needed, appropriate modifications examined.

IV. 27MM AMMUNITION

In pursuit of the objective of evaluating the thermal performance of existing fixtures and ammunition, firing tests, cook-off tests, and analysis were conducted for 27mm caseless ammunition. The firing tests consisted of both single-shots and rapid fire. These firing tests were directed towards evaluating the heat transfer to the firing fixture. The cook-off tests were directed towards evaluating the cook-off susceptability of caseless ammunition to a given thermal environment. Calculation of the thermal response of a weapon is confirmed by the test data and additional calculations are made evaluating test conditions that were not actually fired. Testing and analysis of covered caseless ammunition was also conducted to obtain information on a possible improvement in future weapons and ammunition. The following section fully describes the work performed on 27mm caseless ammunition.

A. Single-Shot Tests

Single-shot firing tests were conducted with 27mm caseless ammunition supplied by three contractors: Hercules Incorporated, Kenvil, New Jersey; Olin Corporation, St. Marks, Florida; and Aerojet Ordnance and Manufacturing Company, Downey, California. The single-shot fixture was made with the same internal configuration as the Philco-Ford CAW-T2 rapid-fire fixture. In these tests, the following data were obtained: heat input at six locations, chamber pressure, muzzle pressure, projectile velocity, ignition delay, time from ignition to muzzle exit, and particle impacts on a target in front of the muzzle. Heat inputs were determined through the use of in-wall thermocouples located at a nominal 0.015 from the bore. The axial locations of the in-wall thermocouples are shown in Figure 18. Appropriate calculation procedures provide heat input data from the temperatures recorded by the in-wall thermocouples. Appendix B explains the data reduction techniques. Piezoelectric pressure transducers were used for pressure measurements. The chamber pressure transducer was located 1.140 in. behind the stop-shoulder.

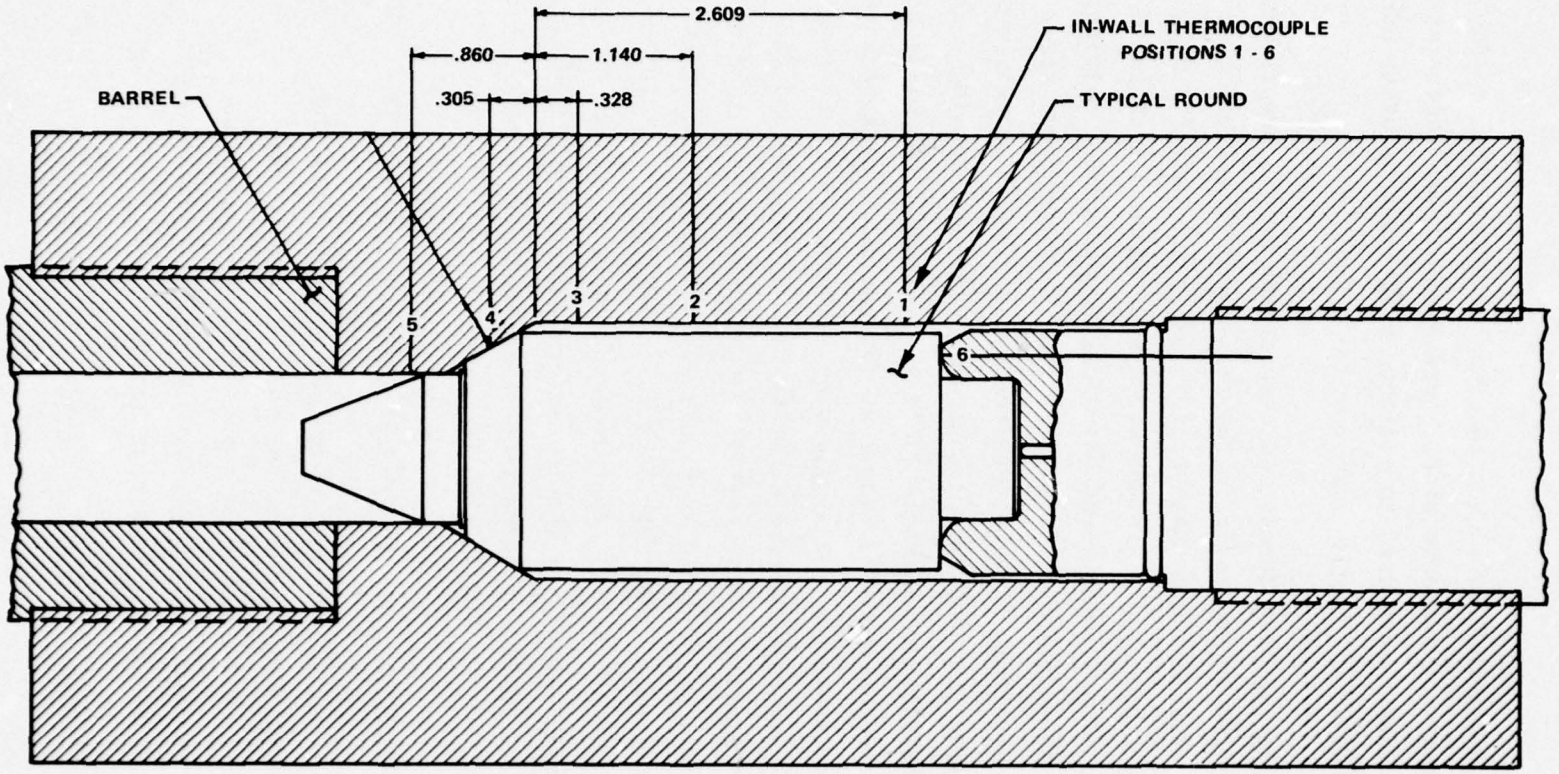

Figure 18 INSTRUMENTATION LOCATIONS IN CALSPAN SINGLE-SHOT CHAMBER SIMULATING PHILCO-FORD 27MM CASELESS FIXTURE, CAW-T2

Ignition timing was determined through a combination of a switch on the firing pin and the start of pressure rise. Cardboard witness sheets at 4.5 ft. in front of the muzzle were used to indicate propellant or other particles exiting from the barrel.

The Hercules and Olin rounds use compression molded propellant made by compacting conventional gun powder in the presence of a solvent binder. The Hercules rounds utilize double base cylindrical grains and the Olin rounds utilize ball powder. The Hercules rounds were supplied both with and without an external coating. The Aerojet round has a cast, monolithic, multiperforated propellant charge. In addition to firing the rounds as supplied, several rounds were covered with thin films to determine the effects on performance. A total of 42 uncovered and 8 covered rounds were fired in the single-shot fixture. The test results are shown in Table IX. In addition, Olin and Hercules rounds covered in the same manner as for the rapid-fire tests discussed in Section IV-B, were tested in the single shot fixture. These Calspan-covered rounds were developed under a separate Calspan program and the environmental protection qualities were tested in that program.[5] A typical covered round of this type is shown in Figure 19. A depth of 0.090 in. was machined from the outside of the propellant for a length of 1.25 in. to reduce the pressure to acceptable levels. The sleeve was shortened from full length to eliminate the residue problem. The results of these covered round tests are given in Table X including comparisons with noncovered rounds of the same type.

An examination of the test results yields the following information:

1). The Hercules and Aerojet rounds produce about the same heating except at the bolt face where the Hercules heat input is about half the Aerojet and at the rear chamber position where Hercules is about 25 percent less than Aerojet.

Table IX
TEST RESULTS - 27MM CASELESS AMMUNITION

Ammunition	Test No.	Heat Input at Given Location,* Btu/ft²/rd 1	2	3	4	5	6	Peak Chamber Pressure, psi	Projectile Velocity at 20 ft., ft/sec	Peak Muzzle Pressure, psi	Muzzle Preblast Pressure, psi	Time I Ignitio Muzzle,
Aerojet, Lot 1	1	30.0	-	-	50.5	-	44.0	52,000	3920	5400	850	2.7
	2	24.5	32.0	41.0	48.0	-	33.0	62,000	4120	5300	780	2.4
	3	27.0	31.0	41.0	47.0	55.0	33.0	58,000	4070	5700	760	2.7
	6	24.0	15.5	27.0	42.0	56.5	31.0	57,000	4075	5850	740	2.5
	38	24.0	31.6	33.3	42.6	60.0	-	68,000	4180	-	810	2.2
	39	22.1	37.4	40.5	46.6	62.0	-	68,000	4250	5140	580	2.3
	40	22.7	29.8	35.8	37.8	57.0	38.0	66,000	-	4760	-	2.6
Averages		24.9	29.6	36.4	44.9	58.1	35.8	61,571	4102	5358	753	2.5
Aerojet, Lot 2	16	-	33.6	35.7	45.4	56.5	24.4	48,000	3920	-	-	-
	17	-	31.5	35.1	37.0	54.2	26.8	58,000	3960	4220	-	2.6
	21	20.0	15.3	39.0	44.0	63.0	30.7	63,000	4080	4040	-	2.4
	22	22.1	33.6	36.5	40.5	55.0	30.0	000	-	-	-	-
	23	26.8	35.8	38.3	40.0	58.2	37.6	57,500	3900	4820	600	2.5
	24	21.0	30.7	32.7	37.5	57.2	35.2	51,000	-	-	-	(3.5
	25	22.0	44.8	41.2	43.7	58.5	-	61,000	3960	4950	880	(3.4
	26	21.0	37.2	35.0	38.4	56.4	28.4	-	4000	-	-	2.6
	30	16.6	37.8	36.2	43.0	61.5	32.0	61,000	3900	4360	-	2.6
	33	22.4	36.2	36.2	40.2	61.8	-	-	4010	-	-	-
Averages		21.5	33.6	36.6	41.0	58.2	30.6	57,438	3966	4478	740	2.5
Hercules	8	-	29.3	31.7	-	53.5	12.6	50,000	3940	4820	960	3.0
	9	17.2	30.1	33.3	43.5	53.2	15.1	57,000	4050	5640	1570	2.7
	10	17.5	30.8	34.0	42.7	52.8	15.2	54,000	4010	5420	1560	2.7
	11	18.1	31.8	35.7	45.2	57.8	17.3	41,000	3860	5420	1200	3.3
	12	18.1	30.8	33.8	43.2	57.8	16.8	51,000	3950	4520	840	3.1
	13	-	30.9	35.8	-	56.2	15.8	48,000	3930	5420	1920	3.2
	14	-	30.8	37.4	42.1	57.0	14.6	48,000	3950	4820	960	3.1
	15	-	31.1	34.2	41.8	55.5	15.3	55,000	4050	4520	-	2.4
	18	12.2	31.0	34.0	39.4	53.1	13.7	54,000	4030	4700	1140	2.9
	27	15.6	34.1	33.1	38.8	54.7	21.2	57,000	4050	4400	760	2.6
Averages		16.4	31.1	34.3	42.1	55.2	15.8	51,500	3982	4968	1212	2.9
Hercules with HES 8028 Coating	19	14.0	29.8	32.3	39.2	56.7	14.7	53,000	4050	5120	840	3.4
	20	15.2	28.2	29.6	32.4	41.2	20.7	54,000	4080	4520	540	2.9
	28	14.4	31.0	30.0	37.2	56.1	16.2	65,000	4200	4440	1160	2.5
	29	14.9	30.3	31.8	38.6	58.6	16.4	54,000	4100	5250	1750	2.7
	50	12.4	26.3	28.7	38.8	56.0	20.0	52,000	4140	3940	870	2.7
Averages		14.2	29.1	30.5	37.2	53.7	17.6	55,600	4114	4654	1032	2.8
Olin	34	16.0	28.4	27.6	31.5	46.5	-	60,000	4300	5250	-	2.4
	35	14.3	25.7	26.6	31.6	47.0	-	58,000	4400	-	-	2.7
	37	13.1	26.4	28.6	32.5	45.0	-	58,000	4380	-	-	2.4
	41	14.7	25.6	26.8	31.5	47.0	19.3	60,000	4440	5340	-	-
	42	15.5	27.9	28.9	34.0	47.7	16.9	57,000	4380	5400	870	2.4
	43	12.9	27.7	29.0	40.5	46.0	18.1	58,000	4430	5450	1450	2.5
	44	13.1	26.7	29.3	-	46.4	15.6	60,000	4390	5280	1040	2.6
	47	13.6	23.5	26.4	35.0	46.6	15.2	60,000	4360	4700	1160	2.7
	48	15.0	27.1	28.6	34.7	45.8	16.8	57,000	4370	4810	695	2.7
	49	12.9	23.8	25.8	33.6	49.2	17.6	60,000	4390	4350	-	2.5
Averages		14.1	26.3	27.8	33.9	46.7	17.1	58,800	4384	5072	1043	2.5
CAL Covered Rounds***	4	19.0	6.5	11.5	20.0	46.0	31.0	65,000	4065	5350	1100	2.5
	5	18.5	22.0	9.0	19.0	46.0	26.0	55,000	4000	5460	935	2.7
	7	16.5	6.0	5.0	-	51.5	28.0	49,000	3880	5350	960	2.6
	31	19.2	7.3	10.3	24.2	53.1	21.0	65,000	4050	4660	990	2.7
	32	16.9	8.8	8.9	19.6	51.0	-	71,000	4150	-	-	2.6
	36	5.2	3.0	3.6	19.5	47.0	-	69,000	4510	5250	-	2.4
	45	14.3	4.2	6.4	-	47.8	21.0	70,000	4300	3880	810	2.3
	46	8.4	10.5	5.2	19.5	55.8	14.7	70,000	4400	3770	1100	2.4

Table IX
- 27MM CASELESS AMMUNITION

Peak Muzzle Pressure, psi	Muzzle Preblast Pressure, psi	Time From Ignition to Muzzle, msec	Ignition Delay, msec	Observations
5400	850	2.74	0.88	Large amount of material striking witness. Small amount of residue in chamber in some tests.
5300	780	2.44	1.17	
5700	760	2.75	0.43	
5850	740	2.58	0.72	
-	810	2.27	0.60	
5140	580	2.36	0.68	
4760	-	2.64	0.60	
5358	753	2.54	0.73	
-	-	-	1.33	Large amount of material impacting witness.
4220	-	2.62	0.76	Small amount of residue in chamber in some tests.
4040	-	2.48	0.98	One round misfired even though pin strike appeared satisfactory.
-	-	-	0.58	
4820	600	2.56	1.05	
-	-	(3.55**)	-	
4950	880	(3.42**)	-	
-	-	2.60	0.72	
4360	-	2.62	-	
-	-	-	-	
4478	740	2.58	0.90	
4820	960	3.06	0.94	Few propellant grains impacting witness. Very small amount of residue in chamber
5640	1570	2.70	1.21	
5420	1560	2.74	1.09	
5420	1200	3.32	1.46	
4520	840	3.16	0.74	
5420	1920	3.24	1.21	
4820	960	3.16	1.05	
4520	-	2.48	1.43	
4700	1140	2.95	0.66	
4400	760	2.67	0.88	
4968	1212	2.95	1.07	
5120	840	3.40	0.96	Few propellant grains impacting witness. Very small amount of residue in chamber, in some tests slightly more than uncoated.
4520	540	2.92	1.05	
4440	1160	2.57	0.86	
5250	1750	2.75	1.42	
3940	870	2.71	1.50	
4654	1032	2.87	1.16	
5250	-	2.48	1.74	Few propellant grains impacting witness.
-	-	2.77	1.79	
-	-	2.42	1.66	
5340	-	-	1.15	
5400	870	2.42	1.40	
5450	1450	2.52	1.85	
5280	1040	2.61	1.17	
4700	1160	2.73	1.21	
4810	695	2.75	1.99	
4350	-	2.50	1.17	
5072	1043	2.58	1.51	
5350	1100	2.56	0.49	0.050 in. x 0.3 in. and 0.5 in. dia. residue in chamber.
5460	935	2.73	0.78	Very small amount of residue.
5350	960	2.64	0.94	Large amount of residue in barrel.
4660	990	2.79	0.82	Base disk intact, no other residue.
-	-	2.61	0.74	Base disk intact, <1 $in.^2$ in chamber, lg. amt. in barrel.
5250	-	2.46	0.88	Large amount of residue in barrel.
3880	810	2.38	0.66	Some base disk, <1 $in.^2$ in chamb., melted pcs. on witness.
3770	1100	2.42	0.58	Large amount in barrel.

NOTES TO TABLE IX

*See Figure 18 for locations.

**Time from pin strike to muzzle.

***Covered rounds consisted of the following:

Test No. 4:	Aerojet, lot No. 2, covered with a single 0.004 in. polyester shoulder cap and a single full-length 0.007 in. polyester sleeve.
Test No. 5:	Aerojet, lot No. 2, covered with a double thickness polyester shoulder cap and a single full-length polyester sleeve.
Test No. 7:	Aerojet, lot No. 2, covered with a double thickness polyester shoulder cap and a double thickness full-length polyester sleeve.
Test No. 31:	Aerojet, lot No. 2, completely covered with 0.001 - 0.002 in. polyethylene, a full-length polyester sleeve, and a 0.016 in. acetate shoulder cap.
Test No. 32:	Same as Test No. 31.
Test No. 36:	Olin covered with the same as Test No. 31.
Test No. 45:	Hercules covered with the same as Test No. 31.
Test No. 46:	Hercules with HES 8028 coating covered with the same as Test No. 31.

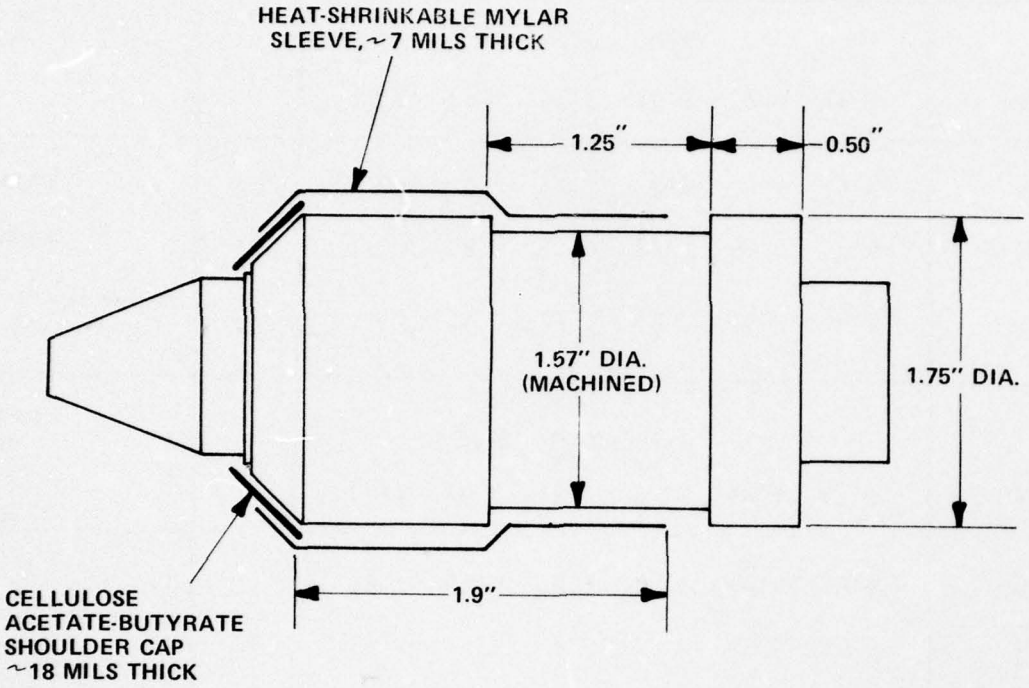

Figure 19 MACHINED AND MYLAR-COVERED 27 MM ROUND CONFIGURATION (HERCULES AND OLIN AMMUNITION)

TABLE X

TEST RESULTS - 27MM COVERED AMMUNITION (AS COVERED FOR RAPID-FIRE TESTS)

Ammunition	Test No.	Heat Input at Given Location,* Btu/ft^2/rd						Peak Chamber Press., psi	Proj. Vel. at 20 ft., ft/sec
		1	2	3	4	5	6		
Olin, As-Received (Avg. of 10 rds., Table IX)	-	14.1	26.3	27.8	33.9	46.7	17.1	58,800	4384
Covered Olin	76	13.5	14.9	7.6	13.6	45.3	15.5	53,000	4100
Covered Olin	77	15.3	21.5	12.7	18.0	45.6	19.4	45,000	3960
Average		14.4	18.2	10.2	15.8	45.4	17.4	49,000	4030
Avg. Reduction From Uncovered		-	31%	63%	53%	-	-		
Hercules, As-Received (Avg. of 10 rds., Table IX)	-	16.4	31.1	34.3	42.1	55.2	15.8	51,500	3982
Covered Hercules	78	16.9	18.6	17.9	27.9	50.8	19.6	51,000	3860
Covered Hercules	79	15.4	20.1	14.3	22.9	53.1	17.6	48,000	3830
Average		16.2	19.4	16.1	25.4	52.0	18.6	49,500	3845
Avg. Reduction From Uncovered		-	38%	53%	40%	-	-		

* 1 - rear chamber, 2 - mid-chamber, 3 - front chamber, 4 - stop-shoulder, 5 - neck, 6 - bolt face. See Figure 18 for exact locations.

2). The Olin rounds have less heat input at nearly every location compared to any of the other uncovered rounds--an average of 26 percent less than Aerojet, lot No. 2, and 16 percent less than the Hercules.

3). The Olin rounds have significantly higher velocity than any other rounds, and the peak chamber pressure is higher than any rounds except Aerojet, lot No. 1. Therefore, the lower heating rate of the Olin rounds is not at the expense of ballistic performance.

4). All of the rounds have about the same time from propellant ignition until the projectile reaches the muzzle.

5). The Olin rounds have the longest ignition delays of any of the rounds.

6). The readability of the peak muzzle pressure and muzzle preblast pressure measurements is not adequate to assess whether these results in Table IX are real or are only variations in readability.

7). The Aerojet rounds produced considerably more debris exiting from the muzzle than the other rounds.

8). The Calspan covered rounds typically produce significantly reduced heat inputs in the chamber compared with uncovered rounds. The largest reductions without residue were of the order of 30 to 50 percent.

9). Hercules HES 8028 coating on Hercules rounds reduces heating somewhat at all chamber locations except at the bolt face. Average reduction is 6.7 percent.

Before the above information can be fully evaluated, cook-off test results must be compared. Cook-off characteristics of each propellant are evaluated in Section IV-C. Also, comparisons made between uncovered rounds may not apply to covered rounds. Sections IV-D-4 and 5 combines the heat

transfer and cook-off data in an analysis that predicts firing limits for cook-off free operation for each type of round.

B. Rapid-Fire Tests

Rapid-fire tests were conducted with 27mm caseless ammunition to further delineate the heat transfer characteristics in rapid-fire. The testing was conducted by Philco-Ford Corporation, Newport Beach, California, in their CAW-T2 27mm caseless fixture. Thermal instrumentation and data reduction were furnished by Calspan. The test ammunition was the same as that used in the single-shot tests; i.e., supplied by Hercules Incorporated, Olin Corporation, and Aerojet Ordnance and Manufacturing Company. Also tested were Calspan-covered versions of the same rounds. The coverings were applied to reduce the heating of the fixture and to reduce the heat transfer back from the fixture to the propellant. Thermal instrumentation consisted of six in-wall thermocouples at locations shown in Figure 20 and external thermocouples on the barrel at distances of 17 in. and 41 in. from the origin of rifling. The in-wall thermocouples were located at 0.010 in. to 0.020 in. from the bore. The thermal instrumentation was utilized to determine the heat input from the ammunition and the residual temperatures within the chamber. Residual temperature is the temperature at the bore surface at the time the succeeding shot is fired. Data reduction techniques for the in-wall thermocouples are described in Appendix B.

The Calspan-covered rounds were developed under another Calspan program and their environmental protection qualities were tested in that program.[5] The portion of the work reported herein includes the rapid-fire of the covered rounds. A typical covered round is shown in Figure 19. Results of single-shot tests with these rounds are given in Table X. All of the rounds were covered in the same manner but the 1.57 in. diameter was not machined on the Aerojet rounds. The machining was determined to be necessary for the Hercules and Olin rounds to reduce peak chamber pressures as a result of single-shot tests. Machining of the Aerojet rounds was not considered feasible because of the construction of the round, i.e., a single, multiperforated grain.

The in-wall temperature measurements of the longest instrumented bursts of noncovered Aerojet, Hercules, and Olin rounds are shown in Figures 21, 22, and 23, respectively. The number of rounds fired for each type of

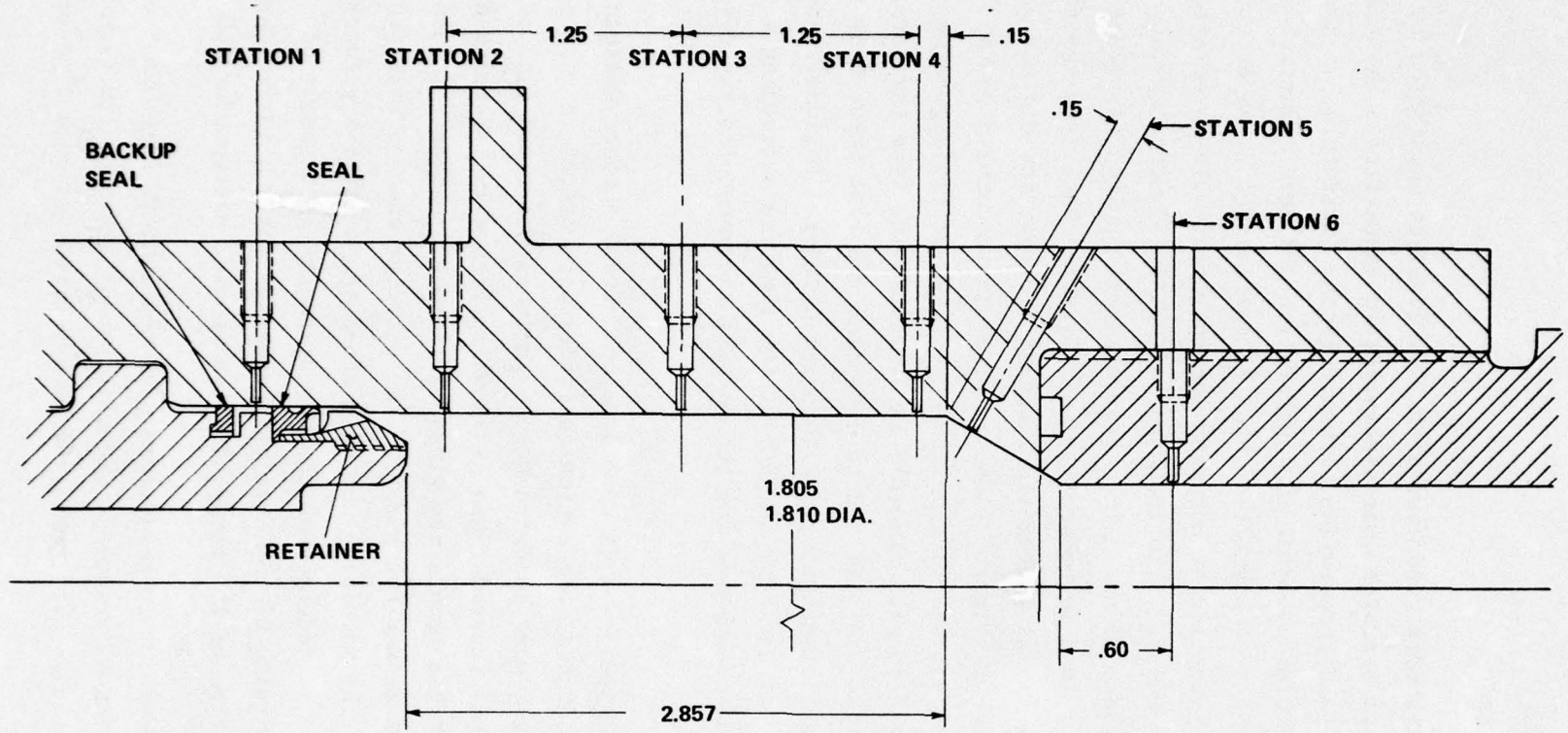

Figure 20 CAW - T2 AUTOMATIC FIXTURE IN-WALL TEMPERATURE LOCATIONS

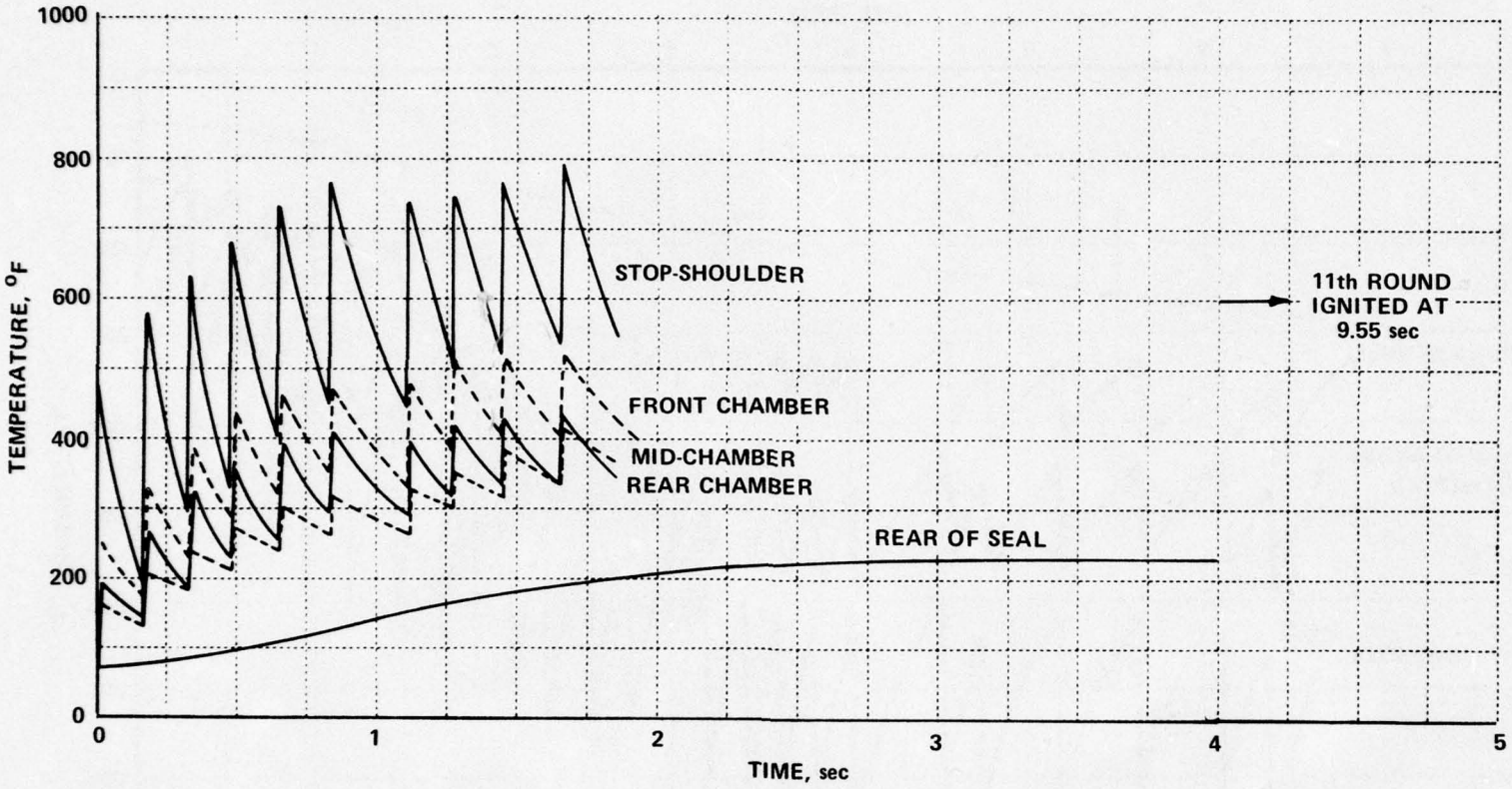

Figure 21 IN-WALL TEMPERATURES DURING A 10 ROUND BURST OF AEROJET AMMUNITION IN THE PHILCO-FORD CAW-T2 AUTOMATIC 27 MM FIXTURE

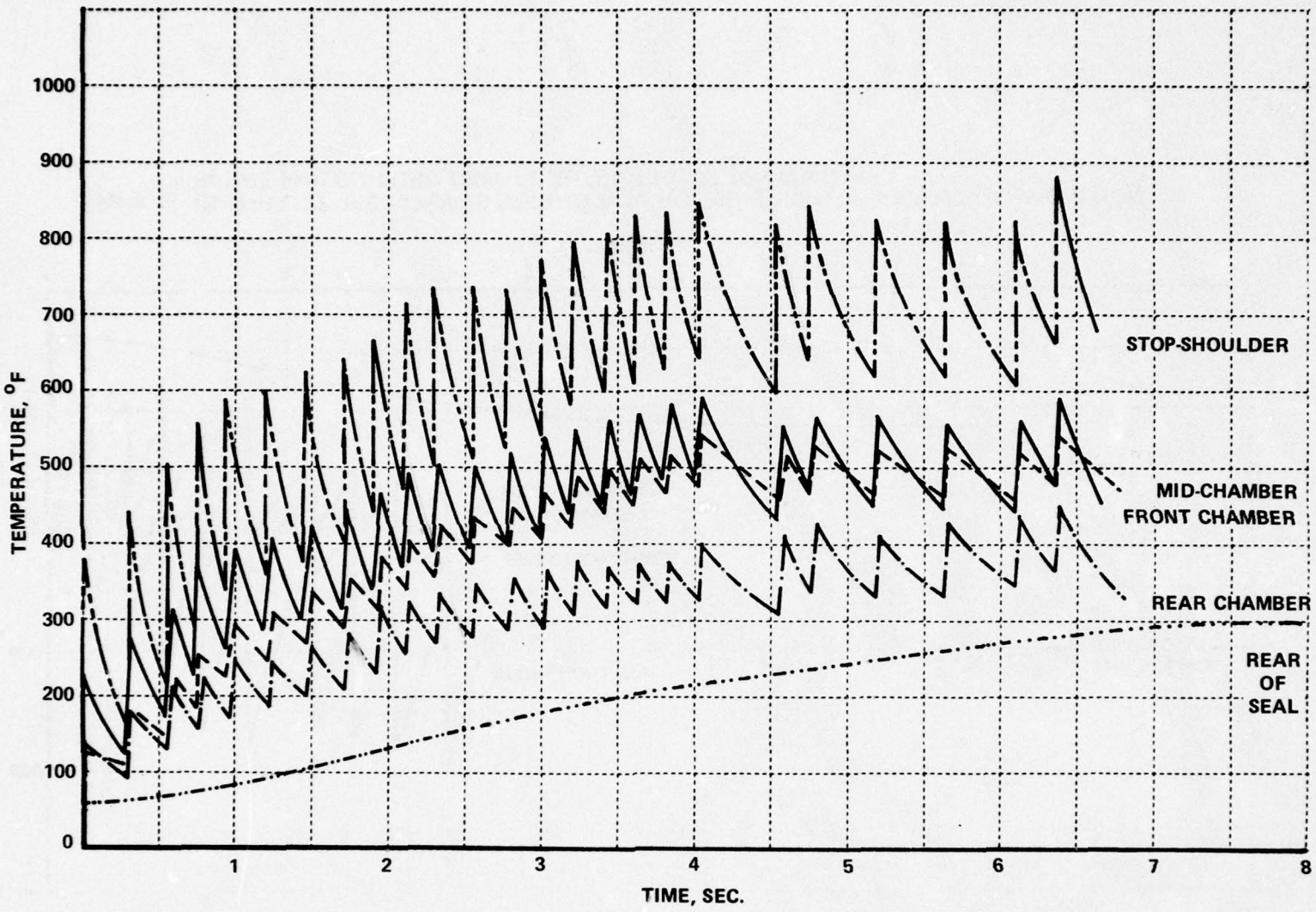

Figure 22 IN-WALL TEMPERATURES DURING A 25 ROUND BURST OF HERCULES AMMUNITION IN THE PHILCO-FORD CAW-T2 AUTOMATIC 27 MM FIXTURE

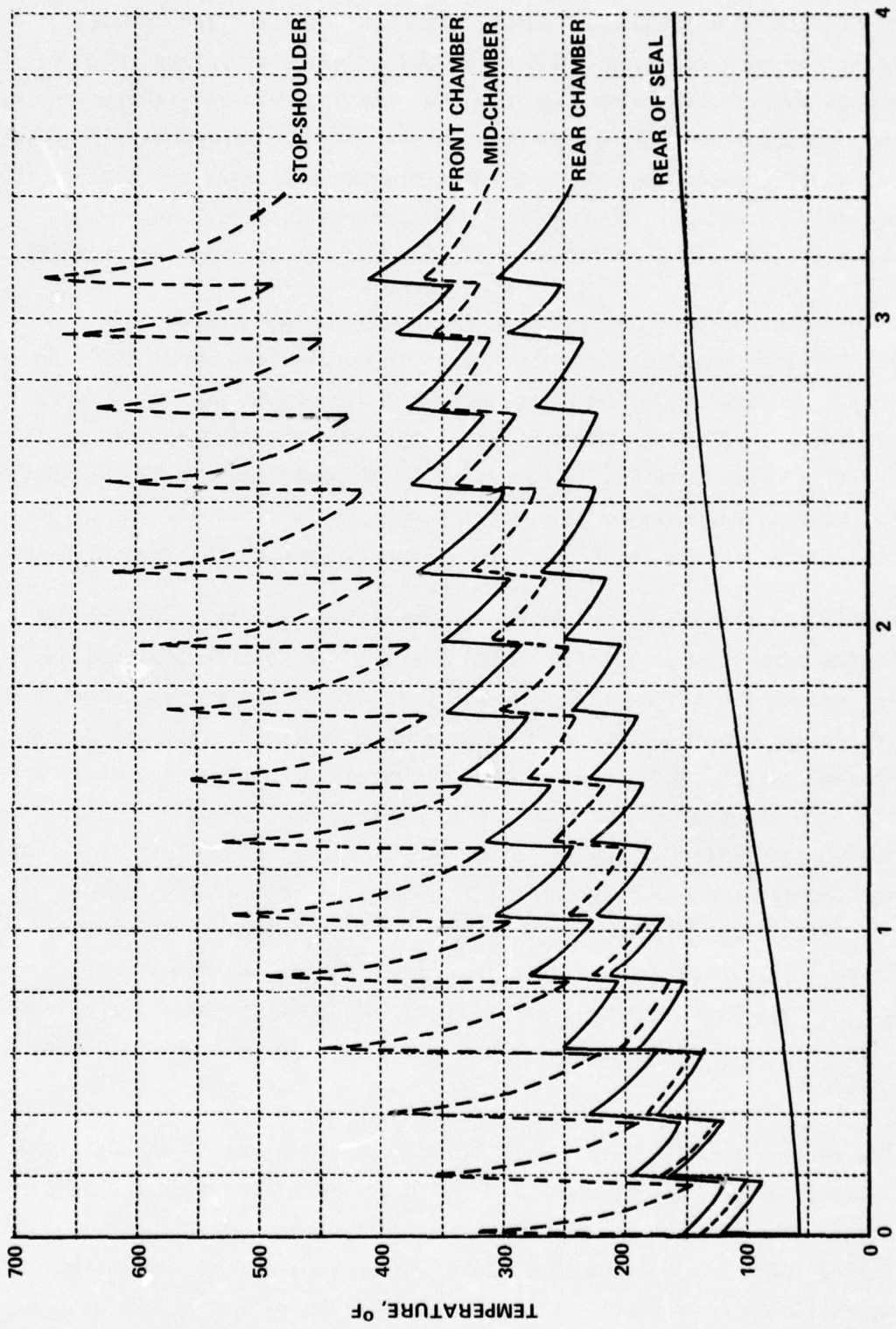

Figure 23 IN-WALL TEMPERATURES DURING A 15 ROUND BURST OF OLIN AMMUNITION IN THE PHILCO-FORD CAW-T2 AUTOMATIC 27 MM FIXTURE

round varied because of malfunctions during the test program. The in-wall thermocouple at the neck position did not respond as expected perhaps because it may have been further away from the bore than the other in-wall thermocouples. Data from this location are not as important as at the chamber locations because propellant does not contact the neck and therefore the neck does not enter into cook-off considerations. Consequently, no corrective action was taken during the test program and the neck in-wall thermocouple data are not reported.

A 10-round burst of Aerojet ammunition was the maximum obtained (Figure 21). The 11th round did not fire normally but ignited after 9.55 sec. The relatively long time before ignition indicates a cook-off due to average temperature. For all of the ammunition types, the low rate of temperature rise at the rear of seal position is caused by axial conduction in the chamber wall and indicates no appreciable gas past the main seal. The heat inputs at the 17 in. and 41 in. barrel positions were 48 and 32 Btu/ft^2/rd, respectively.

A full, 25 round burst of Hercules ammunition was fired (Figure 22). For the Hercules ammunition, the heat input at the 17 in. barrel position was 42 Btu/ft^2/rd and at the 41 in. barrel position it was 27 Btu/ft^2/rd. During the burst, there were four delayed firings, as are evident in the temperature data after rounds 19, 21, 22, and 23. The temperature data give no indication that cook-off occurred near any of the in-wall thermocouple locations. If there had been a cook-off near one of these locations, the in-wall thermocouple would be expected to show a slow temperature rise while the burning begins. This slow temperature rise for cook-off rounds has been noted in 5.56mm caseless ammunition tests (Figure 10). There may have been a cook-off at an uninstrumented location, or the delayed ignitions may have occurred for a reason not associated with cook-off. Section IV-D-4 discusses possible uninstrumented cook-off locations.

The maximum burst length for the Olin ammunition was 15 rounds. The gun stopped firing after the fifteenth round and an ammunition fire consumed the remaining rounds. No heating was noted at any instrumented location for 13 sec after firing ended, indicating that there was no cook-off at any instrumented location within this time. Section IV-D-4 discusses a possible origin

for this fire. Barrel heating was 34 Btu/ft^2/rd at the 17 in. position and 17 Btu/ft^2/rd at the 41 in. position.

A comparison of cook-off performance of each of the 27mm rounds at instrumented locations can be made from the burst temperature data that have been presented. Table XI lists stop-shoulder temperature data after firing 10 rounds of each type of ammunition. The stop-shoulder data were chosen for comparison purposes because this is the highest temperature location in contact with propellant and therefore the likely site of cook-off. The data were obtained at different firing rates which must be adjusted for valid comparisons. A higher firing rate produces higher residual temperatures, other factors being the same. For full comparison of rounds, the cook-off characteristics of each propellant must be known. Cook-off characteristics are reported in Section IV-C of this report and further comparisons of the rounds are included in Section IV-D.

In-wall temperature histories for Calspan-covered rounds are presented in Figures 24, 25, and 26. Figure 24 is for a 7 round burst of covered Aerojet ammunition. Figure 25 is for a 10 round burst of covered Hercules ammunition and Figure 26 is for a 9 round burst of covered Olin ammunition. Each of these figures represents the longest burst fired with the respective covered ammunition.

A comparison of residual temperatures for covered and uncovered ammunition is presented in Table XII. The table is a comparison of raw data, and complete interpretation is hampered by the fact that the firing rates were not precisely the same for all types of ammunition, as indicated by the firing time noted in the table. Also, the round-to-round variation in heating, especially by covered rounds, as evidenced by the figures indicates that more rounds must be fired to obtain valid average temperature data. However, it is clear that the coverings have significantly reduced heating at all covered locations. (The rear chamber location does not have any covering over it and does not show any significant change in heating.) Of course, in addition, the coverings tend to insulate the propellant from the chamber walls, further reducing the possibility of cook-off. This will be discussed further in Section IV-D-4.

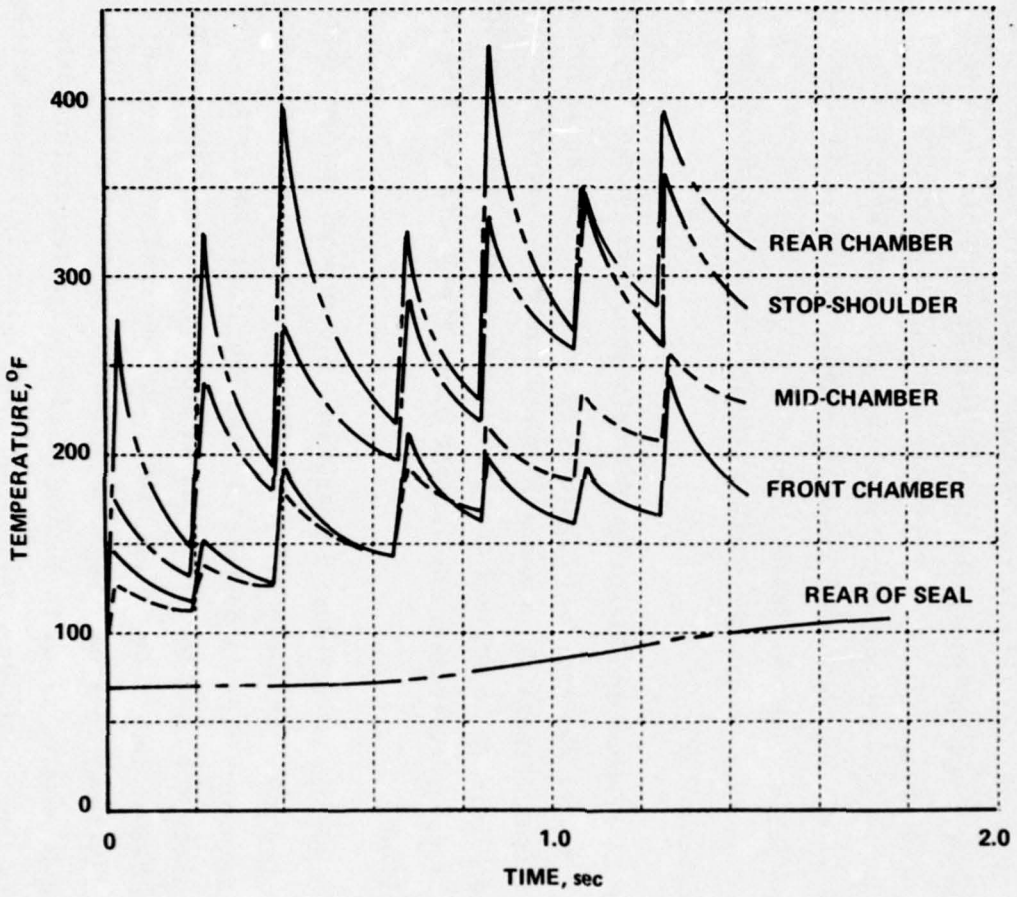

Figure 24 IN-WALL TEMPERATURES DURING A 7 ROUND BURST OF COVERED AEROJET AMMUNITION IN THE PHILCO-FORD CAW-T2 AUTOMATIC 27 MM FIXTURE

TABLE XI

RAPID-FIRE TEST DATA AT STOP-SHOULDER AFTER 10 ROUNDS

Ammunition	Residual Temperature, °F	Average Firing Rate, rds/min	Single-Shot Heat Input, * Btu/ft^2
Aerojet	550	325	41.0
Hercules	505	260	42.1
Olin	405	278	33.9

*Table IX.

TABLE XII

COMPARISON OF MEASURED RESIDUAL TEMPERATURES
FOR CALSPAN-COVERED AND UNCOVERED 27MM CASELESS AMMUNITION

Ammunition Type	Rds. Fired	Time, sec	Stop-Shoulder			Front Chamber			Mid-Chamber			Rear Chamber		
			Residual Temp., °F	Residual Temp. Rise, °F	% Reduction in Temp. Rise for Covered	Residual Temp., °F	Residual Temp. Rise, °F	% Reduction in Temp. Rise for Covered	Residual Temp., °F	Residual Temp. Rise, °F	% Reduction in Temp. Rise for Covered	Residual Temp., °F	Residual Temp. Rise, °F	% Reduction in Temp. Rise for Covered
Aerojet, Uncovered	7	1.10	445	365		337	265		265	188		290	220	
Aerojet, Covered	7	1.25	262	178	51	168	91	66	210	129	31	286	209	5
Hercules, Uncovered	10	2.10	480	413		373	310		345	282		260	200	
Hercules, Covered	10	2.07	349	272	34	280	206	34	292	121	57	270	199	0
Olin, Uncovered	9	1.70	364	304		278	228		242	174		190	138	
Olin, Covered	9	2.01	253	169	44	183	101	56	218	143	18	194	130	6

NOTE: Temperatures given are the in-wall temperatures immediately preceding the last round of the noted rounds fired (the longest burst of covered ammunition).

An additional comparison of covered and noncovered ammunition has been made. The heat input for the first round of every burst fired with the covered rounds was evaluated from in-wall temperature data. (The equations relating in-wall temperatures to heat inputs are not valid after the first round of a burst.) As a comparison of the instrumentation in the CAW-T2 and in the Calspan single-shot fixture, data were also reduced for the first round of bursts that were fired with uncovered Hercules ammunition during the same series of tests. The data obtained in the CAW-T2 and single-shot fixtures were in agrement except at two locations, the mid-chamber and the neck. The data obtained in the single-shot fixture were higher at both of these locations. The in-wall thermocouple locations were not exactly the same in the automatic and single-shot fixtures and therefore a smooth curve was drawn through the heat input data for comparison purposes. The heat input at the neck is not pertinent to the present discussion of heat reductions due to coverings because coverings do not affect heating at the neck. Therefore, heat input data at the neck are not presented here. Heat input data at the mid-chamber are presented with the caution that the uncovered round measurements in the same series of tests were lower than measurements in the single-shot fixture.

The heat input data for each of the covered round types are presented in Table XIII. It may be noted that there is considerable round to round variation in the heat inputs from covered rounds as has been noted in previous testing. This is probably due to differences in the amount of time that the coverings remain insulating the chamber. The coverings did not extend to the rear chamber location and therefore were not expected to have an effect at this location. In fact, for two of the ammunition types, the heat input actually increased compared with the single-shot data. There also appear to be large differences between the different ammunition types but this may be at least partially due to the relatively small sample size. It is again evident, though, that coverings reduce heating a significant amount as was found from the comparison of residual temperatures. The net result of the various comparisons that have been made on the basis of rather limited testing of covered rounds is that significant reductions in heating were obtained although there were

TABLE XIII

FIRST ROUND HEAT INPUT DATA FOR CALSPAN-COVERED AMMUNITION IN CAW-T2 27MM AUTOMATIC FIXTURE

Ammunition	Test No.	Heat Input, Btu/ft^2			
		Stop-Shoulder	Front Chamber	Mid-Chamber	Rear Chamber
Calspan-Covered Aerojet	181-1	14	16	13	24
	181-2	18	10	9	21
	181-3	13	10	11	20
	181-4	31	17	8	20
	181-5	14	8	10	21
	182	23	16	10	22
	183	10	12	9	22
	184	25	13	12	24
	185	10	16	10	23
	186	29	10	13	25
Avg.		19	13	10	22
% Reduction of Covered Round		52	62	69	10(increase)
Calspan-Covered Hercules	172	30	21	19	18
	173	31	22	18	16
	174-1	35	22	18	16
	174-2	34	28	19	17
	174-3	31	22	18	15
	174-4	27	21	19	15
	189	33	22	21	18
Avg.		32	23	19	16
% Reduction of Covered Round		18	35	37	7(increase)
Calspan-Covered Olin	175-1	17	11	12	11
	175-2	19	14	10	11
	175-3	20	17	-	-
	175-4	24	9	15	13
	175-5	19	9	10	11
	176	21	10	12	12
	177	19	14	9	9
	180	23	11	13	12
Avg.		20	12	12	11
% Reduction of Covered Round		35	57	54	15

round-to-round variations and the precise magnitude of reduction that would be obtained in larger scale testing is not known.

C. Cook-Off Tests

Cook-off (autoignition) of caseless propellant may be due to either one or two basic mechanisms. The cook-off may be due to contact with the hot but rapidly cooling interior chamber surface temperature that is present following a rapid-fire burst. The inside surface temperature at the time of insertion of the next round in the burst is called the residual temperature. Cook-off may also be caused by the overall average temperature across the wall thickness at the end of a burst. Cook-off due to the average temperature is called long-time cook-off. At the end of a burst the temperature in contact with a chambered round is the residual temperature which then equilibrates to the average temperature. For cased ammunition, the case isolates the propellant from the residual temperature and cook-off due to average temperature is the only type possible. Similarly for covered caseless ammunition, cook-off tends to be only a function of the average temperature.

Cook-off of caseless propellants due to residual temperatures were determined using a specially constructed test device, discussed earlier in Section III, B-2. This device allows the simulation of the hot but rapidly cooling chamber wall contacted by a caseless round during rapid firing.

Several tests were conducted at different test temperatures and visual note made of whether the propellant burned completely or began to burn and then quenched or did not burn at all. Table XIV gives the minimum temperatures at which the propellant combustion was not quenched, i.e., at higher temperatures the propellant could continue to burn and at lower temperatures the burning would stop or never even start.

The materials are listed in Table XIV in order of increasing cook-off temperatures. The first three types (Hercules, Olin, and Aerojet) represent samples taken from the main body of as-received rounds with the outside surface of the propellant in contact with the hot test surface in every test. Samples of IMR 4809 were molded to provide a comparison with a standard propellant which has been studied extensively as a small caliber caseless propellant. Two plastic coverings were also tested on the IMR 4809 with the

TABLE XIV

MINIMUM COOK-OFF TEMPERATURE OF PROPELLANTS IN CONTACT WITH STEEL SURFACE COOLING AT 250°F/SEC

Type	Minimum Cook-Off Temperature, °F
Hercules (No Covering)	490
Olin (No Covering)	515
Aerojet (No Covering)	545
IMR 4809 (No Covering)	565
IMR 4809 + 0.0008 in. Mylar Covering	565
Hercules + HES 8028 Covering	577
Aerojet Stop-Shoulder Material	665
IMR 4809 + 0.010 in. Acetate Butyrate	825

covering towards the hot surface. The Hercules + HES 8028 coating samples were taken from rounds of this configuration supplied by Hercules and were tested with the HES 8028 coating in contact with the hot surface. The Aerojet rounds have a stop-shoulder made of a different material than the main body of the round, and these were tested separately.

Long-time cook-off tests were conducted by placing propellant samples on a steel plate at a known temperature and the time to cook-off measured. The results of these tests are shown in Figures 27, 28, and 29. As in all cook-off tests, there is considerable variation between the results for specific samples. However, the minimum expected cook-off times must be the important consideration if cook-off prevention is essential. These minimum cook-off values are estimated by the curves on the figures. Instances in which no cook-off was observed are also shown by designation on each figure. Each of the curves appear to approach a temperature below which cook-off does not occur. The longest test times are of the same order as the times that a gun chamber would remain at elevated temperature at the conclusion of firing. Therefore, these temperatures define the long-time cook-off limits. For the several propellants, the values of the long time cook-off limits are taken from the figures to be as listed in Table XV.

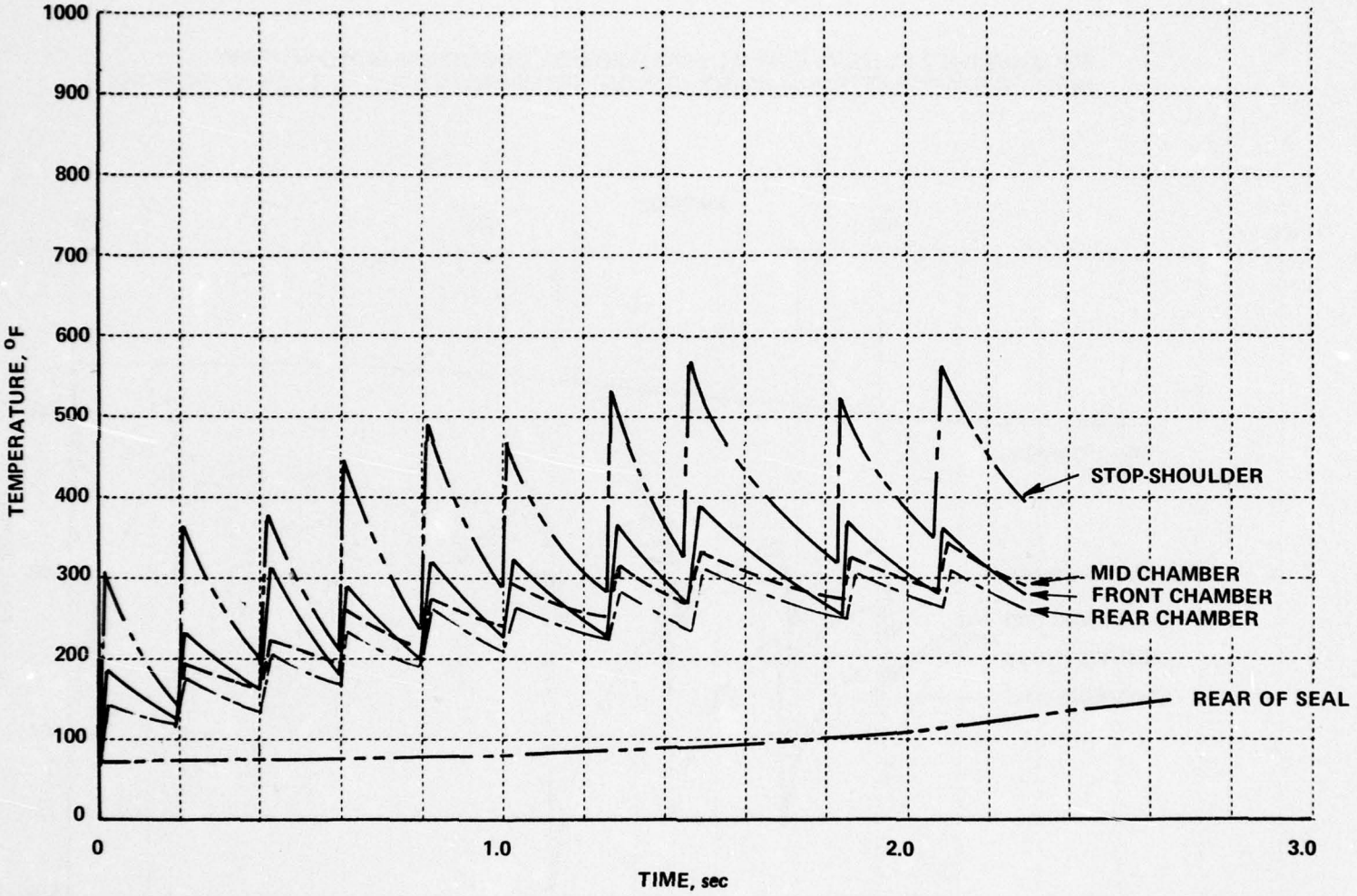

Figure 25 IN-WALL TEMPERATURES DURING A 10 ROUND BURST OF COVERED HERCULES AMMUNITION IN THE PHILCO-FORD CAW-T2 AUTOMATIC 27 MM FIXTURE

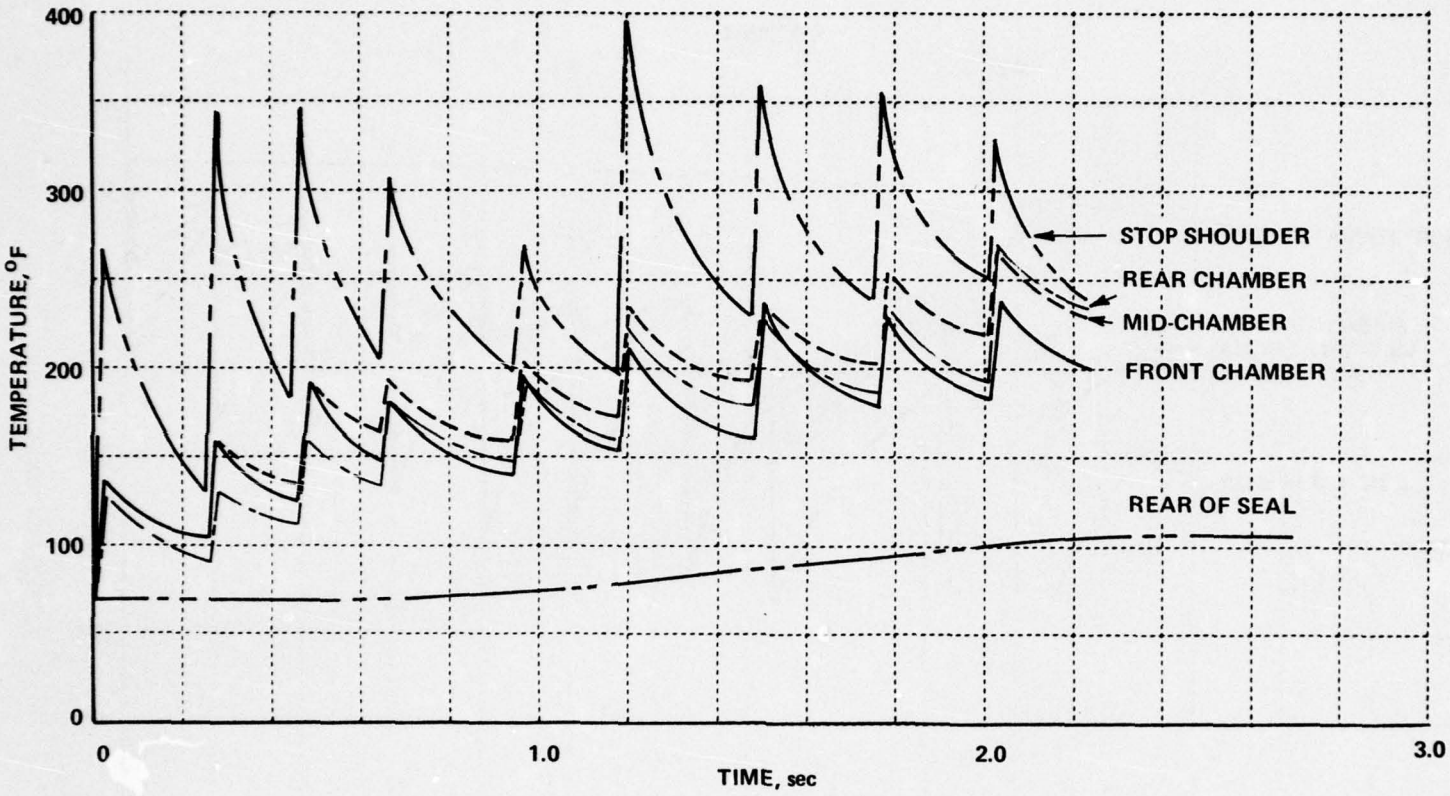

Figure 26 IN-WALL TEMPERATURES DURING A 9 ROUND BURST OF COVERED OLIN AMMUNITION IN THE PHILCO-FORD CAW-T2 AUTOMATIC 27 MM FIXTURE

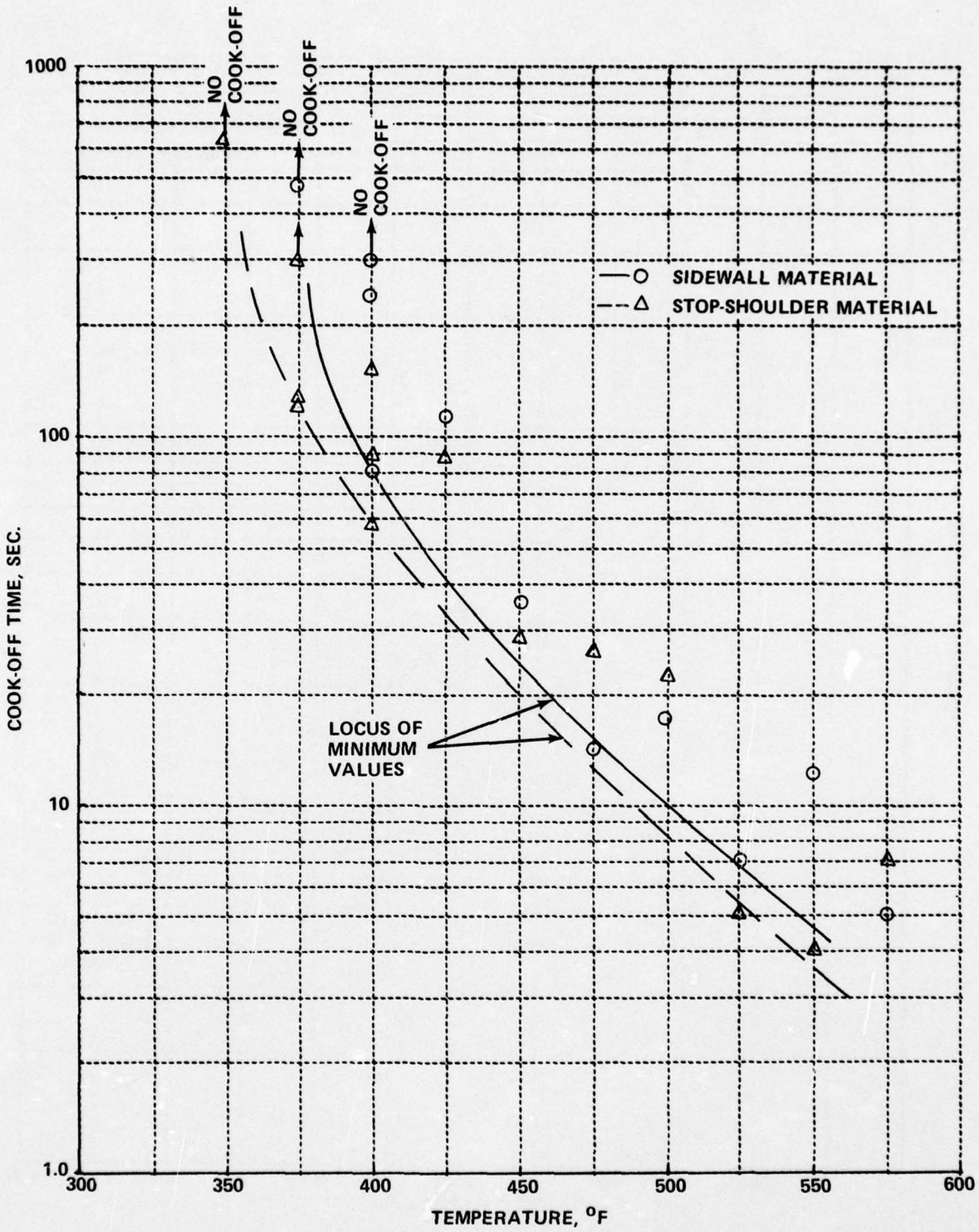

Figure 27 COOK-OFF TEMPERATURES ON CONSTANT TEMPERATURE STEEL PLATE, AEROJET 27 MM CASELESS PROPELLANT

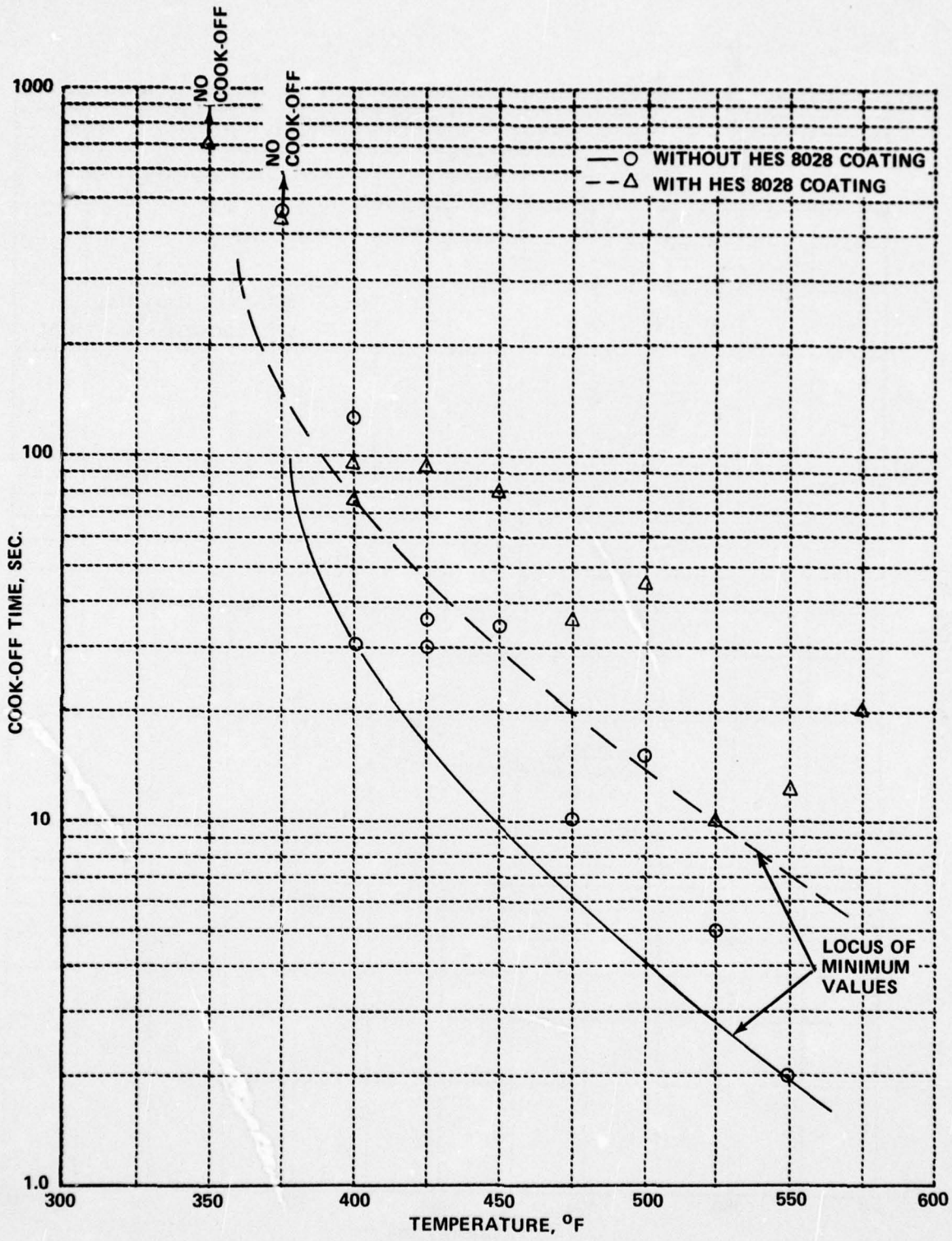

Figure 28 COOK-OFF TEMPERATURES ON CONSTANT TEMPERATURE STEEL PLATE, HERCULES 27 MM CASELESS PROPELLANT

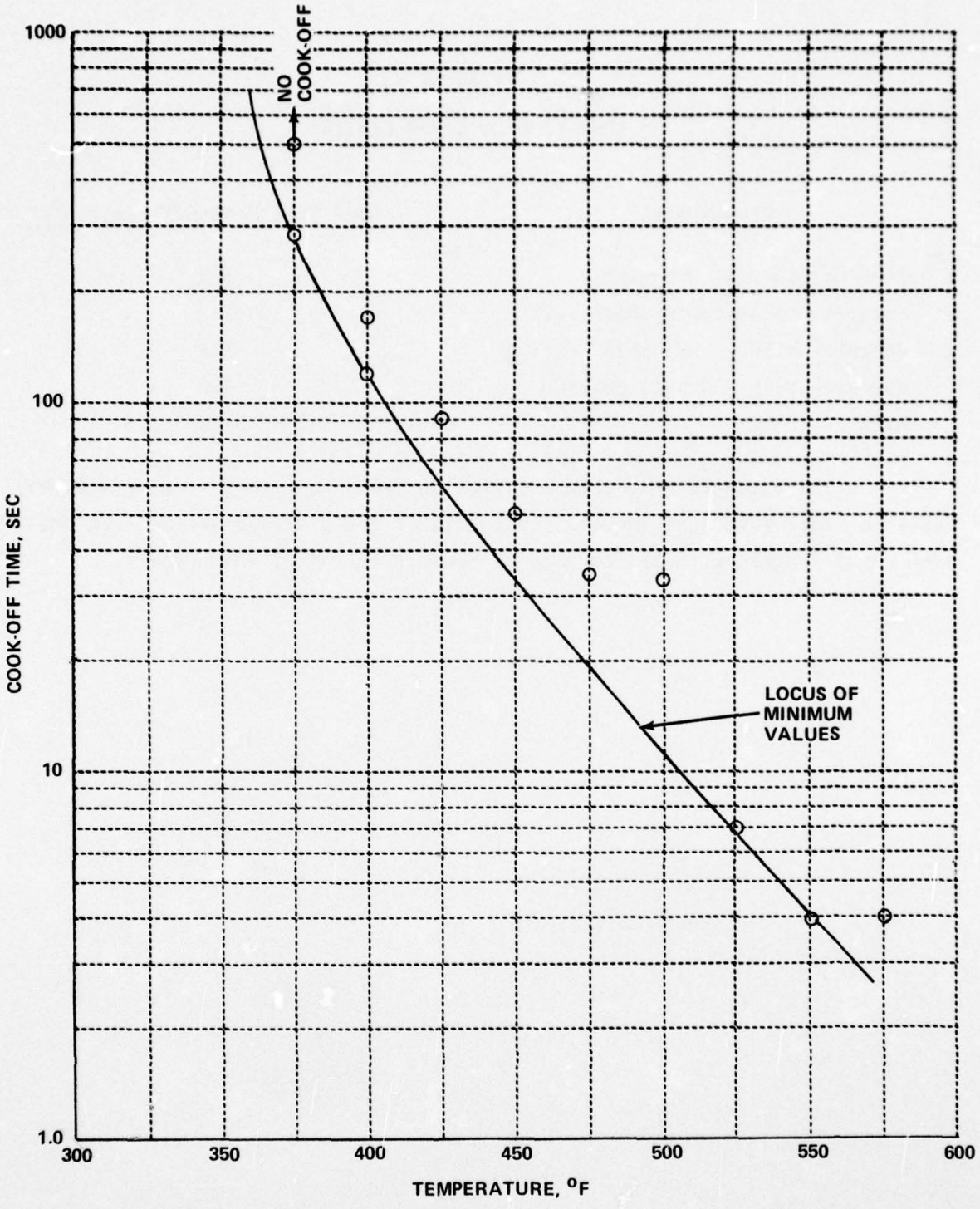

Figure 29 COOK-OFF TEMPERATURES ON CONSTANT TEMPERATURE STEEL PLATE, OLIN 27 MM CASELESS PROPELLANT

Table XV

LONG-TIME COOK-OFF LIMITS

Propellant	Long Time Cook-Off Limit, ^{o}F
Aerojet Sidewall Material	375
Aerojet Stop-Shoulder Material	350
Hercules Without HES 8028 Coating	375
Hercules With HES 8028 Coating	350
Olin	360

The cook-off temperature limits determined in this section will be utilized along with heat input measurements of the previous sections to predict burst lengths without cook-off in Section IV-D-4 of this report.

D. Thermal Evaluations

In this section, the heat input parameters necessary for calculation of temperatures occurring during rapid-fire are presented. These are then used to calculate rapid-fire conditions duplicating the rapid-fire tests in the CAW-T2 and comparisons are made with measurements. Calculations are then made for other firing conditions and cook-off limits are predicted. Calculations for covered ammunition are included.

1. Heat Transfer Parameters

Calculations based on single-shot data were made of the factors relevant to heat transfer. The calculation procedure is given in Appendix A. The calculations were performed on an IBM 370/168 computer. The measurement locations in the single-shot and the rapid-fire fixtures, were not precisely the same. Therefore, any calculations made using single-shot measurements for calculating rapid-fire conditions were adjusted to the rapid-fire locations by a smooth curve through the single-shot data. Figures 30, 31, and 32 present the calculated propellant gas temperature and projectile velocity and measured chamber pressures for Aerojet, Hercules, and Olin ammunition, respectively. The computed heat transfer coefficients at the origin of rifling, stop-shoulder, and mid-chamber are given in Figures 33, 34, and 35.

2. Comparisons Between Measured and Calculated Temperatures

Using the heat transfer parameters calculated above, temperatures at the stop-shoulder and neck of the CAW-T2 while firing Hercules ammunition were calculated. Comparisons of the calculated and measured temperatures are shown in Figures 36 and 37. These curves are plots of the residual temperatures which are the temperatures on the inside surface at the time the next round is ready to be fired. The curves indicate very good agreement between the measured and calculated temperatures, especially considering the lack of precise knowledge of the thermal properties of the gun steels and the round-to-round variation in heating, as evidenced by the non-smooth shape of the measured curves. The stop-shoulder is also a particularly difficult location

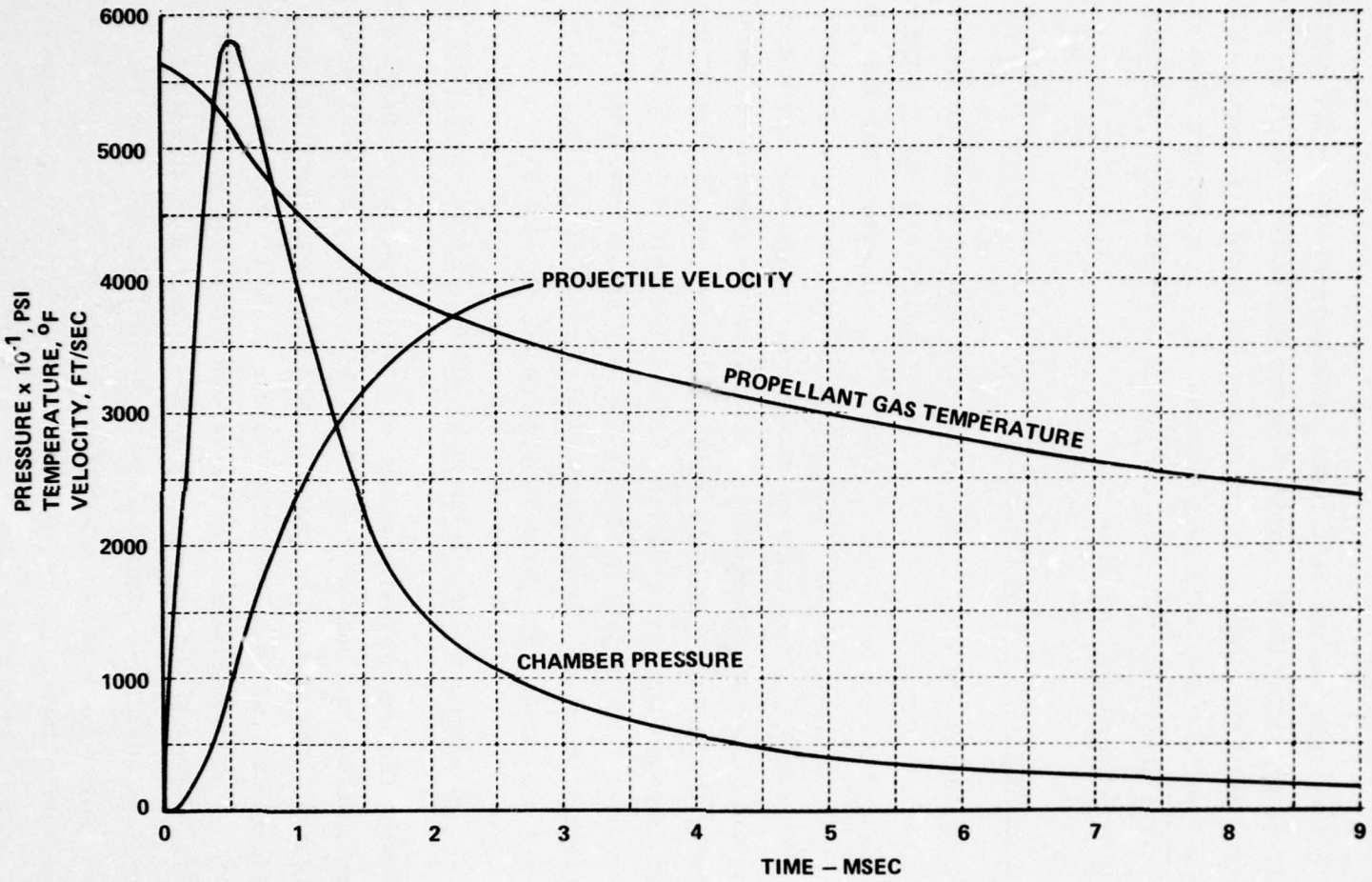

Figure 30 PROPELLANT GAS TEMPERATURE, CHAMBER PRESSURE, AND PROJECTILE VELOCITY AS A FUNCTION OF TIME FOR AEROJET 27 MM CASELESS AMMUNITION

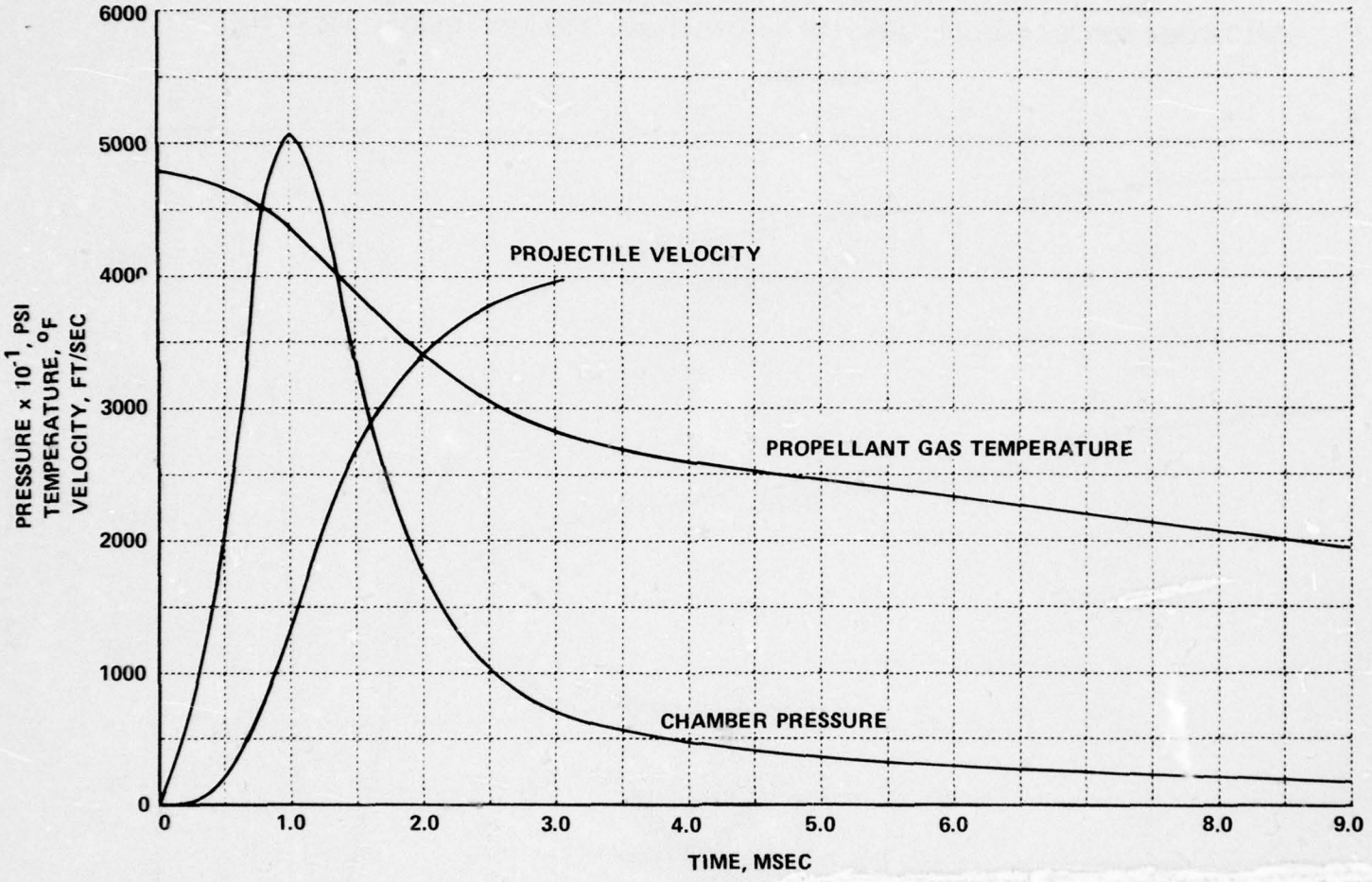

Figure 31 PROPELLANT GAS TEMPERATURE, CHAMBER PRESSURE, AND PROJECTILE VELOCITY AS A FUNCTION OF TIME FOR HERCULES 27 MM CASELESS AMMUNITION

AD-A034 159 CALSPAN CORP BUFFALO N Y F/G 19/1
CASELESS AMMUNITION HEAT TRANSFER. VOLUME III.(U)
APR 76 D E ADAMS, F A VASSALLO DAAG25-70-C-0454
UNCLASSIFIED CALSPAN-GM-2948-Z-3-VOL-3 NL

2 OF 3
AD
A034159

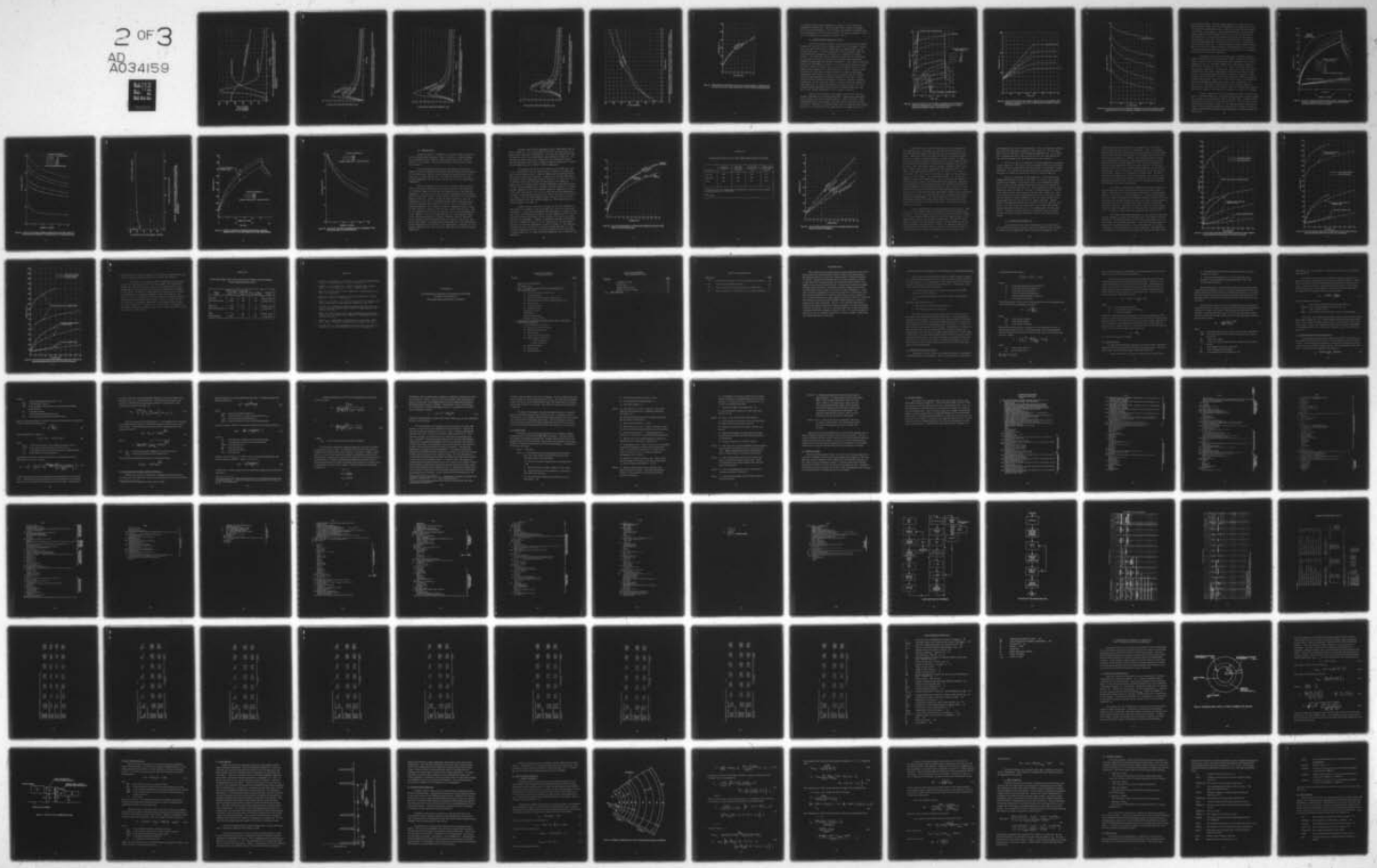

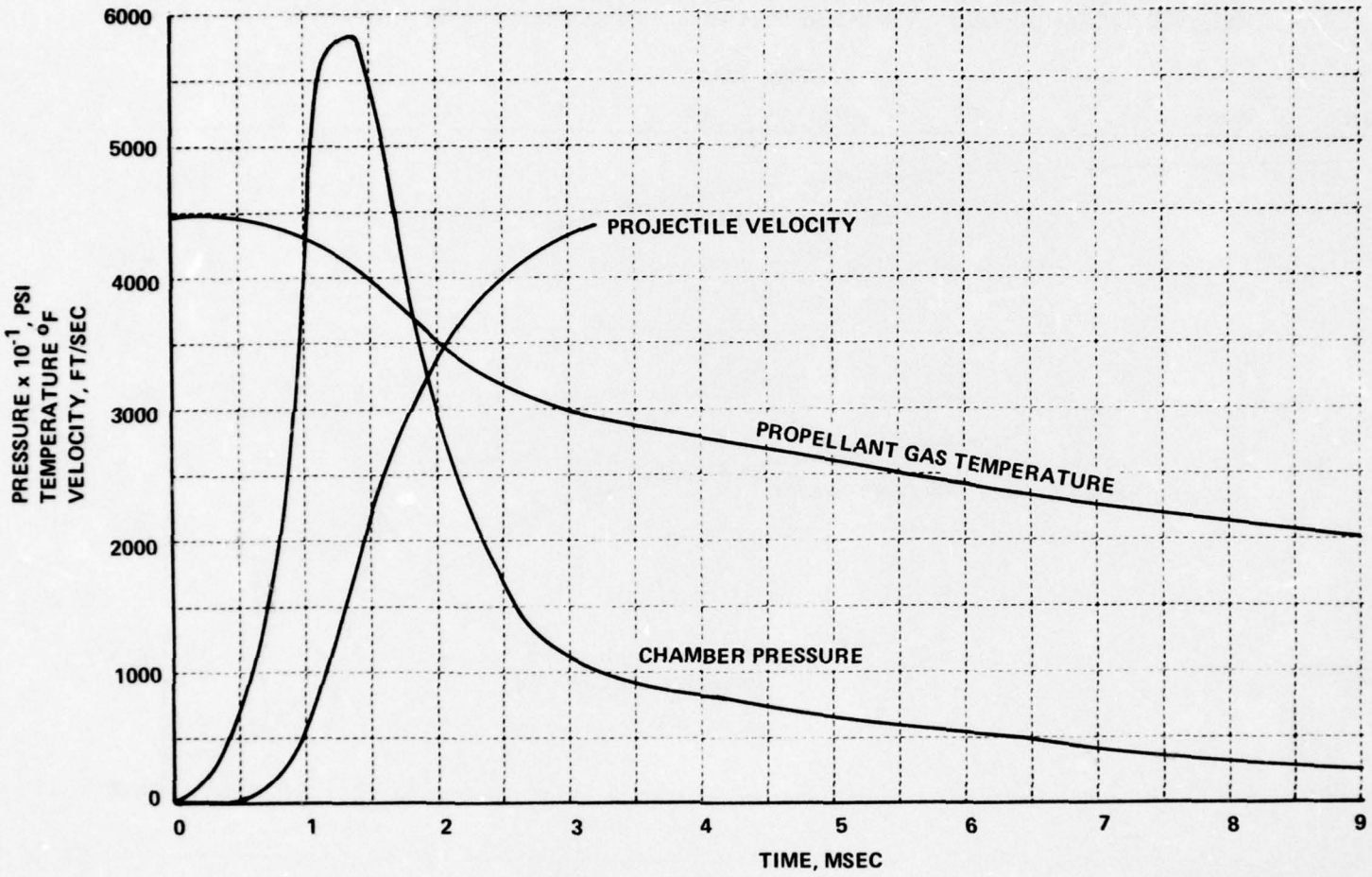

Figure 32 PROPELLANT GAS TEMPERATURE, CHAMBER PRESSURE, AND PROJECTILE VELOCITY AS A FUNCTION OF TIME FOR OLIN 27 MM CASELESS AMMUNITION

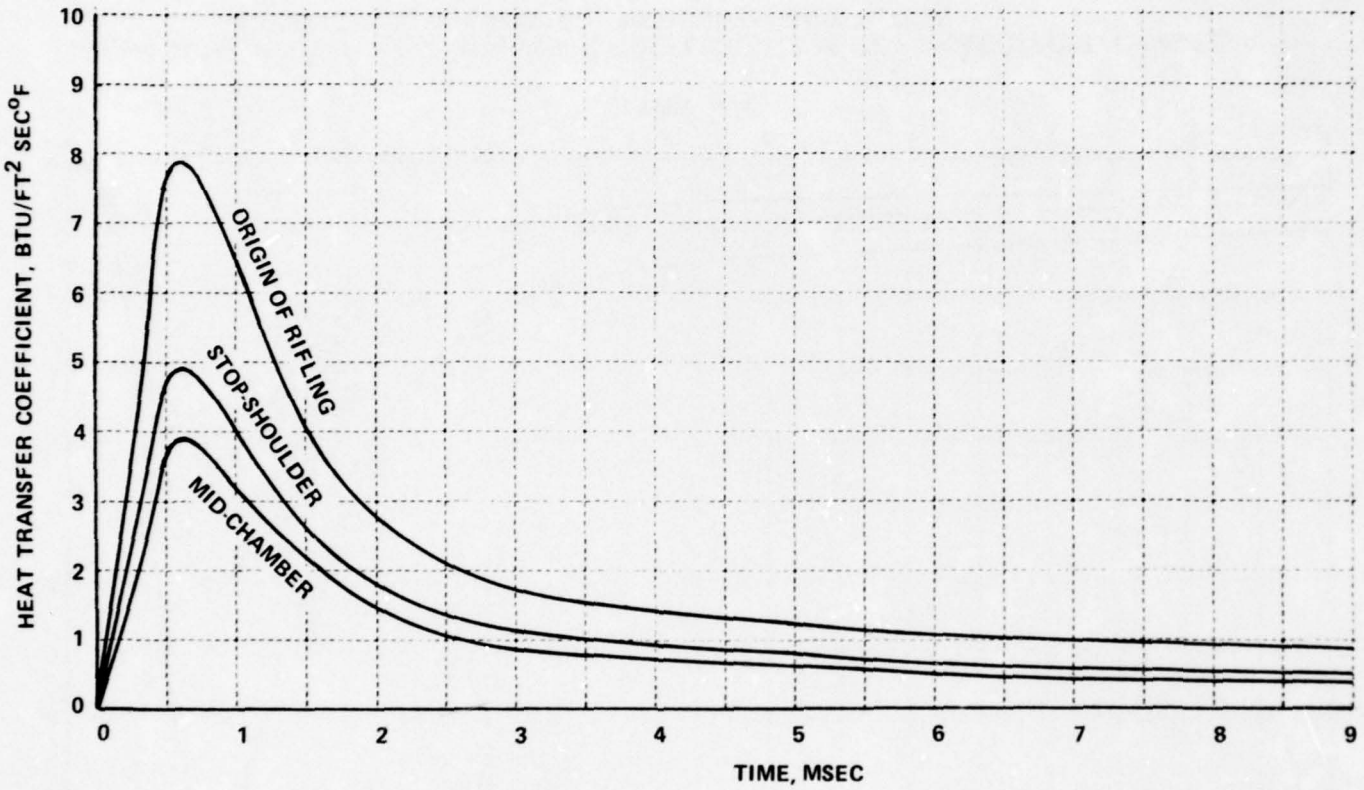

Figure 33 COMPUTED HEAT TRANSFER COEFFICIENTS IN THE PHILCO-FORD CAW-T2 AUTOMATIC 27 MM FIXTURE, AEROJET AMMUNITION

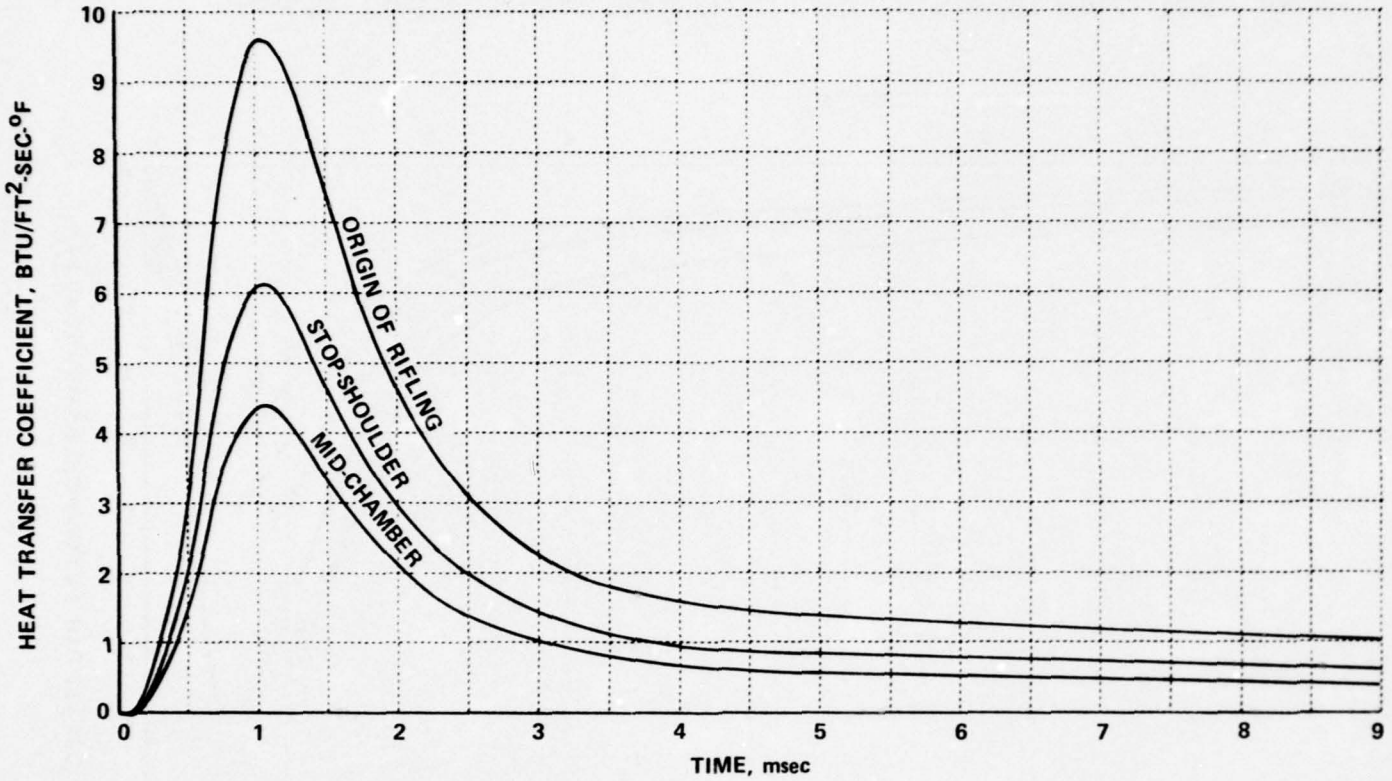

Figure 34 COMPUTED HEAT TRANSFER COEFFICIENTS IN THE PHILCO-FORD CAW-T2 AUTOMATIC 27 mm FIXTURE, HERCULES AMMUNITION

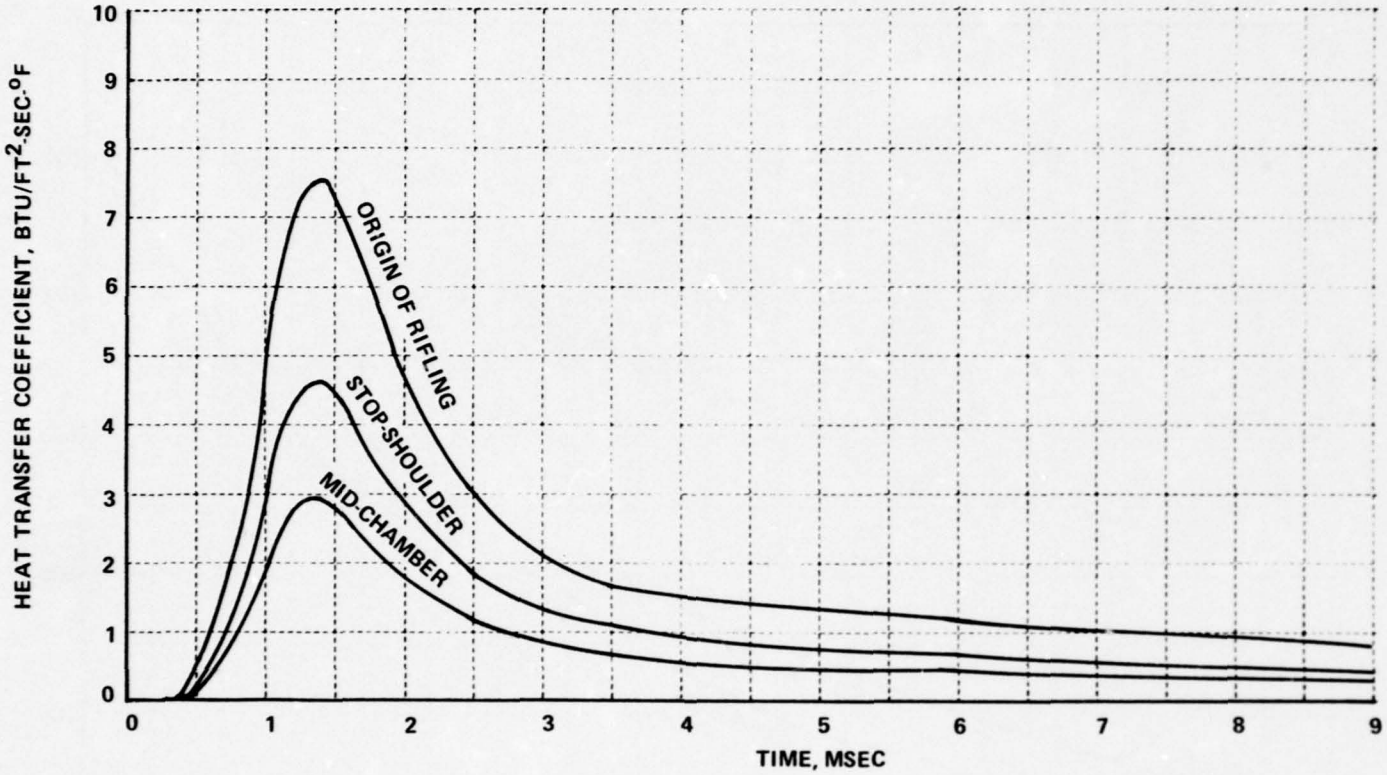

Figure 35 COMPUTED HEAT TRANSFER COEFFICIENTS IN THE PHILCO-FORD CAW-T2 AUTOMATIC 27 MM FIXTURE, OLIN AMMUNITION

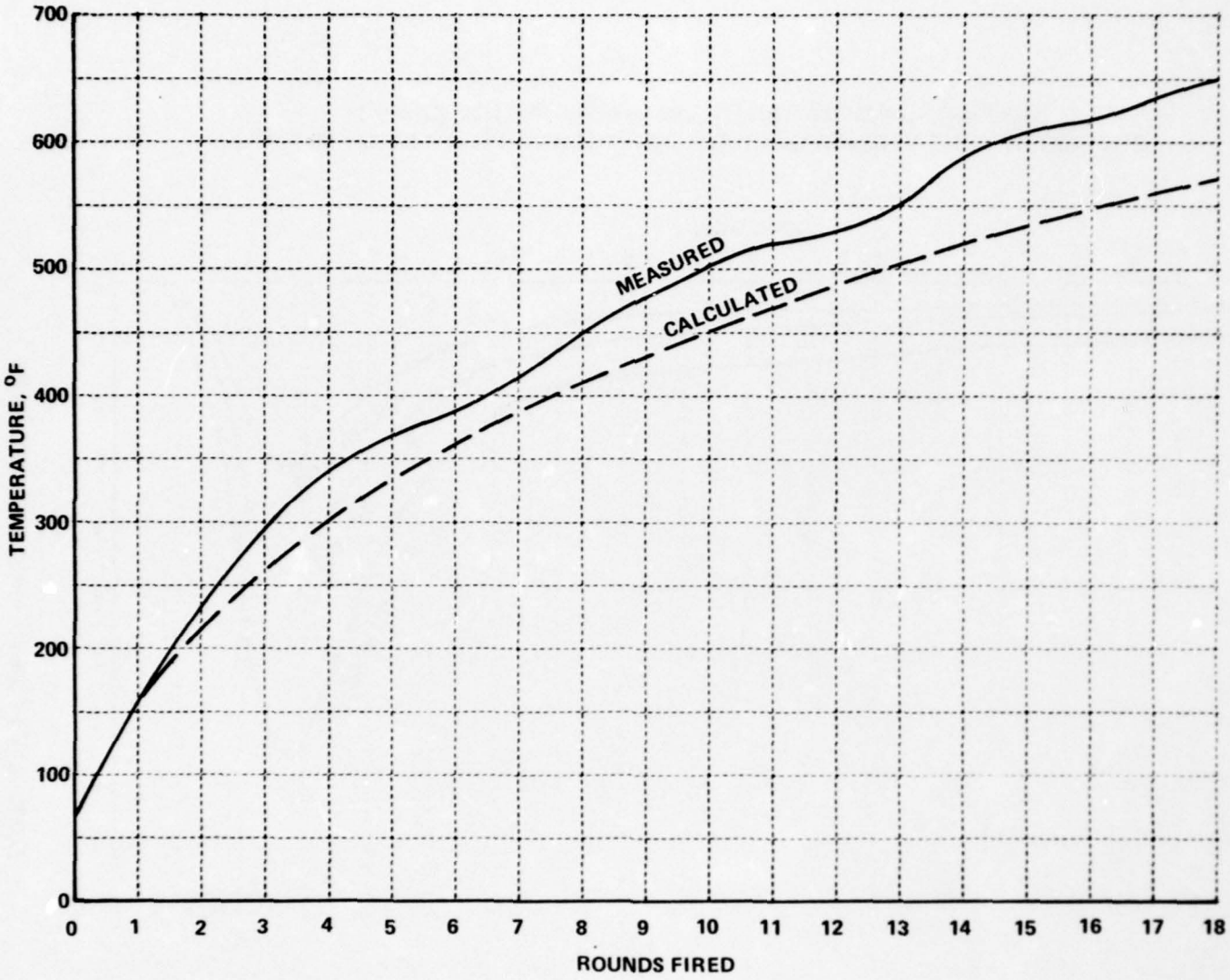

Figure 36 COMPARISON OF MEASURED AND CALCULATED RESIDUAL TEMPERATURES AT STOP-SHOULDER OF CAW-T2 27 MM AUTOMATIC FIXTURE, HERCULES AMMUNITION

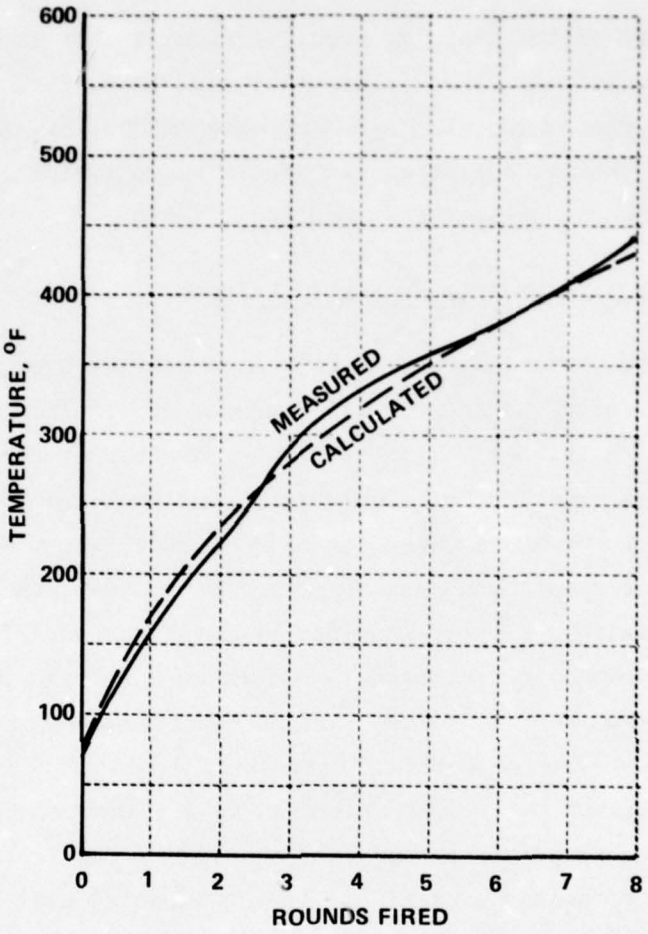

Figure 37 COMPARISON OF MEASURED AND CALCULATED RESIDUAL TEMPERATURES AT NECK OF CAW-T2 27 MM AUTOMATIC FIXTURE, HERCULES AMMUNITION

to calculate because of the changing cross section at this location with attendant axial conduction. These plots then tend to confirm the adequacy of the calculation procedure. The calculation procedure has also agreed quite well with measured results for other fixtures. For example, agreement is good for 5.56mm ammunition as presented in Section III-B-6.

3. Weapon Thermal Conductivity Effects

One of the variables related to weapon heating over which the weapon designer has some control is the thermal conductivity of the weapon. Calculations were made of the effects of chamber material thermal conductivity on chamber temperatures. For these calculations, the heat transfer coefficients and propellant gas temperatures were taken to be independent of chamber material. The coefficients and gas temperatures used were those established for previous calculations of stop-shoulder temperatures when firing 27mm Frankford Arsenal ammunition reported in Reference 2. These inputs are different from those of the ammunitions studied in this report but for general consideration of the effects of thermal conductivity the calculations are valid. The chamber outside diameter in all calculations was 3.6 inches. Figure 38 shows the effect of a wide range of thermal conductivity values (corresponding approximately from ceramics to aluminum) on the expected peak and residual internal surface temperatures during 40-round bursts at 600 rpm. Clearly, increasing thermal conductivity produces a substantial lowering of residual temperatures. On the other hand, there is a general increase in chamber average temperature with increasing conductivity as shown in Figure 39. This increased average temperature results from an increased internal heat load due to lower residual temperatures. This is shown in Figure 40.

Cook-off can be produced in the chamber by virtue of either high residual temperature or high average temperature. High residual temperatures tend to produce short-time cook-off (measured in tenths of seconds). High average temperatures tend to produce long-time cook-off (measured in seconds or minutes). Therefore, in situations where short-time cook-off can be avoided entirely, say by noncontact of the propellant with the chamber walls, or by

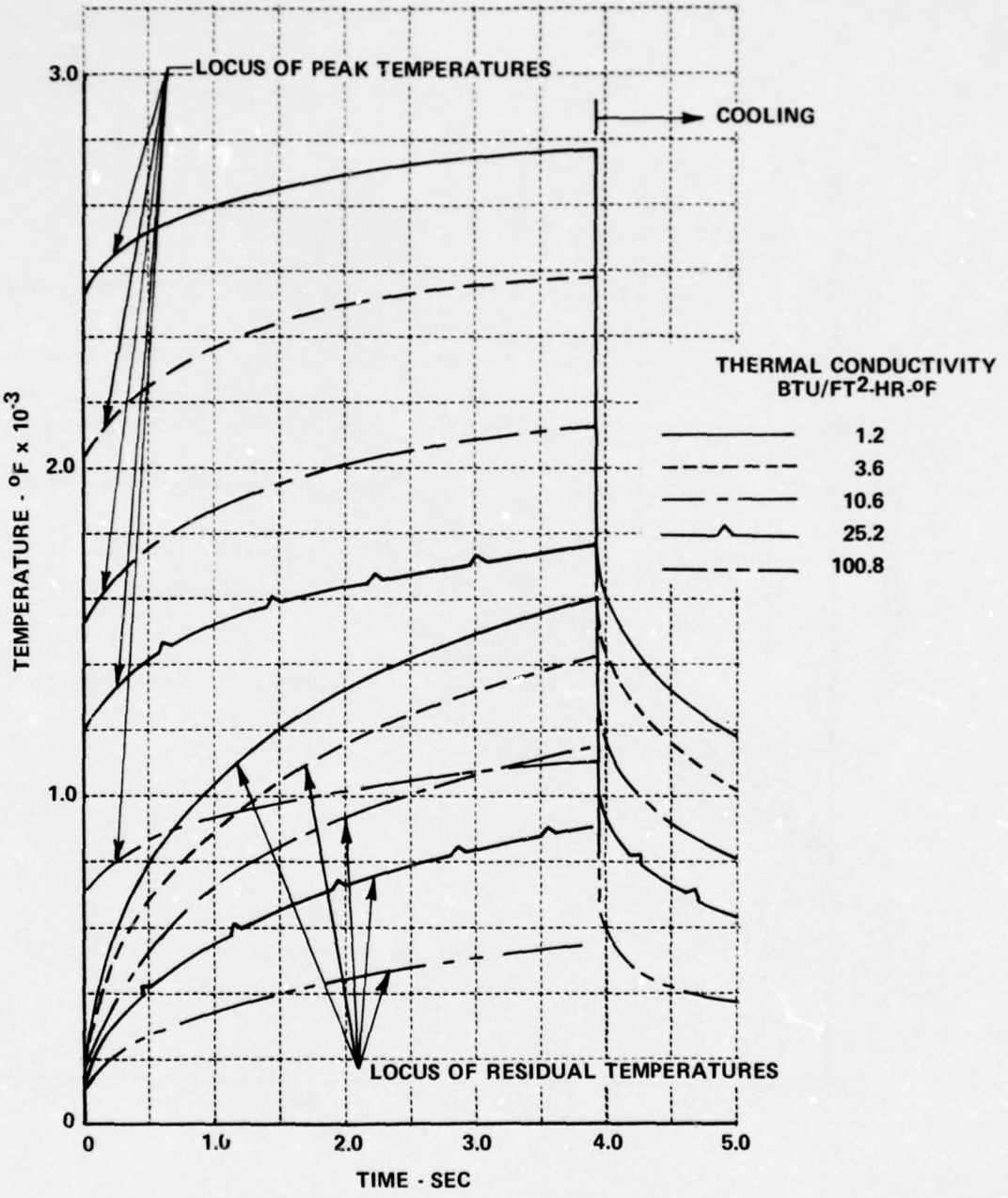

Figure 38 CALCULATED EFFECT OF THERMAL CONDUCTIVITY ON INTERNAL SURFACE TEMPERATURE AT THE STOP SHOULDER OF A 27 MM CASELESS CHAMBER DURING A 40 ROUND BURST

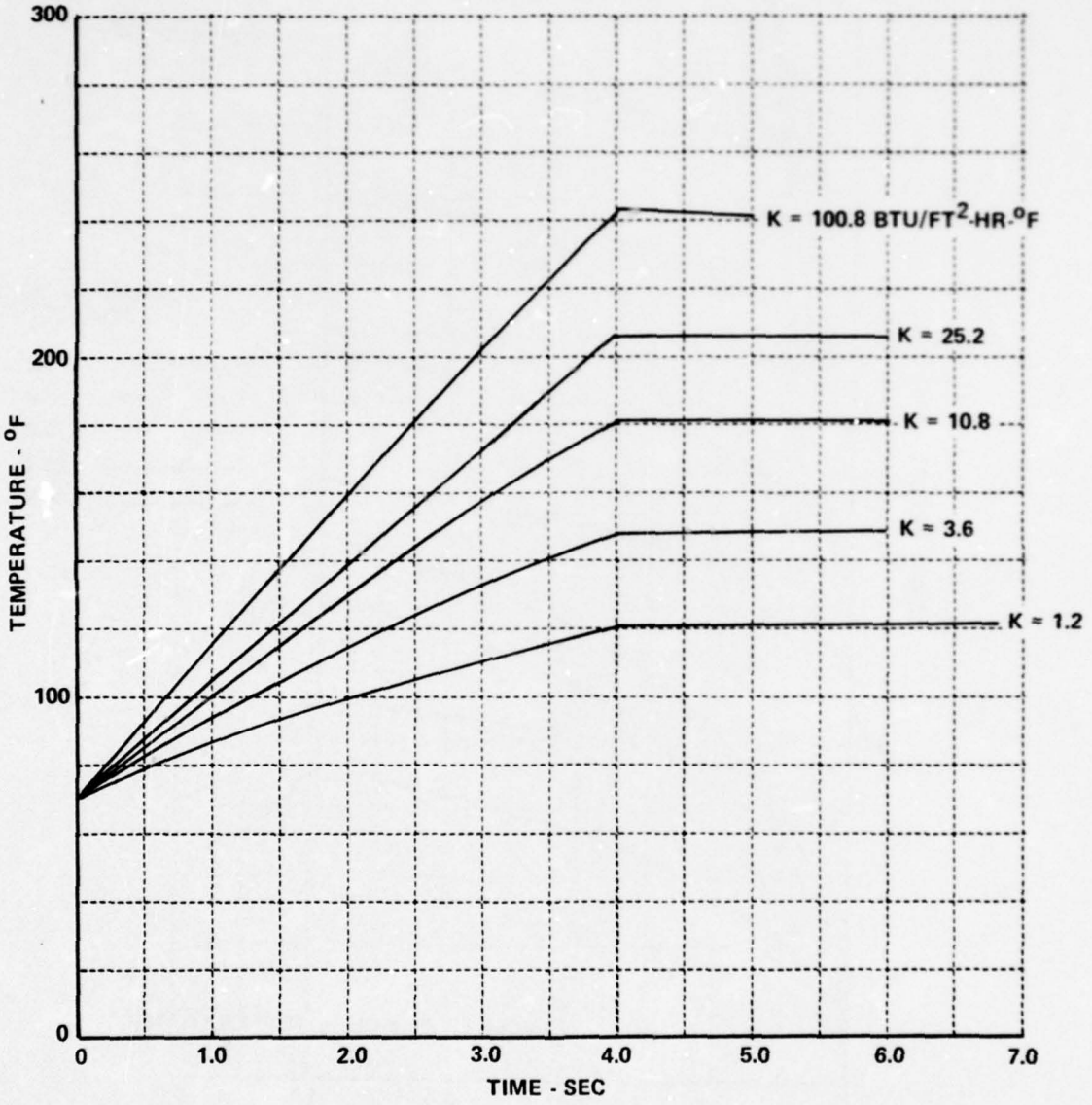

Figure 39 CALCULATED EFFECT OF THERMAL CONDUCTIVITY ON AVERAGE STOP SHOULDER TEMPERATURE FOR A 27 MM CASELESS CHAMBER DURING A 40 ROUND BURST

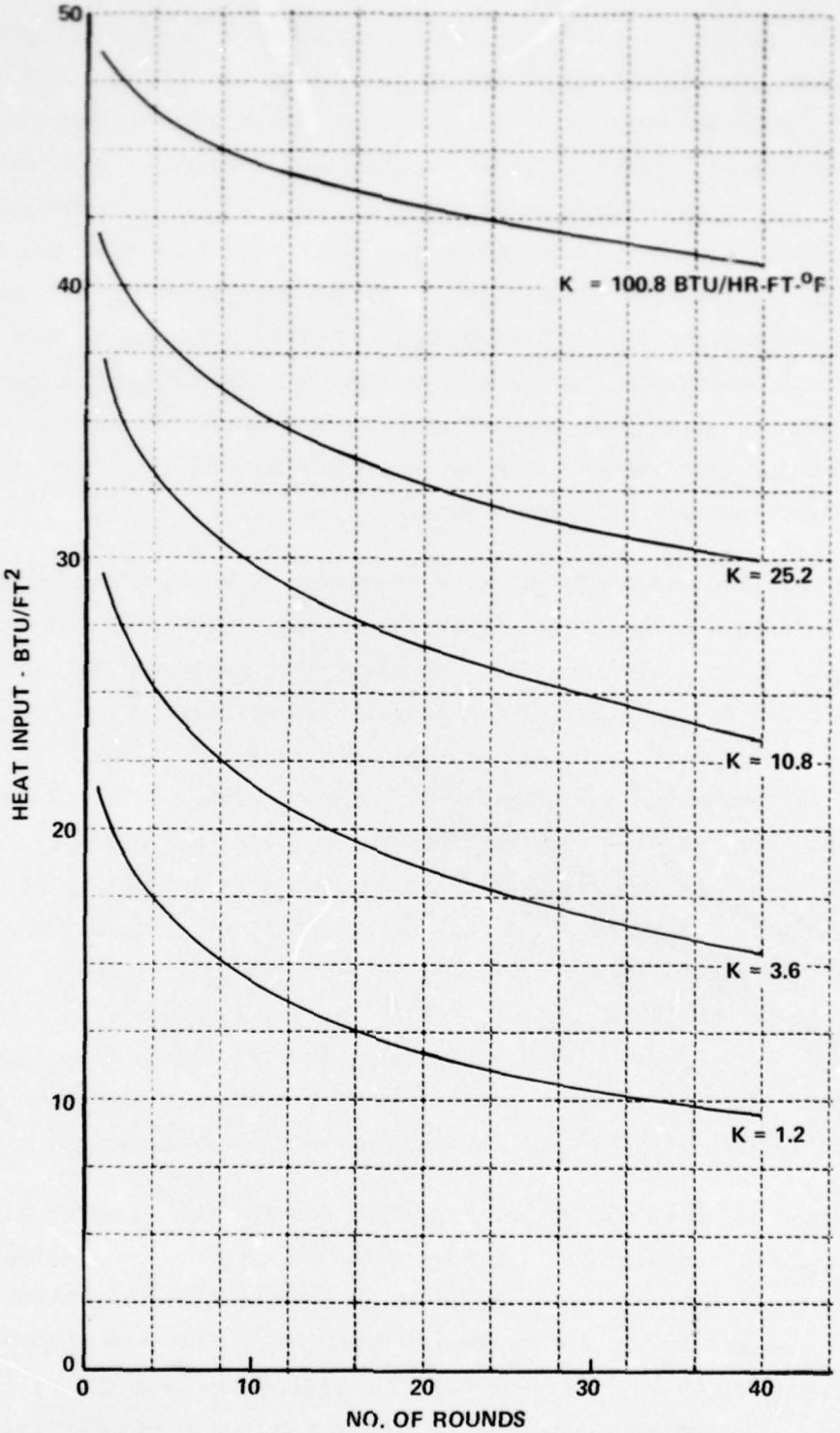

Figure 40 CALCULATED EFFECT OF THERMAL CONDUCTIVITY ON HEAT INPUT TO STOP SHOULDER FOR A 27 MM CASELESS CHAMBER DURING A 40 ROUND BURST

using multiple chambers, the lower thermal conductivity chamber materials can be superior. Where contact of the propellant to the chamber walls cannot be avoided and extended burst firing is desired, the higher thermal conductivity materials can be superior. Burst length requirements and mission-time-supply govern selection of chamber material for best cook-off performance. The effectiveness of coatings for preventing short-time cook-off also has a large influence on the final selection of chamber material. Future ammunition coating development may lead to practical use of very low thermal conductivity chamber materials. It must be recognized, however, that the primary gain in the use of low thermal conductivity chamber materials is a lowering of chamber average temperature which may also be obtained by use of ammunition coverings and/or increase of chamber mass.

Calculations were also made of temperatures in chambers internally coated with materials with several different thermal conductivities and thicknesses. Figure 41 shows the residual and average temperatures for a coating thickness of 0.020 in. and thermal conductivities varying from a ceramic (1.2 Btu/ft hr ^{o}F) to copper (226 Btu/ft hr ^{o}F). Figure 42 shows the heat input for the same circumstances. Increasing heat inputs are in order of increasing conductivities, but residual temperatures do not follow any order of conductivities. The residual temperatures after 25 rounds as a function of conductivity are shown in Figure 43. The residual temperature reaches a minimum at a conductivity of about 7 Btu/ft. hr. ^{o}F, but this residual is only about 70^{o}F less than a homogeneous chamber made of barrel steel (conductivity = 25.2 Btu/ft hr ^{o}F). The copper coating exhibits a higher residual temperature than the barrel steel because the beneficial effect of increased heat conduction away from the surface is overridden by the increased heat input to the copper.

Figure 44 shows the effect of increasing the thickness of copper coating on the residual temperature. Increased thickness decreases residual temperatures. However, a coating of even 0.100 in. thickness gives a residual temperature after 25 rounds only 30^{o}F less than barrel steel. The heat inputs for the same thicknesses are shown in Figure 45. The indication from the calculations is that it does not appear worthwhile to pursue the use of chamber coatings as a means of substantially reducing residual temperatures, thereby reducing cook-off potential.

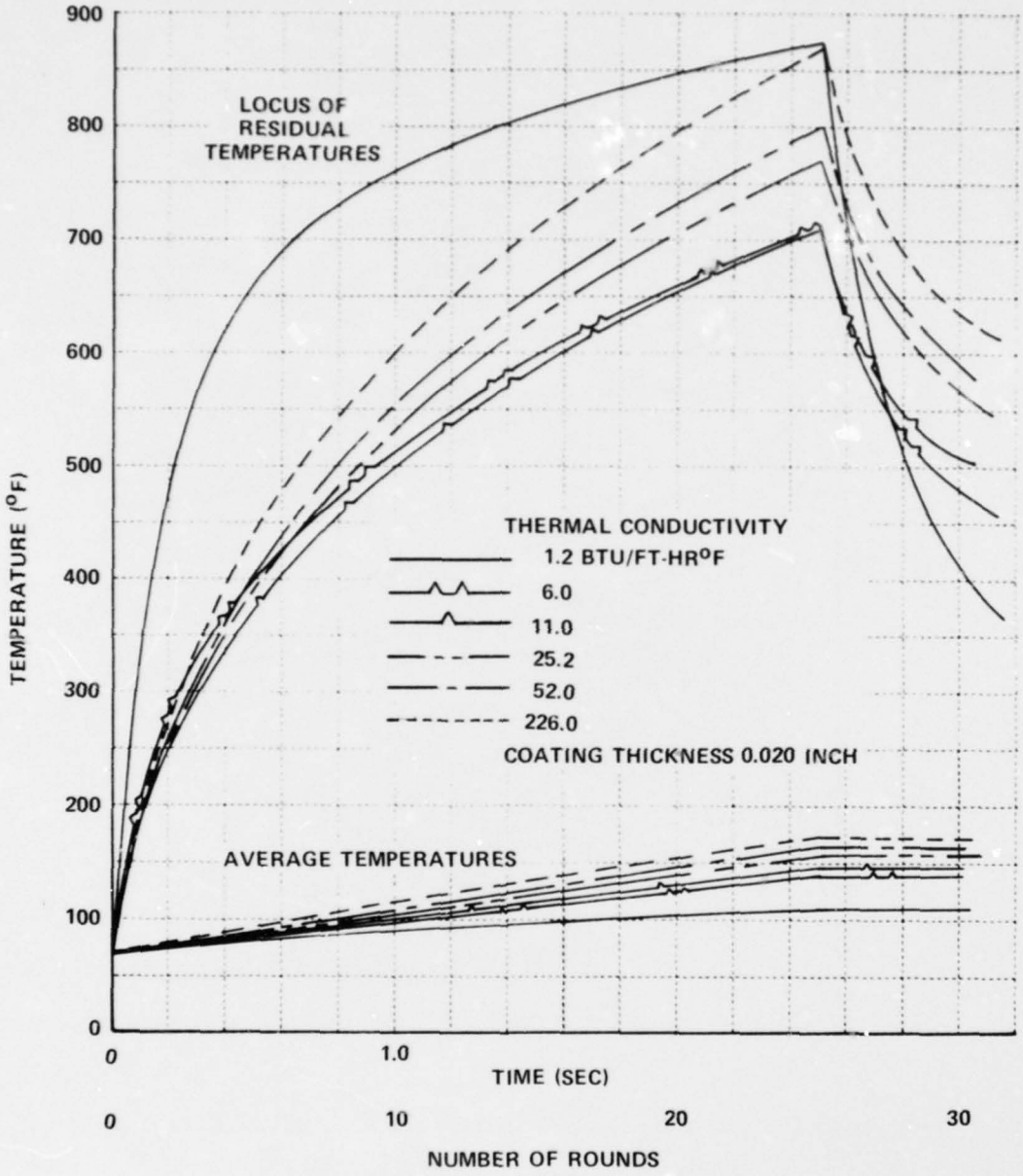

Figure 41 EFFECT OF COATING THERMAL CONDUCTIVITY ON RESIDUAL AND AVERAGE TEMPERATURES AT THE STOP SHOULDER DURING A 25 ROUND BURST (27 MM, 600 RDS/MIN)

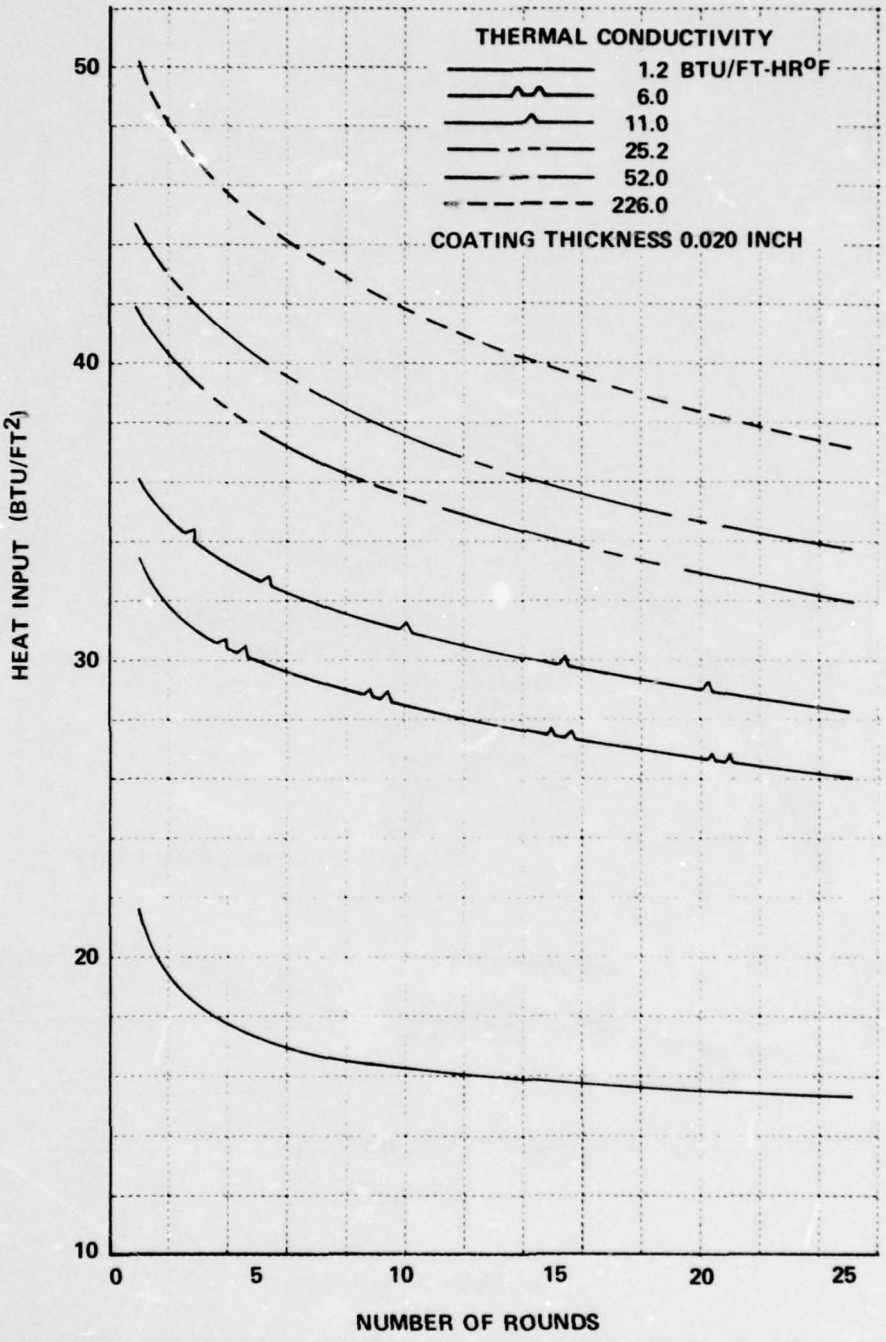

Figure 42 EFFECT OF COATING THERMAL CONDUCTIVITY ON HEAT INPUT TO STOP SHOULDER DURING A 25 ROUND BURST (27 MM, 600 RDS/MIN)

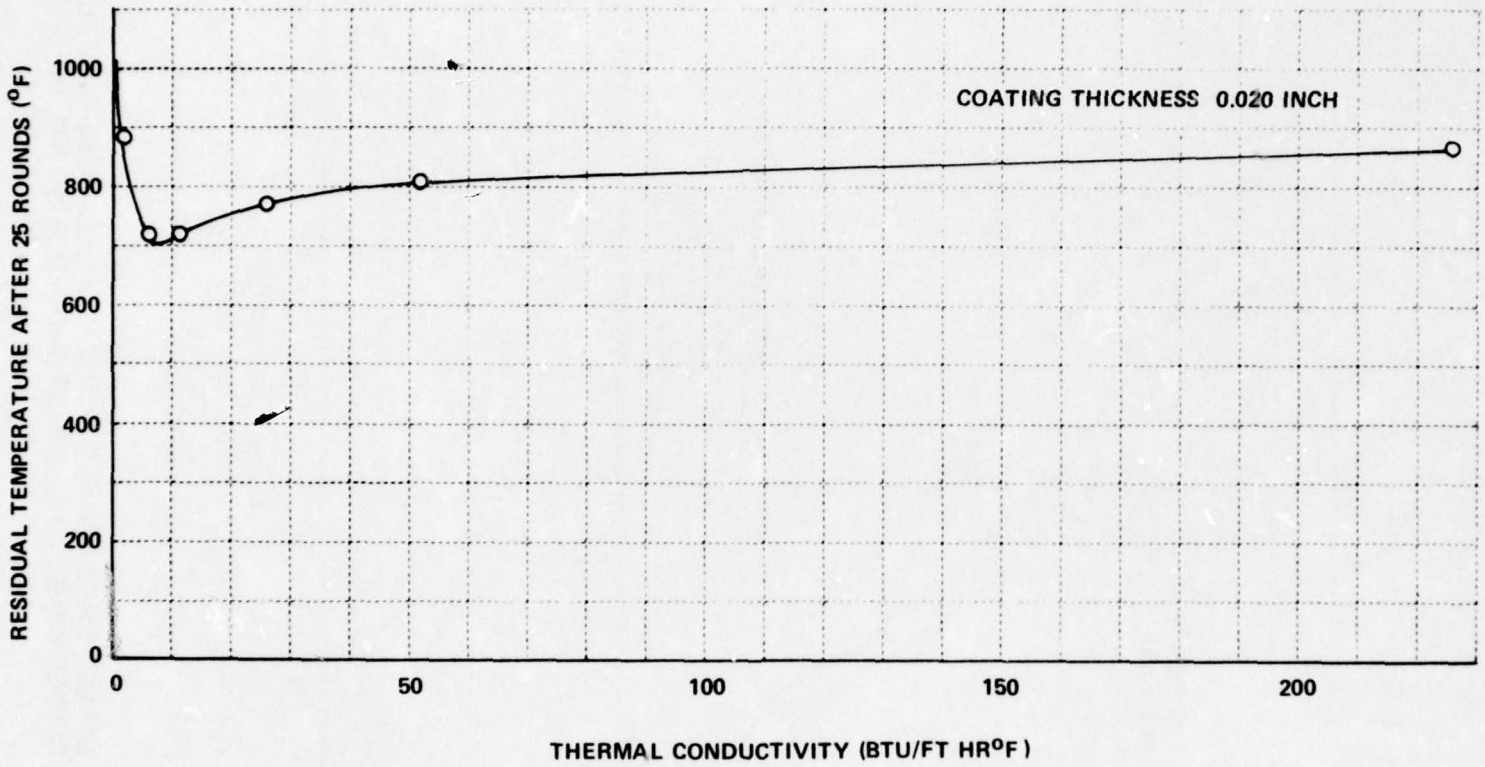

Figure 43 EFFECT OF COATING THERMAL CONDUCTIVITY ON RESIDUAL TEMPERATURE AT STOP SHOULDER AFTER 25 ROUNDS (27 MM, 600 RDS/MIN

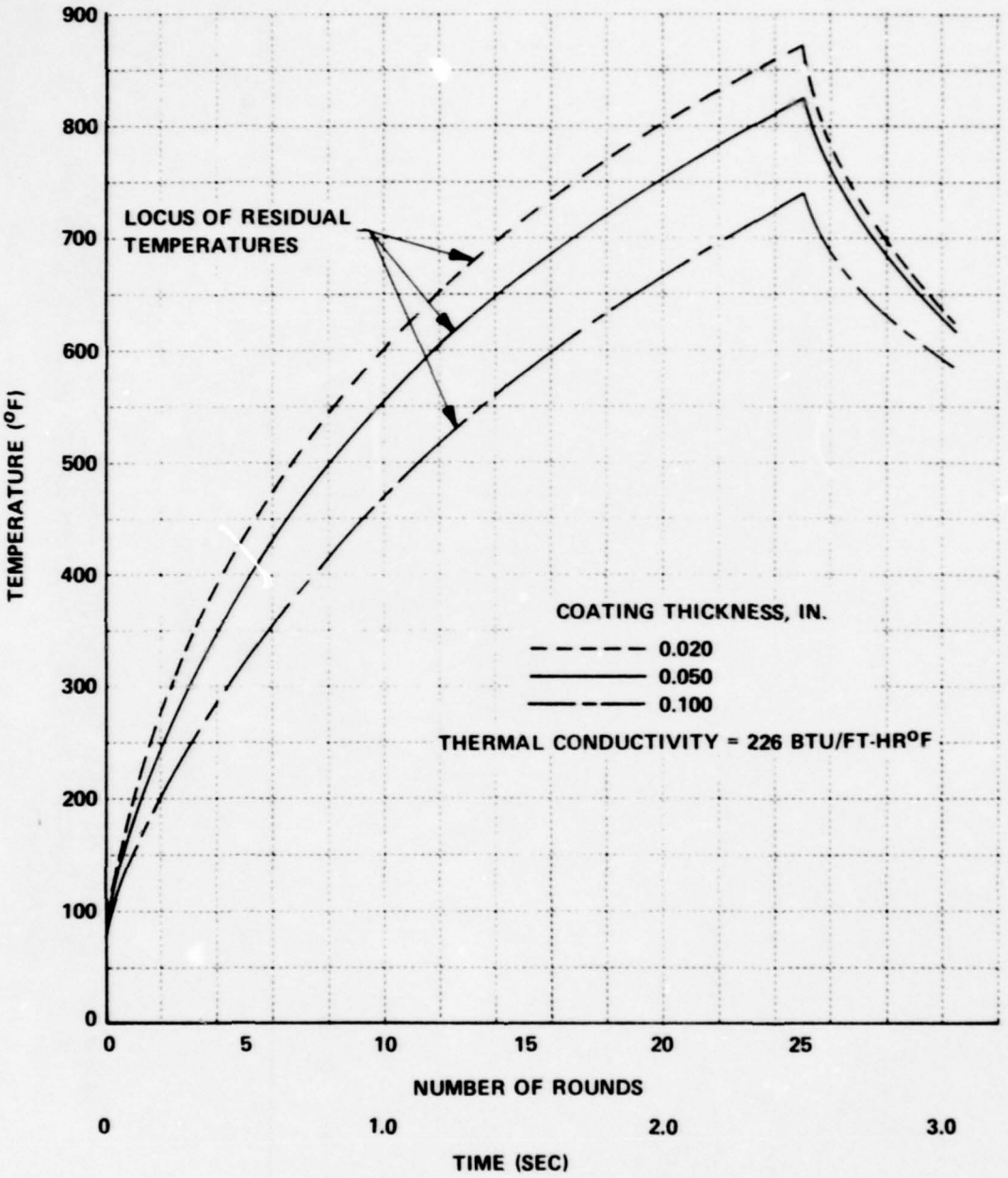

Figure 44 EFFECT OF COATING THICKNESS ON RESIDUAL SURFACE TEMPERATURE AT THE STOP SHOULDER (27 MM, 600 RDS/MIN)

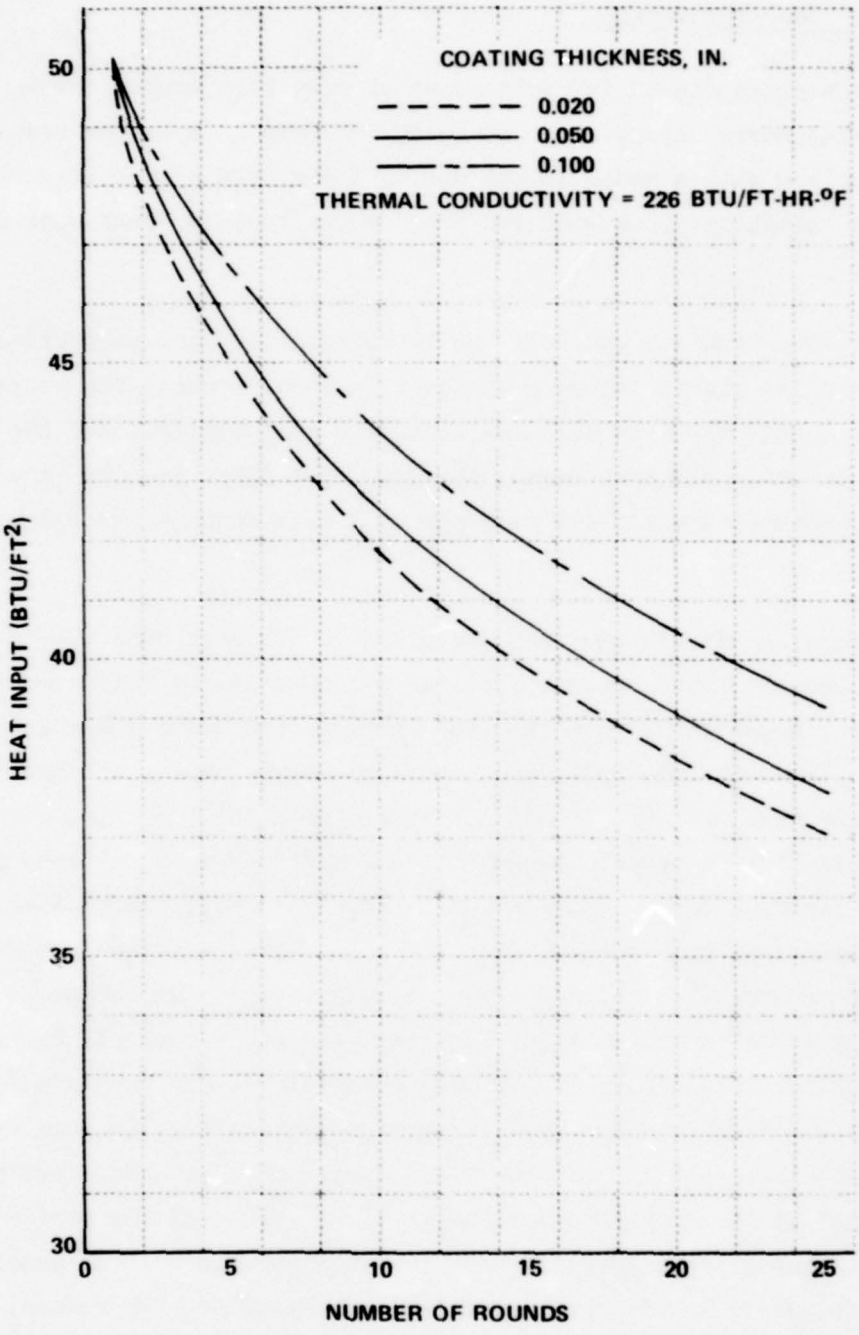

Figure 45 EFFECT OF COATING THICKNESS ON HEAT TRANSFER TO THE STOP SHOULDER (27 MM, 600 RDS/MIN)

4. Cook-Off Limits

Because the CAW-T2 is designed as an open bolt weapon, cook-off can not occur during normal operation. However, if there is a weapon stoppage due to malfunction with a round in contact with portions of the fixture, a cook-off is a possibility. During the development testing, such cook-offs have occurred.

The stop-shoulder and bolt cavity temperatures are of particular importance from the standpoint of propellant cook-off because the stop-shoulder has the highest heat input of any area contacted by propellant and the bolt cavity has a low mass per unit area. The high heat input results in high residual temperatures and the low mass per unit area results in high average temperatures.

Special considerations must be given to the most sensitive cook-off areas of the Aerojet round because the sidewall material of this ammunition is of different composition than the stop-shoulder and has a lower cook-off temperature. The cook-off limit due to residual temperatures for the sidewall material of the Aerojet round is 545^{o}F compared with 665^{o}F for the stop-shoulder material (Table XIV). However, because the sidewall heating is less, the temperatures are also less. The maximum residual sidewall temperature after firing 10 rounds was 420^{o}F (Figure 21). This is 125^{o}F less than the 545^{o}F cook-off temperature. The residual stop-shoulder temperature after 10 rounds was 550^{o}F (Figure 21) which is 115^{o}F less than its 665^{o}F cook-off limit. That is, the temperature was closer to the cook-off limit at the stop-shoulder than at the sidewall. Also, the residual temperature was increasing more rapidly at the stop-shoulder than at the sidewall. Therefore, cook-off conditions will be reached at the stop-shoulder before the sidewall of the Aerojet round. For the other rounds, the sidewalls and stop-shoulders are of the same material, and the temperature rise is greatest at the stop-shoulder. Therefore, the stop-shoulder temperatures will limit the burst length due to cook-off from residual temperatures.

Calculated stop-shoulder temperatures for the three ammunitions are given in Figure 46. All of the calculations were for the same firing rate to permit direct comparison of temperatures. The Figure also indicates the cook-off limits for each of the rounds based on data presented in Table XIV. The calculations indicate that at the firing rate of 270 rds/min, stop-shoulder cook-off conditions prevail after 12 rounds for Hercules ammunition, 22 rounds for Olin ammunition, and 25 rounds for Aerojet ammunition.

The comparison of cook-off limits among the three ammunition types is not in disagreement with the relative order of ranking of the ammunition types based on rapid-fire data. Table XVI repeats the stop-shoulder temperatures after 10 rounds given previously in Table XI for the three ammunitions and adds the cook-off temperatures given in Table XIV. The data were obtained at different firing rates which must be adjusted for valid comparisons. A higher firing rate produces higher residual temperatures, other factors being the same. Hercules ammunition is, therefore, the most susceptible to reaching cook-off temperatures at the stop-shoulder because this ammunition was fired at the lowest rate and was the only one to exceed the cook-off temperature in 10 rounds. Adjusting the firing rate of the Aerojet test to that of the Olin test suggests that the Aerojet ammunition has a cook-off limit at the stop-shoulder slightly better than the Olin ammunition. These comparisons are in general agreement with Figure 46.

Because the bolt cavity has a low mass per unit area compared with other parts of the chamber, it may be expected to be the site of severe cook-off problems. No heat input measurements were made along the sidewalls of the bolt cavity but measurements were made at the rear chamber position. These are believed to be more representative of the sidewalls of the bolt cavity than the bolt face measurements. Therefore, calculations were made of the average bolt cavity temperatures based on the heat input data for the rear chamber position. The resulting temperatures are given in Figure 47. The long-time cook-off limits are also shown in the Figure as taken from Table XV. This calculation indicates that bolt cavity cook-off would occur after 10 rounds of Aerojet ammunition, 14 rounds of Hercules ammunition, and 17 rounds of Olin ammunition.

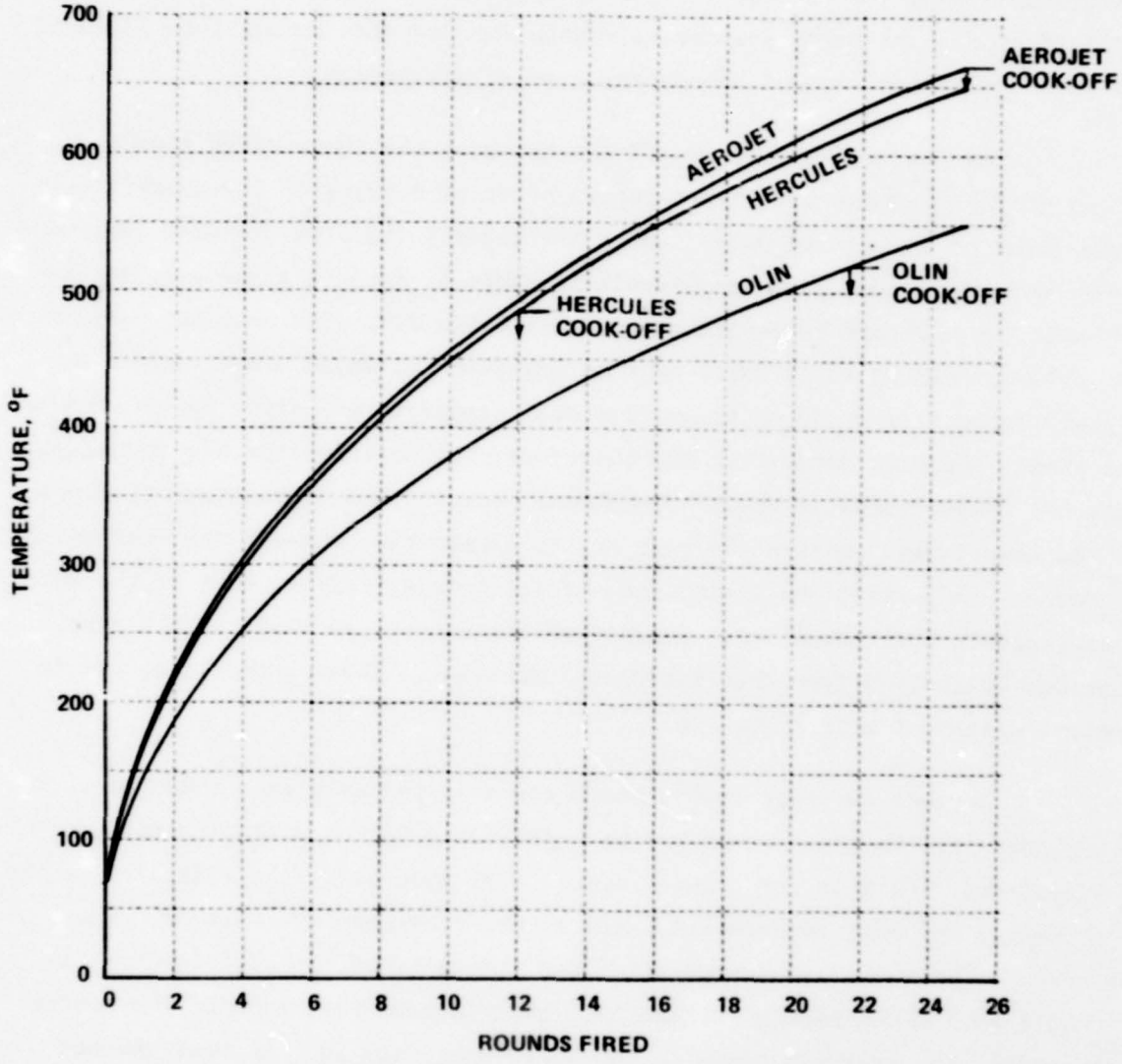

Figure 46 CALCULATED RESIDUAL STOP-SHOULDER TEMPERATURES IN 27 MM CAW-T2 FIXTURE, 270 RDS/MIN

TABLE XVI

RAPID-FIRE TEST DATA AT STOP-SHOULDER AFTER 10 ROUNDS

Ammunition	Residual Temperature, °F	Average Firing Rate, rds/min	Cook-Off Temperature,* °F	Single-Shot Heat Input,** Btu/ft^2
Aerojet	550	325	665	41.0
Hercules	505	260	490	42.1
Olin	405	278	515	33.9

* Minimum cook-off temperature of propellants in contact with steel surface cooling at 250°F/sec, Table XIV.

**Table IX.

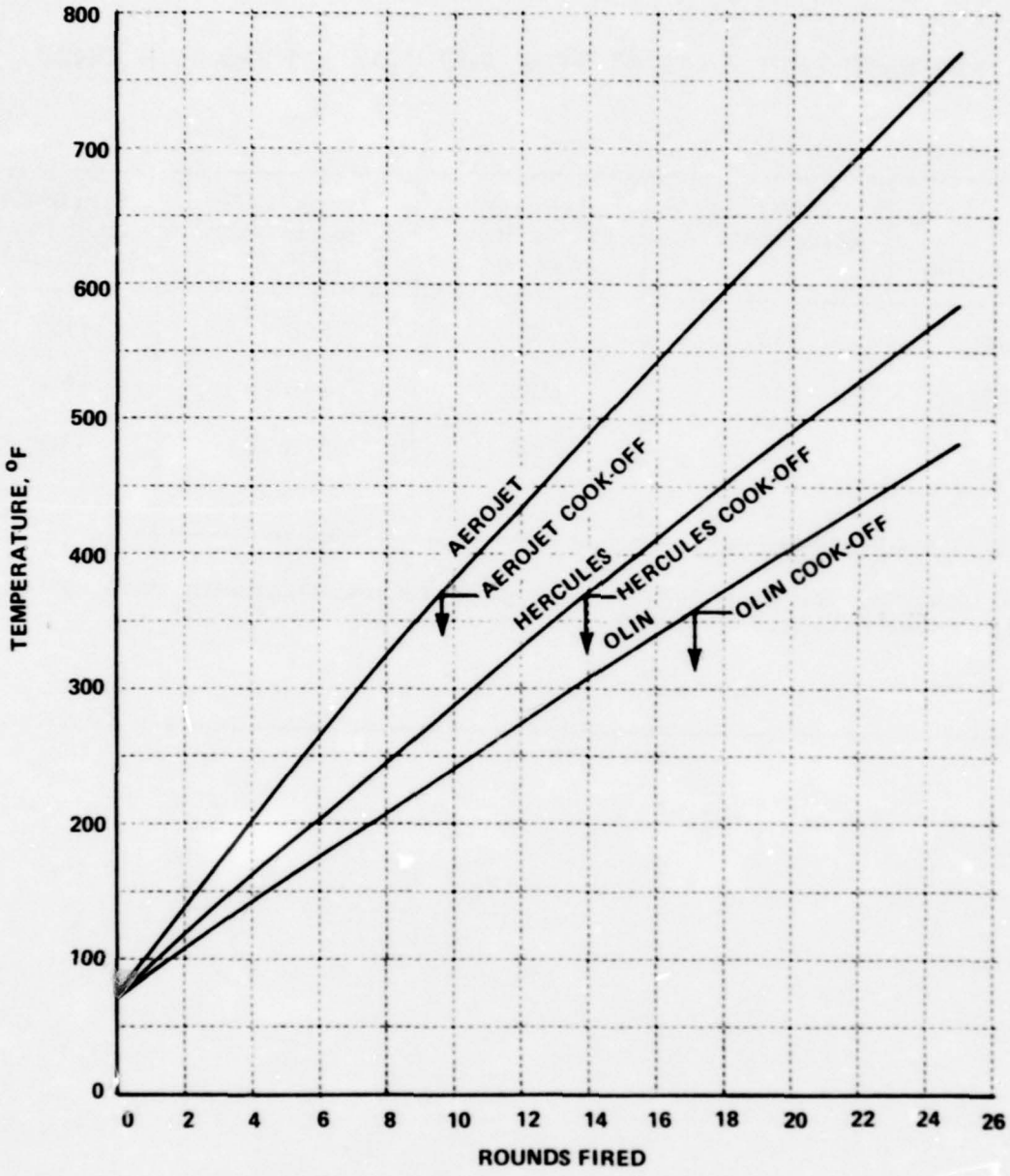

Figure 47 CALCULATED AVERAGE BOLT CAVITY TEMPERATURES IN 27 MM CAW-T2 FIXTURE, 270 RDS/MIN

Figure 46 gives the cook-off conditions at the stop-shoulder for each ammunition type. The shortest possible cook-off limit would occur at the least number of rounds to cook-off either at the stop-shoulder or bolt cavity. Taking these values from Figures 46 and 47, the resulting cook-off limits are: Aerojet, 10 rounds; Hercules, 12 rounds; and Olin, 17 rounds. These cook-off limits represent the calculation of the least number of rounds at which cook-off could occur if a round were left chambered at the end of the burst. After firing these numbers of rounds, a hazardous condition may exist. However, under certain circumstances cook-off may not occur. Of course, if no propellant were exposed to the hot surfaces, there could be no cook-off. This is the desire in an open bolt weapon but a malfunction may negate this safety feature. Also, short-time cook-off, i.e., at the stop-shoulder, requires good thermal contact. Even a relatively small amount of insulation or space between the stop-shoulder and the propellant would allow the stop-shoulder to cool significantly before the propellant were heated to cook-off temperature thereby preventing cook-off. This is not true for long-time (bolt cavity) cook-off because the average temperature remains at cook-off levels for a relatively long time--long enough to conduct across considerable insulation or air gap. This also indicates that coverings may provide significant cook-off improvement at the stop-shoulder but not at the bolt cavity. The primary influence of coverings on bolt cavity cook-off would be in the reduction of heat input to the bolt during firing. Coverings are discussed later in this section.

Several cook-offs have occurred during the rapid-fire testing. After 19, 21, 22, and 23 rounds of Hercules ammunition, delayed firings were noted (Figure 22). These firings are believed to be cook-offs after misfires because the firing pin probably would not have had sufficient impact energy if it had been delayed as long as the temperature records show. Cook-off after these numbers of rounds could have occurred either at the stop-shoulder or the bolt cavity according to the calculations. However, the temperature data give no indication that stop-shoulder cook-off occurred. If there had been cook-off at the stop-shoulder, the in-wall thermocouple would be expected to show a

slow temperature rise while the burning begins. This slow temperature rise has been noted in 5.56mm caseless ammunition tests (Figure 10). No such indication of cook-off occurred in the 27mm Hercules ammunition test. It is, therefore, postulated that poor thermal contact existed at the stop-shoulder and that cook-off occurred at the uninstrumented bolt cavity location.

At 9.55 sec after a 10 round burst of Aerojet ammunition, an ignition occurred (Figure 21). The eleventh round was chambered with the bolt partially locked. The time interval before cook-off indicates a cook-off due to average temperature. The calculations indicate that bolt cavity temperatures should have been just capable of causing cook-off after 10 rounds (Figure 47).

After a 15 round burst of Olin ammunition, a fire occurred which consumed the remaining 10 rounds in the feeder. In this test an over feed caused the gun stoppage. No heating was noted at any instrumented location for 13 sec after the gun stoppage indicating that there was no cook-off at any of these locations within this time. The calculations of cook-off limits indicate that cook-off could not occur until 17 rounds (Figure 47). The bolt of the CAW-T2 contains a seal around its outside surface (Figure 20). This seal is exposed to hot gases during heating and has a very low mass per unit area and, therefore, could be expected to heat very rapidly during a burst. During normal operation, the seal does not contact propellant. However, during an overfeed the propellant may contact the seal and an ignition could result. This type of ignition has also been noted in other tests without thermal instrumentation and one such test was photographed with high speed movies.[9] Evidently, bolt seal cook-off is an additional type of cook-off that must be protected against, presumably by better round control during feeding.

5. Covered Caseless Ammunition

In this section of the report, temperatures at the stop-shoulder of the CAW-T2 27mm caseless fixture firing covered ammunition were calculated for comparison with temperatures while firing uncovered ammunition. The

average heat reductions measured for covered ammunition in the CAW-T2 as given in Table XIII were used in the calculations. There was considerable round-to-round variation in the heating of covered rounds so that the average values used may not precisely represent a true average value because of the relatively small sample size. However, the calculations based on average values should give an indication of the temperature reductions that can be expected while firing covered ammunition. The coverings were applied by Calspan to rounds supplied by Aerojet, Hercules, and Olin. The coverings consisted of a 0.018 in. thick cellulose-acetate-butyrate cap over the stop-shoulder and a 0.007 in. thick mylar sleeve extending 1.9 in. back from the stop-shoulder. Figure 19 is a drawing of the covered round. The knob on the rear of the round was not covered, and therefore, other corrective measures, such as a special knob covering or elimination of the knob, would be required to prevent cook-off in the bolt cavity. The present calculations are concerned only with the stop-shoulder.

The calculated stop-shoulder temperatures are shown in Figures 48, 49, and 50 for both covered and uncovered versions of the three types of rounds. Temperatures were calculated for 50-round bursts of covered ammunition and 25-round bursts of uncovered ammunition. These calculated temperatures are in general agreement with temperatures measured in rapid fire to the end of the burst although firing rates varied in the tests causing differences and, particularly for the covered rounds, round to round variations make comparisons difficult. Therefore, the curves of Figures 48, 49, and 50 may be used as a more convenient source of comparison than the measured temperatures. In addition, longer bursts were calculated than could be fired.

The residual and average temperatures are the important temperatures from the standpoint of number of rounds that may be fired without a cook-off possibility. For uncovered rounds, cook-off at the stop-shoulder will occur first because of the residual temperature. Cook-off of uncovered rounds was discussed in the preceding section. For covered ammunition, it was shown in Reference 2 that cook-off due to residual temperatures could effectively be eliminated by the insulation of the propellant from the hot chamber walls.

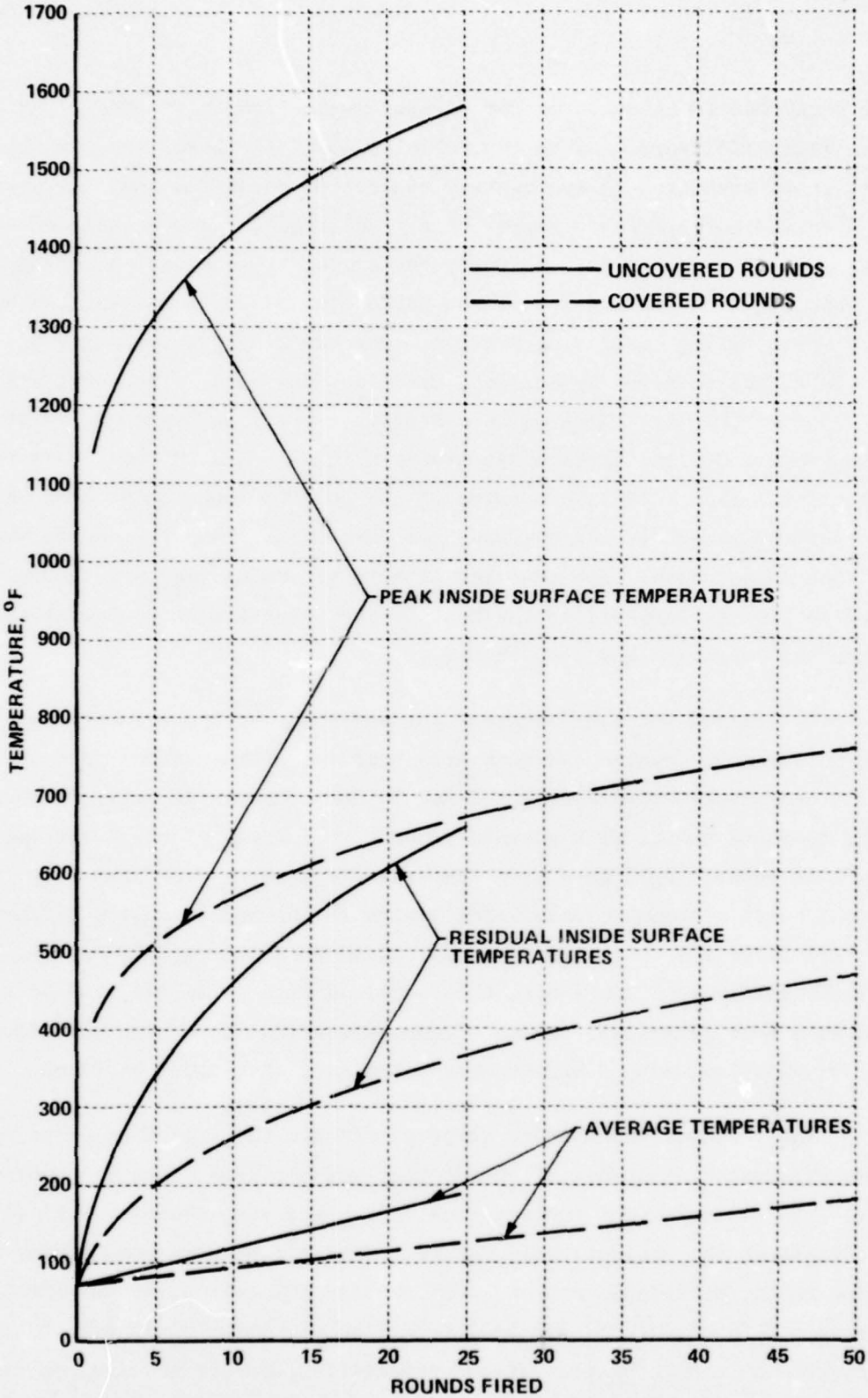

Figure 48 CALCULATED STOP-SHOULDER TEMPERATURES FOR 27 MM AEROJET CASELESS AMMUNITION IN CAW-T2 FIXTURE, 270 RDS/MIN

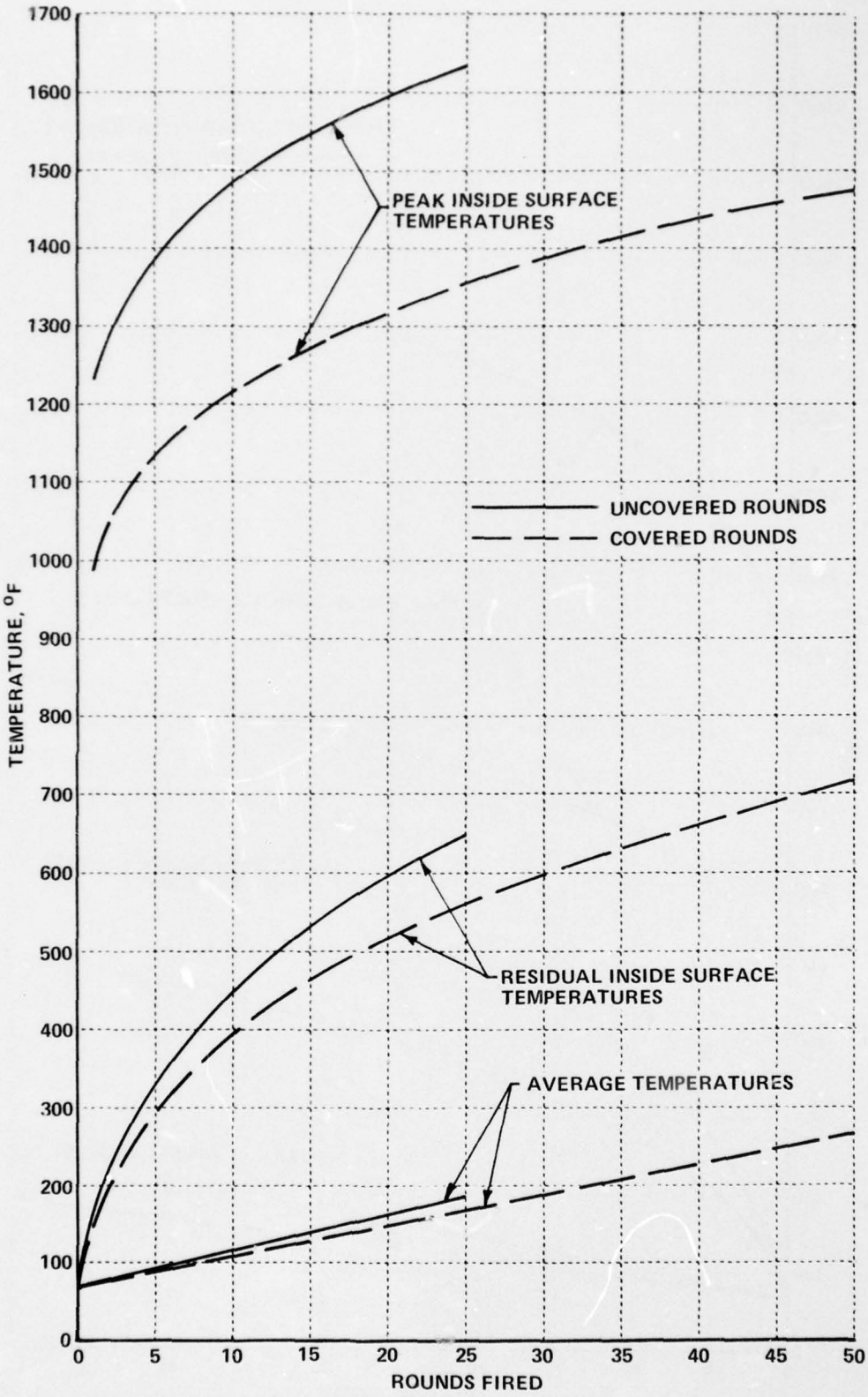

Figure 49 CALCULATED STOP-SHOULDER TEMPERATURES FOR 27 MM HERCULES CASELESS AMMUNITION IN CAW-T2 FIXTURE, 270 RDS/MIN

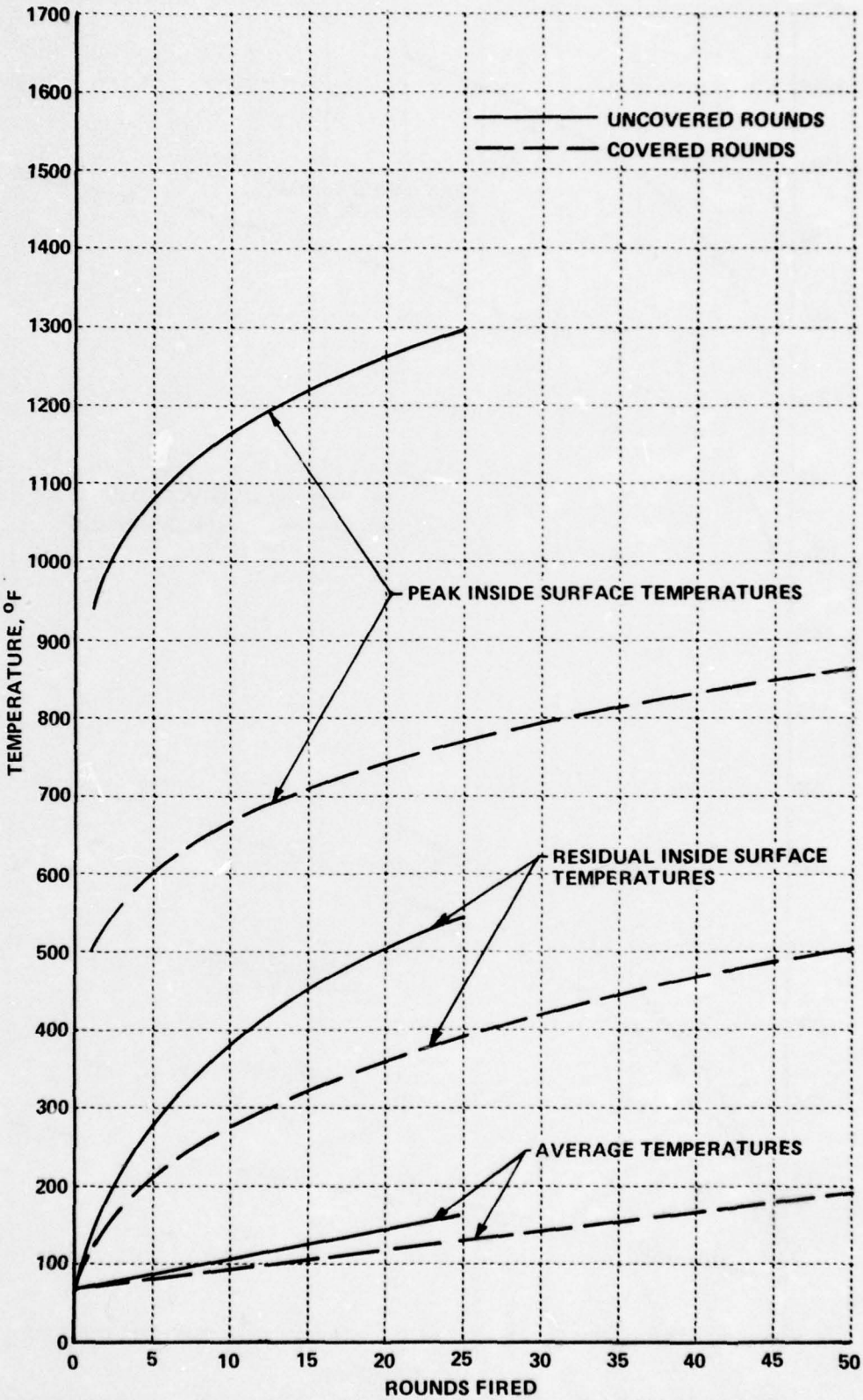

Figure 50 CALCULATED STOP-SHOULDER TEMPERATURES FOR 27 MM OLIN CASELESS AMMUNITION IN CAW-T2 FIXTURE, 270 RDS/MIN

With cook-off due to residual temperature eliminated for covered rounds, cook-off due to average temperature becomes the sole cook-off criterion.

The average (i.e., long-time) cook-off temperature limits are given in Table XV. The values are 350°F for Aerojet rounds, 375°F for Hercules rounds, and 360°F for Olin rounds. None of the average temperatures have reached these cook-off limits in the calculated 50-round bursts of Figures 48, 49, and 50. The number of rounds required for cook-off can be estimated by extrapolation of the average temperature curves in the figures. The results of such an extrapolation are given in Table XVII along with uncovered round cook-off data presented in the previous section. The data in Table XVII indicate the substantial improvement in stop-shoulder cook-off limits that can be obtained with coverings. The cook-off limits are comparable to the number of rounds per chamber that may be fired without cook-off in a cased gun of about the same caliber.

TABLE XVII

STOP-SHOULDER COOK-OFF DATA FOR COVERED AND UNCOVERED 27MM CASELESS AMMUNITION

Round Type	Short-Time Cook-Off Temp., °F	Long-Time Cook-Off Temp., °F	No. of Rds. to Cook-Off	Cook-Off Type
Aerojet	665	350	25	Short-Time
Covered Aerojet	>1000	350	124	Long-Time
Hercules	490	375	12	Short-Time
Covered Hercules	>1000	375	80	Long-Time
Olin	515	360	22	Short-Time
Covered Olin	>1000	360	120	Long-Time

REFERENCES

1. Vassallo, F.A., Adams, D.E., and Taylor, R.D., "Caseless Ammunition Heat Transfer," Calspan Report No. GI-2433-Z-1, October 1967.

2. Vassallo, F.A., and Adams, D.E., "Caseless Ammunition Heat Transfer, Volume II," Calspan Report No. GI-2758-Z-1, October 1969.

3. Brown, W.R., "Coatings for Caseless Ammunition," Calspan Report No. GI-2461-Z-1, Feburary 1968.

4. Brown, W.R., "Protective Coverings for Caseless Ammunition," Calspan Report No. GI-2771-Z-1, Feburary 1970.

5. Brown, W.R., and Sudlik, D.J., "Protective Coverings for 5.56mm and 27mm Caseless Ammunition," Calspan Report No. GM-3012-D-1, July 1972.

6. Vassallo, F.A., "Mathematical Models and Computer Routines Used in Evaluation of Caseless Ammunition Heat Transfer," Calspan Report No. GM-2948-Z-1, June 1971.

7. Adams, D.E., "Heat Transfer From 5.56mm Cased Ammunition and Ignition Characteristics of 5.56mm Caseless Ammunition," Calspan Report No. GM-2948-Z-2, April 1976.

8. Scheuren, J., "Final Report of Engineering Test of Cartridge, 5.56mm, Tracer, XM196," Aberdeen Proving Ground Report DPS-1687, June 1965.

9. Williams, Dean S., "27mm Experimental Caseless Firing Fixture Test Program CAW-T2," Philco-Ford Corporation No. U-4958, 10 August 1972.

APPENDIX A

MATHEMATICAL MODELS AND COMPUTER ROUTINES USED IN EVALUATION OF CASELESS AMMUNITION HEAT TRANSFER

TABLE OF CONTENTS
FOR APPENDIX A

Section		Page
	LIST OF ILLUSTRATIONS	117
	INTRODUCTION	118
I.	HEAT TRANSFER COEFFICIENT AND PROPELLANT GAS TEMPERATURE	119
	A. Projectile Velocity and Position	119
	B. Total Heat Input	121
	C. Estimated Propellant Gas Temperature	123
	D. Estimated Heat Transfer Coefficient Histories	125
	E. Input Format	129
	F. Program Listing	132
	G. Program Output	133
	Computer Listing	134
	Flow Charts	147
	Master Input Format	149
	Sample Computer Output	151
II.	COMPOSITE CYLINDRICAL CONDUCTION HEAT TRANSFER COMPUTER PROGRAM	163
	List of Symbols for Section II	162
	A. Geometrical Considerations	163
	B. Heat Input Parameters	167
	C. Time Factors	168
	D. Output and Print Intervals	170
	E. Heat Conduction Relations	171
	1. Radial Conduction	171
	2. Axial Conduction	176
	F. Computer Routine	177
	G. Input Format	177
	H. Output Format	179

TABLE OF CONTENTS
FOR APPENDIX A (Cont.)

Section		Page
	Computer Listing	181
	Flow Charts	192
	Master Input Format	194
	Sample Computer Output	208
III.	REFERENCES	219

LIST OF ILLUSTRATIONS

Figure No.		Page
A1	Cross Sectional View at a Typical Chamber Axial Section . .	164
A2	Typical Axial Chamber Sections	166
A3	Time Factors for Computer Simulation of Rapid Fire	169
A4	General Subdivision of Axial Sections into Radial Elements .	172

INTRODUCTION

Heat transfer rates as they influence weapon temperatures have direct bearing upon both weapon design and effectiveness of the weapon system. Heat transfer effects are especially important where caseless ammunition is utilized. Chamber wall temperatures can produce thermally initiated firings (cook-off) in extremely short periods (within milliseconds) if little regard is given to heat transfer factors in weapon and/or ammunition design. Through continuing efforts in this study program, methods by which heat transfer factors can be taken into account are under investigation. In this work it has been regarded most accurate and efficient to evaluate the prime heat transfer parameters by a combined experimental-analytical approach and to evaluate influences through computer simulation of rapid fire conditions. The following sections deal with computer models presently in use at this laboratory for these evaluations. Section I describes the experimental-analytical approach by which heat transfer parameters are obtained through computer calculations. Section II discusses application of these parameters to simulated rapid fire through a computer routine. To allow more general application, the two computer routines are not directly linked. Hence, they are treated separately in the report.

I. HEAT TRANSFER COEFFICIENT AND PROPELLANT GAS TEMPERATURE

The purpose of the heat transfer coefficient (HTC) computer program is to convert experimentally determined single-shot heat transfer and ballistics information to a form compatible with the requirements of the composite cylindrical conduction routine discussed in Section II. Prime output information from the HTC routine is therefore:

1. A heat transfer coefficient history at each selected chamber and barrel point of interest.
2. A propellant gas temperature history at each corresponding point.

Secondary output information is:

1. The projectile velocity within the barrel.
2. The projectile position in the barrel.

The input information consists of thermophysical constants, gun geometry, and experimentally determined test data. The thermophysical constants are the adiabatic flame temperature; the gas constant; the specific heat, density, and thermal conductivity of the barrel material; the specific heat at constant volume for the propellant gas; the specific co-volume of the gas; and the ratio of specific heats of the gas. The geometric constants are the inner and outer radii and position from the origin of rifling for each selected position of interest, the chamber length and volume, and the length of the barrel. The experimentally determined input data consist of a breech pressure-time tabulation, the projectile weight, the weight of charge, the muzzle velocity, the time-to-muzzle, and sufficient information to allow determination of the total heat input per unit area as discussed under subsection B, Total Heat Input.

A. Projectile Velocity and Position

The projectile velocity and position within the barrel is estimated by impulse-momentum considerations. Motion of the projectile is considered

to be governed by the relation

$$\int_0^t P_s A dt - F \int_0^t dt = mV(t) \qquad (1)$$

where

P_s is the base pressure on the projectile,
A is the base area of the projectile,
m is the mass of the projectile,
F is a frictional restraining force,
t is the time after pressure increase,
V is the projectile velocity.

The base pressure is taken to be a constant fraction of the input breech pressure as given by the LaGrange corrections*

$$P_s = \frac{P_B}{\left[1 + \frac{w_o}{2w_p}\right]} \qquad (2)$$

where

P_B is the breech pressure,
w_o is the charge weight,
w_p is the projectile weight.

Because the breech pressure is known as an input parameter as well as muzzle time, muzzle velocity, and barrel length, one can determine the value of F required to achieve the correct muzzle velocity at the input muzzle time. Hence,

$$F = \frac{1}{t_m}\left[\int_0^{tm} \frac{P_B A dt}{\left(1 + \frac{w_o}{2w_p}\right)} - m V_m\right] \qquad (3)$$

where

V_m is the muzzle velocity,
t_m is the muzzle time.

*See Ref. 1, p. 219.

Once a value of F has been established, the estimated projectile velocity as a function of time is obtained from Equation 1.

The projectile position within the barrel (distance traveled) is estimated by integration of the projectile velocity history. Integration to the muzzle time should result in the correct barrel length. Because there is likely to be more error in the input muzzle time than in the input barrel length, any discrepancy between projectile travel at the muzzle time and barrel length is taken to be error in input muzzle time. For this reason, the muzzle time is adjusted by the ratio

$$t_{m_o} = t_m \left[1 + 0.6\left(\frac{L}{s_L} - 1 \right) \right] \tag{4}$$

where

t_{m_o} is corrected muzzle time,
s_L is the projectile travel at time t_m,
L is the barrel length.

Values of F, V(t), and projectile position, s, are then recalculated. This iteration is continued until the calculated projectile travel at the muzzle time agrees to within a specified fraction of the input barrel length. Because the above calculation is dependent for the most part on the barrel length and muzzle velocity, significant error in the input muzzle time may be tolerated. In fact, a mere estimate of the time-to-muzzle of

$$t_m = 2 \frac{L}{V_m} \tag{5}$$

will result in adequate convergence.

B. Total Heat Input

At eight selected chamber and barrel points of interest, information relative to total heat input per unit internal area must be given. This computer routine can accept three types of heat input indicators:

1. Direct specification of total heat input per unit area per round.

2. The measured external barrel temperature rise per shot at any point of interest.

3. The measured temperature at a time greater than 50 t_m given by an in-depth thermocouple placed within 0.015 in. of the inner (bore) surface.

Direct specification of the total heat input per unit area at points of interest along the chamber or bore requires no computation by the machine. These input values are used directly in subsequent calculations. Of course, heat input values are generally not directly evaluated experimentally, but this input format allows previously determined heat input values to be used if desired.

The total heat input to the bore (or chamber) per unit internal area is determined by the computer using experimentally determined temperature information of types 2 and 3 above. Where the barrel wall is thin, for example, at locations near the muzzle, total heat input per square foot per round can be obtained through simple external barrel temperature measurements and the relation

$$Q_{in} = \frac{\pi C\rho \, (R_2^2 - R_1^2)\Delta T}{(2\pi R_1 + 2N\mathcal{E})} \tag{6}$$

where

Q_{in} is the total heat input per square foot per round - Btu/ft^2-rd,

$C\rho$ is the heat capacity of the barrel material per unit volume - $Btu/ft^3 \cdot F$,

R_2 is the outer radius,

R_1 is the inner radius measured to the midpoint of the land and groove,

N is the number of rifling projections,

$\mathcal{E}$ is the rifling projection height,

ΔT is the external barrel temperature rise.

When $C\rho$, R_2, R_1, N, $\mathcal{E}$, and ΔT are input for any station, Q_{in} is calculated using Equation 6.

At locations where the barrel is thick, for example, within or at a short distance from the breech, axial conduction effects will limit the applicability of the simple external temperature measurements for determination of Q_{in}. At these locations, in-depth thermocouples placed a short distance from the bore surface can be effective in determining the bore heat input. As described in the appendix, the heat input is given by

$$Q_{in} = \sqrt{\pi k C \rho \theta_o} \quad \frac{\Delta T(\theta_o)}{\eta(R_1)} \tag{7}$$

in which additional terms are:

k	is the thermal conductivity of the barrel material,
$\Delta T(\theta_o)$	is the in-depth temperature rise at time, θ_o,
θ_o	is the time after firing,
$\eta(R_1)$	is a correction factor for radius as given in the appendix.

In general, the in-depth thermocouples should be within 0.015 in. of the bore surface, and the time, θ_o, at which $\Delta T(\theta_o)$ is measured should be beyond 50 t_m. The in-depth technique operates most accurately where barrel thickness is great. Refer to the appendix for details of the method. When $\Delta T(\theta_o)$ at corresponding time, θ_o, is input to the machine, Q_{in} is calculated using Equation 7.

C. Estimated Propellant Gas Temperature

The propellant gas temperature while the projectile is in the bore can be estimated once the projectile position and total heat loss have been determined. The propellant gas temperature is obtained by combining an equation of state for the gas with the energy equation. The state equation, taken from Ref. 1, and selected for computational purposes is

$$T_g = \frac{P_m [As + V_{ch} - (spv) w_o]}{R\zeta} \tag{8}$$

in which

T_g	is the propellant gas temperature - °R,
V_{ch}	is the chamber volume,
spv	is the average of the specific co-volume of the propellant gas and solid,
R	is the gas constant,
ζ	is the amount of propellant burned,
P_m	is the space mean pressure behind the shot.

Again, using the LaGrange corrections, the space mean pressure is expressed in terms of the breech pressure as

$$P_m = \frac{P_B}{\left[1 + \frac{w_o}{3w_p}\right]} \tag{9}$$

The energy equation is taken as

$$(Q_{loss} + W_k) = C_v \zeta (T_A - T_g(t)) \tag{10}$$

where

Q_{loss}	is the total heat loss to the chamber walls up to time, t,
W_k	is the work done on the projectile up to time, t,
C_v	is the specific heat of the propellant gas at constant volume,
T_A	is the adiabatic flame temperature.

Eliminating the amount of propellant burned by simultaneous solution of Equations 8, 9, and 10, one gets

$$T_g = T_A \left[1 - \frac{\left[Q_{loss} + W_k\right]}{\left\{ \left[Q_{loss} + W_k\right] + \frac{P_B C_v (As + V_{ch} - (spv)w_o)}{R\left[1 + \frac{w_o}{3w_p}\right]} \right\}} \right] \tag{11}$$

as the working equation for the propellant gas temperature up to the muzzle time. Computer solution of this equation is accomplished by incrementing the time in finite steps from the start of pressure increase. The heat loss

as a function of time is approximated by taking area-time percentages of the total heat input, Q_{in}, calculated earlier. The work done by the gas on the projectile is determined by summing the product of average force on the projectile and distance traveled, i.e.,

$$W_k = \sum_{o}^{t + \Delta t} \left[\frac{P_s\big|_t + P_s\big|_{t+\Delta t}}{2} \right] A \, (S_{t + \Delta t} - S_t) \tag{12}$$

After the projectile has left the barrel, it is assumed that the remaining gas exhausts from the barrel in an adiabatic expansion with acoustic velocity at the muzzle. The pressure decay in this period is obtained by use of the simplified relation*

$$P_B = P_{Bm} \left(1 + \frac{t - t_m}{Z} \right)^{-\frac{2K}{K-1}} \tag{13}$$

where

$$Z = \frac{2 (V_{ch} + AL)}{(K-1) A} \sqrt{\frac{1}{KRT_{gm}} \left(\frac{K+1}{2} \right)^{\frac{K+1}{K-1}}} \tag{14}$$

and T_{gm} is the propellant gas temperature at the muzzle time,
P_{Bm} is the breech pressure at the muzzle time.

The propellant gas temperature decay is then obtained using

$$T_g / T_{gm} = \left(P_B / P_{Bm} \right)^{\frac{K-1}{K}} \tag{15}$$

D. Estimated Heat Transfer Coefficient Histories

Effective heat transfer coefficients at chamber and barrel positions for which heat input information is given are estimated by an iterative technique

* Modified form of the Hugoniot relation given in Ref. 1.

which results in the correct single-shot heat input. The heat transfer coefficient is defined as

$$h_g(t) = \frac{q(t)}{\left[T_g(t) - T_w(t)\right]} \tag{16}$$

where

$h_g(t)$ is the heat transfer coefficient,
$q(t)$ is the heat flux to a surface of temperature T_w,
$T_g(t)$ is the propellant gas temperature,
$T_w(t)$ is the temperature of the surface absorbing $q(t)$.

The heat transfer coefficient is assumed to follow the form for tube flow, or

$$h_g(t) = \frac{CK_g}{D}\left(\frac{V_g(t)\rho_g(t)D}{\mu_g}\right)^n \tag{17}$$

in which

K_g is the thermal conductivity of the propellant gas,
μ_g is the dynamic viscosity of the propellant gas,
$V_g(t)$ is the gas velocity,
ρ_g is the gas density,
D is the tube diameter,
C, n are constants.

Further, the ratio K_g/μ_g^n is taken to remain constant throughout the temperature range of interest*. Hence, one can write

$$h_g(t) = B\left(\frac{V_g(t)\,P_g(t)}{T_g(t)}\right)^n \tag{18}$$

in which B is a lumped coefficient to be established using the known heat input information.

---

*This assumption is in keeping with the desire for a simplified distributional fit of measured data. Little would be gained by specification of a variation of K_g/μ_g^n with temperature.

Combining Equations 16 and 18 and integrating over the period 0 to ∞, one gets

$$B = \frac{\int_0^\infty q(t)dt}{\int_0^\infty \left[\frac{V_g(t)\,P(t)}{T_g(t)}\right]^n \left[T_g(t) - T_w(t)\right] dt} \tag{19}$$

or

$$B = \frac{Q_{in}}{\int_0^\infty \left[\frac{V_g(t)\,P(t)}{T_g(t)}\right]^n \left[T_g(t) - T_w(t)\right] dt} \tag{20}$$

in which

Q_{in} is the total heat input previously computed.

The numerical integration implied by Equation 20 cannot be allowed to proceed to infinity in time. An estimate of the total heat input period is needed to allow limited numerical calculation of the definite integral. Equations 13, 14, and 15 can be utilized to obtain a reasonable estimate of the heating period. Because the heat transfer coefficient is influenced primarily by the pressure, calculations extending through the time period in which pressure has decayed to a small percentage of the peak breech pressure will be adequate for evaluation of the integral. Generalizing typical propellant properties as

$$K \approx 1.25$$

$$R \approx 65\ \frac{\text{ft-lb}}{\text{lb-}^\circ\text{R}}$$

$$T_A \approx 5000^\circ\text{R}$$

and taking a 100:1 pressure decay, Equation 15 indicates a temperature decay of at least 2.5:1. Hence, T_g is no more than 2000°R. Since the pressure decay is exponential, a good approximation of the average gas temperature during the pressure decay is 3000°R. Utilizing this value in the evaluation of Z of Equation 14 and solving Equation 13 for $t - t_m$ (taken to be the final time of interest), one gets

$$t_f = 2.85 \times 10^{-3} \frac{V_{CH} + AL}{A} \tag{21}$$

Integration should extend at least to this period. With V_{CH}, A, and L expressed in feet, t_f is in seconds.

For any location in the chamber or barrel at which a total heat input is known. a value of B can be established for any selected n*. Because the variation of the wall temperature with time, $T_w(t)$, is unknown and depends upon the value of B, an iterative technique is used to determine B. In the computer solution, an initial value of B is determined by assuming $T_w(t) = T_{w_o}$ = constant**. Given this initial selection of B, the first approximation of $h_g(t)$ can be obtained using Equation C3 with V_g assumed to vary linearly from 0 at the breech to the projectile velocity at its position in the barrel (or acoustic velocity after the projectile exits the muzzle). Once the first approximation of $h_g(t)$ has been established, it is necessary to determine whether this coefficient (and gas temperature) produces the same heat transfer as that actually measured in the experiment (Q_{in}). For this determination, a numerical one-dimensional heat conduction subroutine (slab routine) similar in structure to the cylindrical conduction routine is used. The numerical method employed divides the barrel position of interest into a number of differential elements to which heat input based upon the above heat transfer coefficients and gas temperatures is applied (cf. Ref. 2). Calculation of temperature rise with time at each element is performed in differential time steps during the heating period of interest. At the completion of the heating period, the

*Values of n may range from 0 to 1.0. Comparison of results with experiment indicates a selection of n = 0.5 to give good agreement.

**T_{wo} is the initial wall temperature at which the experimental heat input parameters were obtained.

total heat into the slab per unit area is computed. If the calculated heat input does not agree to within a specified fraction of Q_{in}, the value of B is adjusted by the ratio of Q_{in} to the calculated heat input; new coefficients are formed; and the slab routine is re-entered. This iteration continues until agreement is obtained.

The output of the program consists of projectile velocity, projectile position, and breech pressure as a function of time. In addition, at each axial position, heat transfer coefficient and propellant gas temperature arrays are printed with corresponding time arrays. The heat input per unit area and the maximum single-shot surface temperature at the various axial positions, along with the computed value of B for each position, are also given.

E. Input Format

The above relations have been organized into a complete computer program written for use with the IBM 360/65 computer. In order to apply the program to evaluate measured data, suitable input information must be supplied and in the correct format. Pages 149 and 150 show the master input format and input card organization for use with the program. A description of inputs is as follows.

Card 1. Title card.

Card 2. A. The adiabatic flame temperature of the propellant gas, °R, taken from the literature for the particular propellant used in the experiment.

B. The initial weight of charge used in the experiment - lbs.

C. The approximate chamber volume in cubic inches.

D. The gas constant for the propellant in ft-lb/lb-°R, taken from the literature.

E. The initial wall temperature of the barrel in the experiment - °R.

F. The measured muzzle velocity - ft/sec.

G. The approximate chamber length - in.

H. The barrel length - in.

Card 3. A. The final time or time of interest. (This is the effective heat input period. It should be estimated by Equation 21.)

B. The gun's specific heat is the specific heat of the barrel material in Btu/lb-°R.

C. Barrel material density - lb/ft^3.

D. Muzzle exit time - sec. (If this is not known, take it as twice the barrel length divided by muzzle velocity.)

E. Correlation exponent, n. Although selection is arbitrary, a value of 0.5 is considered most appropriate.

F. Specific heat of the propellant gas at constant volume taken from the literature - Btu/lb-°R.

G. Convergence error. This is the error to be accepted on agreement between calculated and measured heat input. A value of 0.01 would allow ± 1.0 percent error, 0.02 ± 2.0 percent, etc. One should not specify a convergence error of zero.

H. Specific co-volume of charge, spv. This is taken as the average of the specific volume of solid and the co-volume of gaseous propellant - in^3/lb.

Card 4. A. Ratio of specific heats for the propellant gas taken from the literature. The value may be multiplied by 1.05 to partially account for non-adiabatic expansion if desired.

B. Convergence error barrel length is the accepted barrel length error in establishing projectile velocity-position. A value 0.01 allows ± 1 percent error, etc. A value zero should not be used.

C. Projectile weight in the experiment - lb.

D. Barrel thermal conductivity in the experiment - Btu/sec-ft-°R.

Card 5. All items on this card must be right justified.

A. Total number of axial positions in the experiment for which heat input information is given.

B. Number of pressure-time inputs--must be less than 60.

C. Number of chamber points for which heat input data are given should be less than the total number of axial positions.

D. Number of grooves in the barrel rifling.

Card 6. A. The locations of points of interest or axial locations for which heat input data are given are placed on this card. Eight locations must be input with distance given in inches relative to the start of the barrel.

Card 7. A. The corresponding inner radii in inches at the points of interest are placed on this card. These radii should be input as the average of the land and groove of the barrel.

Card 8. A. The corresponding outer radii at the points of interest are placed on this card.

Card 9. A. The projection height of the rifling in inches is input on this card.

Card 10. A. Heating parameters are placed on this card for eight locations. All eight locations must contain input data. If the average temperature rise (°F) at the barrel location in a single shot is input, leave the time group blank (first five digits of each decade). If an in-wall temperature (°F) is given, place time in seconds in time group (up to five digits). If a total heat input (Btu/ft^2) is given, place it in temperature group and put 9999. in time group.

Card 11-25 A. The measured breech pressure-time array is placed on these cards. Up to 60 pressure inputs up to and including the final time of interest may be used.

Input values for the slab subroutine are built into the program and can only be changed by change of program cards in the source deck. This subroutine is actually written in similar logic to that of the cylindrical conduction program of Section II of this report. As such, it could be used with minor modification to determine barrel temperatures during rapid fire of multiple bursts with cooling, provided that the barrel wall thickness is not great.

F. Program Listing

The entire HTC program listing, as written for the Calspan IBM 360/65 computer, including all subroutines is given beginning on page 134. (The program has also been adapted to the Frankford Arsenal CDC-6500 computer by Mr. Peter Ayyoub of Frankford Arsenal.) Comments within the bracketed areas shown indicate the purpose of the various program sections. Simplified flow charts are shown on pages 147 and 148. Basic organization of the flow logic is as described above in subsections A-D of this report.

G. Program Output

The output of the program consists first of an organization of input information as shown on page 151. On the first output page, only the muzzle time and the projectile restraining force are computed quantities. Next, the breech pressure, projectile velocity, and projectile position are printed out at corresponding times. This is shown on page 152. Finally, on successive pages, as shown representatively on pages 153 through 160, the heat transfer coefficients, corresponding gas temperatures, and times are printed for each axial position of interest. In addition, the single-shot heat input per unit area and the maximum computed single-shot inner surface temperature are also given for each position, along with the computed coefficient of Equation 18.

COMPUTER LISTING
FOR HTC PROGRAM
MAIN

```
C   THIS PROGRAM COMPUTES THE HEAT TRANSFER COEFFICIENT TO A GUN
C     BARREL AND THE CORRESPONDING GAS TEMPERATURES
      LOGICAL SNAFU
      DIMENSION R1(8),R2(8),TR(8),P(60),VP(60),S(60),TIME(60),
     1QIN(8),QTOTG(8),QTC(60),HETA(8),IND(8),WORK(60),TG(60),
     2VG(60,8),ZAT(60,8),SUMH(8),A(8),HG(60,8),QTIME(8),EPSD(8)
      DIMENSION THEH(60,8),THETG(60,8),TGD(60,8),DTA(8),TITLE(20)
      DIMENSION XN(8),QINC(8),TIMEX(50),PIX(50),DR(8)
      COMMON DESCP(12),ARG(2)
      COMMON IFPS,IX,IPRNT1,IPRNT2,IM
      COMMON XL,HMAX,THETAF,THETAE,C,RHO,XK,     CTE,HL,NH(10),
     1  NTG(10),DELTAY,TT1,DTHEX,DTHE1,
     2 DTHE2,NFINAL,LAST,T(100,10),M,ACCTHE,IPMAXB,DTHE,TT2,THETA,IP,
     3  HXT,TGXT,TR(100,10),SNAFU,STMAX(8),TIMAX(8)
      COMMON LCOUNT,SUM(10),IBURST,MM
      COMMON MBURST,THETAC,DTHEC,TMAX,LIV,TIMEF,TW
      NAMELIST/NAMY1/ R1,R2,TR,P,VP,S,TIME,QIN,QTOTG,QTG,HETA,IND,XN
      NAMELIST/NAMY/P,VP,S,WORK,TG,VG,ZAT,SUMH,A,HG
      NAMELIST/NAMAL/ NT,J,I,K,TS,PM,BUL,IL,LOT,NUTS,TUM,XO,XOT,IZ,ST,
     1VPT,KT,KS,PF,TGM,AB,PGL
      NAMELIST/NAMY2/ QIN,QINC,A,HG,DTA,AD,KEY
      NIN=5
      NOUT=6
      CON=144.0/778.28
      PIE=3.141593
      READ(NIN,4080) TITLE
 4080 FORMAT(20A4)
      WRITE(NOUT,4090)  TITLE
 4090 FORMAT(1H1,20A4)
      READ(NIN,5000) TA,WO,VCH,GC,TW,VM,CHL,BL,TIMEF,C ,RHO,TIMEM,EX
     1,CV,ERR,SPV,RK,ERBL,WP,XK
 5000 FORMAT(8F10.5)
      READ(NIN,5010) N,NT,NCH,NG,SNAFU
C  A POINT OF INTEREST SHOULD BE SPECIFIED AT ANY CHANGE OF BORE RADIUS
 5010 FORMAT(4I10,L10)
      READ(NIN,5000) (XN(J),J=1,N)
      READ(NIN,5000) (R1(J),J=1,N)
      READ(NIN,5000) (R2(J),J=1,N)
      READ(NIN,5000)(DR(J),J=1,N)
 5005 FORMAT(16F5.2)
      READ(NIN,5005)(QTIME(J),TR(J),J=1,N)
      READ(NIN,5000) (P(I),TIME(I),I=1,NT)
      WRITE(NOUT,6000) TA,TW
 6000 FORMAT(1HO,5X,29HADIABATIC GAS TEMPERATURE(R)=,F9.2,5X,29HINITIAL
     1WALL TEMPERATURE(R)= ,F9.2)
      WRITE(NOUT,6010) TIMEM,TIMEF
 6010 FORMAT(1HO,5X,29HTIME AT PROJECTILE EXIT(SEC)=,F9.5,5X,29HFINAL TI
     1ME OF INTEREST(SEC)= ,F9.5)
      WRITE(NOUT,6020) CHL,BL
 6020 FORMAT(1HO,5X,19HCHAMBER LENGTH(IN)=,10X,F9.2,5X,18HBARREL LENGTH(
     1IN)=,11X,F9.2)
      WRITE(NOUT,6030) C,CV
 6030 FORMAT(1HO,5X,29HSPECIFIC HEAT,GUN (BTU/LB*R)=,F9.3,5X,29HSPECIFIC
     1 HEAT CV (BTU/LB*R)= ,F9.3)
      WRITE(NOUT,6040) WO,SPV
 6040 FORMAT(1HO,5X,29HINITIAL WEIGHT OF CHARGE(LB)=,F9.4,5X,27HSPECIFIC
     1 VOLUME (IN**3/LB)=,2X,F9.3)
      WRITE(NOUT,6050) GC,RK
```

READ INPUT CARDS

WRITE INPUT PARAMETERS

```
6050 FORMAT(1HO,5X,29HGAS CONSTANT (LBF*FT/LBM*R)= ,F9.2,5X,24HRATIO OF
     1 SPECIFIC HEATS=,5X,F9.2)
      WRITE(NOUT,6060) VCH,VM
6060 FORMAT(1HO,5X,23HCHAMBER VOLUME (IN**3)=,6X,F9.2,5X,25HMUZZLE VELO
     1CITY (FT/SEC)=,4X,F9.2)
      WRITE(NOUT,6070) RHC,ERR
6070 FORMAT(1HO,5X,26HBARREL DENSITY (LB/FT**3)=,3X,F9.4,5X,22HCONVERGE
     1NCE ERROR (%)=,7X,F9.4)
      WRITE(NOUT,6080) EX,ERBL
6080 FORMAT(1HO,5X,21HCORRELATION EXPONENT=,8X,F9.3,5X,24HBARREL LENGTH
     1 ERROR (%)=,5X,F9.4)
      WRITE(NOUT,6081)WP,XK
6081 FORMAT(1HO,5X,23HPROJECTILE WEIGHT (LB)=,6X,F9.5,5X,31HBARREL THER
     1M CONDUCTIVITY (BTU/FT-SEC-R)=,F7.5//)
      WRITE(NOUT,6090) N,NT,NCH,NG
6090 FORMAT(1HO,5X,26HNUMBER OF AXIAL POSITIONS=,3X,I4,5X,25HNUMBER OF
     1TIME INTERVALS=,4X,I9/6X,'NUMBER OF CHAMBER POSITIONS=',1X,I9,
     25X,18HNUMBER OF GROOVES=,11X,I9)
      WRITE(NOUT,6093)
      WRITE(NOUT,6092)(J,XN(J),R1(J),R2(J),DR(J),J=1,N)
6092 FORMAT( I10,F12.3,12X,F9.5 ,12X,F9.5,18X,F9.5)
6093 FORMAT(//10X,'AXIAL POSITION-IN',5X,'INNER RADIUS-IN',
     15X,'OUTER RADIUS-IN',5X,'PROJECTION HEIGHT-IN')
      RKP1=(RK+1.0)/(RK-1.0)
      RK2=2.0*RK/(RK-1.0)
      RKM1=(RK-1.0)/RK
      NCHP1=NCH+1
      AVB=0.0
      DO 90 J=NCHP1,N
   90 AVB=AVB+PIE*R1(J)**2
      AN=N-NCH
      AVB=AVB/AN
   93 KFLAG=0
      VP(1)=0.0
      DO 120  K=2,NT
      IF(TIME(K).LE.TIMEM) GO TO 100
      TS=TIMEM
      PM=SI(TIME,P,TS,NT,1,1,1)
      KFLAG=1
      GO TO 110
  100 TS=TIME(K)
      PM=P(K)
  110 VP(K)=VP(K-1)+(P(K-1)+PM)/2.0*(TS-TIME(K-1))
      IF(TS.EQ.TIMEM) GO TO 130
  120 CONTINUE
  130 BUL= (VP(K)*AVB*32.2/((1.+WO/(2.*WP))*WP)-VM)*WP/(32.2*TIMEM)
      IL=K
      IF(KFLAG.EQ.0) GO TO 140
      DO 95 I=K,NT
      PIX(I)=P(I)
   95 TIMEX(I)=TIME(I)
      DO 97 I=K,NT
      P(I+1)=PIX(I)
   97 TIME(I+1)=TIMEX(I)
      NT=NT+1
      P(K)=PM
      TIME(K)=TIMEM
  140 S(1)=0.0
```

WRITE INPUT PARAMETERS

DETERMINE PROJECTILE VELOCITY

MAIN

```
      DO 150  I=2,K
      VP(I)=AVB*32.2*VP(I)/((1.+WO/(2.*WP))*WP)-BUL*TIME(I)*32.2/WP
      S(I)=S(I-1)+(VP(I)+VP(I-1))/2.0*(TIME(I)-TIME(I-1))*12.0
      IF(VP(I)+S(I))151,150,150
  151 VP(I)=0.
        S(I)=0.
  150 CONTINUE
 1151 IF(SNAFU)GO TO 1152
      GO TO 2152
 1152 WRITE (6,6152) S(K),BL
 6152 FORMAT (10X,F15.5,10X,E15.5)
 2152 IF(ABS(S(K)-BL)/BL-EPBL)155,155,152
  152 TIMEM=TIMEM*(1.0+0.6*(BL/S(K)-1.0))
      NT=NT-1
      DO 153 I=K,NT
      P(I)=P(I+1)
  153 TIME(I)=TIME(I+1)
      GO TO 93
  155 WRITE(NOUT,6095) TIMEM,S(K)
 6095 FORMAT(///4X,19H THE MUZZLE TIME IS ,F9.6,2X,'SEC',3X,
     133HFOR A CALCULATED BARREL LENGTH OF, F9.3,2X,'IN')
      WRITE(NOUT,6091) BUL
 6091 FORMAT(1HO,4X,'PROJECTILE RESTRAINING FORCE=',F9.2,2X,'LBS')
      IF(S(K).LT.BL) S(K)=BL
      WRITE(NOUT,6160)
 6160 FORMAT(//5X,'BARREL HEATING INPUTS'/)
      DO 160  J=1,N
      IF(QTIME(J).EQ.0.) GO TO 1160
      IF((QTIME(J)-9999.).EQ.0.) GO TO 2160
      EPSD(J)=1.-0.32*EXP(-3.71*R1(J))
      QIN(J)=SQRT(PIE*XK*C*RHO*QTIME(J))*TR(J)/EPSD(J)
      WRITE(NOUT,6161)J,QTIME(J),J,TR(J)
 6161 FORMAT(5X,'TIME(',I1,')(SEC)=',F9.5,5X,'TEMP RISE (',I1,')(R) =',
     1F9.4)
      GO TO 3160
 1160 XNG=NG
      QIN(J)=PIE*C*RHO*TR(J)*(R2(J)**2-R1(J)**2)/(2.*PIE*R1(J)+2.*XNG*
     1DR(J))/12.
      WRITE(NOUT,6162)J,TR(J)
 6162 FORMAT(5X,'TEMP RISE(',I1,')(R) =',28X,F9.4)
      GO TO 3160
 2160 QIN(J)=TR(J)
      WRITE(NOUT,6163)J,TR(J)
 6163 FORMAT(5X,'HEAT INPUT(',I1,')(BTU/FT**2)=',20X,F9.4)
 3160 QTOTG(J)=0.6667*(BL-XN(J))/(BL+CHL)*QIN(J)
      IF(XN(J).LT.0.) GO TO 4160
      HETA(J)= SIMPS(TIME,XN(J),NT,1,1,1)
      GO TO 160
 4160 HETA(J)=TIME(1)
  160 CONTINUE
      LOT=1
      I=0
      NUTS=NCHP1
      NP1=N+1
      DO 1620 NUTS=1,NCH
 1620 IND(NUTS)=1
  163 I=I+1
      IF(NUTS.EQ.NP1) GO TO 165
```

PROJECTILE VELOCITY

DETERMINE PROJECTILE POSITION AND ADJUST MUZZLE TIME

CALCULATE TOTAL HEAT INPUT

DETERMINE HEAT LOSS TO BARREL AS A FUNCTION OF TIME

```
      IF(TIME(I).GT. HETA(NUTS)) GO TO 180
      IF(TIME(I).LT. HETA(NUTS)) GO TO 165
      LOT=2
      IND(NUTS)=I
  165 QTG(I)=0.0
      TUM=TIME(I)
      XO=0.0
      IF(XN(I).LT.0.)XO=-CHL
  167 DO 170  J=1,NUTS
      IF(J.NE.NUTS) GO TO 168
      XOT=S(I)
      GO TO 169
  168 XOT=XN(J)
  169 QTG(I)=QTG(I)+QTOTG(J)*(TIME(I)-TUM)/TIMEM**(EXP1(J)*(XOT-XO)/72.
      XO=XOT
  170 TUM= HETA(J)
      IF(I.GE.IL) GO TO 200
      GO TO (163,171),LOT
  171 NUTS=NUTS+1
      LOT=1
      GO TO 163
  180 IZ=I
      ST=SI(TIME,S, HETA(NUTS),NT,1,1,1)
      VPT=SI(TIME,VP, HETA(NUTS),NT,1,1,1)
      PMT=SI(TIME,P,HETA(NUTS),NT,IND,1,1)
      KT=NT-IZ+1
      DO 190  K=1,KT
      KS=NT+1-K
      TIME(KS+1)=TIME(KS)
      S(KS+1)=S(KS)
      P(KS+1)=P(KS)
  190 VP(KS+1)=VP(KS)
      TIME(IZ)= HETA(NUTS)
      S(IZ)=ST
      VP(IZ)=VPT
      P(IZ)=PMT
      NT=NT+1
      IL=IL+1
      IND(NUTS)=IZ
      LOT=2
      GO TO 165
  200 J=1
      WRITE(NOUT,7010)
 7010 FORMAT(1H1,5X,65HTHE PROJECTILE TIME,VELOCITY,AND POSITION TO EXIT
     1 ARE GIVEN BELOW//6X,9HTIME(SEC))
      WRITE(NOUT,5070) (TIME(I),I=1,NT)
      WRITE(NOUT,7020) (VP(I),I=1,IL)
 7020 FORMAT(1HO,5X,27HPROJECTILE VELOCITY(FT/SEC)/(8F14.2))
      WRITE(NOUT,7040) (S(I),I=1,IL)
 7040 FORMAT(1HO,5X,23HPROJECTILE POSITION(IN)/(8F14.4))
      WORK(1)=0.0
      DO 205  K=1,N
      VG(1,K)=0.0
      ZAT(1,K)=0.0
      SUMH(K)=0.0
  205 HG(1,K)=0.0
      TG(1)=TA
      KFLAG=0
```

HEAT INPUT TO BARREL (CONT)

INITIALIZES PARAMETERS

```
      DO 230  I=2,NT
      IF(I.LE.IL) GO TO 207
      IF(KFLAG.GT.0) GO TO 206
      PF=(VCH+BL*AVB)/(6.0*(RK-1.0)*AVB)*SQRT(1/(32.2*RK*GC*TGM)*
     1  ((RK+1.0)/2.0)**RKP1)
      KFLAG=1
  206 P(I)=PM*(1.0+(TIME(I)-TIMEM)/PF)**(-RK2)
      TG(I)=TGM*(P(I)/PM)**RKM1
      VP(I)=SQRT(32.2*RK*GC*TG(I))
      S(I)=BL
      GO TO 209
  207 IF(IND(J).LT.I.AND.J.LT.N) J=J+1
      AB=AVB
      WORK(I)=WORK(I-1)+AB*(P(I)+P(I-1))*(S(I)-S(I-1))/((1.+WC/(2.*WP))
     1*24.)
      PGL=P(I)*(1.+WC/(3.*WP))*CV*(AB*S(I)+VCH-WC*SPV)/(12.*GC
     1*(1.+WC/(2.*WP)))
      TG(I)=TA*(PGL/(QTG(I)+WORK(I)/778.26+PGL))
      IF(TIME(I).EQ.TIMEM)TGM=TG(I)
  209 DO 230  K=1,N
      IF(I.LE.IND(K)) GO TO 210
      VG(I,K)=(XN(K)+CHL)/(S(I)+CHL)*VP(I)
  220 ZAT(I,K)=(P(I)*VG(I,K)/TG(I)*CON)**EX
      SUMH(K)  =SUMH(K)     +ZAT(I,K)*(TG(I)-Tw)*(TIME(I)-TIME(I-1))
      GO TO 230
  210 ZAT(I,K)=0.0
      VG(I,K)=0.0
      SUMH(K)  =0.0
  230 CONTINUE
      DO 240 K=1,N
      A(K)=QIN(K)/SUMH(K)
      DO 240 I=1,NT
  240 HG(I,K)=A(K)*ZAT(I,K)
      WRITE(NOUT,7050) (P(I),I=1,NT)
 7050 FORMAT(1HO,5X,43HPRESSURE UNTIL END OF CALCULATION TIME(PSI)
     1/ (8F14.1))
      DO 250  J=1,N
      DO 250  I=1,NT
      THEH(I,J) = TIME(I)
      THETG(I,J)=TIME(I)
  250 TGD(I,J)=TG(I)
      KEY=1
  255 CALL SLAB(HG,THEH,THETG,TGD,N,NT,DTA,CTO,KEY)
      DO 260  J=1,N
  260 QINC(J)=C*RHO*XL*(DTA(J)-CTO)
      DO 265 J=1,N
      IF((ABS(QIN(J)-QINC(J)))/QIN(J)-ERR)265,265,270
  265 CONTINUE
      GO TO 300
  270 DO 280 J=1,N
      AD=QIN(J)/QINC(J)
      A(J)=A(J)*AD
      DO 280 I=1,NT
  280 HG(I,J)=HG(I,J)*AD
      KEY=KEY+1
      IF(KEY.LT.25) GO TO 255
  300 WRITE(NOUT,5050)EX
 5050 FORMAT(1H1,62HTHE HEAT TRANSFER COEFFICIENT ARRAY FOLLOWS FOR AN E
```

CALCULATE PRESSURE AND TEMPERATURE AFTER MUZZLE EXIT

CALCULATE WORK AND PROPELLANT GAS TEMP.

CALCULATE HEAT TRANSFER COEFFICIENT (FIRST APPROXIMATION)

ADJUST COEFFICIENT TO MATCH HEAT INPUT

```
     1XPONENT OF,F13.5)
      DO 320  J=1,N
      WRITE(NOUT,5055) XA(J)
5055 FORMAT(1H1,//47HOTHE FOLLOWING PROPERTIES ARE AT AXIAL POSITION,
     1  F14.2)
5060 FORMAT(1HO,5X,25HHEAT TRANSFER COEFFICIENT )
      WRITE(NOUT,5060)
      WRITE(NOUT,5070) (HG(I,J),I=1,NT)
5070 FORMAT(8F14.5)
      WRITE(NOUT,5080)
5080 FORMAT(1HO,5X,17H''A'' COEFFICIENT)
      WRITE(NOUT,5070) A(J)
      WRITE(NOUT,5090)
5090 FORMAT(1HO,5X,10HTIME ARRAY)
      WRITE(NOUT,5070) ( TIME(I),I=1,NT)
      WRITE(NOUT,5091)
      WRITE(NOUT,5092)(TG(I),I=1,NT)
5091 FORMAT(1HO,5X,'GAS TEMPERATURE-DEG R')
5092 FORMAT(8F14.2)
5071 FORMAT(F14.5,39X,F14.5,16X,F14.5)
      WRITE(NOUT,5100)
5100 FORMAT(1HO,5X,37HHEAT TRANSFER PER UNIT AREA,BTU/FT**2,10X,
     1 'MAXIMUM SURFACE TEMPERATURE-DEG R AND TIME-SEC')
 320 WRITE(NOUT,5071)QIN(J),STMAX(J),TIMAX(J)
      CALL EXIT
      END
```

WRITE OUTPUT

SI

```
      FUNCTION SI(X,Y,X1,NE,IN1,IN2,IN3)
      DIMENSION X(1),Y(1)
C     XTBL=INDEPENDANT VARIABLE ARRAY
C     YTBL=  DEPENDANT VARIABLE ARRAY
C     XX   =KNOWN INDEPENDANT VALUE
C     NN   =NUMBER OF ENTRIES IN THE ARRAY
      DO 100  I=1,NE
      IF(X(I).GE.X1) GO TO 120
  100 CONTINUE
  120 IF(X(I).EQ.X1) GO TO 150
  130 SI=Y(I-1)+(X1-X(I-1))/(X(I)-X(I-1))*(Y(I)-Y(I-1))
      GO TO 160
  150 SI=Y(I)
  160 RETURN
      END
```

TABLE LOOK UP

```
      SUBROUTINE SLAB(H,THEH,THETG,TG,IS,NUM,DTA,CTC,KEY)
      LOGICAL SNAFU
      COMMON DESCP(12),ARG(2)
      COMMON IEPS,IX,IPRNT1,IPRNT2,IM
      COMMON XL,HMAX,THETAF,THETAE,C,RHO,XK,     CTF,HL,NH(10),
     1  NTG(10),DELTAY,TTL,DTHEX,DTHE1,
     2 DTHE2,NFINAL,LAST,T(100,10),M,ACCTHE,IPMAXB,DTHE,TT2,THETA,IP,
     3  HXT,TGXT,TB(100,10),SNAFU,STMAX(8),TIMAX(8)
      COMMON LCOUNT,SUM(10),IBURST,MM
      COMMON MBURST,THETAC,DTHEC,TMAX,DIV,TIMEF,TW
      DIMENSION H(60,8),THEH(60,8),THETG(60,8),TG(60,8),DTA(F),
     1TEST(8),TTM1(8)
C   FIRST DIMENSION OF A TWO DIMENSIONAL ARRAY WHICH IS A SUBROUTINE ARGUEMENT
C   MUST BE THE SAME AS IN THE CALLING PROGRAM
C   MAIN PROGRAM
C
C
1     LCOUNT=0
      IX=IS
      IBURST=1
      DO 30  I=1,IX
      NH(I)=NUM
   30 NTG(I)=NUM
      IF(KEY.GT.1) GO TO 342
      IEPS=60
      HL=0.
      IPRNT1=10000
      IPRNT2=10000
      IM=1
      MBURST=1
      XL=0.02
      HMAX=15.0
      THETAF=TIMEF
      THETAE=TIMEF
      CTC=TW
      CTF=TW
      DTHEC=0.0
      THETAC=0.0
      TMAX=5000.
      DIV=12.
   20 FORMAT(8E15.5)
C   PRINT OF TABULAR DATA
      IF(SNAFU)GO TO 179
      GO TO 242
  179 DO 241  I=1,IX
  180 FORMAT(1H1,25H TABULAR DATA FOR SECTION,I3)
      WRITE(6,190) NH(I)
  190 FORMAT(1HO,29H  H TABLE - NUMBER OF ENTRIES,I3)
      WRITE(6,200)
  200 FORMAT(1HO,2X,5HTHETA)
      NUM=NH(I)
      WRITE(6,210) (THEH(K,I),K=1,NUM)
  210 FORMAT(1X,1P8E15.7)
      WRITE(6,220)
  220 FORMAT(1HO,2X,8HH(THETA))
      WRITE(6,210) (H(K,I),K=1,NUM)
      WRITE(6,230) NTG(I)
  230 FORMAT(/////3X,26HTG TABLE NUMBER OF ENTRIES,I3)
```

INITIALIZE PARAMETERS

GO TO 242

```
      NUM=NTG(I)
      WRITE(6,200)
      WRITE(6,210) (THETG(K,I),K=1,NUM)
      WRITE(6,240)
  240 FORMAT(1HO,2X,9HTG(THETA))
      WRITE(6,210) (TG(K,I),K=1,NUM)
  241 CONTINUE
C PRINT OF INPUT DATA AND TABLES COMPLETED
C  START OF CALCULATION
242     CONTINUE
      DELTAY = XL/FLOAT(IEPS)
      TT1 = XK/DELTAY
      DTHEX = (C*RHO*DELTAY**2)/(2.0*(HMAX*DELTAY+XK))
      DTHEX=DTHEX/DIV +5.0E-8
      DO 250  J=1,50
      ITEMP = DTHEX*10.0 **J
      IF(ITEMP.GT.0) GO TO 260
  250 CONTINUE
  251 RETURN
  260 DTHEX = FLOAT(ITEMP)*10.0**(-J)
  270 DTHE1=DTHEX
      DTHE2=DIV*DTHEX
      NFINAL=IEPS
      LAST=IEPS+1
      M=0
      ACCTHE=0.0
      IF(SNAFU)GO TO 273
      GO TO 272
  273 WRITE(6,271)DELTAY,DTHE1,DTHE2
271   FORMAT(1X,8H DELTAY=,1PE15.6,8X,6HDTHE1=,1PE15.6,
     X 8X,6HDTHE2=,1PE15.6)
272     CONTINUE
      DO 290  I=1,IX
      DO 280  J=1,LAST
  280 T(J,I)=CTO
      TEST(I)=0.
  290 CONTINUE
       THETA=0.0
       CALL PRINT
  300 IPMAXB=IPRNT1
      M=M+1
      DTHE=DTHE1
      IGOTO=1
       THETA=DTHE1
       ACCTHE=ACCTHE+DTHE1
  302 IP=0
  301 TT2=DTHE /(C*RHO*DELTAY)
      TT3=TT1*TT2
      DO 303 I=1,IX
      TTM1(I)=T(1,I)
  303 CONTINUE
      DO 380  I=1,IX
C  TABLE LOOKUP FOR N(THETA) AND TG(THETA)
      NUM=NH(I)
      DO 310 J=2,NUM
      IF(THETA.GT.THEH(J,I)) GO TO 310
      IF(THEH(J,I)-THEH(J-1,I))309,309,308
  308 HXT=H(J-1,I)+((THETA-THEH(J-1,I))*(H(J,I)-H(J-1,I)))/(THEH(J,I)-
```

DETERMINE TIME AND DISTANCE INTERVALS

GO TO 272

START CALCULATION OF THERMAL GRADIENTS AND HEAT INPUT

```
     X      THEH(J-1,I))
            GO TO 311
  309 HXT=H(J-1,I)
  311 CONTINUE
      GO TO 320
310   CONTINUE
      HXT=H(NUM,I)
320   NUM=NTG(I)
      DO 330  J=2,NUM
      IF(THETA.GT.THETG(J,I)) GO TO 330
      IF(THETG(J,I)-THETG(J-1,I))328,328,326
  326 TGXT=TG(J-1,I)+((THETA-THETG(J-1,I))*(TG(J,I)-TG(J-1,I)))/(THETG(
     X      J,I)-THETG(J-1,I))
      GO TO 329
  328 TGXT=TG(J-1,I)
  329 CONTINUE
      GO TO 360
330   CONTINUE
      TGXT=TG(NUM,I)
  360 TB(1,I)=2.0*TT2*(HXT*(TGXT-T(1,I))-TT1*(T(1,I)-T(2,I)))+T(1,I)
      IF(T(1,I).LT.TMAX  ) GO TO 10020
      WRITE(6,10010)
10010 FORMAT (1X,29H MAXIMUM TEMPERATURE EXCEEDED)
      CALL PRINT
      STOP
10020 CONTINUE
      DO 370  J=2,NFINAL
  370 TB(J,I)=TT3*(T(J-1,I)-T(J,I)-T(J,I)+T(J+1,I))+T(J,I)
      TB(LAST,I)=2.0*TT2*(TT1*(T(LAST-1,I)-T(LAST,I))-HI*
     X           (T(LAST,I)-CTF))+T(LAST,I)
  380 CONTINUE
      DO 400  I=1,IX
      DO 390  J=1,LAST
  390 T(J,I) = TB(J,I)
  400 CONTINUE
      DO 409 I=1,IX
       IF(TEST(I).NE.0.)GO TO 409
      IF(T(1,I)-TTM1(I)) 401,409,409
  401 STMAX(I)=TTM1(I)
      TIMAX(I)=THETA
      TEST(I)=1.
  409 CONTINUE
      IP=IP+1
      GO TO (410,440,450,480),IGOTO
  410 IF((THETA+DTHE).LT.THETAF) GO TO 420
       IF(  IP  .NE.  IPMAXB)  GO TO 411
       CALL PRINT
       IP=0
411    CONTINUE
      DTHE=THETAF-THETA
      ACCTHE=ACCTHE+DTHE
      THETA=THETA+DTHE
      IP=0
      IF(THETAE.EQ.THETAF) IGOTO=4
      IGOTO=2
      GO TO 301
  420 IF (IP.NE.IPMAXB) GO TO 430
      CALL PRINT
```

CALCULATION OF TEMPERATURES IN SLAB AT ALL AXIAL LOCATIONS

INCREASE TIME BY ACCUMULATION

```
      IP=0
  430 ACCTHE=ACCTHE + DTHE
      THETA=THETA+DTHE
      GO TO 301
  440 CALL PRINT
      IPMAXB=IPRNT2
      DTHE=DTHE2
      ACCTHE=ACCTHE+DTHE
      THETA=THETA+DTHE
      IP=0
      IGOTO=3
      GO TO 301
  450 IF((THETA+DTHE) .LT. THETAE) GO TO 460
      IF(IP  .NE.  IPMAXB) GO TO 451
       CALL PRINT
       IP=0
  451  CONTINUE
      DTHE=THETAE-THETA
      ACCTHE=ACCTHE+DTHE
      THETA=THETA+DTHE
      IP=0
      IGOTO=4
      GO TO 301
  460 IF(IP .NE. IPMAXB) GO TO 470
      CALL PRINT
      IP=0
  470 ACCTHE=ACCTHE+DTHE
      THETA=THETA+DTHE
      GO TO 301
  480 CALL PRINT
       IP=0
      IF(M.LT.IM) GO TO 300
      TAVE=SUM(1)
      DO 482 I=1,IX
  482 DTA(I)=SUM(I)
      IF (SNAFU) GO TO 483
      GO TO 484
  483 WRITE(6,20)(DTA(I),I=1,IX)
  484 XTHETA=THETA
       XTHET1=XTHETA+THETAC
  481  IF((THETA+DTHEC).LT.XTHET1)  GO TO 490
       TEMP1=XTHET1-THETA
      ACCTHE=ACCTHE+TEMP1
      THETA=THETA+TEMP1
      TAVEB=TAVE-(HL*TEMP1*(TAVE-CTE))/(XL*C*RHO)
      TAVE=TAVEB
      GO TO 500
  490 ACCTHE=ACCTHE+DTHEC
      THETA=THETA+DTHEC
      TAVEB=TAVE-(HL*DTHEC*(TAVE-CTE))/(XL*C*RHO)
      TAVE=TAVEB
      GO TO 481
  500 IF(SNAFU)GO TO 1500
      GO TO 502
 1500 WRITE(6,501)IBURST,M,ACCTHE,TAVE
  501  FORMAT(1X,I8,I8,F15.6,7X,1PE12.5)
  502 IF(IBURST.EQ.MBURST) GO TO 510
      IBURST=IBURST+1
```

```
      M=0
      CTO= TAVE
      GO TO 272
510   LCOUNT=0
      IHURST=1
      GO TO 251  (RETURN TO MAIN)
      END
```

MAIN

```
CIBFTC LGM2     LIST,DECK,REF
       SUBROUTINE PRINT
       LOGICAL SNAFU
       COMMON DESCP(12),ARG(2)
       COMMON IEPS,IX,IPRNT1,IPRNT2,IM
       COMMON XL,HMAX,THETAF,THETAE,C,RHO,XK,     CTI,HL,NH(10),
      1  NTG(10),DELTAY,TT1,DTHEX,DTHEL,
      2 DTHE2,NFINAL,LAST,T(100,10),M,ACCTHE,IPMAXB,DTHE,TT2,THETA,IP,
      3  HXT,TGXT,TB(100,10),SNAFU,STMAX(8),TIMAX(8)
       COMMON LCOUNT,SUM(10),IBURST,MM
       COMMON MBURST,THETAC,DTHEC,TMAX,DIV,TIMEF,TW
       DO 40  I=1,IX
       SUM(I)=T(1,I)/2.0
       DO 30  J=2,NFINAL
    30 SUM(I)=SUM(I)+T(J,I)
    40 SUM(I)=(SUM(I)+T(LAST,I)/2.0)/FLOAT(IEPS)
       IF(SNAFU)GO TO 105
       GO TO 115
   105 IF(MOD(LCOUNT,50)  .NE.   0)  GO TO 100
       WRITE(6,120)
   120  FORMAT(1H1,2X,5HBURST,3X,5HRCUND,5X,11HTHETA(SEC.),7X,9HT(AVE),14X
      X,4HT(1),16X,7HT(LAST))
   100   WRITE(6,110)IBURST, M,ACCTHE,SUM(1),T(1,1),T(LAST,1)
   110  FORMAT(1X,I8,I8,F15.6,7X,1PE12.5,8X,1PE12.5,8X,1PE12.5)
   115 CONTINUE
       LCOUNT=LCOUNT+1
       RETURN
       END
```

DETERMINE AVERAGE TEMPERATURE

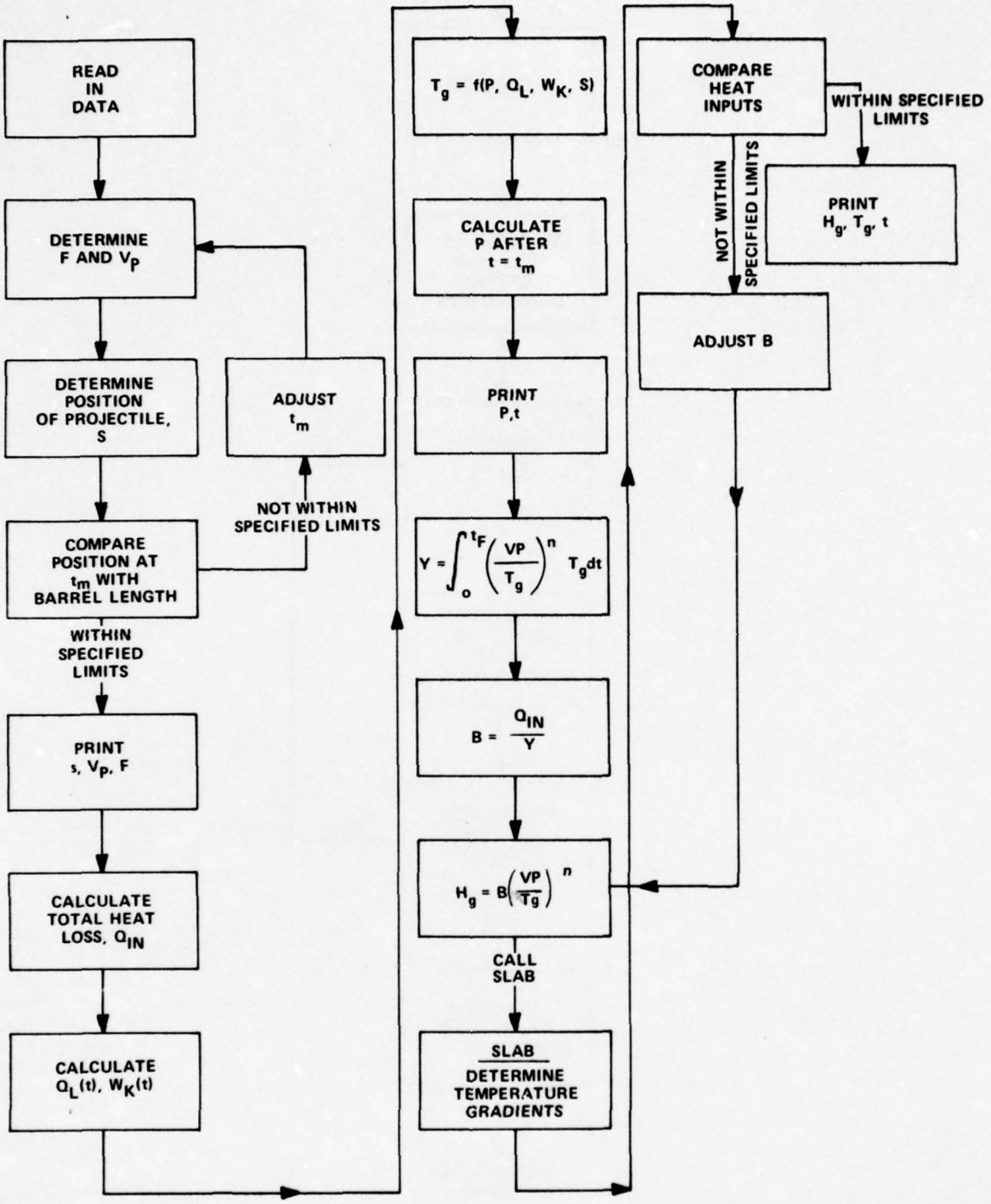

FLOW CHART FOR HTC PROGRAM

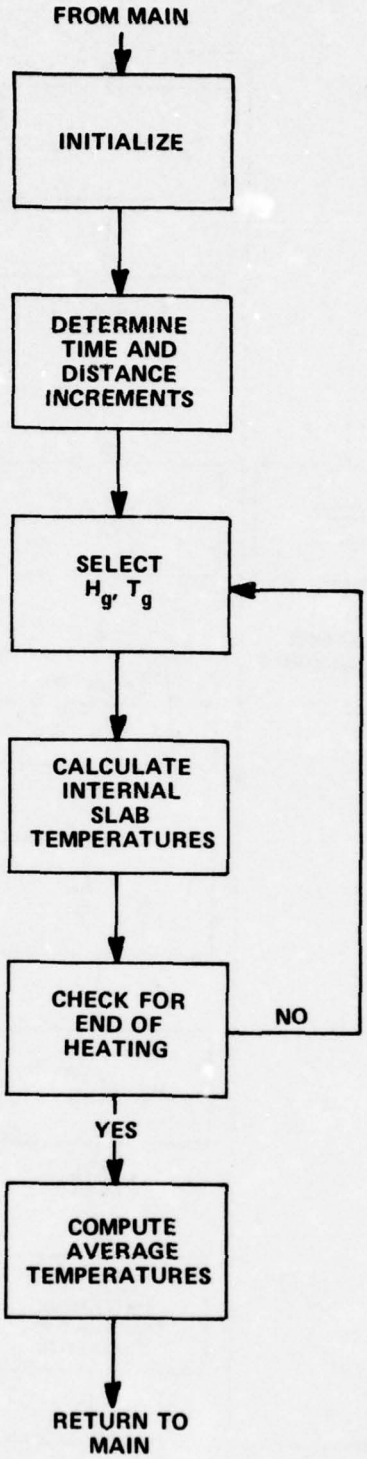

FLOW CHART FOR SUBROUTINE SLAB

IBM System 360 Assembler Coding Form

PROGRAM: HTC - MASTER INPUT | PUNCHING INSTRUCTIONS | GRAPHIC | PAGE 1 OF 2
PROGRAMMER | DATE | PUNCH | CARD ELECTRO NUMBER

STATEMENT — Name | Operation | Operand | Comments | Identification-Sequence

CD										
1	HTC TITLE 20A4									
2	ADIABATIC GAS TEMP-°R	INITIAL CHARGE WEIGHT - LBM	CHAMBER VOLUME IN^3	GAS CONSTANT FT-LBF/LBM-°R	INITIAL WALL TEMP - °R	MUZZLE VELOCITY FT/SEC	CHAMBER LENGTH IN.	BARREL LENGTH IN.		
3	FINAL TIME SEC	SPECIFIC HEAT GUN - BTU/LBM-°R	BARREL DENSITY LBM/FT^3	MUZZLE EXIT TIME SEC	CORRELATION EXPON.	SPECIFIC HEAT GAS CV - BTU/LBM-°R	CONVERGENCE ERROR	SPECIFIC VOLUME CHARGE - IN^3/LBM		
4	RATIO OF SPEC HEATS	CONVERGENCE ERROR - BARREL LENGTH	PROJECTILE WEIGHT LBM	BARREL THERMAL CONDUCT - BTU/SEC-FT-°R						
5	NO. POINTS IN CHAMBER & BARREL	NO. PRESSURE-TIME INPUTS	NO. OF CHAMBER POINTS	NO. OF GROOVES						
6	LOCATION OF POINTS OF INTEREST (IN.)									
7	CORRESPONDING INNER RADII (IN.)									
8	CORRESPONDING OUTER RADII (IN.)									
9	PROJECTION HEIGHT (IN.)									

MASTER INPUT FORMAT

IBM System 360 Assembler Coding Form

PROGRAM
PROGRAMMER
DATE
PAGE 2 OF 2
CARD ELECTRO NUMBER

	Name	Operation	Operand	Comments	Identification Sequence
10	HEATING PARAMETER*				
	TIME TEMP				
11-25	PRESSURE, TIME TABLE 8F10.3, UP TO 60 PRESSURES				
	PRESSURE** PSI	TIME SEC	PRESSURE	TIME	PRESSURE	TIME	PRESSURE	TIME

*1 AVE TEMP RISE - LEAVE TIME BLANK
2 IN-WALL TEMP & TIME (ΔT°F + SEC)
3 TOTAL HEAT INPUT:TIME = 9999.. TEMP = QIN(BTU/FT^2)
**THE INITIAL VALUE OF PRESSURE MUST BE DIFFERENT FROM ZERO.

HTC PROGRAM

ADIABATIC GAS TEMPERATURE(R)=	5060.00	INITIAL WALL TEMPERATURE(R)=	535.00
TIME AT PROJECTILE EXIT(SEC)=	0.00120	FINAL TIME OF INTEREST(SEC)=	0.00500
CHAMBER LENGTH(IN)=	1.25	BARREL LENGTH(IN)=	20.00
SPECIFIC HEAT,GUN (BTU/LB*R)=	0.126	SPECIFIC HEAT CV (BTU/LB*R)=	0.336
INITIAL WEIGHT OF CHARGE(LB)=	0.0037	SPECIFIC VOLUME (IN**3/LB)=	21.300
GAS CONSTANT (LBF*FT/LBM*R)=	65.20	RATIO OF SPECIFIC HEATS=	1.25
CHAMBER VOLUME (IN**3)=	0.12	MUZZLE VELOCITY (FT/SEC)=	3060.00
BARREL DENSITY (LB/FT**3)=	490.0000	CONVERGENCE ERROR (%)=	0.0500
CORRELATION EXPONENT=	0.800	BARREL LENGTH ERROR (%)=	0.0050
PROJECTILE WEIGHT (LB)=	0.00781	BARREL THERM CON(BTU/FT-SEC-R)=	0.00700

NUMBER OF AXIAL POSITIONS=	8	NUMBER OF TIME INTERVALS=	20
NUMBER OF CHAMBER POSITIONS=	3	NUMBER OF GROOVES=	6

	AXIAL POSITION-IN.	INNER RADIUS-IN	OUTER RADIUS-IN	PROJECTION HEIGHT-IN
1	-1.100	0.18700	0.62500	0.0
2	-0.600	0.18700	0.62500	0.0
3	-0.050	0.18700	0.62500	0.0
4	0.0	0.11100	0.62500	0.00225
5	5.000	0.11100	0.62500	0.00225
6	10.000	0.11100	0.62500	0.00225
7	15.000	0.11100	0.62500	0.00225
8	20.000	0.11100	0.62500	0.00225

THE MUZZLE TIME IS 0.001114 SEC FOR A CALCULATED BARREL LENGTH OF 20.087 IN
PROJECTILE RESTRAINING FORCE= 133.68 LBS

BARREL HEATING INPUTS

TIME(1)(SEC)=	0.30000	TEMP RISE (1)(R) =	17.3000
TIME(2)(SEC)=	0.30000	TEMP RISE (2)(R) =	19.9800
TIME(3)(SEC)=	0.30000	TEMP RISE (3)(R) =	25.9800
TIME(4)(SEC)=	0.30000	TEMP RISE (4)(R) =	37.3000
TIME(5)(SEC)=	0.30000	TEMP RISE (5)(R) =	23.9800
HEAT INPUT(6)(BTU/FT**2)=			15.0000
TEMP RISE(7)(R) =			1.4400
TEMP RISE(8)(R) =			1.3300

THE PROJECTILE TIME,VELOCITY,AND POSITION TO EXIT ARE GIVEN BELOW

TIME(SEC)

0.00005	0.00005	0.00015	0.00025	0.00035	0.00045	0.00055	0.00064
0.00065	0.00075	0.00082	0.00085	0.00095	0.00097	0.00105	0.00111
0.00111	0.00115	0.00125	0.00135	0.00185	0.00235	0.00285	0.00335
0.00385	0.00500						

PROJECTILE VELOCITY(FT/SEC)

0.0	0.0	0.0	139.64	522.21	1063.75	1612.21	2013.99
2063.90	2402.69	2574.63	2653.93	2842.95	2873.37	2985.90	3057.24
3060.00							

PROJECTILE POSITION(IN)

0.0	0.0	0.0	0.0838	0.4809	1.4325	3.0380	5.0000
5.2437	7.9237	10.0000	10.9576	14.2557	15.0000	17.7531	20.0000
20.0869							

PRESSURE UNTIL END OF CALCULATION TIME(PSI)

3750.0	3750.0	7143.0	25000.0	42857.0	49643.0	43929.0	35669.0
34643.0	26429.0	22762.2	21071.0	16786.0	16178.0	13929.0	12533.5
12479.5	11987.4	10717.4	9594.0	5613.3	3375.0	2079.9	1310.7
843.0	327.1						

THE FOLLOWING PROPERTIES ARE AT AXIAL POSITION 20.00

HEAT TRANSFER COEFFICIENT

0.0	0.0	0.0	0.0	0.0	0.0	0.0	0.0
0.0	0.0	0.0	0.0	0.0	0.0	0.0	0.0
3.51111	3.39717	3.23022	3.07320	2.41456	1.92051	1.54457	1.25478
1.02876	0.67186						

"A" COEFFICIENT

0.07643

TIME ARRAY

0.00005	0.00005	0.00015	0.00025	0.00035	0.00045	0.00055	0.00064
0.00065	0.00075	0.00082	0.00085	0.00095	0.00097	0.00105	0.00111
0.00111	0.00115	0.00125	0.00135	0.00185	0.00235	0.00285	0.00335
0.00385	0.00500						

GAS TEMPERATURE-DEG R

5060.00	5060.00	4667.06	4790.78	4673.28	4459.46	4219.01	4005.51
3984.22	3797.57	3705.85	3655.00	3508.95	3485.46	3398.60	3337.21
3334.46	3307.74	3234.48	3163.64	2842.04	2567.10	2330.20	2124.65
1945.14	1609.59						

HEAT TRANSFER PER UNIT AREA,BTU/FT**2 MAXIMUM SURFACE TEMPERATURE-DEG R AND TIME-SEC

11.22611 830.95947 0.00234

THE FOLLOWING PROPERTIES ARE AT AXIAL POSITION 15.00

HEAT TRANSFER COEFFICIENT

0.0	0.0	0.0	0.0	0.0	0.0	0.0	0.0
0.0	0.0	0.0	0.0	0.0	0.0	3.84585	3.52278
3.51104	3.39710	3.23015	3.07314	2.41451	1.92047	1.54454	1.25476
1.02874	0.67185						

"A" COEFFICIENT

0.08740

TIME ARRAY

0.00005	0.00005	0.00015	0.00025	0.00035	0.00045	0.00055	0.00064
0.00065	0.00075	0.00082	0.00085	0.00095	0.00097	0.00105	0.00111
0.00111	0.00115	0.00125	0.00135	0.00185	0.00235	0.00285	0.00335
0.00385	0.00500						

GAS TEMPERATURE-DEG R

5060.00	5060.00	4667.06	4790.78	4673.28	4459.46	4219.01	4005.51
3984.22	3797.57	3705.85	3655.00	3508.95	3489.46	3398.60	3337.21
3334.46	3307.74	3234.48	3163.64	2842.04	2567.10	2330.20	2124.65
1945.14	1609.59						

HEAT TRANSFER PER UNIT AREA, BTU/FT**2 — MAXIMUM SURFACE TEMPERATURE-DEG R AND TIME-SEC

12.15458	853.01685	0.00224

THE FOLLOWING PROPERTIES ARE AT AXIAL POSITION 10.00

HEAT TRANSFER COEFFICIENT

0.0	0.0	0.0	0.0	0.0	0.0	0.0	0.0
0.0	0.0	0.0	5.72865	4.79235	4.63316	4.10639	3.76143
3.74890	3.62725	3.44899	3.28133	2.57809	2.09058	1.64918	1.33976
1.09843	0.71737						

"A" COEFFICIENT

0.11216

TIME ARRAY

0.00005	0.00005	0.00015	0.00025	0.00035	0.00045	0.00055	0.00064
0.00065	0.00075	0.00082	0.00085	0.00095	0.00097	0.00105	0.00111
0.00111	0.00115	0.00125	0.00135	0.00185	0.00235	0.00285	0.00335
0.00385	0.00500						

GAS TEMPERATURE-DEG R

5060.00	5060.00	4667.06	4790.78	4673.28	4459.46	4219.01	4005.51
3984.22	3797.57	3705.85	3655.00	3508.95	3489.46	3398.60	3337.21
3334.46	3307.74	3234.48	3163.64	2842.04	2567.10	2330.20	2124.65
1945.14	1609.59						

HEAT TRANSFER PER UNIT AREA,BTU/FT**2
15.00000

MAXIMUM SURFACE TEMPERATURE-DEG R AND TIME-SEC
927.07324 0.00198

THE FOLLOWING PROPERTIES ARE AT AXIAL POSITION 5.00

HEAT TRANSFER COEFFICIENT

0.0	0.0	0.0	0.0	0.0	0.0	0.0	0.0
9.08985	7.38223	6.48286	6.12139	5.12098	4.95080	4.38792	4.01931
4.00592	3.87593	3.68545	3.50630	2.75484	2.19116	1.76224	1.43161
1.17374	0.76655						

"A" COEFFICIENT

0.16079

TIME ARRAY

0.00005	0.00005	0.00015	0.00025	0.00035	0.00045	0.00055	0.00064
0.00065	0.00075	0.00082	0.00085	0.00095	0.00097	0.00105	0.00111
0.00111	0.00115	0.00125	0.00135	0.00185	0.00235	0.00285	0.00335
0.00385	0.00500						

GAS TEMPERATURE-DEG R

5060.00	5060.00	4667.06	4790.78	4673.28	4459.46	4219.01	4005.51
3984.22	3797.57	3705.85	3655.00	3508.95	3489.46	3398.60	3337.21
3334.46	3307.74	3234.48	3163.64	2842.04	2567.10	2330.20	2124.65
1945.14	1609.59						

HEAT TRANSFER PER UNIT AREA,BTU/FT**2	MAXIMUM SURFACE TEMPERATURE-DEG R	AND TIME-SEC
19.42145	1949.85425	0.00156

THE FOLLOWING PROPERTIES ARE AT AXIAL POSITION 0.0

HEAT TRANSFER COEFFICIENT

0.0	0.0	0.0	3.96834	8.93024	11.28022	10.62255	9.09458
8.92506	7.24840	6.36533	6.01041	5.02806	4.86105	4.30837	3.94645
3.93330	3.80566	3.61863	3.44273	2.70490	2.15144	1.73029	1.40566
1.15246	0.75265						

A COEFFICIENT

0.35303

TIME ARRAY

0.00005	0.00005	0.00015	0.00025	0.00035	0.00045	0.00055	0.00064
0.00065	0.00075	0.00082	0.00085	0.00095	0.00097	0.00105	0.00111
0.00111	0.00115	0.00125	0.00135	0.00185	0.00235	0.00285	0.00335
0.00385	0.00500						

GAS TEMPERATURE-DEG R

5060.00	5060.00	4667.96	4790.78	4673.28	4459.46	4219.01	4005.51
3984.22	3797.57	3705.85	3655.00	3508.95	3449.46	3398.60	3337.21
3334.46	3307.74	3234.48	3163.64	2842.04	2567.10	2330.20	2124.65
1945.14	1609.59						

HEAT TRANSFER PER UNIT AREA, BTU/FT**2	MAXIMUM SURFACE TEMPERATURE-DEG R	AND TIME-SEC
30.20935	1482.91431	0.00082

THE FOLLOWING PROPERTIES ARE AT AXIAL POSITION -0.05

HEAT TRANSFER COEFFICIENT

0.0	0.0	0.0	2.39960	5.40000	6.42101	6.42332	5.49938
5.39687	4.38301	3.84903	3.63442	3.04040	2.93941	2.60522	2.38637
2.37842	2.30123	2.18814	2.08178	1.63562	1.30095	1.04629	0.84999
0.69688	0.45512						

"A" COEFFICIENT

0.21797

TIME ARRAY

0.00005	0.00005	0.00015	0.00025	0.00035	0.00045	0.00055	0.00064
0.00065	0.00075	0.00082	0.00085	0.00095	0.00097	0.00105	0.00111
0.00111	0.00115	0.00125	0.00135	0.00185	0.00235	0.00285	0.00335
0.00385	0.00500						

GAS TEMPERATURE-DEG R

5060.00	5060.00	4667.06	4790.78	4673.28	4459.46	4219.01	4005.51
3984.22	3797.57	3705.85	3655.00	3508.95	3489.46	3398.50	3337.21
3334.46	3307.74	3234.48	3163.64	2842.04	2567.10	2330.20	2124.65
1945.14	1[illegible]9.59						

HEAT TRANSFER PER UNIT AREA,BTU/FT**2

19.73676

MAXIMUM SURFACE TEMPERATURE-DEG R AND TIME-SEC

1156.26953 0.00084

THE FOLLOWING PROPERTIES ARE AT AXIAL POSITION -0.60

HEAT TRANSFER COEFFICIENT

0.0	0.0	0.0	1.78220	4.01062	5.06602	4.77065	4.08443
4.00930	3.25530	2.85871	2.69931	2.25813	2.18313	1.93491	1.77237
1.76647	1.70914	1.62515	1.54615	1.21478	0.96622	0.77709	0.63129
0.51758	0.33802						

"A" COEFFICIENT

0.21987

TIME ARRAY

0.00005	0.00005	0.00015	0.00025	0.00035	0.00045	0.00055	0.00064
0.00065	0.00075	0.00082	0.00085	0.00095	0.00097	0.00105	0.00111
0.00111	0.00115	0.00125	0.00135	0.00185	0.00235	0.00285	0.00335
0.00385	0.00500						

GAS TEMPERATURE-DEG R

5060.00	5060.00	4667.06	4790.78	4673.28	4459.46	4219.01	4005.51
3984.22	3797.57	3705.85	3655.00	3508.95	3489.46	3398.60	3337.21
3334.46	3307.74	3234.48	3163.64	2842.04	2567.10	2330.20	2124.65
1945.14	1609.59						

HEAT TRANSFER PER UNIT AREA, BTU/FT**2 — MAXIMUM SURFACE TEMPERATURE-DEG R AND TIME-SEC

15.17862 — 1011.86670 — 0.00086

THE FOLLOWING PROPERTIES ARE AT AXIAL POSITION -1.10

HEAT TRANSFER COEFFICIENT

0.0	0.0	0.0	1.51898	3.41827	4.31778	4.06604	3.48117
3.41629	2.77450	2.43649	2.30063	1.92461	1.86069	1.64913	1.51060
1.50556	1.45671	1.38512	1.31779	1.03537	0.82352	0.66231	0.53805
0.44113	0.28810						

A COEFFICIENT

0.39009

TIME ARRAY

0.00005	0.00005	0.00015	0.00025	0.00035	0.00045	0.00055	0.00064
0.00065	0.00075	0.00082	0.00085	0.00095	0.00097	0.00105	0.00111
0.00111	0.00115	0.00125	0.00135	0.00185	0.00235	0.00285	0.00335
0.00385	0.00500						

GAS TEMPERATURE-DEG R

5060.00	5060.00	4667.06	4790.78	4673.28	4459.46	4219.01	4005.51
3984.22	3797.57	3705.85	3655.00	3508.95	3489.46	3398.60	3337.21
3334.46	3307.74	3234.48	3163.64	2842.04	2567.10	2330.20	2124.65
1945.14	1609.59						

HEAT TRANSFER PER UNIT AREA, BTU/FT**2
13.14264

MAXIMUM SURFACE TEMPERATURE-DEG R AND TIME-SEC
947.32104 0.00086

List of Symbols for Section II

A_s	heat input area of modified axial section 3 of Figure 2 - ft^2
A_{taper}	actual heat input area of tapered axial section 3 of Figure 2 - ft^2
A_{1-2}	area for conduction between axial sections 1 and 2 - ft^2
A_{2-3}	area for conduction between axial sections 2 and 3 - ft^2
C	specific heat of the material - Btu/lb - °F
h_I	interface coefficient - Btu/ft^2 - sec - °F
h_L	loss coefficient - Btu/ft^2 - sec - °F
$h(\theta)$	propellant gas heat transfer coefficients tabular values with time - Btu/ft^2 - sec - °F
K	thermal conductivity - Btu/ft - sec - °F
L_s	length of axial section 3 of Figure 2 - ft
L_1	length of axial section 1 - ft
L_2	length of axial section 2 - ft
L_3	length of axial section 3 - ft
$q(\theta)$	general heat input per square foot per second as a function of time - Btu/ft^2 - sec
q_L	heat loss rate - Btu/ft^2 - sec
R_I	radius to interface measured from chamber centerline - ft
R_1	radius to inner chamber wall - ft
R_{OD}	radius to outer chamber wall - ft
R_2	radius defined by Figure 2 - ft
$T_{ave_o}( )$	average temperature of section ( ) at the beginning of a shot - °F
$T_{ave}( )$	average temperature of section ( ) after a time interval θ_E - °F
$T_L(\theta)$	temperature of outer element as a function of time - °F
T_n	temperature of element n - °F
T'_n	temperature of element n after a time interval, $\Delta\theta$ - °F
$T_g(\theta)$	temperature of the propellant gases in tabular form - °F
T_1	temperature of the surface element - °F
T_{ENV}	temperature of the environment - °F
V_{taper}	actual volume of axial section 3 of Figure 2 - ft^3
V_s	modified volume of axial section 3 of Figure 2 - ft^3
θ	time - sec
θ_f	heat input period - sec
θ_E	cycle period - sec

θ_c	cooling period between bursts - sec
$\Delta\theta$	time increment for computer calculations - sec
δ	element size - ft
ρ	density - lb/ft^3
ε	emissivity
σ	Stefan-Boltzmann constant
$(\ )_c$	refers to coating
$(\ )_m$	refers to metal

II. COMPOSITE CYLINDRICAL CONDUCTION HEAT TRANSFER COMPUTER PROGRAM

Calculation of temperatures within the chamber or barrel walls during firing of multiple rounds can be performed once the time history of propellant gas temperature and local heat transfer coefficients are known. The composite cylindrical conduction computer program written at CAL performs this function with consideration to balance of machine time with computational accuracy. In the program, radial conduction into the chamber is given chief emphasis, but the effects of axial conduction along the chamber are included by an approximation which limits the required machine time normally associated with three-dimensional conduction computer programs.

A. Geometrical Considerations

The key to reduction of computer time is an introduction of a change of dimension at an arbitrary distance, R_I, within the chamber wall as measured from the chamber axis. This is shown in Figure A1. For generalization, at this location an arbitrary interface coefficient can also be specified if composite chambers are to be studied. Parameters within the cross section between R_1 and R_I are, for generality, given the subscript $()_{coat}$. Between R_I and R_{OD} they are given the subscript $()_{metal}$. Each cross section is divided into a chosen number of elements, and the element size is determined by the computer. The thermal conductivity, K, specific heat, C, and density, ρ, are input for both the "coating" and the "metal" as well as the interface coefficient, h_I.

The chamber can also be divided into as many as five axial sections of arbitrary length and diameter. This option is used when axial conduction effects are to be considered. When this option is exercised, the thermal properties of the "coating" must be the same as those of the "metal". In effect, the "coating" cross section simply serves to provide a reduction in element size near the heated surface, improving the accuracy of the calculation.

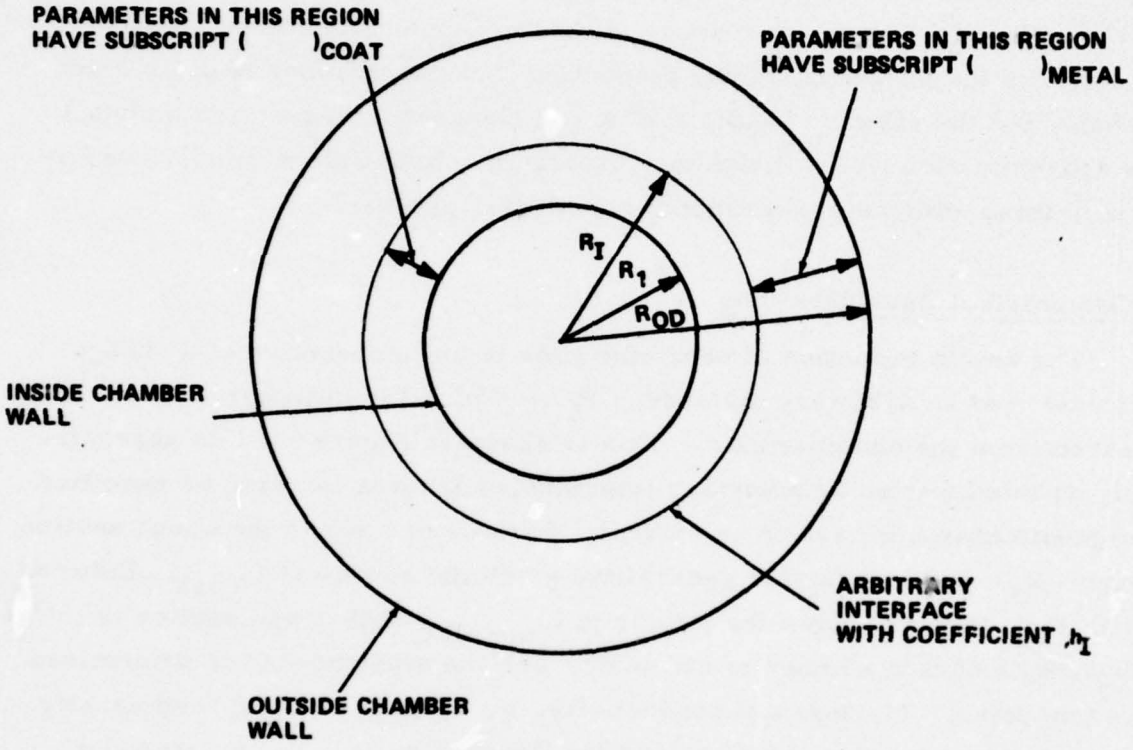

Figure A-1 CROSS SECTIONAL VIEW AT A TYPICAL CHAMBER AXIAL SECTION

The actual geometry is simplified by choosing length and inner and outer radii so that the correct mass per unit internal surface area is maintained at each section. Figure A2 indicates a typical chamber with possible axial divisions. The inner and outer radii of sections 1, 2, and 5 can be left unchanged. The outer radius of section 4 (shown by the dashed line) is adjusted to maintain the same volume in that section as in the original tapered section. Section 3 has both its inner and outer radii adjusted as given by the following method: First, the inner radius is taken as the average of the inner tapered surface $(R_1 + R_2)/2$. The new inside surface area is computed from

$$A_s = \pi(R_1 + R_2)\, L_s \tag{22}$$

The original inside area on the taper is

$$A_{taper} = \pi(R_1 + R_2)\sqrt{L_s^2 + (R_1 - R_2)^2} \tag{23}$$

The volume of the original section is

$$V_{taper} = \pi\left[R_{OD}^2 - \left(\frac{R_1 + R_2}{2}\right)^2\right] L_s \tag{24}$$

because $\dfrac{V_{taper}}{A_{taper}} = \dfrac{V_s}{A_s}$,

$$V_s = \frac{\pi\left[R_{OD}^2 - \left(\frac{R_1 + R_2}{2}\right)^2\right] L_s^2}{\sqrt{L_s^2 + (R_1 - R_2)^2}} = \pi\left[R_s^2 - \left(\frac{R_1 + R_2}{2}\right)^2\right] L_s \tag{25}$$

$$R_s = \sqrt{\left(\frac{R_1 + R_2}{2}\right)^2 + \frac{\left[R_{OD}^2 - \left(\frac{R_1 + R_2}{2}\right)^2\right] L_s}{\sqrt{L_s^2 + (R_1 - R_2)^2}}} \tag{26}$$

Use of the radius R_s for R_{OD} will thus yield the same volume per unit internal surface area as in the original section. It is important to note that the volume per unit internal area must be correct in order that the average temperature rise of the section be correct.

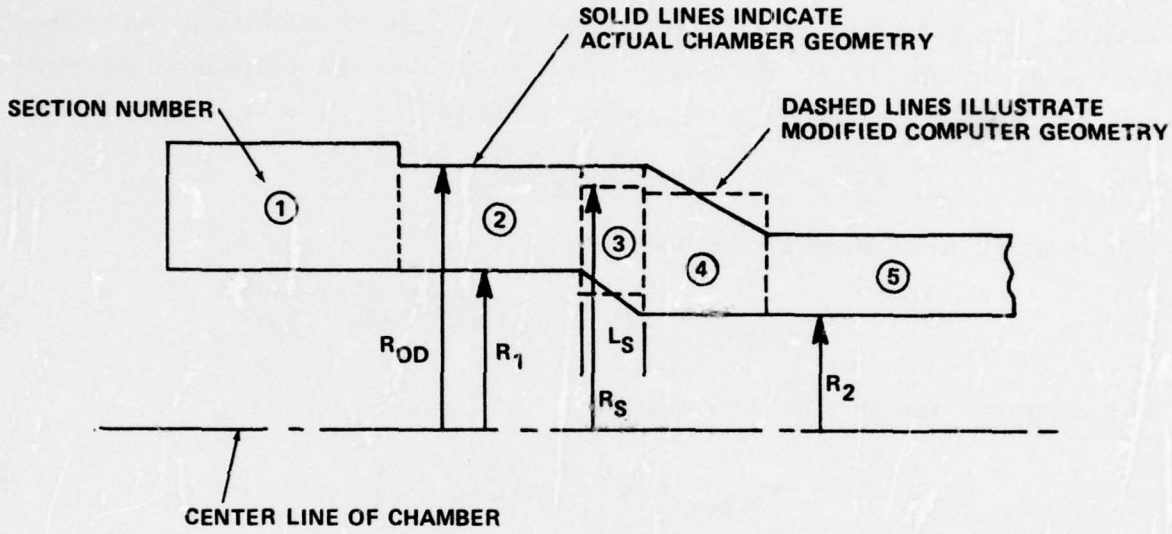

Figure A-2 TYPICAL AXIAL CHAMBER SECTIONS

B. Heat Input Parameters

The heat input at each axial section during the firing of individual shots is dependent upon a convection heat transfer coefficient history, a propellant gas temperature history, and the temperature of the inner surface element. At each axial section, the heat flux rate to the inner surface is represented by

$$q(\theta) = h(\theta)\left[T_g(\theta) - T_1(\theta)\right] \tag{27}$$

where

- $q(\theta)$ is the heat flux rate as a function of time,
- $h(\theta)$ is the convection coefficient history specified for the section,
- $T_g(\theta)$ is the propellant gas temperature history specified for the section,
- $T_1(\theta)$ is the computed temperature of the inner surface element as a function of time,
- θ is the time.

Hence, at any time, θ, the heat input rate can be computed which affects the future calculated inner surface temperature $T_1(\theta)$, according to the conduction relations to be discussed later.

Heat losses from each axial section at the outer surface also depend upon given heat transfer coefficients and the temperature of the environment as well as the temperature of the outer element. But here, in addition, radiation heat transfer is considered. Thus, the equation for heat loss rate is

$$q_L = h_L\left[T_L(\theta) - T_{ENV}\right] + \sigma\epsilon\left[T_L(\theta)^4 - T_{ENV}^4\right] \tag{28}$$

where

- h_L is a specified convection coefficient for loss,
- $T_L(\theta)$ is the absolute temperature of outer surface elements,
- T_{ENV} is the absolute environmental temperature,
- σ is the Stefan-Boltzmann constant,
- ϵ is a specified emissivity factor.

Again, the loss depends upon a calculated temperature ($T_L(\theta)$), and this in turn affects all future calculated temperatures.

C. Time Factors

There are several time periods of interest during computer simulations of rapid-fire conditions. These are depicted by Figure A3. First, the relatively short period in which the total heat per shot is introduced into the inner chamber wall is of importance and is specified by the time factor, θ_f, in the figure. This time is derived from the convection coefficient history at the time after firing at which $h(\theta)$ can be taken as negligible (i.e., $h(\theta) = 0$). Second, the cycle time or the period between shots is required. This time is designated by θ_E in the figure. Third, if temperatures for more than one burst are to be computed, the cooling interval between bursts must be specified. This is indicated by θ_c in Figure A3. During each of the above time intervals, there are used separate and distinct time increments, $\Delta\theta$, for temperature calculations. For the first time interval during each shot, the time increment to be used is based upon either the maintenance of stability in the solution or adequate subdivision of the heat input period, whichever is the smaller. Subdivision of the heat input period is specified by input of a time increment factor during firing (see Sample Computer Output) selected by the programmer. This factor effectively divides the firing period into a selected number of time increments. For example, if the firing (heat input) period were 10 milliseconds, one may chose to divide this period into at least 100 increments. To do this, a time increment factor of 99 would be selected (one less than the number of increments desired). The computer also determines a maximum allowable time increment for stability, as discussed in subsection E. For the time interval during firing, the smaller of these time increments is used.

In the second time period, the time between shots, only the time increment required for stability of the solution is used.

In the cooling interval, the time increment remains the same as that for the second time period until a convergence criterion relating to thermal gradient in the chamber wall is met. This is designated as the cooling convergence error, with value 0 - 1.0. The convergence error is simply the ratio of outer to inner wall temperature. Hence, a convergence error of 0.5 indicates that calculations will continue using the time increment of the second time

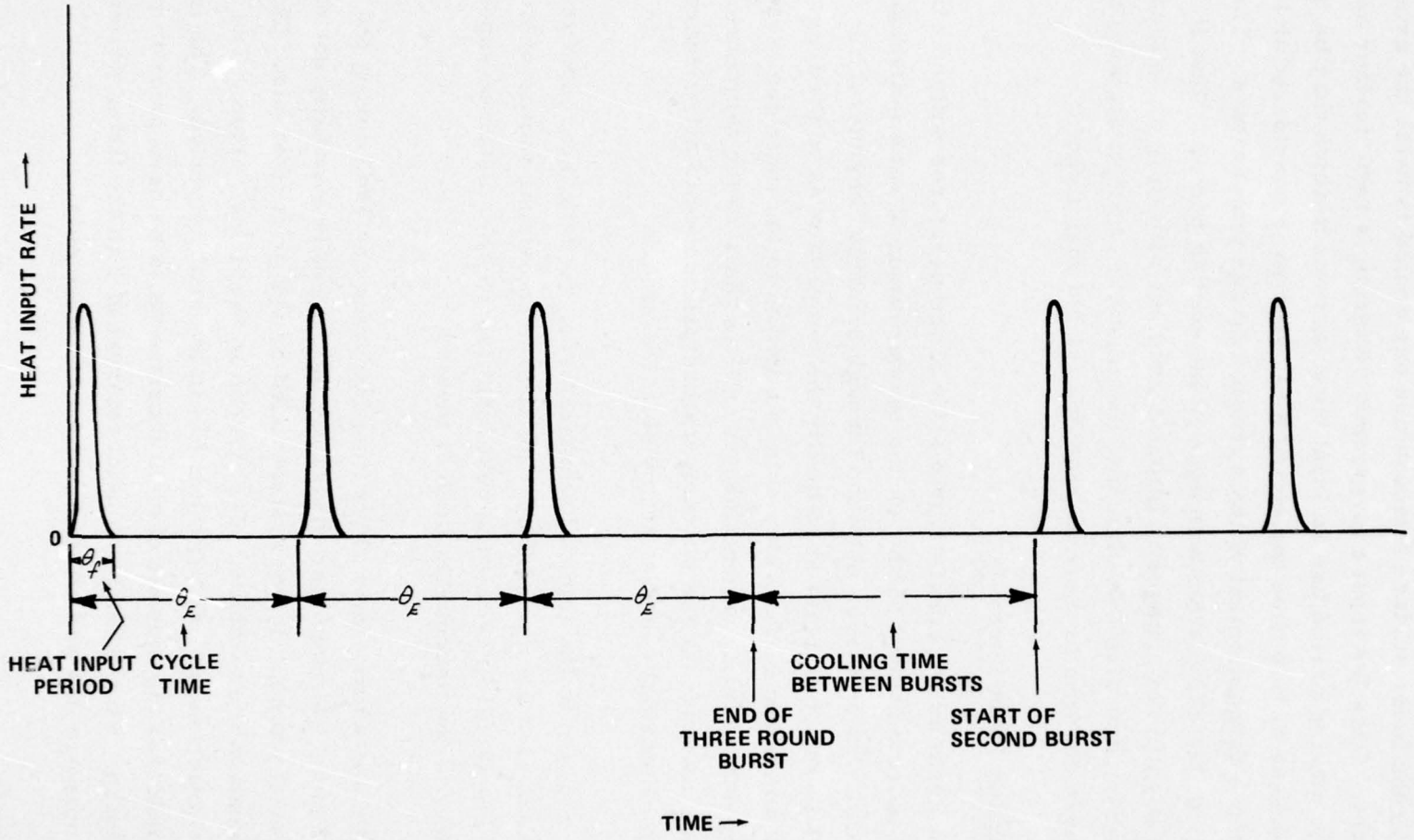

Figure A-3 TIME FACTORS FOR COMPUTER SIMULATION OF RAPID FIRE

period until the inner surface temperature has cooled to twice the external temperature. Once the input convergence criterion is met, further calculations in the cooling period use an input time increment which may be much larger, because at this time the entire axial section is considered to be cooling as one large element of the correct average temperature. The chief advantage of this calculation technique in the cooling period is that it can allow investigation of changes in internal gradient with time while these changes are significant, and also can eliminate meaningless, time consuming calculations where changes in thermal gradient are not significant.

D. Output and Print Intervals

Program output consists primarily of temperatures within each axial section at selected times. Although the temperatures of each individual element of each axial section can be obtained through printout, in general use, the output format is set up to print specifically the temperatures of the inner surface, interface, and outer surface elements in addition to the individual averages of the coating and metal cross sections as well as the average temperature of the entire axial section. These six temperature printouts can allow reasonable estimation of thermal gradient at any selected time.

In addition to the internal temperatures, the total heat input to the inner surface element during the firing of each individual shot is printed out. This is found useful in evaluating heat input information obtained experimentally through in-wall thermocouples or heat meters.

As noted above, very short time intervals are used during the calculations. Printout at each individual time increment is generally not needed. The amount of printout desired is specified by the print intervals. Three intervals are input to the machine. The first is in the firing period. The second is in the extraction period. The third is in the cooling period. The input print interval indicates the number of time increments to be used prior to printout in each period. For example, a print interval of 5 in the firing period indicates that printouts are desired after each 5 time increments.

Several printouts are given in addition to those called for by the print interval. These occur at any maximum of the above six temperatures. Also, printouts are given at the end of the heat input period, θ_f, the cycle period θ_E, and at the time the cooling convergence error is satisfied.

E. Heat Conduction Relations

1. Radial Conduction

Conduction of heat to the interior of the composite cylinder at each axial section is determined by use of finite difference relations based upon subdivision of the cylindrical section. Figure A4 indicates a general subdivision of a particular axial section. In region I (or the coating region) the central elements are of thickness δ_c and the two end elements are half sized, $\delta_c/2$. In region II the same general geometry is used, but the element thickness is δ_m. At the interface between regions (designated by I in the figure), there is a given interface coefficient, h_I.

Temperatures within each element as a function of time are determined by heat balances in which a new temperature of each element after a specific time interval is calculated based upon its and neighboring element temperatures. At the surface the heat input per unit length in the time interval $\Delta\theta$ is

$$q_{in} = 2\pi R_1 h(\theta) \left(T_g - T_1\right)\Delta\theta \tag{29}$$

The heat out of element 1 to element 2 is

$$q_{1-2} = 2\pi(R_1 + .5\delta_c) \frac{K_c}{\delta_c} (T_1 - T_2)\Delta\theta \tag{30}$$

The heat stored in element 1 is

$$q_{stored} = \pi R_1 \delta_c C_c \rho_c (T_1' - T_1) \tag{31}$$

but

$$q_{stored} = q_{in} - q_{out} \tag{32}$$

Hence with good approximation,

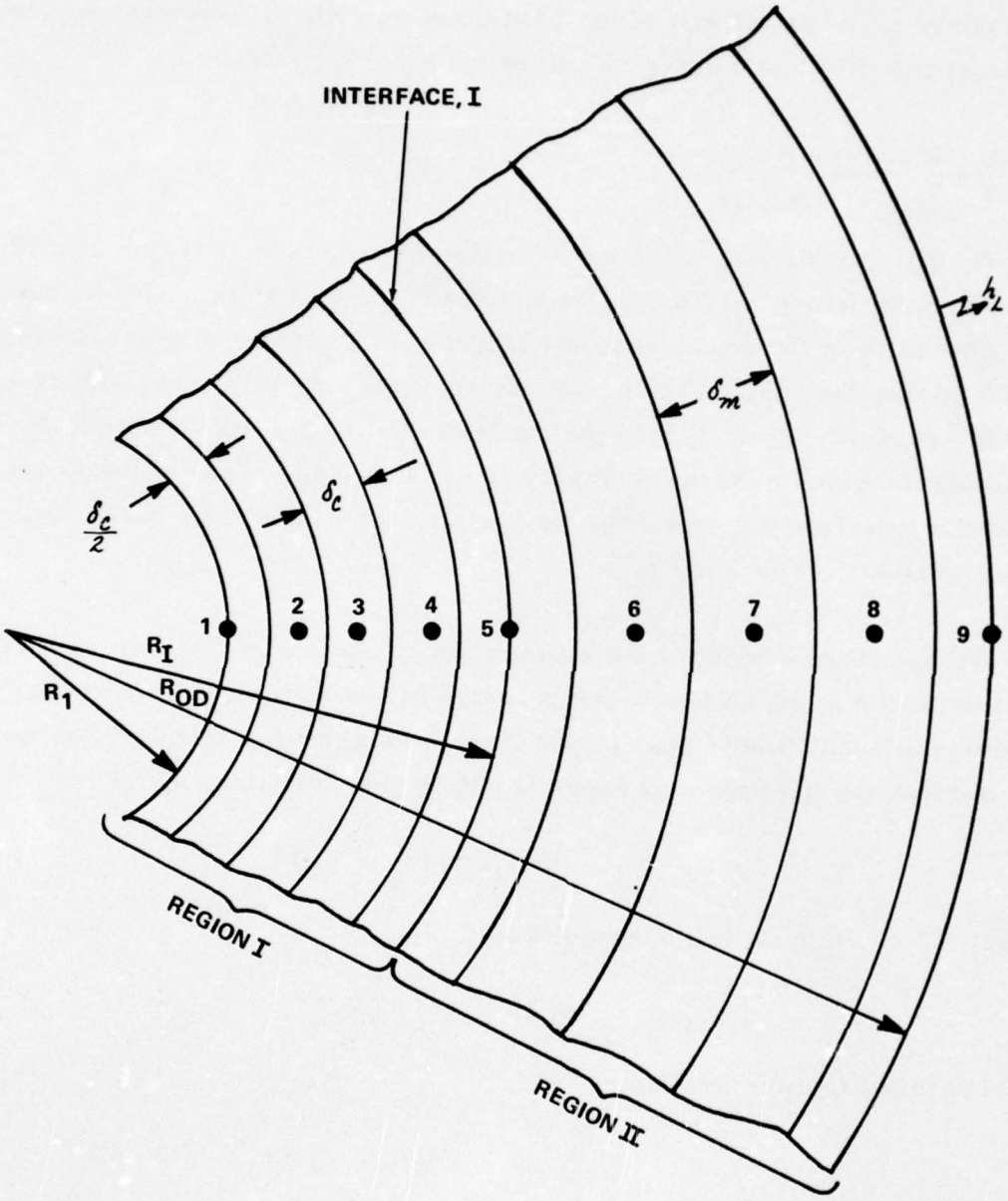

Figure A-4 GENERAL SUBDIVISION OF AXIAL SECTIONS INTO RADIAL ELEMENTS

$$T_1' = \frac{2\Delta\theta}{C_c\rho_c\delta_c} h(\theta)\left(T_g - T_1\right) - \frac{2(R_1 + .5\delta_c)K_c\Delta\theta}{C_c\rho_c\delta_c^2 R_1}(T_1 - T_2) + T_1 \quad (33)$$

By similar treatment, the internal elements in region I (elements 2 and 3 of Figure A4) are computed from

$$T_n' = \frac{K_c\Delta\theta}{C_c\rho_c\delta_c^2}\left[\frac{\left(R_1 + .5(2n-3)\delta_c\right)(T_{n-1} - T_n)}{R_1 + (n-1)\delta_c} - \frac{\left(R_1 + .5(2n-1)\delta_c\right)(T_n - T_{n+1})}{R_1 + (n-1)\delta_c}\right] + T_n \quad (34)$$

$2 < n < I - 2$

where I is the number of the interface element. The temperature of the last full element in region I (element 4 of Figure A4) is obtained from

$$T_n' = \frac{K_c\Delta\theta}{C_c\rho_c\delta_c^2(R_1 + (n-1)\delta_c)}\left[\left[R_1 + .5\delta_c(2n-3)\right]\left[T_{n-1} - T_n\right] - \left(\frac{h_I}{K_c + 2\delta_c h_I}\right)\left[R_1 + .5\delta_c(2n-1)\right](T_n - T_{n+1})\right] + T_n \quad (35)$$

$n = I - 1$

At the interface $n = I$

$$T_{mass_1} = \frac{4\Delta\theta h_I}{C_c\rho_c\delta_c(R_I - .25\delta_c) + C_m\rho_m\delta_m(R_I + .25\delta_m)}$$

$$T_n = T_{mass_1}\left[\left(\frac{K_c}{K_c + 2\delta_c h_I}\right)(R_I - .5\delta_c)(T_{n-1} - T_n) - \left(\frac{K_m}{K_m + 2\delta_m h_I}\right)(R_I + .5\delta_m)(T_n - T_{n+1})\right] + T_n \quad (36)$$

The temperatures of the first full element of region II, n = I+ 1, are obtained from

$$T_{mass_2} = \frac{K_m \Delta\theta}{C_m \rho_m \delta_m^2 (R_I + \delta_m)} \tag{37}$$

$$T_n' = T_{mass_2} \left[\left(\frac{2h_I \delta_m}{K_m + 2h_I \delta_m} \right) (R_I + .5\delta_m)(T_{n-1} - T_n) - (R_I + 1.5\delta_m)(T_n - T_{n+1}) \right] + T_n \tag{38}$$

The temperatures of the internal elements of region II are obtained from

$I + 1 < n < I_L$ (the number of the last element)

$$T_n' = \frac{\Delta\theta K_m}{C_m \rho_m \delta_m^2 \left[R_I + (n - I)\delta_m \right]} \times \left[\left(R_I + .5\left[2(n - I) - 1 \right] \delta_m \right) (T_{n-1} - T_n) - \left[\left(R_I + .5\left[2(n - I) + 1 \right] \delta_m \right) (T_n - T_{n+1}) \right] + T_n \right] \tag{39}$$

The temperatures in the final element (last element) are determined from

$n = I_L$

$$T_n' = \frac{2\Delta\theta K_m (R_{OD} - .5\delta_m)(T_{n-1} - T_n)}{C_m \rho_m R_{OD} \delta_m^2} - \frac{2h_L \Delta\theta (T_n - T_{amb})}{C_m \rho_m \delta_m} - \frac{2\sigma\varepsilon\Delta\theta \left[(T_n + 460)^4 - (T_{amb} + 460)^4 \right]}{C_m \rho_m \delta_m} + T_n \tag{40}$$

In order to maintain stability of the solution, the time interval for each calculation must be selected with consideration of element size and thermal properties of the material. Stability is insured if the coefficients of the temperature at all nodal points or elements are equal to or slightly greater than zero. Three positions within the section are of most importance relative to stability, (1) at the surface, (2) at the interface, and (3) at the last element. Setting the coefficients of T_1 equal to zero and solving for $\Delta\theta$, we get

$$\Delta\theta_1 = \frac{1}{2} \frac{C_c \rho_c \delta_c^2}{(\delta_c h(\theta) + K_c)} \tag{41}$$

as the maximum time interval for stability based on the surface equation. This equation must be applied to all axial sections. For simplicity, the maximum value of $h(\theta)$ taken from the input tables of heat transfer coefficients for all sections may be used.

From the interface equation

$$\Delta\theta_2 = \frac{C_c \rho_c \delta_c + C_m \rho_m \delta_m}{\left(\frac{4K_c h_I}{K_c + 2\delta_c h_I} + \frac{4K_m h_I}{K_m + 2\delta_m h_I} \right)} \tag{42}$$

determines the maximum allowable time interval.

The maximum time interval based on the last element is

$$\Delta\theta_3 = \frac{C_m \rho_m \delta_m^2}{2K_m + 2h_L \delta_m + 2\sigma\varepsilon\delta_m (T_{L_{max}} + 460)^3} \tag{43}$$

But, in general,

$$K_m >> h_L \delta_m + \sigma\varepsilon (T_{L_{max}} + 460)^3 \delta_m$$

Thus, one can take

$$\Delta\theta_3 = \frac{1}{4} \frac{C_m \rho_m \delta_m^2}{K_m} \tag{44}$$

which assumes

$$K_m = h_L \delta_m + \sigma \mathcal{E} \delta_m (T_{L_{max}} + 460)^3 \qquad (45)$$

To assure stability, the minimum of $\Delta\theta_1$, $\Delta\theta_2$, and $\Delta\theta_3$ must be used for the computations. This minimum is determined by the computer prior to the beginning of calculations.

2. Axial Conduction

Conduction between axial sections is obtained by considering each axial section to be one large element conducting heat to neighboring axial sections. The temperature of the large element is taken to be the average of all radially internal elements in the axial section. This average is computed by summing the energy content of elements within the "coating" and "metal" individually and dividing by the combined thermal capacity of the section. In order to reduce computation time, axial conduction and its effect on the average temperatures of each section is computed only once for each round fired. In this computation, the average temperature of each axial section over the firing period is used to compute the total change in average temperature of each section in the cycle period. As an example of the axial conduction relations, the following describes the change in average temperature of axial section 2.

$$\Delta T_{ave}(2) = -\left\{ \frac{K_m A_{1-2} \left[T_{ave_o}(2) - T_{ave_o}(1) + T_{ave}(2) - T_{ave}(1) \right]}{(L_1 + L_2)\, \pi C_m \rho_m L_2 \left[R_{OD}^2(2) - R_1^2(2) \right]} \theta_E + \right.$$

$$\left. \frac{K_m A_{2-3} \left[T_{ave_o}(2) - T_{ave_o}(3) + T_{ave}(2) - T_{ave}(3) \right]}{(L_2 + L_3)\, \pi C_m \rho_m L_2 \left[R_{OD}^2(2) - R_1^2(2) \right]} \theta_E \right\} \qquad (46)$$

The change computed by this equation is then added to $T_{ave}(2)$ to find the new average temperature of section 2 at the end of the cycle period, θ_E. The other axial sections are handled in similar fashion. After having computed new average temperatures at each axial section, calculations then continue through the next firing period.

F. Computer Routine

The entire computer routine for temperature calculations written for use with an IBM 360/65 computer consists of several parts. First, the main program contains the majority of the program logic and performs some preliminary calculations as, for example, determination of element size and time increments. The main program also calls several subroutines including:

1. Subroutine CALC

   This subroutine calculates all internal temperatures within each axial section as well as average temperatures of each section.

2. Subroutine PRINT

   This subroutine prints out all temperature histories.

3. Subroutine INTAB

   This subroutine reads in heat transfer coefficient and gas temperature tables.

4. Subroutine INDAT

   This subroutine reads in the input data for the calculation.

5. Subroutine INTER

   This subroutine determines axial conduction effects on average temperatures.

Each of the above subroutines is called for at appropriate sequence by the main program. The entire program listing is given on pages 181 through 191. Sufficient comment cards are provided within the listing to allow basic understanding of logical flow. As a further aid, the simplified flow charts of pages 192 and 193 indicate the logical flow for the main program and subroutine CALC. A complete set of cards, including a set of sample input data cards, has been supplied to Frankford Arsenal.

G. Input Format

As indicated for the HTC program, application of the program to determining temperatures during and after heating, input information must be supplied to the machine and in the correct format. The master input

format for the cylindrical conduction program is given in pages 194 through 207. This format is along commonly accepted computational rules and should be easily applied by an experienced programmer. For clarity, the following indicates symbolism used where it may be unclear in the input format statements:

N	Number of axial sections up to 5.
NH( )	Number of entries in heat transfer coefficient array (up to 60).
THETAH (,)	Time array for heat transfer coefficients.
H(,)	Corresponding heat transfer coefficient array. The final entry should be zero.
NTG( )	Number of entries in propellant gas temperature array (up to 60).
THETAG(,)	Time array for propellant gas temperature.
TG(,)	Corresponding propellant gas temperature array.
THETA F	The time at which the last coefficient becomes equal to zero.
THETA E	The cycle time.
THETA C	The cooling interval between bursts.
DTHEC	The time increment during cooling (should be about 0.01 THETAC).
CLER	The cooling convergence error (should not be equal to 1.0).
XCOOL	Set XCOOL at zero (not applicable to this calculation).
HMAX	Maximum coefficient appearing in the heat transfer coefficient arrays.
HINT	Interface heat transfer coefficient.
EPS	Emissivity of outer surface (0 - 1.0).

MINC	Time increment factor as discussed under Section C, Time Factor.
SCALE	Set this equal to 1.0.
IPRINT 1	Number of time steps to be calculated before PRINT in the period 0-THETA F.
IPRINT 2	Number of time steps to be calculated before PRINT in the period THETA F - THETA E.
IPRINT 3	Number of time steps to be calculated before PRINT in the period THETA E - THETA C.

The other input quantities should be evident by inspection of the master input statement.

H. Output Format

The output of the machine for a sample calculation is shown in pages 208 through 218. Output begins by a printout of all heat transfer coefficient, gas temperature, and time arrays. Following this is a printout of all input information used in the calculation, as well as some preliminary calculations of distance and time increments. Finally, the calculated temperatures for each section are given as a function of time during the input firing schedule. Again, for clarity the following is given to describe output information:

T(1)	The temperature of the bore surface element - °F.
T(INTER)	The temperature of the interface element - °F.
T(LAST)	The temperature of the outer surface element - °F.
T(CT)AVE	The average temperature in the coating - °F.
T(ML)AVE	The average temperature in the metal.
TAVE	The combined average temperature of the section.
QIN	The heat input per unit internal area for the section - Btu/ft^2.

AD-A034 159 CALSPAN CORP BUFFALO N Y F/G 19/1
CASELESS AMMUNITION HEAT TRANSFER. VOLUME III.(U)
APR 76 D E ADAMS, F A VASSALLO DAAG25-70-C-0454
UNCLASSIFIED CALSPAN-GM-2948-Z-3-VOL-3 NL

3 OF 3
AD
AD34159

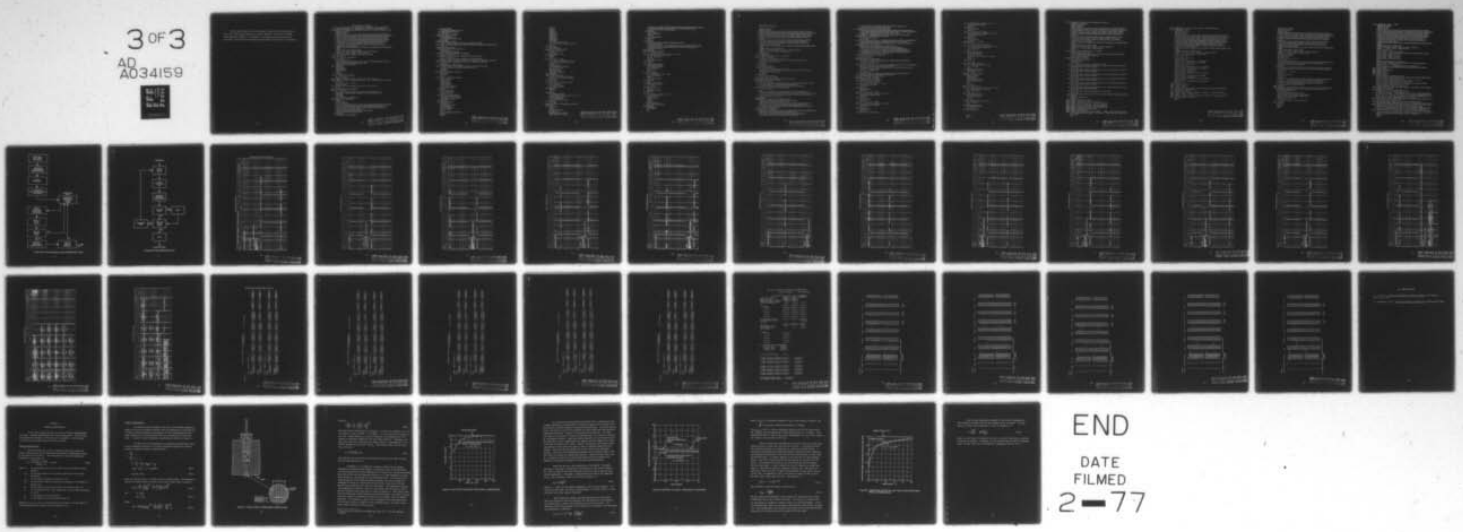

END
DATE FILMED
2-77

These output values can allow adequate estimation of thermal gradients. Of course, additional temperatures could be obtained, if desired, by change in the subroutine PRINT. For example, a secondary print statement could be written to print the entire temperature distribution if this were of importance.

COMPUTER LISTING
FOR COMPOSITE CYLINDRICAL CONDUCTION PROGRAM

```
C THIS PROGRAM COMPUTES THE TEMPERATURE HISTORY OF A CYLINDRICAL
C COMPOSITE GUN CHAMBER WITH MULTIPLE BURSTS AND VARIOUS COOLING CYCLES
      IMPLICIT REAL(K)
      INTEGER SCALE
      COMMON TABTIT(20),TITLE(20),ACCTHE,CCOAT,CMETL,DELC(5),DELM(5),
     1 DTH1,DTH2,DTH3,DTH4,DTHE,DTHEC,DTHEF,DTHEF,EPS,H(5,60),HINT,HLOSS
     2,HXT(5),IBURST,ICOAT,IGO,IMETL,IP,IROUND,IPRINT,IPRNT1,IPRNT2,
     3 IPRNT3,ITOT,KCOAT,KMETL,LFTML,LINTC,LINTM,LINTR,LLTCT,LLTML,
     4 LPRNT(5),MBURST,MINC,MPRNT,MROUND,N,TAVOLD(5),DTAVG(5),ACCOLD
      COMMON NH(5),NTG(5),RCOAT,RID(5),RINT(5),RMETL,ROD(5),SIGMA,
     1 T(5,400),TAMB,TAVCT(5),TAVML(5),TB(5),TG(5,60),TGXT(5),
     2 THEH(5,60),THETA,THETAC,THETAE,THETAF,THETG(5,60),TINT(5),
     3 TMASS(5),TP(5,400),SCALE
      COMMON TENV,MGOTH,THMAX,MGOTI,TIMAX,MGOTO,TOMAX,MGTAC,TCMAX,MGTAM,
     1 TMMAX
      COMMON HMAX,QIN(5),TCHAM,XCOOL
      COMMON CLER,IAVG,AREA(4),SECTL(5),ISKIP,TMASS2(5)
      COMMON LT, LSUB1, LSUB2, LSUB3,ALPH(2)
C READ IN AND PRINTOUT TABULAR HEAT FLUX HISTORIES
    1 CALL INTAB
C READ IN DATA FOR COMPUTATION
    2 CALL INDAT
      DO 2222 ISECT=1,N
      TMASS2(ISECT)=CCOAT*RCOAT*(RINT(ISECT)**2-RID(ISECT)**2)+CMETL*
     1 RMETL*(ROD(ISECT)**2-RINT(ISECT)**2)
      TAVOLD(ISECT)=TINT(ISECT)
 2222 CONTINUE
      ACCOLD=0.0
      STDTHC=DTHEC
      STHETC=THETAC
      IAVG=0
      ISKIP=0
C CHECK FOR MIN NO OF SLABS
      IF (ICOAT.GT.4) GO TO 3
      WRITE (6,9000)
 9000 FORMAT (1H1//40X,'ERROR'/25X,'ICOAT LESS THAN 5')
 5000 FORMAT(1HO,'LAST ROUND OF BURST NO.',I5,' BEGIN UNIFORM COOLING')
      GO TO 2
    3 IF(IMETL.GT.4) GO TO 2223
      WRITE (6,9001)
 9001 FORMAT (1H1//40X,'ERROR'/25X,'IMETL LESS THAN 5')
      GO TO 2
C DETERMINE DISTANCE INCREMENTS
 2223 DO 6 ISECT=1,N
      DELC(ISECT)=(RINT(ISECT)-RID(ISECT))/(FLOAT(ICOAT)-1.)
      DELM(ISECT)=(ROD(ISECT)-RINT(ISECT))/(FLOAT(IMETL)-1.)
    6 CONTINUE
      TENV=TAMB
      CALL CLEAR(QIN(1),QIN(5))
C DETERMINE TIME INCREMENTS
      IDUM=2
      DTHE=10.0**10
      DO 10 ISECT=1,N
      DTH1=(0.5*CCOAT*RCOAT*DELC(ISECT)**2)/(HMAX*DELC(ISECT)*1.0+KCOAT)
      DTH2=(CCOAT*RCOAT*DELC(ISECT)+CMETL*RMETL*DELM(ISECT))*0.25/
     1 ((HINT*KCOAT)/(KCOAT+2.0*DELC(ISECT)*HINT)+(HINT*KMETL)/
     2 (KMETL+2.0*DELM(ISECT)*HINT))
      DTH3=(.25*CMETL*RMETL*DELM(ISECT)**2)/KMETL
      DTHE=AMIN1(DTH1,DTH2,DTH3,DTHE)
   10 CONTINUE
      DTH4=THETAF/(FLOAT(MINC))
```


COPY AVAILABLE TO DDC DOES NOT PERMIT FULLY LEGIBLE PRODUCTION

```
   11 DTHE=0.5*DTHE
      IF (DTHE.LT.DTH4) GO TO 30
   12 IDUM=2.0*DTHE/DTH4+0.6
      DTHE=DTH4
C ROUND OFF TIME INCREMENT
   30 DO 35 J=1,50
      ITEMP=DTHE*10.0**J
      IF (ITEMP.GT.0) GO TO 36
   35 CONTINUE
C PRINT OUT ERROR MESSAGE
      WRITE (6,2000) DELC,DELM,DTH1,DTH2,DTH3,DTH4,DTHE
 2000 FORMAT (1H1,20X,'ERROR IN DTHETA'/20X,2E15.6/20X,4E15.6/40X,E15.6)
      GO TO 2
C CONTINUE CALCULATIONS
   36 DTHE=FLOAT(ITEMP)*10.0**(-J)
      DTHEF=DTHE
      DTHEE=DTHE*FLOAT(IDUM)
C PRINT OUT TIME AND DISTANCE INCREMENTS
      WRITE (6,999) CLER
  999 FORMAT (//10X,'COOLING CONVERGENCE ERROR',F14.4/)
      DO 37 ISECT=1,N
      WRITE(6,1000) ISECT,DELC(ISECT),ISECT,DELM(ISECT)
 1000 FORMAT( /10X,'DISTANCE INCREMENT IN COATING OF SECTION',I2,F18.6/,
     1 10X,'DISTANCE INCREMENT IN METAL OF SECTION',I2,E20.6)
   37 CONTINUE
      WRITE(6,1001) DTHEF,DTHEE
 1001 FORMAT(//10X,'TIME INCREMENT DURING FIRING',E19.6/,10X,
     1 'TIME INCREMENT DURING EXTRACTION',E15.6)
      IROUND=0
      IBURST=1
C COMPUTE TEMPERATURE HISTORIES
      THETA=0.
      ACCTHE=0.0
      IP=0
C INITIALIZE TEMPERATURE TABLES
      LLTCT=ICOAT-2
      LINTC=ICOAT-1
      LINTR=ICOAT
      LINTM=ICOAT+1
      LFTML=ICOAT+2
      LLTML=ICOAT+IMETL-2
      ITOT=ICOAT+IMETL-1
   40 MPRNT=1
      DO 47 ISECT=1,N
      LPRNT(ISECT)=100
      DO 45 I=1,ITOT
   45 T(ISECT,I)=TINT(ISECT)
      TAVCT(ISECT)=TINT(ISECT)
      TAVML(ISECT)=TINT(ISECT)
      CALL PRINT(ISECT)
   47 CONTINUE
   50 IROUND=IROUND+1
      DTHF=DTHEF
      ACCTHF=ACCTHF+DTHF
      STACCT=ACCTHE
      DO 102 ISECT=1,N
      IPRINT=IPRNT1
      IGO=1
      CALL CLEAR(QIN(1),QIN(5))
      MGOTH=1
      MGOTI=1
```

COPY AVAILABLE TO DDC DOES NOT
PERMIT FULLY LEGIBLE PRODUCTION

```
      MGOTO=1
      MGTAC=1
      MGTAM=1
      THMAX=0.0
      TIMAX=0.0
      TOMAX=0.0
      TCMAX=0.0
      TMMAX=0.0
      DTHE=DTHEF
      THETA=DTHE
      CALL CALC(ISECT,&355)
      IF (ISECT .LT. N) ACCTHE=STACCT
      IP=0
  102 CONTINUE
      CALL INTER(N)
C PRINT OUT AT END OF CYCLE
      DO 300 ISECT=1,N
      MPRNT=8
      CALL PRINT(ISECT)
  300 CONTINUE
      IAVG=0
      IP=0
C TEST FOR END OF BURST
      IF (IROUND.LT.MROUND) GO TO 50
      IF (THETAC.EQ.0.0) GO TO 500
      ISKIP=1
      IPRINT=IPRNT3
      DTHE=DTHEF*FLOAT(SCALE)
      DO 310 ISECT=1,N
      QIN(ISECT)=0.0
      HXT(ISECT)=0.0
      TGXT(ISECT)=1000.0
  310 CONTINUE
  355 DO 356 ISECT=1,N
      TEST=T(ISECT,ITOT)/T(ISECT,1)
      IF(TEST .LT. CLER) GO TO 357
  356 CONTINUE
      GO TO 395
  357 IF(IP .NE. IPRINT)GO TO 360
      CALL INTER(N)
      DO 358 ISECT=1,N
      CALL PRINT (ISECT)
  358 CONTINUE
      IAVG=0
      IP=0
  360 IP=IP+1
      ACCTHE=ACCTHE+DTHE
      IF ((THETAC-DTHE).LT.0.0) GO TO 395
      THETAC=THETAC-DTHE
      DO 365 ISECT=1,N
      CALL AT125(ISECT,&365)
  365 CONTINUE
      GO TO 355
C COMPUTED COOLING TEMPERATURE HISTORIES
  395 IAVG=1
      THETA=0.0
      IGO=1
      DO 396 ISECT=1,N
      NN=ISECT+5
      WRITE(NN,5000) IBURST
      TAVOLD(ISECT)=TB(ISECT)
```

COPY AVAILABLE TO DDC DOES NOT
PERMIT FULLY LEGIBLE PRODUCTION

```
      TB(ISECT)=CCOAT*RCOAT*(RINT(ISECT)**2-RID(ISECT)**2)*TAVCT(ISECT)+
     1 CMETL*RMETL*(ROD(ISECT)**2-RINT(ISECT)**2)*TAVML(ISECT)
      TB(ISECT)=TB(ISECT)/TMASS2(ISECT)
  396 CONTINUE
      CALL INTER(N)
      DO 397 ISECT=1,N
      MPRNT=7
      CALL PRINT(ISECT)
  397 CONTINUE
      IP=0
  400 IP=IP+1
      TAMB=TCHAM+(TENV-TCHAM)/(EXP(XCOOL*ACCTHE))
      DO 1111 ISECT=1,N
      TB(ISECT)=TB(ISECT)-(1.0/TMASS2(ISECT))*(2.0*ROD(ISECT)*DTHEC*
     1 (HLOSS*(TB(ISECT)-TAMB)+SIGMA*EPS*((TB(ISECT)+460.0)**4-
     2 (TAMB+460.0)**4)))
 1111 CONTINUE
C TEST FOR END OF COOLING
      GO TO (401,450),IGO
  401 IF ((THETA+DTHEC).LT.THETAC) GO TO 410
      IF (IP.NE.IPRINT) GO TO 405
      DO 402 ISECT=1,N
      MPRNT=7
      CALL PRINT(ISECT)
  402 CONTINUE
      IP=0
  405 DTHEC=THETAC-THETA
      ACCTHE=ACCTHE+DTHEC
      THETA=THETA+DTHEC
      CALL INTER(N)
      IGO=2
      GO TO 400
  410 CALL INTER(N)
      IF (IP.NE.IPRINT) GO TO 420
      DO 415 ISECT=1,N
      MPRNT=7
      CALL PRINT(ISECT)
  415 CONTINUE
      IP=0
  420 ACCTHE=ACCTHE+DTHEC
      THETA=THETA+DTHEC
      GO TO 400
  450 DO 460 ISECT=1,N
      MPRNT=7
      CALL PRINT(ISECT)
  460 CONTINUE
      IP=0
  500 IF (IBURST.EQ.MBURST) GO TO 1
      IBURST=IBURST+1
      IROUND =0
      THETAC=STHETC
      IAVG=0
      ISKIP=0
      DO 510 ISECT=1,N
      TINT(ISECT)=TB(ISECT)
  510 CONTINUE
      DTHEC=STDTHC
      GO TO 40
      END
C
```


COPY AVAILABLE TO DDC DOES NOT
PERMIT FULLY LEGIBLE PRODUCTION

```
      SUBROUTINE CALC(N,*)

      IMPLICIT REAL(K)
      INTEGER SCALE
      COMMON TABTIT(20),TITLE(20),ACCTHE,CCOAT,CMETL,DELC(5),DELM(5),
     1 DTH1,DTH2,DTH3,DTH4,DTHE,DTHFC,DTHEE,DTHFF,EPS,H(5,60),HINT,HLOSS
     2,HXT(5),IBURST,ICOAT,IGO,IMETL,IP,IROUND,IPRINT,IPRNT1,IPRNT2,
     3 IPRNT3,ITOT,KCOAT,KMETL,LFTML,LINTC,LINTM,LINTR,LLTCT,LLTML,
     4 LPRNT(5),MBURST,MINC,MPRNT,MROUND,IDUMMY,TAVOLD(5),DTAVG(5),
     5 ACCOLD
      COMMON NH(5),NTG(5),RCOAT,RID(5),RINT(5),RMETL,ROD(5),SIGMA,
     1 T(5,400),TAMB,TAVCT(5),TAVML(5),TB(5),TG(5,60),TGXT(5),
     2 THEH(5,60),THETA,THETAC,THETAE,THETAF,THETG(5,60),TINT(5),
     3 TMASS(5),TP(5,400),SCALE
      COMMON TENV,MGOTH,THMAX,MGOTI,TIMAX,MGOTO,TOMAX,MGTAC,TCMAX,MGTAM,
     1 TMMAX
      COMMON HMAX,QIN(5),TCHAM,XCOOL
      COMMON CLER,IAVG,AREA(4),SECTL(5),ISKIP,TMASS2(5)
      COMMON LT, LSUB1, LSUB2, LSUB3,ALPH(2)
      NHSUBN=NH(N)
      NTGSBN=NTG(N)
C TABLE LOOKUP FOR H(THETA) AND TG(THETA)
  100 DO 105 I=2,NHSUBN
      IF (THETA.GT.THEH(N,I)) GO TO 105
      HXT(N)=H(N,I-1)+((THETA-THEH(N,I-1))*(H(N,I)-H(N,I-1)))/
     1 (THEH(N,I)-THEH(N,I-1))
      GO TO 110
  105 CONTINUE
      HXT(N)=H(N,NH(N))
  110 DO 115 I=2,NTGSBN
      IF (THETA.GT.THETG(N,I)) GO TO 115
      TGXT(N)=TG(N,I-1)+((THETA-THETG(N,I-1))*(TG(N,I)-TG(N,I-1)))/
     1 (THETG(N,I)-THETG(N,I-1))
      GO TO 120
  115 CONTINUE
      TGXT(N)=TG(N,NTG(N))
C CALCULATE TOTAL HEAT INPUT
  120 QIN(N)=QIN(N)+HXT(N)*DTHE*(TGXT(N)-T(N,1))
C TEMPERATURE OF HEATED SURFACE
      ENTRY ATI25(N,*)
  125 TP(N,1)=(2.0*DTHE/(CCOAT*RCOAT*DELC(N)))*HXT(N)*(TGXT(N)-T(N,1))
     1 -(2.0*DTHE*KCOAT /(CCOAT*RCOAT*DELC(N)**2))*
     2 ((RID(N)+.5*DELC(N))/RID(N))*(T(N,1)-T(N,2))+T(N,1)
C TEMPERATURE OF INTERNAL COATING SECTIONS
      DO 130 I=2,LLTCT
      XI=I
      TP(N,I)=(DTHE*KCOAT/(CCOAT*RCOAT*DELC(N)**2))*((RID(N)+.5*
     1 (2.0*XI-3.0)*DELC(N))*(T(N,I-1)-T(N,I))/(RID(N)+(XI-1.0)*DELC(N))
     2 -(RID(N)+.5*(2.0*XI-1.0)*DELC(N))*(T(N,I)-T(N,I+1))/(RID(N)+
     3 (XI-1.0)*DELC(N)))+T(N,I)
  130 CONTINUE
C TEMPERATURE IN LAST FULL COATING SECTION
      TMASS(N)=DTHE*KCOAT/(CCOAT*RCOAT*DELC(N)**2*
     1 (RID(N)+DELC(N)*FLOAT(LINTC-1)))
      TP(N,LINTC)=TMASS(N)*((RID(N)+0.5*DELC(N)*FLOAT(2*LINTC-3))*
     1 (T(N,LLTCT)-T(N,LINTC))-(HINT/(KCOAT+2.*DELC(N)*HINT))*
     2 (RID(N)+.5*DELC(N)*FLOAT(2*LINTC-1))*(T(N,LINTC)-T(N,LINTR))*
     3 DELC(N)*2.0)+T(N,LINTC)
C TEMPERATURE OF INTERFACE
      TMASS(N)=4.0*DTHE*HINT/(CCOAT*RCOAT*DELC(N)*(RINT(N)-0.25*DELC(N))
     1+CMETL*RMETL*DELM(N)*(RINT(N)+0.25*DELM(N)))
      TP(N,LINTR)=TMASS(N)*((KCOAT/(KCOAT+2.*DELC(N)*HINT))*
     1 (RINT(N)-.5*DELC(N))*(T(N,LINTC)-T(N,LINTR))-
```


COPY AVAILABLE TO DDC DOES NOT
PERMIT FULLY LEGIBLE PRODUCTION

```
     2 (KMETL/(KMETL+2.*DELM(N)*HINT))*(RINT(N)+.5*DELM(N))*
     3 (T(N,LINTR)-T(N,LINTM)))+T(N,LINTR)
C TEMPERATURE IN FIRST FULL METAL SECTION
      TMASS(N)=DTHE*KMETL/(CMETL*RMETL*DELM(N)**2*(RINT(N)+DELM(N)))
      TP(N,LINTM)=TMASS(N)*((HINT*2.0*DELM(N)/(KMETL+2.0*DELM(N)*HINT))*
     1 (RINT(N)+0.5*DELM(N))*(T(N,LINTR)-T(N,LINTM))-
     2 (RINT(N)+1.5*DELM(N))*(T(N,LINTM)-T(N,LFTML)))+T(N,LINTM)
C TEMPERATURE OF INTERNAL METAL SECTIONS
      DO 140 I=LFTML,LLTML
      XI=I-ICOAT
  140 TP(N,I)=(DTHE*KMETL/(CMETL*RMETL*DELM(N)**2*(RINT(N)+XI*DELM(N))))
     1 *((RINT(N)+0.5*(2.0*XI-1.0)*DELM(N))*(T(N,I-1)-T(N,I))-
     2 (RINT(N)+0.5*(2.0*XI+1.0)*DELM(N))*(T(N,I)-T(N,I+1)))+T(N,I)
C TEMPERATURE OF FINAL SECTION
      TAMB=TCHAM+(TENV-TCHAM)/(EXP(XCOOL*ACCTHE))
      TP(N,ITOT)=((2.0*DTHE*KMETL)*(ROD(N)-0.5*DELM(N))*
     1 (T(N,LLTML)-T(N,ITOT))/(CMETL*RMETL*ROD(N)*DELM(N)**2))-
     2 ((HLOSS*DTHE)*(T(N,ITOT)-TAMB)*2.0/(CMETL*RMETL*DELM(N)))-
     3 ((SIGMA*EPS*DTHE)*((T(N,ITOT)+460.0)**4-(TAMB+460.0)**4)/
     4 (CMETL*RMETL*0.5*DELM(N)))+T(N,ITOT)
C STORE NEW TEMPERATURE DISTRIBUTION
      DO 150 I=1,ITOT
  150 T(N,I)=TP(N,I)
C COMPUTE AVERAGE TEMPERATURES
      TAVCT(N)=DELC(N)*(T(N,1)*(RID(N)+0.25*DELC(N))+T(N,LINTR)*
     1 (RINT(N)-0.25*DELC(N)))
      DO 155  I=2,LINTC
  155 TAVCT(N)=TAVCT(N)+2.0*T(N,I)*DELC(N)*(RID(N)+(FLOAT(I-1))*DELC(N))
      TAVCT(N)=TAVCT(N)/(RINT(N)**2-RID(N)**2)
      TAVML(N)=DELM(N)*(T(N,LINTR)*(RINT(N)+0.25*DELM(N))+T(N,ITOT)*
     1 (ROD(N)-0.25*DELM(N)))
      DO 160  I=LINTM,LLTML
      XI=I-LINTR
  160 TAVML(N)=TAVML(N)+2.0*T(N,I)*DELM(N)*(RINT(N)+XI*DELM(N))
      TAVML(N)=TAVML(N)/(ROD(N)**2-RINT(N)**2)
C END OF TEMPERATURE CALCULATIONS
C DETERMINE LOGICAL SEQUENCE
      IF(ISKIP .EQ. 1) RETURN 1
C TEST FOR MAXIMUM TEMPERATURES
      GO TO (161,163), MGOTH
  161 IF (T(N,1).LT.THMAX) GO TO 162
      THMAX=T(N,1)*0.9995
      GO TO 163
  162 MPRNT=2
      CALL PRINT(N)
      MGOTH=2
  163 GO TO (164,166), MGOTI
  164 IF (T(N,LINTR).LT.TIMAX) GO TO 165
      TIMAX=T(N,LINTR)*0.9995
      GO TO 166
  165 MPRNT=3
      CALL PRINT(N)
      MGOTI=2
  166 GO TO (167,169), MGOTO
  167 IF (T(N,ITOT).LT.TOMAX) GO TO 168
      TOMAX=T(N,ITOT)*0.9995
      GO TO 169
  168 MPRNT=4
      CALL PRINT(N)
      MGOTO=2
  169 GO TO (170,172),MGTAC
```


COPY AVAILABLE TO DDC DOES NOT
PERMIT FULLY LEGIBLE PRODUCTION

```
  170 IF (TAVCT(N).LT.TCMAX) GO TO 171
      TCMAX=TAVCT(N)*0.9995
      GO TO 172
  171 MPRNT=5
      CALL PRINT(N)
      MGTAC=2
  172 GO TO (173,190), MGTAM
  173 IF (TAVML(N) .LT. TMMAX) GO TO 174
      TMMAX=TAVML(N)*0.9995
      GO TO 190
  174 MPRNT=6
      CALL PRINT(N)
      MGTAM=2
C TEST FOR END OF FIRING
  190 IP=IP+1
      GO TO (200,250,300,350),IGO
  200 IF((THETA+DTHE).LT.THETAF) GO TO 210
      IF (IP.NE.IPRINT) GO TO 205
      CALL PRINT(N)
      IP=0
  205 DTHE=THETAF-THETA
      ACCTHE=ACCTHE+DTHE
      THETA=THETA+DTHE
      IF(THETAF .EQ. THETAF) GO TO 206
      IGO=2
      GO TO 100
  206 IGO=4
      GO TO 100
C TEST FOR PRINT INTERVAL
  210 IF (IP.NE.IPRINT) GO TO 220
      CALL PRINT(N)
      IP=0
  220 ACCTHE=ACCTHE+DTHE
      THETA=THETA+DTHE
      GO TO 100
C PRINT AT END OF FIRING
  250 CALL PRINT(N)
      IPRINT=IPRNT2
      DTHE=DTHEF
      THETA=THETA+DTHE
      ACCTHE=ACCTHE+DTHE
      IP=0
      IGO=3
      GO TO 100
C TEST FOR END OF CYCLE
  300 IF ((THETA+DTHE).LT.THETAF) GO TO 310
      IF (IP.NE.IPRINT) GO TO 305
      CALL PRINT(N)
      IP=0
  305 DTHE=THETAF-THETA
      ACCTHE=ACCTHE+DTHE
      THETA=THETA+DTHE
      IGO=4
      GO TO 100
  310 IF (IP.NE.IPRINT) GO TO 320
      CALL PRINT(N)
      IP=0
  320 ACCTHE=ACCTHE+DTHE
      THETA=THETA+DTHE
      GO TO 100
  350 CALL PRINT(N)


      RETURN
      END
```

COPY AVAILABLE TO DDC DOES NOT
PERMIT FULLY LEGIBLE PRODUCTION

```
C
C THIS SUBROUTINE PRINTS OUT TEMPERATURE HISTORIES
      SUBROUTINE PRINT(N)
      IMPLICIT REAL(K)
      INTEGER SCALE
      COMMON TABTIT(20),TITLE(20),ACCTHE,CCOAT,CMETL,DELC(5),DELM(5),
     1 DTH1,DTH2,DTH3,DTH4,DTHE,DTHEC,DTHEE,DTHEF,EPS,H(5,60),HINT,HLOSS
     2,HXT(5),IBURST,ICOAT,IGO,IMETL,IP,IROUND,IPRINT,IPRNT1,IPRNT2,
     3 IPRNT3,ITOT,KCOAT,KMETL,LFTML,LINTC,LINTM,LINTR,LLTCT,LLTML,
     4 LPRNT(5),MBURST,MINC,MPRNT,MROUND,IDUMMY,TAVOLD(5),DTAVG(5),
     5 ACCOLD
      COMMON NH(5),NTG(5),RCOAT,RID(5),RINT(5),RMETL,ROD(5),SIGMA,
     1 T(5,400),TAMB,TAVCT(5),TAVML(5),TB(5),TG(5,60),TGXT(5),
     2 THEH(5,60),THETA,THETAC,THETAE,THETAF,THETG(5,60),TINT(5),
     3 TMASS(5),TP(5,400),SCALE
      COMMON TENV,MGOTH,THMAX,MGOTI,TIMAX,MGOTO,TOMAX,MGTAC,TCMAX,MGTAM,
     1 TMMAX
      COMMON HMAX,QIN(5),TCHAM,XCOOL
      COMMON CLER,TAVG,AREA(4),SECTL(5),ISKIP,TMASS2(5)
      COMMON LT, LSUB1, LSUB2, LSUB3,ALPH(2)
      NN=N+5
C CALCULATE AVERAGE TEMPERATURE OF CHAMBER
      IF(IAVG .EQ. 1) GO TO 1
      TB(N)=CCOAT*RCOAT*(RINT(N)**2-RID(N)**2)*TAVCT(N)+CMETL*RMETL*
     1 (ROD(N)**2-RINT(N)**2)*TAVML(N)
      TB(N)=TB(N)/TMASS2(N)
C DETERMINE PRINTOUT FORMAT
    1 IF (LPRNT(N).LT.51) GO TO 5
      WRITE(NN,2000) N
      LPRNT(N)=0
    5 GO TO (10,20,30,40,50,60,70,80,100), MPRNT
   10 WRITE (NN,1010) IBURST,IROUND,ACCTHE,T(N,1),T(N,LINTR),T(N,ITOT),
     1 TAVCT(N),TAVML(N),TB(N),QIN(N)
      GO TO 100
   20 WRITE (NN,1020) IBURST,IROUND,ACCTHE,T(N,1),T(N,LINTR),T(N,ITOT),
     1 TAVCT(N),TAVML(N),TB(N),QIN(N)
      GO TO 100
   30 WRITE (NN,1030) IBURST,IROUND,ACCTHE,T(N,1),T(N,LINTR),T(N,ITOT),
     1 TAVCT(N),TAVML(N),TB(N),QIN(N)
      GO TO 100
   40 WRITE (NN,1040) IBURST,IROUND,ACCTHE,T(N,1),T(N,LINTR),T(N,ITOT),
     1 TAVCT(N),TAVML(N),TB(N),QIN(N)
      GO TO 100
   50 WRITE (NN,1050) IBURST,IROUND,ACCTHE,T(N,1),T(N,LINTR),T(N,ITOT),
     1 TAVCT(N),TAVML(N),TB(N),QIN(N)
      GO TO 100
   60 WRITE (NN,1060) IBURST,IROUND,ACCTHE,T(N,1),T(N,LINTR),T(N,ITOT),
     1 TAVCT(N),TAVML(N),TB(N),QIN(N)
      GO TO 100
   70 WRITE (NN,1070) IBURST,ACCTHE,TB(N),TB(N),TB(N)
      GO TO 100
   80 WRITE(NN,1080) T(N,1),T(N,LINTR),T(N,ITOT),TAVCT(N),TAVML(N),TB(N)
  100 MPRNT=1
      LPRNT(N)=LPRNT(N)+1
      RETURN
 1010 FORMAT (2I8,F13.6,7F12.2)
 1020 FORMAT (2I8,F13.6,' **',F9.2,6F12.2)
 1030 FORMAT (2I8,F13.6,1F12.2,' **',F9.2,5F12.2)
 1040 FORMAT (2I8,F13.6,2F12.2,' **',F9.2,4F12.2)
 1050 FORMAT (2I8,F13.6,3F12.2,' **',F9.2,3F12.2)
 1060 FORMAT (2I8,F13.6,4F12.2,' **',F9.2,2F12.2)
 1070 FORMAT (I8,8X,F13.6,36X,3F12.2)
 1080 FORMAT (29X,6F12.2)
 2000 FORMAT(1H1,'SECTION',I2,//3X,'BURST   ROUND  TIME (SEC)',6X,'T(1)'
     1,6X,'T(INTER)',5X,'T(LAST)   T(CT) AVE   T(ML) AVE',4X,'T AVE',7X,
     2 'Q IN'//)
      END
```


COPY AVAILABLE TO DDC DOES NOT
PERMIT FULLY LEGIBLE PRODUCTION

```
C
C THIS SUBROUTINE READS IN HEAT TRANSFER COEFFICIENT AND
C GAS TEMPERATURE TABLES
      SUBROUTINE INTAB
      IMPLICIT REAL(K)
      INTEGER SCALE
      COMMON TABTIT(20),TITLE(20),ACCTHE,CCOAT,CMETL,DELC(5),DELM(5),
     1 DTH1,DTH2,DTH3,DTH4,DTHF,DTHEC,DTHEE,DTHEF,EPS,H(5,60),HINT,HLOSS
     2,HXT(5),IBURST,ICOAT,IGO,IMETL,IP,IROUND,IPRINT,IPRNT1,IPRNT2,
     3 IPRNT3,ITOT,KCOAT,KMETL,LFTML,LINTC,LINTM,LINTR,LLTCT,LLTML,
     4 LPRNT(5),MBURST,MINC,MPRNT,MROUND,N,TAVOLD(5),DTAVG(5),ACCOLD
      COMMON NH(5),NTG(5),RCOAT,RID(5),RINT(5),RMETL,ROD(5),SIGMA,
     1 T(5,400),TAMB,TAVCT(5),TAVML(5),TB(5),TG(5,60),TGXT(5),
     2 THEH(5,60),THETA,THETAC,THETAE,THETAF,THETG(5,60),TINT(5),
     3 TMASS(5),TP(5,400),SCALE
      COMMON TENV,MGOTH,THMAX,MGOTI,TIMAX,MGOTO,TOMAX,MGTAC,TCMAX,MGTAM,
     1 TMMAX
      COMMON HMAX,QIN(5),TCHAM,XCOOL
      COMMON CLER,IAVG,AREA(4),SECTL(5),ISKIP,TMASS2(5)
      COMMON LT, LSUB1, LSUB2, LSUB3,ALPH(2)
      READ(5,1000) TABTIT,N
      DO 10 ISECT=1,N
      READ(5,1001) NH(ISECT)
      NHSUB=NH(ISECT)
      READ(5,1002) (THEH(ISECT,I),I=1,NHSUB)
      READ(5,1002) (H(ISECT,I), I=1,NHSUB)
      READ(5,1001) NTG(ISECT)
      NTGSUB=NTG(ISECT)
      READ(5,1002) (THETG(ISECT,I), I=1,NTGSUB)
      READ(5,1002) (TG(ISECT,I), I=1,NTGSUB)
      WRITE(6,2000) TABTIT,ISECT
      WRITE(6,3000) NH(ISECT)
      WRITE(6,2002) (THEH(ISECT,I),I=1,NHSUB)
      WRITE(6,3001)
      WRITE(6,2002) (H(ISECT,I),I=1,NHSUB)
      WRITE(6,4000) NTG(ISECT)
      WRITE(6,2002) (THETG(ISECT,I),I=1,NTGSUB)
      WRITE(6,4001)
      WRITE(6,2002) (TG(ISECT,I),I=1,NTGSUB)
   10 CONTINUE
 1000 FORMAT (20A4/,I10)
 1001 FORMAT (6I10)
 1002 FORMAT (6E12.4)
 2000 FORMAT (1H1,24X,'TABULAR HEAT TRANSFER AND GAS TEMPERATURES'/
     125X,20A4/,' SECTION',I2)
 2002 FORMAT (10X,8E15.7)
 3000 FORMAT(//9X,'H TABLE - NUMBER OF ENTRIES =',I3//10X,'THETA')
 3001 FORMAT (//10X,'H(THETA)')
 4000 FORMAT (//9X,'TG TABLE - NUMBER OF ENTRIES =',I3//10X'THETA')
 4001 FORMAT (//10X,'TG(THETA)')
      RETURN
      END
C
```

COPY AVAILABLE TO DDC DOES NOT
PERMIT FULLY LEGIBLE PRODUCTION

```
C
      SUBROUTINE INTER(N)
      IMPLICIT REAL(K)
      INTEGER SCALE
      COMMON TABTIT(20),TITLE(20),ACCTHE,CCOAT,CMETL,DELC(5),DELM(5),
     1 DTH1,DTH2,DTH3,DTH4,DTHE,DTHEC,DTHEF,DTHEF,EPS,H(5,60),HINT,HLOSS
     2,HXT(5),IBURST,ICOAT,IGO,IMETL,IP,IROUND,IPRINT,IPRNT1,IPRNT2,
     3 IPRNT3,ITOT,KCOAT,KMETL,LFTML,LINTC,LINTM,LINTR,LLTCT,LLTML,
     4 LPRNT(5),MBURST,MINC,MPRNT,MROUND,IDUMMY,TAVOLD(5),DTAVG(5),
     5 ACCOLD
      COMMON NP(5),NTG(5),RCOAT,RID(5),RINT(5),RMETL,ROD(5),SIGMA,
     1 T(5,400),TAMB,TAVCT(5),TAVML(5),TB(5),TG(5,60),TGXT(5),
     2 THEH(5,60),THETA,THETAC,THETAF,THETAF,THETG(5,60),TINT(5),
     3 TMASS(5),TP(5,400),SCALE
      COMMON TENV,MGOTH,THMAX,MGOTI,TIMAX,MGOTO,TOMAX,MGTAC,TCMAX,MGTAM,
     1 TMMAX
      COMMON HMAX,QIN(5),TCHAM,XCOOL
      COMMON CLER,IAVG,AREA(4),SECTL(5),ISKIP,TMASS2(5)
      COMMON LT, LSUB1, LSUB2, LSUB3,ALPH(2)
      IF(N .EQ. 1) RETURN
      DTHP=ACCTHE-ACCOLD
      ACCOLD=ACCTHE
      IF(IAVG .EQ. 1) GO TO 10
      DO 5 ISECT=1,N
      TB(ISECT)=CCOAT*RCOAT*(RINT(ISECT)**2-RID(ISECT)**2)*TAVCT(ISECT)+
     1 CMETL*RMETL*(ROD(ISECT)**2-RINT(ISECT)**2)*TAVML(ISECT)
      TB(ISECT)=TB(ISECT)/TMASS2(ISECT)
    5 CONTINUE
   10 DTAVG(1)=-KMETL*AREA(1)*(TAVOLD(1)-TAVOLD(2)+TB(1)-TB(2))*DTHP/
     1 (CMETL*RMETL*SECTL(1)*3.141593*(ROD(1)**2-RID(1)**2)*(SECTL(1)+
     2 SECTL(2)))
      IF(N .EQ. 2) GO TO 500
      NM1=N-1
      DO 100 ISECT=2,NM1
      J=ISECT+1
      I=ISECT-1
      DTAVG(ISECT)=-(KMETL*AREA(I)*(TAVOLD(ISECT)-TAVOLD(I)+TB(ISECT)-
     1 TB(I))     /(SECTL(I)+SECTL(ISECT))+KMETL*AREA(ISECT)*
     2 (TAVOLD(ISECT)-TAVOLD(J)+TB(ISECT)-TB(J)) /(SECTL(ISECT)+
     3 SECTL(J)))*DTHP/(CMETL*RMETL*SECTL(ISECT)*3.141593*
     4 (ROD(ISECT)**2-RID(ISECT)**2))
  100 CONTINUE
  500 DTAVG(N)=-KMETL*AREA(NM1)*(TAVOLD(N)-TAVOLD(NM1)+TB(N)-TB(NM1))*
     1DTHP/((SECTL(NM1)+SECTL(N))*CMETL*RMETL*SECTL(N)*3.141593*
     2(ROD(N)**2-RID(N)**2))
      DO 600 ISECT=1,N
      TB(ISECT)=TB(ISECT)+DTAVG(ISECT)
      TAVCT(ISECT)=TAVCT(ISECT)+DTAVG(ISECT)
      TAVML(ISECT)=TAVML(ISECT)+DTAVG(ISECT)
      TAVOLD(ISECT)=TB(ISECT)
      DO 550 IJ=1,ITOT
      T(ISECT,IJ)=T(ISECT,IJ)+DTAVG(ISECT)
  550 CONTINUE
  600 CONTINUE
      IAVG=1
      RETURN
      END
```


COPY AVAILABLE TO DDC DOES NOT
PERMIT FULLY LEGIBLE PRODUCTION

```
C THIS SUBROUTINE READS IN DATA
      SUBROUTINE INDAT
      IMPLICIT REAL(K)
      INTEGER SCALE
      COMMON TABTIT(20),TITLE(20),ACCTHE,CCOAT,CMETL,DELC(5),DELM(5),
     1 DTH1,DTH2,DTH3,DTH4,DTHE,DTHEC,DTHEE,DTHEF,EPS,H(5,60),HINT,HLOSS
     2,HXT(5),IBURST,ICOAT,IGO,IMETL,IP,IROUND,IPRINT,IPRNT1,IPRNT2,
     3 IPRNT3,ITOT,KCOAT,KMETL,LFTML,LINTC,LINTM,LINTR,LLTCT,LLTML,
     4 LPRNT(5),MBURST,MINC,MPRNT,MROUND,N,TAVOLD(5),DTAVG(5),ACCOLD
      COMMON NH(5),NTG(5),RCOAT,RID(5),RINT(5),RMETL,ROD(5),SIGMA,
     1 T(5,400),TAMB,TAVCT(5),TAVML(5),TB(5),TG(5,60),TGXT(5),
     2 THEH(5,60),THETA,THETAC,THETAE,THETAF,THETG(5,60),TINT(5),
     3 TMASS(5),TP(5,400),SCALE
      COMMON TENV,MGOTH,THMAX,MGOTI,TIMAX,MGOTO,TCMAX,MGTAC,TCMAX,MGTAM,
     1 TMMAX
      COMMON HMAX,QIN(5),TCHAM,XCOOL
      COMMON CLER,TAVG,AREA(4),SECTL(5),ISKIP,TMASS2(5)
      COMMON LT, LSUB1, LSUB2, LSUB3,ALPH(2)
      READ (5,1000) ALPH
      READ (5,1000) (TITLE(I),I=1,20)
      READ (5,1010) CCOAT,RCOAT,KCOAT,ICOAT,CMETL,RMETL,KMETL,IMETL
      READ(5,1020) (RID(L), L=1,N)
      READ(5,1020) (RINT(L),L=1,N)
      READ(5,1020) (ROD(L),L=1,N)
      READ(5,1020) (SECTL(L),L=1,N)
      M=N-1
      READ(5,1040)(AREA(ISECT),ISECT=1,M)
      READ (5,1020) THETAF,THETAE,THETAC,DTHEC, CLER,TCHAM,XCOOL
      READ(5,1020) (TINT(L),L=1,N)
      READ (5,1020)       TAMB,HMAX,HINT,HLOSS,SIGMA,EPS
      READ (5,1030) MBURST,MROUND,MINC,SCALE,IPRNT1,IPRNT2,IPRNT3
 1000 FORMAT (20A4)
 1010 FORMAT (3E10.3,I10)
 1020 FORMAT (8E10.3)
 1030 FORMAT (7I5)
 1040 FORMAT(4E10.3)
      WRITE (6,2000) (TITLE(I),I=1,20)
      WRITE (6,2010) MBURST,MROUND,CCOAT,CMETL,RCOAT,RMETL,KCOAT,KMETL,
     1ICOAT,IMETL,TINT(1),TINT(1),TAMB
      WRITE (6,2015) (ALPH,L,RID(L),RINT(L),ROD(L), L=1,N)
      WRITE (6,2020) HMAX,HINT,HLOSS,SIGMA,EPS
      WRITE (6,2030) THETAF,THETAE,THETAC,MINC,SCALE,DTHEC,IPRNT1,
     1IPRNT2,IPRNT3,(ALPH,L,SECTL(L), L=1,N)
      WRITE(6,2040)(AREA(ISECT),ISECT=1,M)
 2000 FORMAT(1H1,19X,'INPUT DATA FOR COMPOSITE CYLINDRICAL GUN CHAMBER P
     1ROGRAM'//10X,20A4//)
 2010 FORMAT (25X,'THIS RUN CONSISTS OF ',I4,
     A' BURST(S) OF',I4,' ROUNDS EACH'/43X,
     1'COATING',6X,'METAL    ENVIRONMENT'/10X,'SPECIFIC HEAT (BTU/LBM)',
     27X,2E12.4/10X,'DENSITY (LBM/FT3)',13X,2E12.4/10X,'CONDUCTIVITY (BT
     3U/FT  SEC DF) ',2E12.4/10X,'NUMBER OF DISTANCE INCREMENTS',4X,I4,
     48X,I4/10X,'INITIAL TEMPERATURE (DF)',6X,3F12.4/)
 2015 FORMAT (43X,'INSIDE',5X,'INTERFACE',4X,'OUTSIDE'/10X,'RADIUS (FT)'
     1 /,( 15X,2A4,I1,16X,3F12.4)/)
 2020 FORMAT(10X,'HEAT TRANSFER COEFFICIENT',5X,3E12.4/10X,
     1'STEFAN-BOLTZMANN CONSTANT',29X,E12.4/10X,'EMISSIVITY',44X,F12.4/)
 2030 FORMAT (43X,'FIRING',4X,'EXTRACTION',4X,'COOLING'/10X,'TIME (SEC)'
     1,20X,3E12.4/10X,'TIME INCREMENT FACTORS',12X,I4,19X,I4/
     210X,'TIME INCREMENT (SEC)',34X,F12.4/,10X,'PRINT INTERVALS',19X,
     3 I4,8X,I4,8X,I4///,10X,'LENGTH OF'/,( 15X,2A4,I1,16X,E12.4)/)
 2040 FORMAT(10X,'CROSS SECTIONAL AREA BETWEEN SECTIONS'/15X,'SECTIONS 1
     1 AND 2',5X,E12.4/,15X,'SECTIONS 2 AND 3',5X,E12.4/,15X,'SECTIONS 3
     2 AND 4',5X,E12.4/,15X,'SECTIONS 4 AND 5',5X,E12.4/)
      RETURN
      END
```


COPY AVAILABLE TO DDC DOES NOT
PERMIT FULLY LEGIBLE PRODUCTION

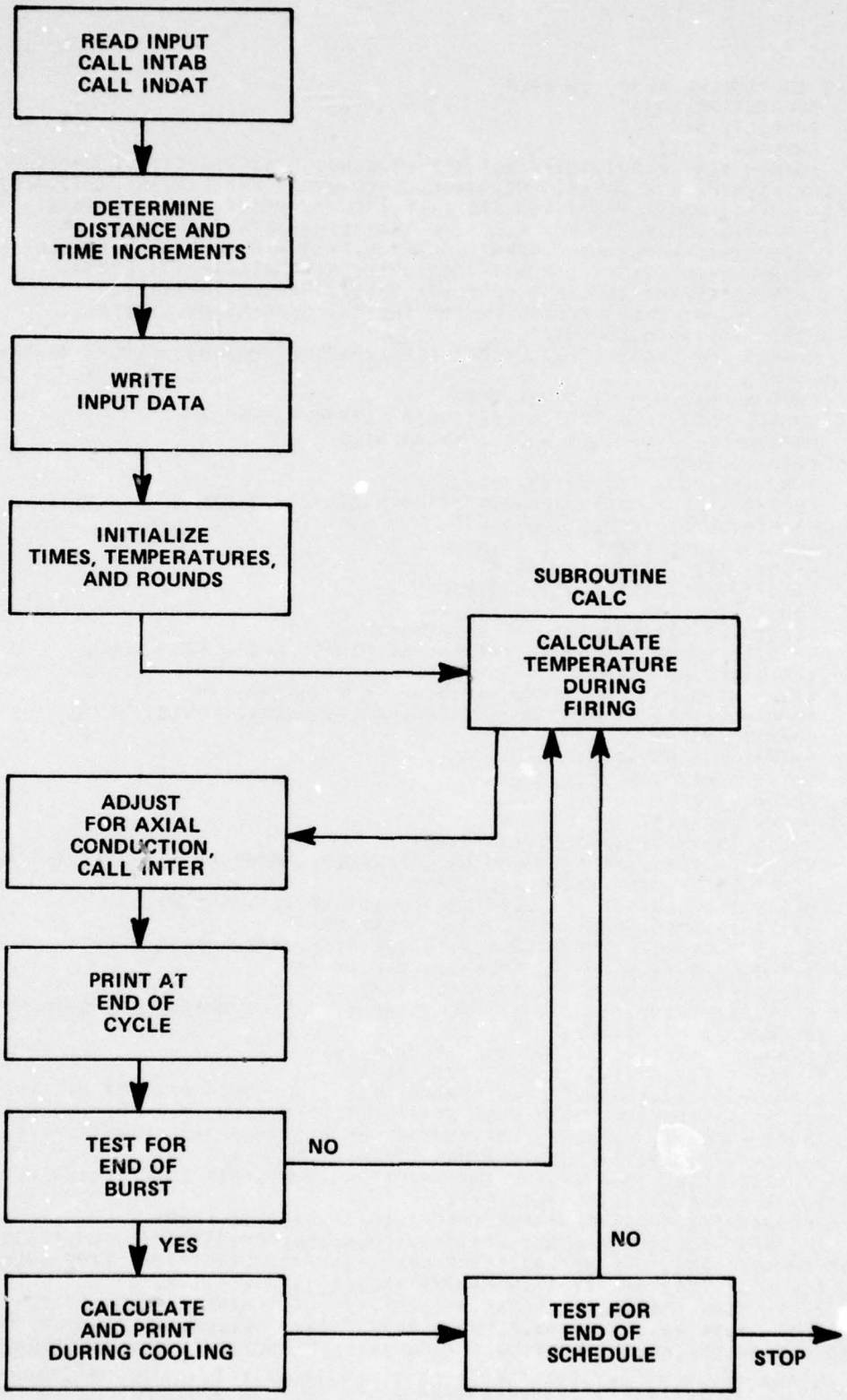

FLOW CHART FOR CYLINDRICAL HEAT CONDUCTION - MAIN

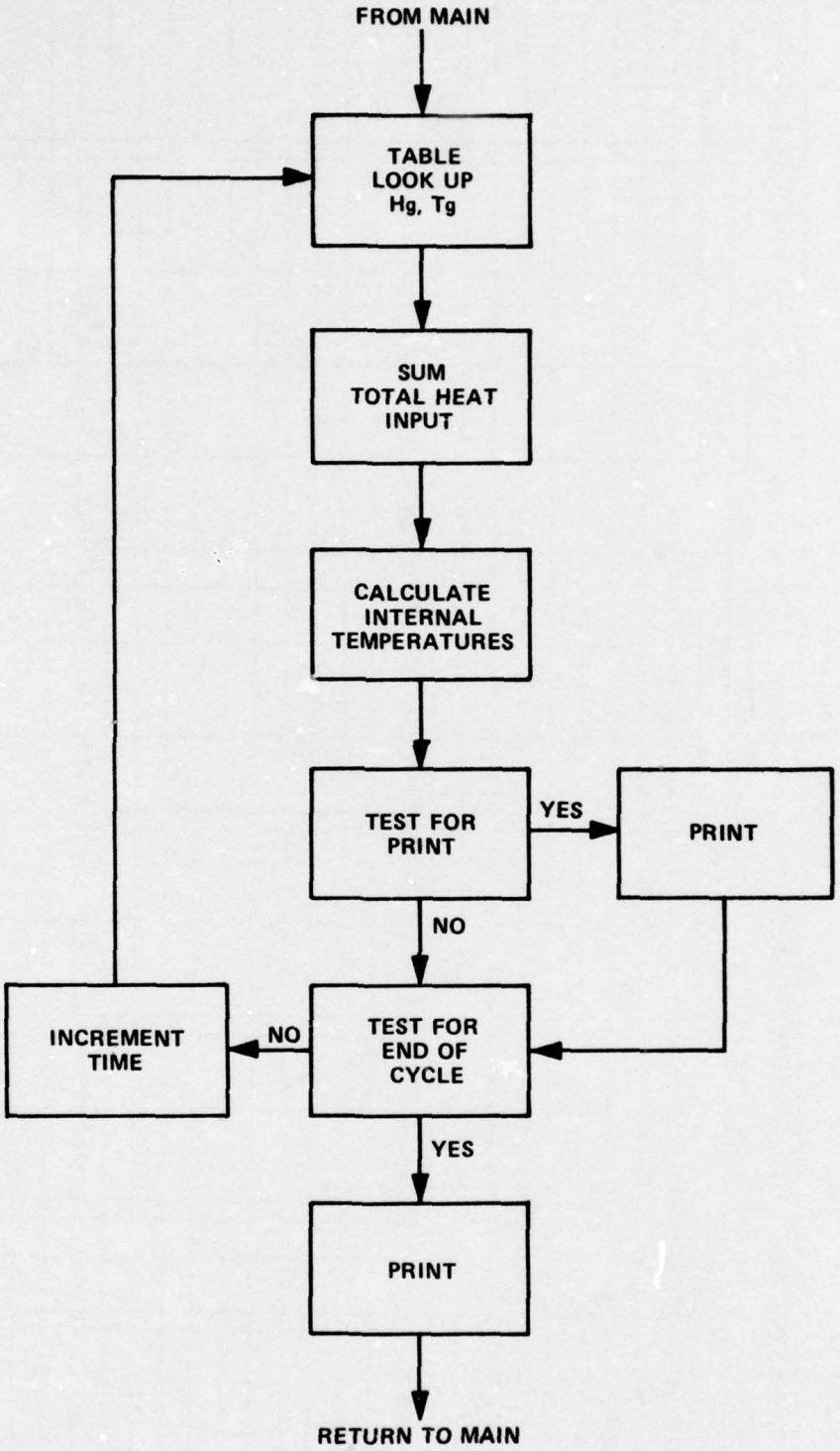

FLOW CHART FOR SUBROUTINE CALC

IBM System/360 Assembler Coding Form

PROGRAM: FIVE SECTION CYLINDRICAL CHAMBER PROGRAM | PUNCHING INSTRUCTIONS | GRAPHIC | PUNCH | PAGE 1 OF 14 | CARD ELECTRO NUMBER *

PROGRAMMER | DATE

STATEMENT — Name | Operation | Operand | Comments | Identification-Sequence

TITLE CARD FORMAT (20A4)

N

NO. OF SECTIONS

1

NH(1) ← RIGHT JUSTIFY

NO. OF ENTRIES IN H TABLE, SECT. 1

1

THETAH (1, I) I = 1, NH(1) FORMAT (6E 12.4) 10 CARD MAXIMUM FOR ANY SECTION (IN SECONDS)

1
2
3
4
5
6
7
8
9
10

H(1, I) I = 1, NH(1) FORMAT (6E 12.4) 10 CARD MAXIMUM (IN BTU/FT^2-SEC)

1
2
3

MASTER INPUT FORMAT

COPY AVAILABLE TO DDC DOES NOT PERMIT FULLY LEGIBLE REPRODUCTION

IBM System 360 Assembler Coding Form

PROGRAM | PUNCHING INSTRUCTIONS | GRAPHIC | PAGE 2 OF 14

PROGRAMMER | DATE | PUNCH | CARD ELECTRO NUMBER

STATEMENT

Name	Operation	Operand	Comments	Identification-Sequence
H(1, I) CONTINUED				
NTG(1)				
NO. OF ENTRIES	← RIGHT JUSTIFY			
IN TG TABLE				
THETAG (1, I)	I = 1, NTG(1)	FORMAT (6E12.4)	MAXIMUM 10 COS (IN SECONDS)	

COPY AVAILABLE TO DDC DOES NOT PERMIT FULLY LEGIBLE PRODUCTION

IBM System 360 Assembler Coding Form

PROGRAM | PUNCHING INSTRUCTIONS | GRAPHIC | PUNCH | PAGE 3 OF 14

PROGRAMMER | DATE | CARD ELECTRO NUMBER

STATEMENT

Name	Operation	Operand	Comments	Identification Sequence
TG (I, I)	I = 1, NTG(I)	FORMAT (6E12.4)	10 CARDS MAXIMUM (IN °F)	
NH(2)				
NO. OF ENTRIES IN H TABLE, SECT. 2	← RIGHT JUSTIFY			
THETAH (2, I)	I = 1, NH(2)	FORMAT (6E12.4)	(IN SECONDS)	

COPY AVAILABLE TO DDC DOES NOT PERMIT FULLY LEGIBLE PRODUCTION

IBM System 360 Assembler Coding Form

PROGRAM | PUNCHING INSTRUCTIONS | GRAPHIC | PAGE 4 OF 14

PROGRAMMER | DATE | PUNCH | CARD ELECTRO NUMBER

STATEMENT

Name	Operation	Operand	Comments	Identification-Sequence
		THETAH (2, I) CONT.		
		H (2, I) I = 1, NH(2) FORMAT (6E12.4) 10 CARDS MAXIMUM (IN BTU/FT^2-SEC)		
		NTG(2) NO. OF ENTRIES IN TG TABLE, SECT. 2 ← RIGHT JUSTIFY		
		THETAG (2, I) I = 1, NTG(2) FORMAT (6E12.4) MAXIMUM 10 CARDS (IN SECONDS)		

COPY AVAILABLE TO DDC DOES NOT PERMIT FULLY LEGIBLE PRODUCTION

IBM System 360 Assembler Coding Form

PROGRAM | PROGRAMMER | DATE | PUNCHING INSTRUCTIONS | GRAPHIC | PUNCH | PAGE 5 OF 14 | CARD ELECTRO NUMBER

STATEMENT: Name | Operation | Operand | Comments | Identification-Sequence

```
THETAG (2, I) CONT.
TG(4, I)        I = 1, NTG(2)      FORMAT (6E12.4)      10 CARDS MAXIMUM      (IN °F)
NH(3)
NO. OF ENTRIES
IN H TABLE,
SECT. 3                  <-- RIGHT JUSTIFY
THETAH (3, I)       I = 1, NH(3)      FORMAT (6E12.4)      MAXIMUM 10 CARDS      (IN SECONDS)
```


COPY AVAILABLE TO DDC DOES NOT
PERMIT FULLY LEGIBLE PRODUCTION

IBM System/360 Assembler Coding Form

PROGRAM | PUNCHING INSTRUCTIONS | GRAPHIC | PAGE 6 OF 14

PROGRAMMER | DATE | PUNCH | CARD ELECTRO NUMBER

STATEMENT

Name	Operation	Operand	Comments	Identification-Sequence
	THETAH (3, I) CONT.			
	H (3, I) I = 1, NH(3)	FORMAT (6E12.4)	MAXIMUM 10 CARDS (IN BTU/FT^2-SEC)	
	NTG(3)			
	NO. OF ENTRIES IN TG TABLE, SECT. 3	← RIGHT JUSTIFY		

COPY AVAILABLE TO DDC DOES NOT PERMIT FULLY LEGIBLE PRODUCTION

IBM System 360 Assembler Coding Form

PROGRAM | PUNCHING INSTRUCTIONS | GRAPHIC | PAGE 7 OF 14
PROGRAMMER | DATE | PUNCH | CARD ELECTRO NUMBER

STATEMENT

	Name	Operation	Operand	Comments	Identification Sequence
1	THETAG (3, I)	I = 1, NTG(3)	FORMAT (6E12.4)	MAXIMUM 10 CARDS (IN SECONDS)	
2					
3					
4					
5					
6					
7					
8					
9					
10					
1	TG(3, I)	I = 1, NTG(3)	FORMAT (6E12.4)	MAXIMUM 10 CARDS (IN °F)	
2					
3					
4					
5					
6					
7					
8					
9					
10					

200

COPY AVAILABLE TO DDC DOES NOT PERMIT FULLY LEGIBLE REPRODUCTION

IBM System 360 Assembler Coding Form

PROGRAM | PROGRAMMER | DATE | GRAPHIC PUNCTUATION INSTRUCTIONS | PAGE 8 OF 14 | CARD ELECTRO NUMBER

STATEMENT | Name | Operation | Operand | Comments | Identification Sequence

NH(4)
NO. OF ENTRIES IN H TABLE, SECT. 4 ← RIGHT JUSTIFY

THETAH (4, I) I = 1, NH(4) FORMAT (6E12.4) MAXIMUM 10 CARDS (IN SECONDS)

H(4, I) I = 1, NH(4) FORMAT (6E12.4) MAXIMUM 10 CARDS (IN BTU/FT^2-SEC)

201
COPY AVAILABLE TO DDC DOES NOT
PERMIT FULLY LEGIBLE PRODUCTION

IBM System 360 Assembler Coding Form

PAGE 9 OF 14

CARD ELECTRO NUMBER

PROGRAM

PROGRAMMER

DATE

PUNCHING INSTRUCTIONS

GRAPHIC

PUNCH

STATEMENT

Name | Operation | Operand | Comments | Identification-Sequence

```
H(4,I) CONT.
9
10
NTG(4)
NO. OF ENTRIES
IN TG TABLE,
SECT. 4          <-- RIGHT JUSTIFY

THETAG (4, I)    I = 1, NTG(4)    FORMAT (6E12.4)    MAXIMUM 10 CARDS    (IN SECONDS)
1
2
3
4
5
6
7
8
9
10
TG(4,I)          I = 1, NTG(4)    FORMAT (6E12.4)    MAXIMUM 10 CARDS    (IN °F)
1
2
3
4
5
```


COPY AVAILABLE TO DDC DOES NOT PERMIT FULLY LEGIBLE REPRODUCTION

IBM System/360 Assembler Coding Form

PROGRAM | PUNCHING INSTRUCTIONS | GRAPHIC | PAGE 10 OF 14
PROGRAMMER | DATE | PUNCH | CARD ELECTRO NUMBER

STATEMENT

Name | Operation | Operand | Comments | Identification-Sequence

TG(4, I) CONT.

NH(5)
NO. OF ENTRIES IN H TABLE SECT. 5 ——— RIGHT JUSTIFY

THETAH(5, I) I = 1, NH(5) FORMAT (6E12.4) MAXIMUM 10 CARDS (IN SECONDS)

H(5, I) I = 1, NH(5) FORMAT (6E12.4) MAXIMUM 10 CARDS (IN BTU/FT^2-SEC)

COPY AVAILABLE TO DDC DOES NOT
PERMIT FULLY LEGIBLE PRODUCTION

IBM System 360 Assembler Coding Form

PROGRAM | PUNCHING INSTRUCTIONS | GRAPHIC | PAGE 11 OF 14

PROGRAMMER | DATE | PUNCH | CARD ELECTRO NUMBER

STATEMENT

	Name	Operation	Operand	Comments	Identification-Sequence
		1 8 10 14 16 20 25 30 35 40 45 50 55 60 65 71			73 80
	H(5, 1) CONT.				
3					
4					
5					
6					
7					
8					
9					
10					
	NTG (5)				
	NO. OF ENTRIES IN TG TABLE, SECT. 5	← RIGHT JUSTIFY			
	THETAG (5,I)	I = 1, NTG(5)	FORMAT (6E12.4)	MAXIMUM 10 CARDS	(IN SECONDS)
1					
2					
3					
4					
5					
6					
7					
8					
9					

COPY AVAILABLE TO DDC DOES NOT PERMIT FULLY LEGIBLE REPRODUCTION

IBM System 360 Assembler Coding Form

PROGRAM | PROGRAMMER | DATE | PUNCHING INSTRUCTIONS | GRAPHIC | PUNCH | PAGE 12 OF 14 | CARD ELECTRO NUMBER

STATEMENT: Name | Operation | Operand | Comments | Identification-Sequence

```
THETAG (5, I)  CONT.
TG (5, I)      I = 1, NTG(5)   FORMAT (6E12.4)   MAXIMUM 10 CARDS   (IN °F)
ALPHANUMERIC FORMAT 20A4 PRINT THE WORD "SECTION" IN THE 1ST 8 SPACES - USED IN SEVERAL WRITE STATEMENTS
SECTION
TITLE CARD  FORMAT 20A4
```

C COAT	R COAT	K COAT	I COAT
COATING SPECIFIC HEAT (BTU/LB°F)	COATING DENSITY (LB/FT^3)	COATING THERM. CONDUCTIVITY AT 0°F BTU/FT-SEC-°F	NO. OF SECTIONS IN COATING

COPY AVAILABLE TO DDC DOES NOT PERMIT FULLY LEGIBLE PRODUCTION

IBM System/360 Assembler Coding Form

| | | |

IBM System/360 Assembler Coding Form

PROGRAM | PROGRAMMER | DATE | PUNCHING INSTRUCTIONS | GRAPHIC | PUNCH | PAGE 14 OF 14 | CARD ELECTRO NUMBER *

Name	Operation	Operand	Comments
THETAF HEAT INPUT TIME (SEC)	THETAF ELAPSED TIME FOR 1 ROUND (SEC)	THETAC COOLING TIME (SEC)	DTHEC COOLING TIME Δ (SEC)	CLER COOLING CONV. FACTOR	TCHAM INITIAL TEMP. OF CHAMBER (°F)	XCOOL COOLING CONST.
TINT(1) INITIAL TEMP SECT. 1 (°F)	TINT(2) SECT. 2 (°F)	TINT(3) SECT. 3 (°F)	TINT(4) SECT. 4 (°F)	TINT(5) SECT. 5 (°F)		
TAMB AMBIENT TEMP °F	HMAX MAX H. T. COEF IN SECT. 1 TO 5 BTU/FT^2-°F-SEC	HINT INTERFACE H. T. COEF. BTU/FT^2-°F-SEC	HLOSS H. T. COEF. FOR OUTER SURFACE BTU/FT^2-°F-SEC	SIGMA STEFAN-BOLTZ. CONST. 4.7595E-13	EPS EMISSIVITY OF OUTER SURFACE	
MBURST NO. OF BURSTS	MROUND NO. OF RNDS/ BURST	MINC MAX. TIME INCRE.	SCALE TIME FACTOR CONV.	IPRINT 1 PRINT INTERV. 0 TO θ_F	IPRINT 2 PRINT INTERV. θ_F TO θ_C	IPRINT 3 PRINT INTERV. END OF BURST TO θ_C	← RIGHT JUSTIFY	

COPY AVAILABLE TO DDC DOES NOT PERMIT FULLY LEGIBLE PRODUCTION

TABULAR HEAT TRANSFER AND GAS TEMPERATURES
5.56MM FIXTURE GEOM. RUN 6 900 RND/MIN

SECTION 1

H TABLE - NUMBER OF ENTRIES = 22

THETA							
0.0	0.9999999E-04	0.2000000E-03	0.3000000E-03	0.3999998E-03	0.3999998E-03	0.4999998E-03	0.5999999E-03
0.7000000E-03	0.7999998E-03	0.8999999E-03	0.9999999E-03	0.1100000E-02	0.1200000E-02	0.1300000E-02	0.1400000E-02
0.1500000E-02	0.1600000E-02	0.1700000E-02	0.1800000E-02	0.1900000E-02	0.2000000E-02		

H(THETA)							
0.0	0.1349999E 01	0.2400000E 01	0.3179999E 01	0.3299999E 01	0.3290000E 01	0.2950000E 01	0.2610000E 01
0.2370000E 01	0.2089999E 01	0.1910000E 01	0.1770000E 01	0.1629999E 01	0.1500000E 01	0.1400000E 01	0.1299999E 01
0.1259999E 01	0.1250000E 01	0.1219999E 01	0.1110000E 01	0.8699999E 00	0.0		

TG TABLE - NUMBER OF ENTRIES = 22

THETA							
0.0	0.9999999E-04	0.2000000E-03	0.3000000E-03	0.3999998E-03	0.3999998E-03	0.4999998E-03	0.5999999E-03
0.7000000E-03	0.7999998E-03	0.8999999E-03	0.9999999E-03	0.1100000E-02	0.1200000E-02	0.1300000E-02	0.1400000E-02
0.1500000E-02	0.1600000E-02	0.1700000E-02	0.1800000E-02	0.1900000E-02	0.2000000E-02		

TG(THETA)							
0.4690000E 04	0.4600000E 04	0.4480000E 04	0.4280000E 04	0.4200000E 04	0.4025000E 04	0.3720000E 04	0.3350000E 04
0.3075000E 04	0.2850000E 04	0.2650000E 04	0.2480000E 04	0.2340000E 04	0.2220000E 04	0.2140000E 04	0.2050000E 04
0.2030000E 04	0.1920000E 04	0.1860000E 04	0.1810000E 04	0.1780000E 04	0.1760000E 04		

COPY AVAILABLE TO DDC DOES NOT
PERMIT FULLY LEGIBLE PRODUCTION

TABULAR HEAT TRANSFER AND GAS TEMPERATURES
5.56MM FIXTURE GEOM. RUN 6 900 RND/MIN

SECTION 2

H TABLE - NUMBER OF ENTRIES = 22

THETA

0.0	0.9999999E-04	0.2000000E-03	0.3000000E-03	0.3999998E-03	0.3999998E-03	0.4999998E-03	0.5999999E-03
0.7000000E-03	0.7999998E-03	0.8999999E-03	0.9999999E-03	0.1100000E-02	0.1200000E-02	0.1300000E-02	0.1400000E-02
0.1500000E-02	0.1600000E-02	0.1700000E-02	0.1800000E-02	0.1900000E-02	0.2000000E-02		

H(THETA)

0.0	0.2980000E 01	0.5320000E 01	0.7080000E 01	0.7330000E 01	0.7309999E 01	0.6540000E 01	0.5780000E 01
0.5250000E 01	0.4650000E 01	0.4250000E 01	0.3929999E 01	0.3639999E 01	0.3339999E 01	0.3120000E 01	0.2860000E 01
0.2799999E 01	0.2780000E 01	0.2709999E 01	0.2459999E 01	0.1910000E 01	0.0		

TG TABLE - NUMBER OF ENTRIES = 22

THETA

0.0	0.9999999E-04	0.2000000E-03	0.3000000E-03	0.3999998E-03	0.3999998E-03	0.4999998E-03	0.5999999E-03
0.7000000E-03	0.7999998E-03	0.8999999E-03	0.9999999E-03	0.1100000E-02	0.1200000E-02	0.1300000E-02	0.1400000E-02
0.1500000E-02	0.1600000E-02	0.1700000E-02	0.1800000E-02	0.1900000E-02	0.2000000E-02		

TG(THETA)

0.4690000E 04	0.4600000E 04	0.4480000E 04	0.4280000E 04	0.4200000E 04	0.4025000E 04	0.3720000E 04	0.3350000E 04
0.3075000E 04	0.2850000E 04	0.2650000E 04	0.2680000E 04	0.2340000E 04	0.2220000E 04	0.2140000E 04	0.2050000E 04
0.2030000E 04	0.1920000E 04	0.1860000E 04	0.1810000E 04	0.1780000E 04	0.1760000E 04		

COPY AVAILABLE TO DDC DOES NOT
PERMIT FULLY LEGIBLE PRODUCTION

TABULAR HEAT TRANSFER AND GAS TEMPERATURES
5.56MM FIXTURE GEOM. RUN 6 900 RND/MIN

SECTION 3

H TABLE - NUMBER OF ENTRIES = 22

THETA							
0.0	0.9999999E-04	0.2000000E-03	0.3000000E-03	0.3999998E-03	0.3999998E-03	0.4999998E-03	0.5999999E-03
0.7000000E-03	0.7999998E-03	0.8999999E-03	0.9999999E-03	0.1100000E-02	0.1200000E-02	0.1300000E-02	0.1400000E-02
0.1500000E-02	0.1600000E-02	0.1700000E-02	0.1800000E-02	0.1900000E-02	0.2000000E-02		

H(THETA)							
0.0	0.2270000E 01	0.4040000E 01	0.5219999E 01	0.5549999E 01	0.5540000E 01	0.4959999E 01	0.4400000E 01
0.3969999E 01	0.3520000E 01	0.3219999E 01	0.2990000E 01	0.2740000E 01	0.2520000E 01	0.2360000E 01	0.2179999E 01
0.2120000E 01	0.2099999E 01	0.2070000E 01	0.1849999E 01	0.1450000E 01	0.0		

TG TABLE - NUMBER OF ENTRIES = 22

THETA							
0.0	0.9999999E-04	0.2000000E-03	0.3000000E-03	0.3999998E-03	0.3999998E-03	0.4999998E-03	0.5999999E-03
0.7000000E-03	0.7999998E-03	0.8999999E-03	0.9999999E-03	0.1100000E-02	0.1200000E-02	0.1300000E-02	0.1400000E-02
0.1500000E-02	0.1600000E-02	0.1700000E-02	0.1800000E-02	0.1900000E-02	0.2000000E-02		

TG(THETA)							
0.4690000E 04	0.4600000E 04	0.4480000E 04	0.4280000E 04	0.4200000E 04	0.4025000E 04	0.3720000E 04	0.3350000E 04
0.3075000E 04	0.2850000E 04	0.2650000E 04	0.2480000E 04	0.2340000E 04	0.2220000E 04	0.2140000E 04	0.2050000E 04
0.2030000E 04	0.1920000E 04	0.1860000E 04	0.1810000E 04	0.1780000E 04	0.1760000E 04		

COPY AVAILABLE TO DDC DOES NOT
PERMIT FULLY LEGIBLE PRODUCTION

TABULAR HEAT TRANSFER AND GAS TEMPERATURES
5.56MM FIXTURE GEOM. RUN 6 900 RND/MIN

SECTION 4

H TABLE - NUMBER OF ENTRIES = 22

THETA							
0.0	0.9999999E-04	0.2000000E-03	0.3000000E-03	0.3999998E-03	0.3999998E-03	0.4999998E-03	0.5999999E-03
0.7000000E-03	0.7999998E-03	0.8999999E-03	0.9999999E-03	0.1100000E-02	0.1200000E-02	0.1300000E-02	0.1400000E-02
0.1500000E-02	0.1600000E-02	0.1700000E-02	0.1800000E-02	0.1900000E-02	0.2000000E-02		

H(THETA)							
0.0	0.3450000E 01	0.6150000E 01	0.8110000E 01	0.8459999E 01	0.8440000E 01	0.7549999E 01	0.6690000E 01
0.6049999E 01	0.5370000E 01	0.4889999E 01	0.4540000E 01	0.4179999E 01	0.3839999E 01	0.3589999E 01	0.3320000E 01
0.3230000E 01	0.3200000E 01	0.3139999E 01	0.2839999E 01	0.2219999E 01	0.0		

TG TABLE - NUMBER OF ENTRIES = 22

THETA							
0.0	0.9999999E-04	0.2000000E-03	0.3000000E-03	0.3999998E-03	0.3999998E-03	0.4999998E-03	0.5999999E-03
0.7000000E-03	0.7999998E-03	0.8999999E-03	0.9999999E-03	0.1100000E-02	0.1200000E-02	0.1300000E-02	0.1400000E-02
0.1500000E-02	0.1600000E-02	0.1700000E-02	0.1800000E-02	0.1900000E-02	0.2000000E-02		

TG(THETA)							
0.4690000E 04	0.4600000E 04	0.4480000E 04	0.4280000E 04	0.4200000E 04	0.4025000E 04	0.3720000E 04	0.3350000E 04
0.3075000E 04	0.2850000E 04	0.2650000E 04	0.2480000E 04	0.2340000E 04	0.2220000E 04	0.2140000E 04	0.2050000E 04
0.2030000E 04	0.1920000E 04	0.1860000E 04	0.1810000E 04	0.1780000E 04	0.1760000E 04		

COPY AVAILABLE TO DDC DOES NOT
PERMIT FULLY LEGIBLE PRODUCTION

TABULAR HEAT TRANSFER AND GAS TEMPERATURES
5.56MM FIXTURE GEOM. RUN 6 900 RND/MIN

SECTION 5

H TABLE - NUMBER OF ENTRIES = 22

THETA

0.0	0.9999999E-04	0.2000000E-03	0.3000000E-03	0.3999998E-03	0.4999998E-03	0.5999999E-03	
0.7000000E-03	0.7999998E-03	0.8999999E-03	0.9999999E-03	0.1100000E-02	0.1200000E-02	0.1300000E-02	0.1400000E-02
0.1500000E-02	0.1600000E-02	0.1700000E-02	0.1800000E-02	0.1900000E-02	0.2000000E-02		

H(THETA)

0.0	0.4040000E 01	0.7200000E 01	0.9549999E 01	0.9910000E 01	0.9889999E 01	0.8839999E 01	0.7839999E 01
0.7089999E 01	0.6290000E 01	0.5730000E 01	0.5309999E 01	0.4900000E 01	0.4500000E 01	0.4209999E 01	0.3889999E 01
0.3790000E 01	0.3750000E 01	0.3669999E 01	0.3330000E 01	0.2599999E 01	0.0		

TG TABLE - NUMBER OF ENTRIES = 22

THETA

0.0	0.9999999E-04	0.2000000E-03	0.3000000E-03	0.3999998E-03	0.3999998E-03	0.4999998E-03	0.5999999E-03
0.7000000E-03	0.7999998E-03	0.8999999E-03	0.9999999E-03	0.1100000E-02	0.1200000E-02	0.1300000E-02	0.1400000E-02
0.1500000E-02	0.1600000E-02	0.1700000E-02	0.1800000E-02	0.1900000E-02	0.2000000E-02		

TG(THETA)

0.4690000E 04	0.4600000E 04	0.4480000E 04	0.4280000E 04	0.4200000E 04	0.4025000E 04	0.3720000E 04	0.3350000E 04
0.3075000E 04	0.2850000E 04	0.2650000E 04	0.2480000E 04	0.2340000E 04	0.2220000E 04	0.2140000E 04	0.2050000E 04
0.2030000E 04	0.1920000E 04	0.1860000E 04	0.1810000E 04	0.1780000E 04	0.1760000E 04		

COPY AVAILABLE TO DDC DOES NOT PERMIT FULLY LEGIBLE PRODUCTION

INPUT DATA FOR COMPOSITE CYLINDRICAL GUN CHAMBER PROGRAM

5.56 MM FIXTURE GEOM. RUN 6 900 RND/MIN

THIS RUN CONSISTS OF 1 BURST(S) OF 2 ROUNDS EACH

	COATING	METAL	ENVIRONMENT
SPECIFIC HEAT (BTU/LBM)	0.1260E 00	0.1260E 00	
DENSITY (LBM/FT3)	0.5000E 03	0.5000E 03	
CONDUCTIVITY (BTU/FT SEC DF)	0.7000E-02	0.7000E-02	
NUMBER OF DISTANCE INCREMENTS	5	40	
INITIAL TEMPERATURE (DF)	70.0000	70.0000	70.0000

	INSIDE	INTERFACE	OUTSIDE
RADIUS (FT)			
SECTION 1	0.2040E-01	0.2165E-01	0.5520E-01
SECTION 2	0.1570E-01	0.1695E-01	0.4400E-01
SECTION 3	0.1570E-01	0.1695E-01	0.4100E-01
SECTION 4	0.1240E-01	0.1365E-01	0.3940E-01
SECTION 5	0.9250E-02	0.1050E-01	0.3320E-01
HEAT TRANSFER COEFFICIENT	0.9910E 01	0.1000E 07	0.1400E-02
STEFAN-BOLTZMANN CONSTANT			0.4759E-12
EMISSIVITY			1.0000

	FIRING	EXTRACTION	COOLING
TIME (SEC)	0.2000E-02	0.6700E-01	0.1000E 02
TIME INCREMENT FACTORS	19		1
TIME INCREMENT (SEC)			0.1000E 00
PRINT INTERVALS	5	50	200

LENGTH OF	
SECTION 1	0.4590E-01
SECTION 2	0.3780E-01
SECTION 3	0.3780E-01
SECTION 4	0.1200E-01
SECTION 5	0.5000E-01

CROSS SECTIONAL AREA BETWEEN SECTIONS

SECTIONS 1 AND 2	0.5950E-02
SECTIONS 2 AND 3	0.4510E-02
SECTIONS 3 AND 4	0.4100E-02
SECTIONS 4 AND 5	0.2980E-02

COOLING CONVERGENCE ERROR 0.2000

DISTANCE INCREMENT IN COATING OF SECTION 1	0.312500E-03
DISTANCE INCREMENT IN METAL OF SECTION 1	0.860256E-03
DISTANCE INCREMENT IN COATING OF SECTION 2	0.312500E-03
DISTANCE INCREMENT IN METAL OF SECTION 2	0.693590E-03
DISTANCE INCREMENT IN COATING OF SECTION 3	0.312500E-03
DISTANCE INCREMENT IN METAL OF SECTION 3	0.616667E-03
DISTANCE INCREMENT IN COATING OF SECTION 4	0.312500E-03
DISTANCE INCREMENT IN METAL OF SECTION 4	0.660256E-03
DISTANCE INCREMENT IN COATING OF SECTION 5	0.312501E-03
DISTANCE INCREMENT IN METAL OF SECTION 5	0.582051E-03

TIME INCREMENT DURING FIRING	0.100000E-03
TIME INCREMENT DURING EXTRACTION	0.300000E-03

COPY AVAILABLE TO DDC DOES NOT PERMIT FULLY LEGIBLE PRODUCTION

SECTION 1

BURST	ROUND	TIME (SEC)	T(1)	T(INTER)	T(LAST)	T(CT) AVE	T(ML) AVE	T AVE	Q IN
1	0	0.0	70.00	70.00	70.00	70.00	70.00	70.00	0.0
1	1	0.000500	428.94	70.01	70.00	133.56	70.00	71.27	5.14
1	1	0.000800 **	434.61	70.24	70.00	156.76	70.00	71.73	7.04
1	1	0.001000	415.06	70.86	70.00	166.22	70.01	71.93	7.82
1	1	0.001500	368.24	75.01	70.00	180.06	70.04	72.24	9.08
1	1	0.002000	321.47	82.30	70.00 **	185.19	70.10	72.40	9.74
1	1	0.002000	321.47	82.30	70.00	185.19	70.10	72.40	9.74
1	1	0.002000	321.47	82.30	70.00	185.19	70.10	72.40	9.74
1	1	0.008600	156.79 **	126.53	70.00	145.32	70.91	72.40	9.74
1	1	0.017000	130.46	118.88	70.00	126.26	71.30	72.40	9.74
1	1	0.032000	113.17	108.43	70.00	111.48	71.60	72.40	9.74
1	1	0.047000	105.02	102.30	70.00	104.05	71.75	72.40	9.74
1	1	0.062000	100.04	98.24	70.00	99.41	71.85	72.40	9.74
1	1	0.067000	98.77	97.17	70.00	98.21	71.87	72.40	9.74
			98.78	97.17	70.00	98.21	71.88	72.40	
1	2	0.067500	455.02	97.08	70.00	161.21	71.88	73.66	5.11
1	2	0.067800 **	460.20	97.25	70.00	184.12	71.88	74.12	6.98
1	2	0.068000	440.54	97.83	70.00	193.41	71.89	74.31	7.76
1	2	0.068499	393.64	101.84	70.00	206.94	71.92	74.62	9.00
1	2	0.068999	347.09	108.97	70.00 **	211.85	71.98	74.78	9.65
1	2	0.068999	347.09	108.97	70.00	211.85	71.98	74.78	9.65
1	2	0.068999	347.09	108.97	70.00	211.85	71.98	74.78	9.65
1	2	0.075299	184.62 **	151.69	70.00	172.13	72.79	74.78	9.65
1	2	0.083999	155.23	142.62	70.00	150.67	73.23	74.78	9.65
1	2	0.098998	135.86	130.27	70.00	133.87	73.57	74.78	9.65
1	2	0.113998	126.00	122.59	70.00	124.79	73.76	74.78	9.65
1	2	0.128997	119.61	117.23	70.00	118.77	73.88	74.78	9.65
1	2	0.133998	117.93	115.77	70.00	117.16	73.91	74.78	9.65
			117.94	115.78	70.02	117.18	73.93	74.79	

LAST ROUND OF BURST NO. 1 BEGIN UNIFORM COOLING

1		0.133998				74.79	74.79	74.79	
1		10.133996				76.36	76.36	76.36	

COPY AVAILABLE TO DDC DOES NOT PERMIT FULLY LEGIBLE REPRODUCTION

SECTION 2

BURST	ROUND	TIME (SEC)		T(1)	T(INTER)	T(LAST)	T(CT) AVE	T(ML) AVE	T AVE	Q IN
1	0	0.0		70.00	70.00	70.00	70.00	70.00	70.00	0.0
1	1	0.000500		815.29	70.01	70.00	202.36	70.00	73.20	10.80
1	1	0.000700	**	821.09	70.25	70.00	234.59	70.00	73.98	13.45
1	1	0.001000		753.52	72.11	70.00	263.27	70.02	74.68	15.84
1	1	0.001500		651.90	81.68	70.30	288.09	70.09	75.36	18.14
1	1	0.002000		558.67	97.65	70.00	** 296.89	70.24	75.71	19.34
1	1	0.002000		558.67	97.65	70.00	296.89	70.24	75.71	19.34
1	1	0.002000		558.67	97.65	70.00	296.89	70.24	75.71	19.34
1	1	0.008000		248.67	** 181.37	70.00	222.93	72.06	75.71	19.34
1	1	0.017000		188.37	165.17	70.00	179.90	73.13	75.71	19.34
1	1	0.032000		153.75	144.39	70.00	150.39	73.86	75.70	19.34
1	1	0.047000		137.59	132.26	70.00	135.69	74.22	75.70	19.34
1	1	0.062000		127.78	124.25	70.00	126.52	74.45	75.70	19.34
1	1	0.067000		125.28	122.13	70.00	124.16	74.50	75.70	19.34
				125.27	122.12	69.99	124.15	74.50	75.69	
1	2	0.067500		859.99	121.94	69.99	254.49	74.50	78.85	10.66
1	2	0.067700	**	864.56	122.09	69.99	286.04	74.50	79.61	13.25
1	2	0.068000		796.51	123.81	69.99	313.91	74.52	80.30	15.59
1	2	0.068499		694.89	133.05	69.99	337.73	74.60	80.96	17.82
1	2	0.068999		602.74	148.57	69.99	** 345.90	74.75	81.30	18.98
1	2	0.068999		602.74	148.57	69.99	345.90	74.75	81.30	18.98
1	2	0.068999		602.74	148.57	69.99	345.90	74.75	81.30	18.98
1	2	0.074999		297.10	** 228.44	69.99	270.91	76.60	81.29	18.98
1	2	0.083999		234.68	209.68	69.99	225.57	77.72	81.29	18.98
1	2	0.098998		196.29	185.36	69.99	192.37	78.54	81.29	18.98
1	2	0.113998		176.93	170.29	69.99	174.56	78.98	81.29	18.98
1	2	0.128997		164.44	159.81	69.99	162.80	79.27	81.29	18.98
1	2	0.133998		161.14	156.95	69.99	159.66	79.35	81.29	18.98
				161.12	156.93	69.96	159.63	79.32	81.26	

LAST ROUND OF BURST NO. 1 BEGIN UNIFORM COOLING

1	0.133998	81.26	81.26	81.26
1	10.133996	78.77	78.77	78.77

COPY AVAILABLE TO DDC DOES NOT PERMIT FULLY LEGIBLE PRODUCTION

SECTION 3

BURST	ROUND	TIME (SEC)		T(1)		T(INTER)	T(LAST)	T(CT) AVE		T(ML) AVE	T AVE	Q IN
1	0	0.0		70.00		70.00	70.00	70.00		70.00	70.00	0.0
1	1	0.000500		648.72		70.01	70.00	172.26		70.00	72.91	8.35
1	1	0.000700	**	660.76		70.21	70.00	198.42		70.00	73.65	10.49
1	1	0.001000		612.87		71.73	70.00	222.01		70.01	74.34	12.46
1	1	0.001500		534.83		79.57	70.00	242.71		70.08	74.99	14.35
1	1	0.002000		460.77		92.59	70.00	250.40	**	70.21	75.34	15.34
1	1	0.002000		460.77		92.59	70.00	250.40		70.21	75.34	15.34
1	1	0.002000		460.77		92.59	70.00	250.40		70.21	75.34	15.34
1	1	0.004000		212.43	**	158.46	70.00	191.81		71.92	75.33	15.34
1	1	0.017000		164.08		145.53	70.00	157.30		72.93	75.33	15.34
1	1	0.032000		136.46		129.01	70.00	133.79		73.62	75.33	15.34
1	1	0.047000		123.61		119.39	70.00	122.11		73.96	75.33	15.34
1	1	0.062000		115.83		113.03	70.00	114.83		74.17	75.33	15.34
1	1	0.067000		113.84		111.35	70.00	112.96		74.23	75.33	15.34
				113.85		111.35	70.00	112.96		74.23	75.33	
1	2	0.067500		686.03		111.21	70.00	213.94		74.24	78.21	8.26
1	2	0.067700	**	697.22		111.34	70.00	239.66		74.24	78.95	10.37
1	2	0.068000		648.94		112.75	70.00	262.72		74.26	79.62	12.30
1	2	0.068499		570.85		120.35	70.00	282.75		74.33	80.26	14.15
1	2	0.068999		497.43		133.05	70.00	289.99	**	74.46	80.59	15.12
1	2	0.068999		497.43		133.05	70.00	289.99		74.46	80.59	15.12
1	2	0.068999		497.43		133.05	70.00	289.99		74.46	80.59	15.12
1	2	0.074699		254.57	**	196.34	70.00	232.30		76.15	80.59	15.12
1	2	0.083999		201.19		181.14	70.00	193.88		77.27	80.59	15.12
1	2	0.098998		170.47		161.75	70.00	167.35		78.05	80.59	15.12
1	2	0.113998		155.04		149.75	70.00	153.16		78.46	80.59	15.12
1	2	0.128997		145.10		141.41	70.00	143.79		78.73	80.59	15.12
1	2	0.133998		142.48		139.14	70.00	141.29		78.81	80.58	15.12
				142.49		139.15	70.01	141.30		78.82	80.60	

LAST ROUND OF BURST NO. 1 BEGIN UNIFORM COOLING

1		0.133998						80.60		80.60	80.60	
1		10.133996						80.61		80.61	80.61	

COPY AVAILABLE TO DDC DOES NOT
PERMIT FULLY LEGIBLE PRODUCTION

SECTION 4

BURST	ROUND	TIME (SEC)		T(1)	T(INTER)	T(LAST)	T(CT) AVE	T(ML) AVE	T AVE	Q IN
1	0	0.0		70.00	70.00	70.00	70.00	70.00	70.00	0.0
1	1	0.000500		912.87	70.02	70.00	218.90	70.00	73.47	12.27
1	1	0.000700	**	913.66	70.29	70.00	254.26	70.00	74.29	15.20
1	1	0.001000		833.10	72.46	70.00	285.42	70.02	75.03	17.83
1	1	0.001500		716.70	83.43	70.00	312.18	70.10	75.74	20.34
1	1	0.002000		612.38	101.49	70.00	321.57	70.25	76.10	21.66
1	1	0.002000		612.38	101.49	70.00	321.57	70.25	76.10	21.66
1	1	0.002000		612.38	101.49	70.00	321.57	70.25	76.10	21.66
1	1	0.008000		267.72	192.76	70.00	238.90	72.22	76.10	21.66
1	1	0.017000		200.13	174.32	70.00	190.65	73.37	76.10	21.66
1	1	0.032000		161.43	151.06	70.00	157.69	74.15	76.10	21.66
1	1	0.047000		143.42	137.54	70.00	141.31	74.54	76.10	21.66
1	1	0.062000		132.52	128.63	70.00	131.13	74.78	76.10	21.66
1	1	0.067000		129.74	126.28	70.00	128.50	74.85	76.10	21.66
				129.74	126.27	70.00	128.50	74.84	76.09	
1	2	0.067500		959.71	126.07	70.00	274.97	74.85	79.51	12.09
1	2	0.067700	**	959.07	126.26	70.00	309.52	74.85	80.32	14.96
1	2	0.068000		878.00	128.25	70.00	339.73	74.87	81.04	17.53
1	2	0.068499		761.66	138.84	70.00	365.32	74.96	81.72	19.95
1	2	0.068999		658.69	156.38	70.00	373.96	75.12	82.07	21.22
1	2	0.068999		658.69	156.38	70.00	373.96	75.12	82.07	21.22
1	2	0.068999		658.69	156.38	70.00	373.96	75.12	82.07	21.22
1	2	0.074699		323.97	243.52	70.00	293.01	77.04	82.07	21.22
1	2	0.083999		249.74	222.00	70.00	239.58	78.31	82.07	21.22
1	2	0.098998		206.94	194.86	70.00	202.59	79.19	82.07	21.22
1	2	0.113998		185.43	178.12	70.00	182.81	79.66	82.06	21.22
1	2	0.128997		171.59	166.49	70.00	169.77	79.97	82.06	21.22
1	2	0.133998		167.94	163.33	70.00	166.29	80.06	82.06	21.22
				167.93	163.33	69.99	166.29	80.05	82.06	

LAST ROUND OF BURST NO. 1 BEGIN UNIFORM COOLING

1	0.133998		82.06	82.06	82.06
1	10.133996		81.49	81.49	81.49

COPY AVAILABLE TO DDC DOES NOT
PERMIT FULLY LEGIBLE PRODUCTION

SECTION 5

BURST	ROUND	TIME (SEC)	T(1)	T(INTER)	T(LAST)	T(CT) AVE	T(ML) AVE	T AVE	Q IN
1	0	0.0	70.00	70.00	70.00	70.00	70.00	70.00	0.0
1	1	0.000500	1033.56	70.02	70.00	238.68	70.00	74.10	14.10
1	1	0.000700 **	1025.30	70.37	70.00	277.33	70.00	75.04	17.36
1	1	0.001000	927.22	73.01	70.00	311.05	70.02	75.87	20.26
1	1	0.001500	792.54	86.07	70.00	339.87	70.12	76.67	23.02
1	1	0.002000	674.49	106.99	70.00 **	349.83	70.29	77.08	24.46
1	1	0.002000	674.49	106.99	70.00	349.83	70.29	77.08	24.46
1	1	0.002000	674.49	106.99	70.00	349.83	70.29	77.08	24.46
1	1	0.007700	294.30 **	205.49	70.00	259.76	72.52	77.07	24.46
1	1	0.017000	212.78	183.93	70.00	202.08	73.96	77.07	24.46
1	1	0.032000	169.20	157.70	70.00	165.01	74.88	77.07	24.46
1	1	0.047000	149.06	142.57	70.00	146.71	75.33	77.07	24.46
1	1	0.062000	136.92	132.64	70.00	135.37	75.62	77.07	24.46
1	1	0.067000	133.83	130.02	70.00	132.46	75.69	77.07	24.46
			133.83	130.02	70.00	132.46	75.69	77.06	
1	2	0.067500	1081.64	129.80	70.00	298.22	75.69	81.10	13.88
1	2	0.067700 **	1071.77	130.04	70.00	335.91	75.70	82.02	17.07
1	2	0.068000	973.19	132.49	70.00	368.53	75.72	82.83	19.89
1	2	0.068499	838.66	145.10	70.00	395.98	75.82	83.59	22.55
1	2	0.068999	722.29	165.39	70.00 **	405.07	76.00	83.99	23.93
1	2	0.068999	722.29	165.39	70.00	405.07	76.00	83.99	23.93
1	2	0.068999	722.29	165.39	70.00	405.07	76.00	83.99	23.93
1	2	0.074699	349.08 **	259.03	70.00	314.15	78.25	83.98	23.93
1	2	0.083999	265.19	234.28	70.00	253.76	79.75	83.98	23.93
1	2	0.098998	217.17	203.82	70.00	212.31	80.78	83.98	23.93
1	2	0.113998	193.20	185.16	70.00	190.29	81.33	83.98	23.93
1	2	0.128997	177.85	172.26	70.00	175.83	81.69	83.98	23.93
1	2	0.133998	173.80	168.76	70.00	171.99	81.78	83.98	23.93
			173.80	168.76	69.99	171.98	81.78	83.97	
LAST ROUND OF BURST NO. 1 BEGIN UNIFORM COOLING									
1		0.133998				83.97	83.97	83.97	
1		10.133996				82.72	82.72	82.72	

COPY AVAILABLE TO DDC DOES NOT PERMIT FULLY LEGIBLE PRODUCTION

III. REFERENCES

1. Corner, J., Theory of the Interior Ballistics of Guns, John Wiley & Sons, Inc. (1950).

2. Dusinberre, G. M., Numerical Analysis of Heat Flow, McGraw-Hill (1949).

APPENDIX B

THERMAL INSTRUMENTATION

In the tests reported herein, two types of thermal instrumentation were used: external thermocouples and in-wall thermocouples. Each of these instrumentation techniques is discussed in this appendix. Each technique was used at the locations where it was most suitable.

External Thermocouples

Where the barrel wall is thin, total heat input can be obtained through simple external barrel temperature measurements (thermocouples welded to the outside of the barrel). The relationship of converting temperature measurement to heat input is:

$$Q = \frac{\pi c\rho (D_o^2 - D_i^2)\Delta T}{4(\pi D_i + L)} \quad Btu/ft^2 \qquad (B-1)$$

where Q is the average heat input per square foot of internal surface, Btu/ft^2,

$c\rho$ is the heat capacity of the barrel material per unit volume, $Btu/ft^3\text{-}^oR$,

D_o is the outside diameter of the barrel, ft,

D_i is the inside diameter measured to the midpoint of the lands and grooves, ft,

ΔT is the external barrel temperature rise after the shot, ^oF,

L is the additional heat input length due to the rifling projection, $L = 2N\mathcal{E}$,

N is the number of rifling grooves,

$\mathcal{E}$ is the height of the rifling projection, ft.

Because $c\rho$, D_o, D_i, and L are specified at each location, the heat input, Q, is proportional to the external barrel temperature rise.

In-Wall Thermocouples

At locations where the barrels were thick or of complex geometrical shapes so that axial conduction effects limit the readability or applicability of simple external temperature measurements, in-wall thermocouples placed a short distance from the bore surface were used to determine the local heat input. A typical in-wall thermocouple installation is shown in Figure B -1.

The derivation of the equation for calculating the heat input based on the temperature measured by an in-wall thermocouple proceeds as follows. Consider a heating situation as depicted below.

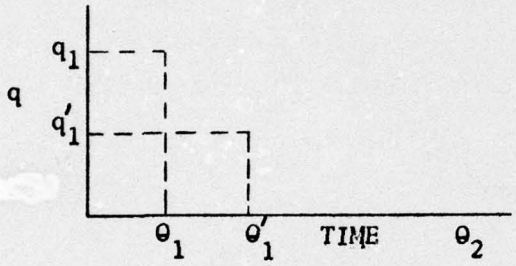

$$q_1\theta_1 = q_1'\theta_1' = Q = \text{constant} \tag{B-2}$$

$$\theta_2 \gg \theta_1 \text{ or } \theta_1' \tag{B-3}$$

where q is the heat flux, θ is time, and Q is the heat input. The temperature rise of the surface above its level at the start of heat input is given by:

$$\Delta T_2 = \frac{2q_1}{K}\left(\frac{K\theta_2}{\pi c\rho}\right)^{1/2} - \frac{2q_1}{K}\left(\frac{K(\theta_2 - \theta_1)}{\pi c\rho}\right)^{1/2} \tag{B-4}$$

But,

$$Q = q_1\theta_1$$

$$q_1 = Q/\theta_1 \tag{B-5}$$

Hence,

$$\Delta T_2 = \frac{2Q}{K}\left(\frac{K}{\pi c\rho\,\theta_2}\right)^{1/2}\left[\frac{\theta_2}{\theta_1}\left\{\left(\frac{\theta_2}{\theta_1}\right)^2 - \frac{\theta_2}{\theta_1}\right\}^{1/2}\right] \tag{B-6}$$

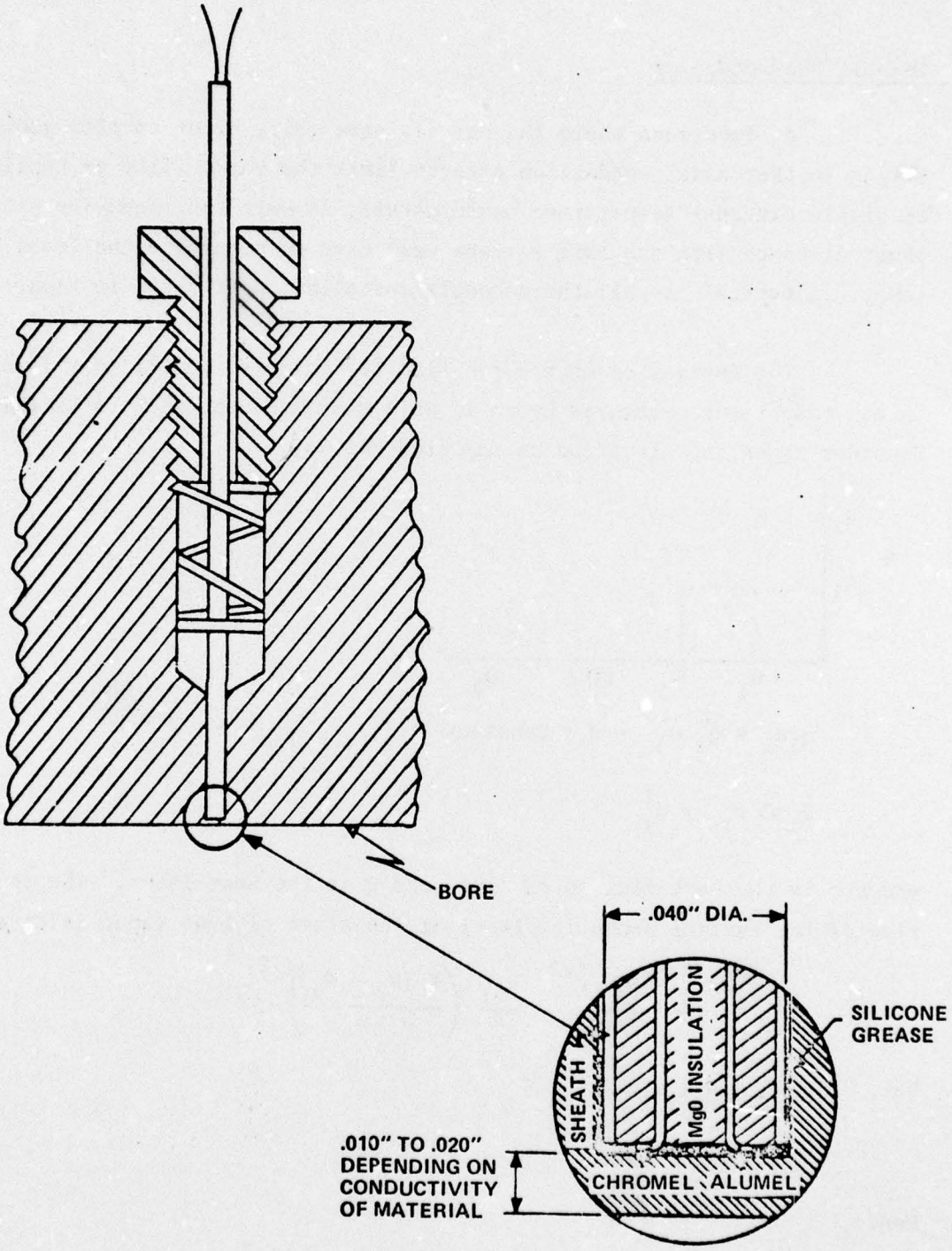

Figure B-1 TYPICAL IN-WALL THERMOCOUPLE INSTALLATION

Defining

$$F\left(\frac{\theta_2}{\theta_1}\right) = \frac{\theta_2}{\theta_1} - \left\{\left(\frac{\theta_2}{\theta_1}\right)^2 - \frac{\theta_2}{\theta_1}\right\}^{1/2} \tag{B-7}$$

one observes that $F(\theta_2/\theta_1) \rightarrow 0.5$ as $\theta_2/\theta_1 \rightarrow \infty$. In fact, the approach to 0.5 is very rapid as θ_2/θ_1 increases. For example, at a ratio θ_2/θ_1 of 10, $F(\theta_2/\theta_1)$ is 0.514. Hence, when θ_2 is at least 10 times θ_1, the temperature of the surface is negligibly affected by the heat input period θ_1. Conversely, the total heat input may be obtained with little error by a determination of the surface temperature existing at time θ_2. From Equation (B-6) and the limit on θ_1, one gets:

$$Q = \sqrt{\pi k c \rho \theta_2}\ \Delta T_2 \tag{B-8}$$

This equation can be used with the restriction that θ_2 be at least 10 times the heat input duration,* θ_1.

In general, it is difficult to obtain a measure of the surface temperature in short-duration heating. Fortunately, only little difference will exist between the surface temperature and a point, say, several thousandths below the surface when the measuring period, θ_2, is long compared to the heat input period, θ_1, as required for use of Equation (B-8). To illustrate this, a one-dimensional heat conduction computer program was used to compute the temperature history in a thick sheet of steel after a heat flux of 20,000 Btu/ft^2-sec was applied for a time of 0.001 second. The temperature rise and time computed for a depth of 0.015 inch was substituted into Equation (B-8), and the calculated total heat input is shown in Figure B-2. This figure shows that the method does indeed calculate the true heat input. The ratio of θ_1/θ_2, where this method is applicable, increases as the distance from the surface increases. From Figure B-2, $\theta_2/\theta_1 = 80$ is required for an exact calculation of total heat input for a depth of 0.015, although $\theta_2/\theta_1 = 40$ yields a heat input within 5 percent of the true value.

*If it is not, the error due to taking the limit of F = 0.5 will increase slightly.

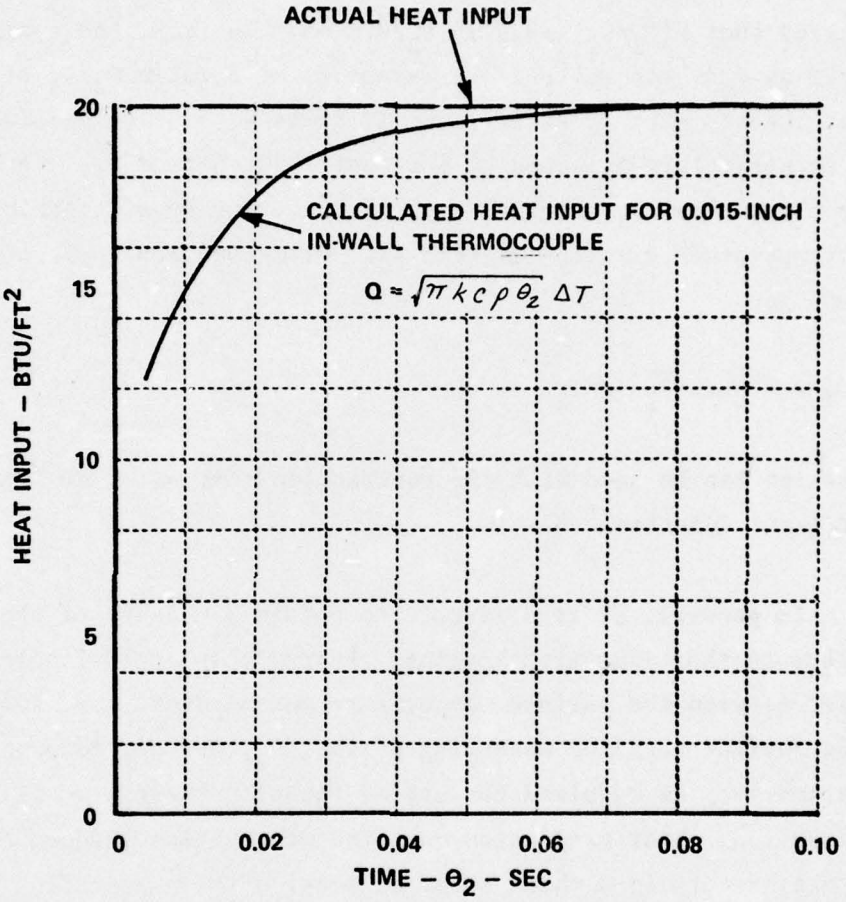

Figure B-2 HEAT INPUT CALCULATED FROM IN-WALL TEMPERATURES

As an illustration of operation where heat flux is varying with time, a sample calculation was performed on the digital computer for a typical 27mm bore heating situation (based on experimental observations). For these calculations, heat input to the bore was governed by given coefficient and propellant temperature histories. Figure B-3 illustrates values obtained. The total heat input to the surface is shown by the dashed line; this value was obtained by the computer directly. Heat input values obtained by use of Equation (B-8) and temperature values determined by the computer for the surface and a point 0.020 inch in depth are also shown. Clearly, the Equation (B-8) gives a good approximation of the total heat input as time is extended beyond 100 milliseconds. Note that both the surface and in-wall values yield reasonable accuracy. Hence, in-wall thermocouple placement at any location within 0.020 inch from the surface will operate successfully. Because the heat input time, θ_1, is generally less than 10 milliseconds during ballistic heating, the technique is especially adaptable to bore heat input measurements.

There are, however, some limitations to the method. The method applies to a slab that is effectively semi-infinite in the time of interest, θ_2. That is, heat has not been conducted through the slab to heat the back surface appreciably. Therefore, a constraint must be made on the magnitude of θ_2. This constraint, based on the Fourier Modulus, is:

$$\theta_2 \leq 0.5 \frac{\rho c \delta^2}{K} \tag{B-9}$$

where ρ, c, and K are the material properties, and δ is the thickness. For steel 0.25 inch thick, this time is approximately 1.7 seconds, which is little constraint for normal weapons evaluation.

Other limitations concern non-one-dimensional heat flow effects which are created by heat flux gradients over the surface and slab geometrical considerations, such as the cylindrical shape of a gun barrel. The influence of heat flow parallel to the surface will be minimal if the following time constraint is satisfied:

$$\theta_2 \leq 1.15 \times 10^{-5} \frac{\rho c}{K} \left(\frac{\Delta T_{max}}{dt/ds} \right)^2 \tag{B-10}$$

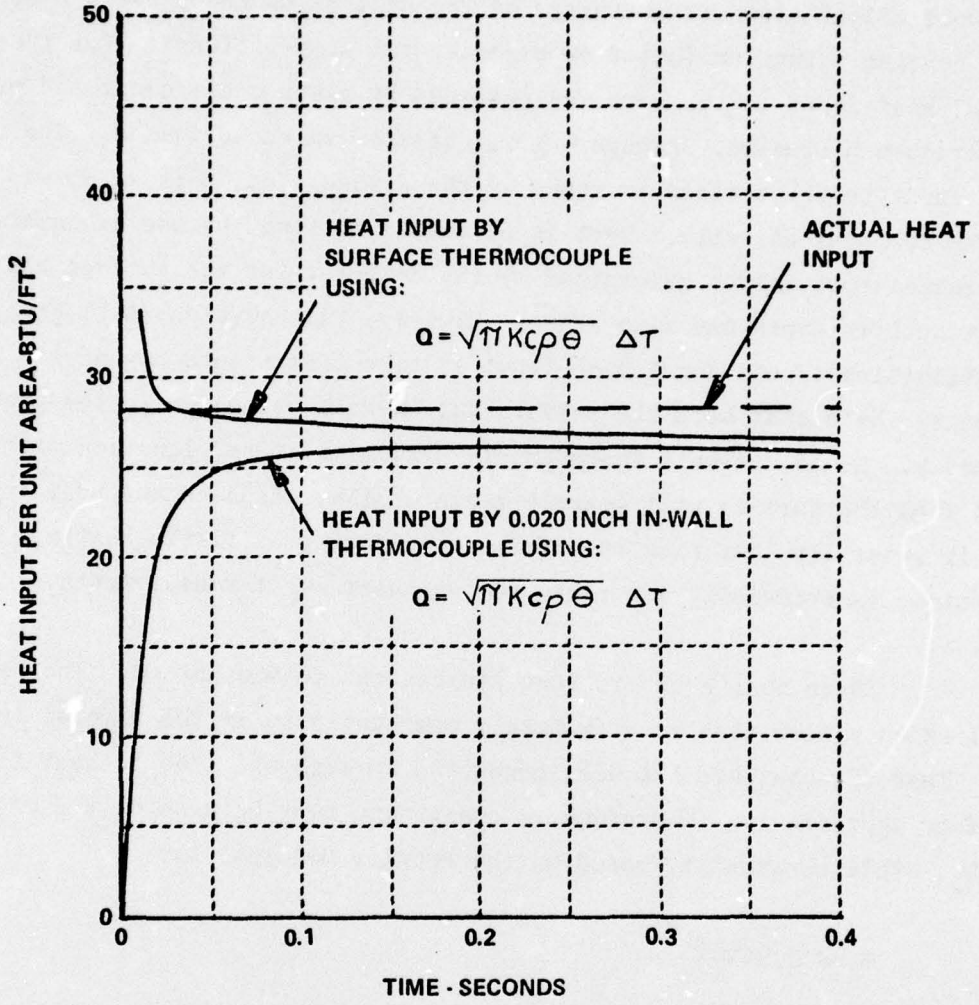

Figure B-3 ACCURACY OF IN-WALL THERMOCOUPLE TECHNIQUE

where ΔT_{max} is the maximum temperature rise at the points of interest, and

$\frac{dt}{ds}$ is the surface temperature gradient in ^{o}F/inch.

For $\Delta T_{max} = 500^{o}F$, a surface temperature gradient of $100^{o}F$ per inch should not influence the one-dimensional results significantly for 2 seconds. This relationship holds as long as the in-wall thermocouple is close to the surface, for example, on the order of 0.02 inch.

The one-dimensional relationship will hold as long as the heat penetration distance is much less than the wall thickness. A correction factor for cylindrical geometry was determined as a function of inner radius. A cylindrical-coordinate heat-conduction computer program was used to generate the temperature distribution 0.015 inch from the inner surface in steel tubes of different radii. In similar fashion to that used for the slab discussed above, a heat flux of 20,000 Btu/ft^2-sec was applied for a period of 0.001 second. The temperature history was used with Equation (B-8) to compute the total heat input. A curve showing the ratio of computed to actual heat input as a function of radius is presented in Figure B-4. This curve was taken for a ratio of $\theta_2/\theta_1 = 50$ and is representative of time ratios from 20 to over 100. An equation was fit to the curve in Figure B-4 and is valid for inner radii larger than 0.10 inch. The equation is:

$$\eta(r) = 1 - 0.32e^{-3.71r} \qquad \text{(B-11)}$$

The corrected or true heat input is then given by:

$$Q_{corr.} = \frac{Q_{calc.}}{\eta(r)} \qquad \text{(B-12)}$$

The heat input values presented in this report were calculated from in-wall thermocouple data using the above relations. For each test, the heat input was calculated at increments of about 25 msec up to 150 milliseconds. A plot of calculated heat input as a function of time was then drawn similar to Figure B-3. The intersection of the straight line portion of the curve with the heat input axis is the value given in the report as the heat input.

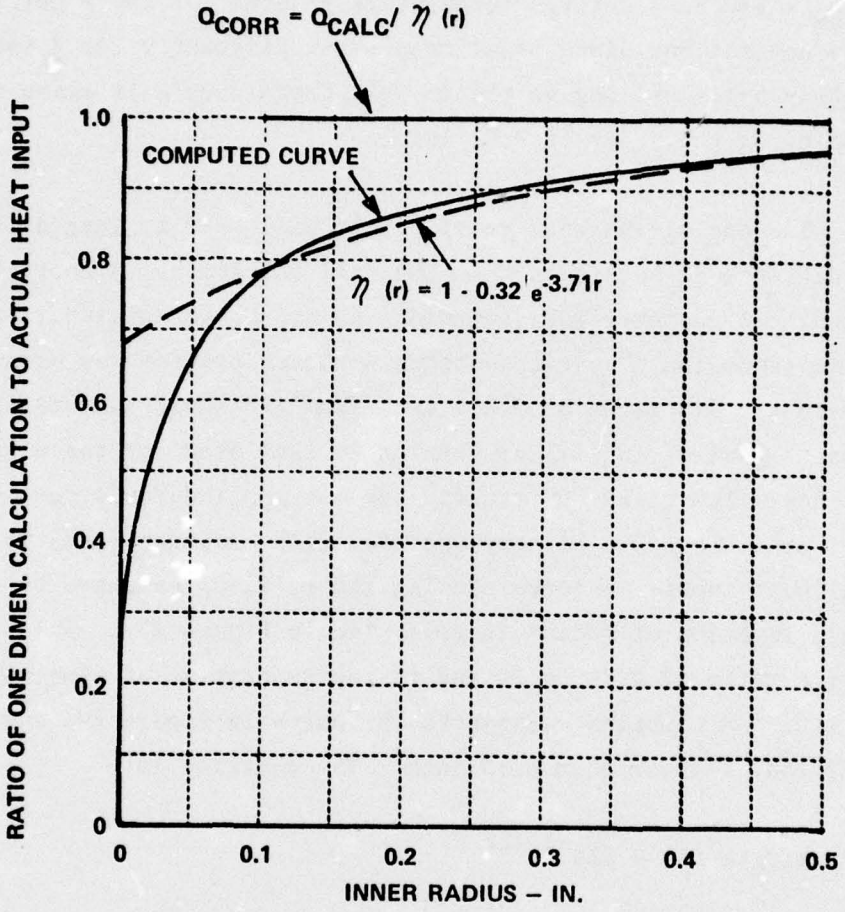

Figure B-4 CORRECTION FACTOR FOR HEAT INPUT CALCULATED FROM IN-WALL THERMOCOUPLES

From the peak temperatures measured by the in-wall thermocouples, their effective distance from the bore surface can be calculated. The equation that relates peak temperature ΔT max to distance x is

$$x = \sqrt{\frac{2}{e\pi}} \quad \frac{Q}{c\rho \Delta T_{max}} \tag{B-13}$$

where e is the base of the natural log, and c is specific heat and ρ is density of the barrel material. Conversely, if the distance from the bore is accurately known, the heat input can be calculated by rearranging equation (B-13).